Universidad de Valladolid

FACULTAD DE CIENCIAS

DEPARTAMENTO DE FÍSICA DE LA MATERIA CONDENSADA, CRISTALOGRAFÍA Y MINERALOGÍA

TESIS DOCTORAL:

DEVELOPMENT OF ENVIRONMENTALLY FRIENDLY CELLULAR POLYMERS FOR PACKAGING AND STRUCTURAL APPLICATIONS. STUDY OF THE RELATIONSHIP CELLULAR STRUCTURE-MECHANICAL PROPERTIES

Presentada por Alberto López Gil para optar al grado de doctor por la Universidad de Valladolid

Dirigida por:
Miguel Ángel Rodríguez Pérez

FINANCIACIÓN

He de agradecer la financiación para llevar a cabo esta investigación que he recibido de diversas instituciones. En primer lugar agradecer al MICINN por la beca FPI referencia BES-2010-038746. Además quiero agradecer la financiación recibida por el grupo CellMat, proveniente de los siguientes proyectos de investigación:

- Desarrollo de plásticos sub-microcelulares y nanocelulares: fabricación, estructura, propiedades y potenciales aplicaciones (MAT2012-34901). Financiado por el Programa Nacional de Materiales (MICIN).
- Desarrollo de una nueva generación de aislantes térmicos avanzados basados en la obtención de estructuras porosas nanocelulares (VA035U13). Financiado por la Junta de Castilla y León.
- Envasado activo y biodegradable para alimentos frescos (ACTIBIOPACK). Financiado por el Ministerio de Economía y Competitividad. Ref: IPT-2011-1662-060000.
- Nancore: Microcellular nanocomposite for substitution of Balsa wood and PVC core material (FP7. 214148). Fiananciado por VII Framework Program (Comisión Europea).

FUNDING

Financial support from FPI grant ref: BES-2010-038746 from MICINN is gratefully acknowledged. Financial assistance provided by the following research projects is also acknowledged:

- Desarrollo de plásticos sub-microcelulares y nanocelulares: fabricación, estructura, propiedades y potenciales aplicaciones (MAT2012-34901). Financiado por el Programa Nacional de Materiales (MICIN).
- Desarrollo de una nueva generación de aislantes térmicos avanzados basados en la obtención de estructuras porosas nanocelulares (VA035U13). Financiado por la Junta de Castilla y León.
- Envasado activo y biodegradable para alimentos frescos (ACTIBIOPACK). Financiado por el Ministerio de Economía y Competitividad. Ref: IPT-2011-1662-060000.
- Nancore: Microcellular nanocomposite for substitution of Balsa wood and PVC core material (FP7. 214148). Fiananciado por VII Framework Program (Comisión Europea).

CONTENTS

0- Resumen en Español.

1- Introduction.

2- Background and State of the Art.

3- Materials, production processes and characterization techniques.

4- Development of starch-based materials.

5- Development of polypropylene foams.

6- Production of prototypes. Applicability of the developed materials.

7- Conclusions and Future work.

ANNEX. Anicell Patent: Method for producing cellular materials having a thermoplastic matrix

CHAPTER 0:

RESUMEN EN ESPAÑOL

Contenidos

0.1- Introducción.

La industria del plástico y la comunidad científica, ante la problemática medioambiental causada por las enormes cantidades de residuos plásticos que se generan, están dirigiendo sus esfuerzos hacia el desarrollo de nuevos procesos y materiales poliméricos que sean más sostenibles con el medio ambiente. Este trabajo tratará de aportar soluciones a este problema dentro de los sectores del envasado de alimentos, del embalaje de protección y de paneles estructurales de baja densidad mediante el desarrollo de formulaciones y procesos a escala de laboratorio que se puedan emplear para la producción de materiales celulares poliméricos ambientalmente sostenibles.

En este sentido se emplearán dos tipos de matrices poliméricas con características muy diferentes: por un lado, un polímero completamente bioderivado y biodegradable como el almidón y por otro lado, un polipropileno ramificado con alta resistencia en fundido y que no requiere de un proceso de reticulación para alcanzar altos ratios de expansión. A pesar de las interesantes propiedades que estos polímeros presentan de partida, todavía se necesitan resolver ciertos aspectos para su aplicación extensiva en los sectores mencionados anteriormente.

Por una parte, el almidón es un polímero que requiere de un proceso previo de plastificación para obtener una matriz termoplástica que pueda ser procesada en equipos industriales (extrusoras, prensas de termoconformado etc.). Este proceso de plastificación disminuye de forma considerable las propiedades mecánicas del polímero (dependiendo del contenido de plastificante) lo que ocasiona que no tenga la rigidez y resistencia adecuadas para remplazar a polímeros derivados del petróleo habitualmente empleados en la fabricación de envases sólidos como el polietileno-tereftalato (PET) y el polipropileno (PP). Además, cuando el almidón es sometido a un proceso de espumado para su aplicación como material de envasado y de embalaje de protección, las estructuras celulares que se obtienen son poco homogéneas y por tanto, las propiedades mecánicas resultantes son inferiores a las de materiales celulares basados en polímeros sintéticos como el XPS y el EPS habitualmente empleados en estos sectores. Por otra parte, los materiales celulares basados en polipropilenos ramificados que se han producido hasta ahora mediante procesos de espumado por extrusión presentan estructuras celulares muy pobres. Este hecho ha impedido la utilización extensiva de este material en el sector de los paneles estructurales de baja densidad en el que se requieren materiales celulares con estructuras celulares homogéneas y con celdas cerradas.

El trabajo desarrollado en esta tesis ha afrontado el desafío de desarrollar materiales celulares basados en estos polímeros con propiedades mecánicas óptimas. Para ello se han utilizado estrategias basadas en la modificación pre-espumado de las propiedades del polímero mediante el uso de partículas micro y nanométricas y se han utilizado procesos de producción a escala de laboratorio novedosos en el campo de los materiales celulares. En el caso del almidón, se ha utilizado un proceso de expansión por radiación microondas con menores consumos de energía y con transferencias de calor más homogéneas (calentamiento en volumen) que en los procesos

convencionales (extrusión y *baking*). En el caso del polipropileno, se ha utilizado un proceso de espumado desarrollado en el propio grupo de investigación (*CellMat Laboratory*) y conocido como moldeo por compresión mejorado (ICM), el cual permite obtener materiales celulares de baja densidad y con una forma definida sin la necesidad de reticular el polímero previamente. Además, se ha utilizado una metodología de trabajo basada en establecer la relación estructura celular-propiedades mecánicas, y que ha sido apoyada en el uso de modelos analíticos ampliamente utilizados en el campo de los materiales celulares. Esta metodología de trabajo ha permitido entender de forma más clara lo que ocurre en el proceso de producción y las estructuras y propiedades mecánicas finalmente obtenidas

0.2- Marco de desarrollo de la tesis dentro del grupo de investigación.

Esta tesis se ha desarrollado en el Laboratorio de Materiales Celulares (*CellMat Laboratory*) de la Universidad de Valladolid, un grupo de investigación fundado en 1999 por los profesores Jose Antonio de Saja Sáez y Miguel Ángel Rodríguez Pérez con el objetivo de desarrollar nuevo conocimiento científico en el área de los materiales celulares. En sus comienzos, el grupo estuvo centrado principalmente en establecer la relación estructura-propiedades pero a lo largo del tiempo se han establecido varias líneas de investigación relacionadas con el desarrollo de nuevos materiales celulares avanzados. Uno de los propósitos del grupo es proveer a la industria con nuevas formulaciones y procesos capaces de mejorar a los materiales celulares existentes actualmente en el mercado y al mismo tiempo, contribuir a crear nuevo conocimiento científico en relación a los mecanismos de espumado inherentes a estos procesos de fabricación y a la relación proceso-formulación-estructura-propiedades en los materiales desarrollados.

Las líneas de investigación que actualmente son abordadas por el grupo de investigación relacionadas con materiales celulares poliméricos son: materiales microcelulares, materiales nanocelulares, nanocomposites celulares y biomateriales celulares (Figura 1.9). Esta tesis se enmarca en dos de estas líneas. Concretamente en las referentes al desarrollo de ***nanocomposites celulares*** y al desarrollo de ***biomateriales celulares***.

El creciente uso de materiales celulares poliméricos en diversos sectores (envasado, construcción, automoción etc.) y la consecuente generación de enormes cantidades de residuos derivados de los mismos han repercutido en que una de las líneas de investigación que más crecimiento ha experimentado en los últimos años en *CellMat Laboratory* sea la relacionada con el desarrollo de biomateriales celulares. En este sentido, una parte muy representativa de las investigaciones realizadas por el grupo tienen relación con este tema [1-13].

Además, el grupo de investigación ha estado involucrado de forma muy intensa en el desarrollo de proyectos de investigación con financiación pública relacionados con los temas de investigación abordados en esta tesis. Por un lado, ACTIBIOPACK es un proyecto financiado por el gobierno español en la convocatoria INNPACTO de 2011 en el cual se desarrollaron formulaciones bioderivadas y biodegradables para la fabricación de bandejas de alimentación sólidas y espumadas. El proyecto fue constituido por un consorcio muy amplio con

representación de los ámbitos tanto académico como privado. Los miembros de este consorcio se recogen en la Tabla 1.1. Por otro lado, el proyecto NANCORE fue un proyecto financiado por el séptimo programa marco de la Unión Europea (FP7) y cuyo principal objetivo fue el desarrollo de paneles rígidos basados en nanocomposites microcelulares de baja densidad con propiedades similares y con un coste inferior a los que se emplean actualmente en el mercado (espuma de PVC y madera de balsa). Es por ello que una de las soluciones planteadas en el proyecto fue el uso de matrices poliméricas basadas en poliolefinas como es el caso del polipropileno ramificado que se ha empleado a lo largo de esta tesis. El proyecto fue constituido por un consorcio muy variado de instituciones públicas y privadas de distintos países de la Unión Europea como se puede ver en la Tabla 1.2.

0.3- Objetivos.

El principal objetivo de este trabajo es el desarrollo y fabricación de nuevos materiales poliméricos sólidos y celulares que sean capaces de ofrecer alternativas ambientalmente sostenibles a los materiales que actualmente se emplean en envases de alimentación, embalajes de protección y en paneles estructurales ligeros. Este será el objetivo común a todos los trabajos desarrollados en esta tesis aunque se han establecido objetivos específicos para cada uno de los polímeros estudiados: almidón y polipropileno.

0.3.1- Almidón

El uso de almidón como matriz polimérica para la producción de bandejas de alimentación y de embalajes de protección todavía requiere afrontar ciertos desafíos relacionados por un lado, con las pobres propiedades mecánicas obtenidas tras el proceso de plastificación y por otro lado, con su pobre comportamiento en espumado, lo cual repercute en la obtención de materiales celulares con estructuras celulares no homogéneas y por tanto, con pobres propiedades mecánicas.

Una de las estrategias implementadas durante esta tesis ha sido la modificación de las propiedades del polímero mediante su **refuerzo con fibras naturales**. En principio, la producción de este tipo de biocomposites debería repercutir en un incremento de las propiedades mecánicas de la matriz termoplástica de almidón de partida ya que la composición química de ambos materiales es similar (moléculas de glucosa). Sin embargo, después de realizar una exhaustiva revisión de la literatura científica relacionada (sección 2.5.2) se detectó que todavía existe un gran desconocimiento sobre como fibras naturales con tamaños micrométricos (como las empleadas en esta tesis) influyen en los mecanismos de espumado básicos y por tanto, en las estructuras celulares y propiedades mecánicas finalmente obtenidas. En cuanto al método de fabricación de las espumas, todavía existen pocos trabajos en literatura que aborden la obtención de espumas de almidón para aplicaciones no alimenticias mediante la utilización de microondas. Además, no se han encontrado estudios en los que se utilicen fibras naturales como refuerzo de la matriz de almidón en este tipo de proceso de espumado.

Teniendo en cuenta todos estos factores se han establecido varios objetivos como los que se enumeran a continuación:

1- Desarrollo de formulaciones bioderivadas y biodegradables basadas en almidón termoplástico (TPS) y optimización de los métodos de fabricación empleados a escala de laboratorio: extrusión, termoconformado y expansión por radiación microondas, necesarios para la obtención de materiales sólidos y espumados.

2- Mejora de los propiedades mecánicas de los materiales sólidos y espumados basados en TPS mediante el refuerzo con fibras naturales.

3- Estudio del efecto que las fibras naturales tienen en las propiedades mecánicas de los materiales desarrollados. En el caso de los materiales celulares el estudio abordará también cuál es el efecto que estas fibras tienen en los mecanismos básicos de formación de una estructura celular.

4- Analizar en detalle la relación estructura-propiedades mecánicas en estos materiales.

5- Describir los resultados mecánicos obtenidos mediante el empleo de modelos analíticos encontrados en literatura como es el caso del modelo de celda abierto de *Gibson* y *Ashby* [14].

6- Evaluar si los métodos de fabricación y las formulaciones desarrolladas pueden ser empleadas para la producción de bandejas de envasado alimenticio y para la producción de embalajes de protección espumados con formas definidas.

0.3.2- Polipropileno.

El uso de espumas de polipropileno en aplicaciones estructurales ha estado de alguna forma limitado hasta hoy por el pobre rendimiento de este polímero en proceso de espumado y como consecuencia, por las pobres propiedades mecánicas finalmente obtenidas. A pesar de los mejores rendimientos ofrecidos por los polipropilenos ramificados (mayor capacidad de expansión volumétrica) con respecto a polipropilenos de cadena lineal, las estructuras celulares así como las propiedades mecánicas de los materiales celulares finalmente desarrollados están todavía lejos de las estructuras y propiedades de materiales como la madera de balsa y las espumas de PVC reticuladas de celda cerrada (materiales que acaparan la mayor cuota de mercado en estas aplicaciones). En principio, el uso de nanoarcillas como partícula de refuerzo en la matriz polimérica debería suponer una solución innovadora a este problema. Sin embargo, aunque es una solución ampliamente utilizada y estudiada en literatura científica, todavía no ha dado los resultados esperados. En esta tesis se ha llevado a cabo una extensa revisión de la literatura científica relacionada con el tema (secciones 2.6.3y sección 5.3) que ha permitido detectar como todavía existe un claro desconocimiento sobre la relación proceso-estructura-propiedades de estos materiales heterogéneos (polímero-gas-nanopartícula). Este trabajo tratará de afrontar estos desafíos estableciendo los siguientes objetivos:

1- Desarrollo de formulaciones y optimización de un proceso de producción a escala de laboratorio conocido como moldeo por compresión mejorado (ICM)y que fue previamente desarrollado en *CellMat Laboratory* [15].

2- Evaluar la influencia que parámetros de producción como la presión, temperatura/tiempo y el contenido de agente espumante (claves en el proceso ICM) pueden tener en la estructura celular y por tanto, en las propiedades mecánicas de los materiales celulares desarrollados.

3- Evaluar el efecto de las nanoarcillas y de la presión externa aplicada sobre el material precursor en la estructura celular y por tanto, en las propiedades mecánicas de espumas de polipropileno de baja densidad.

4- Correlacionar las propiedades mecánicas medidas experimentales con las estructuras celulares (análisis de la relación estructura-propiedades)

5- Utilizar modelos analíticos encontrados en literatura para describir con mayor precisión el comportamiento mecánico de los materiales celulares desarrollados como el modelo de *Huber* y *Gibson* y el modelo de *Kelvin* [16,17,18].

6- Evaluar si las espumas de polipropileno finalmente obtenidas podrían reemplazar a materiales poliméricos habitualmente empleados para aplicaciones estructurales como es el caso de las espumas de PVC reticuladas de celda cerrada y espumas de PET.

0.4- Contenidos.

Esta tesis se divide en siete capítulos, de los cuales dos de ellos (4 y 5) incluyen un compendio de cuatro artículos: tres de ellos ya publicados en revistas científicas internacionales y un cuarto enviado pero aún no publicado. En el capítulo 4 se incluyen los artículos relacionados con los materiales basados en almidón mientras que en el capítulo 5 se recogen los artículos relacionados con los materiales celulares basados en polipropileno ramificado. Además, se incluye un capítulo introductorio (capítulo 1), una revisión del estado del arte y de los principales conceptos abordados durante la tesis (capítulo 2), una descripción de los materiales, procesos de fabricación y técnicas de caracterización empleados (capítulo 3), un capítulo que describe con detalle como los procesos de fabricación desarrollados a escala de laboratorio se han adaptado a la fabricación de prototipos de bandejas de envasado de alimentos y de paneles estructurales de baja densidad (capítulo 6) y finalmente, las principales conclusiones obtenidas y el trabajo futuro que se plantea a raíz de la investigación planteada en esta tesis (capítulo 7). Además, se incluye un anexo que recoge una patente elaborada a raíz del trabajo desarrollado con las espumas de polipropileno.

0.5- Publicaciones, congresos y actividades relacionadas con la tesis.

El trabajo desarrollado en esta tesis ha tenido como resultado la publicación de varios trabajos científicos en revistas internacionales y la elaboración de otros que aún no están publicados pero que se han enviado y están en proceso de revisión. La Tabla 0.1muestra una compilación detallada de los mismos. Además, se incluyen trabajos que aunque no han sido incluidos en la tesis (capítulos 4 y 5) sí que han sido elaborados en el marco de la misma.

Materiales basados en almidón.		Sección
1	**Almidón termoplástico celular reforzado con fibras naturales. Una opción bioderivada y biodegradable para el envasado de alimentos.** López-Gil, A.; Bellucci, F.S.; Ardanuy, M.; Rodríguez-Pérez, M.A.; de Saja, J.A. *Revista de plásticos modernos*. Núm. 671. Enero 2013.	-
2	**Strategies to improve the mechanical properties of starch-based materials: plasticization and natural fibres reinforcement.** López-Gil, A.; Bellucci, F.S.; Ardanuy, M.; Rodríguez-Pérez, M.A.; de Saja, J.A. *Polímeros. Ciência e Tecnologia.* vol. 24, n. Especial, 36-42. 2014.	4.2
3	**Cellular structure and mechanical properties of starch-based foamed blocks reinforced with natural fibres and produced by microwave heating.** Lopez-Gil, A.; Silva-Bellucci, F.; Velasco, D.; Ardanuy, M.; Rodriguez-Perez, M.A. *Industrial Crops and Products*. 66, 194–205. 2015.	4.3
Materiales basados en polipropileno.		**Section**
1	**Structure property relationships of medium-density polypropylene foams.** Saiz-Arroyo, C.; Rodríguez-Pérez, M.A.; Tirado, J.; López-Gil, A.; de Saja, J.A.; *Polymer International*. 62, 1324-1333. 2013.	-
2	**Production of non-crosslinked thermoplastic foams with a controlled density and a wide range of cellular structures.** Lopez-Gil,A.; Saiz-Arroyo, C.; Tirado, J.; Rodríguez-Pérez, M.A. *Journal of Applied Polymer Science*. 132, 2015.	5.2
3	**Anisotropic polypropylene foams filled with nanoclays: microstructure and properties.** Lopez-Gil, A.; Benanti, M.; Lopez-Gonzalez, E.; Ruiz-Herrero J.L.; Briatico, F.; Rodriguez-Perez, M.A. *Submitido*	5.3

Tabla 0.1. Artículos científicos.

Además, el trabajo desarrollado se ha diseminado en congresos y jornadas nacionales e internacionales como los que se muestran en la Tabla 0.2.

Materiales basados en almidón.	
1	**Mechanical properties of biocomposites based on thermoplastic starch and cellulosic fibres from agricultural residues.** Ardanuy, M.; Algaba, I.; García-Hortal, J.A.; López-Gil, A.; Rodríguez-Pérez, M.A. 4th International Textiles Congress. Estambul, Turquía. 16-18 de Mayo. 2010. *Oral.*
2	**Development of starch biobased and biodegradable plastics for their use in trays for food-packaging.**López-Gil, A.; Rodríguez-Pérez M.A.; de Saja, J.A.; Bellucci, F.S.; Ardanuy. M. EUROTEC 2011. Barcelona. España. 14-15 Noviembre 2011. *Oral.*
3	**Productos bioderivados y biodegradables de bajo coste basados en almidón. Aplicación en bandejas para alimentación.** López-Gil, A.; Rodríguez-Pérez, M.A.; de Saja, J.A.; V Jornadas de Innovación y Tecnología Alimentaria CTIC-CITA. Calahorra, España. 25 de Abril 2012. *Oral.*
4	**Development of low density starch-biobased and biodegradable plastics reinforced with natural fibres.** López-Gil, A.; Silva-Bellucci F.; Ardanuy, M.; Rodríguez-Pérez, M.A.; de Saja, J.A. XI Brazilian MRS Meeting (SBP mat). Florianópolis, Brasil. 27 de Septiembre. 2012. *Oral.*
Materiales basados en polipropileno.	
1	**Multi-level characterization of the compressive behaviour of novel cellular nanocomposites.** Shishkina, O.; Zhu, Y.; Escudero, J.; Lopez-Gil, A.; Rodriguez Perez, M.A.; Gorbatikh, L.; Lomov, S.V.; Verpoest, I. European Conference on Composite Materials. ECCM15. Venecia, Italia. 24-28 Junio 2012. *Oral.*
2	**Production of non-crosslinked polyolefin foams with controlled density and tailored cellular structure and physical properties.** Saiz-Arroyo, C.; Escudero, J.; López-Gil, A.; Rodríguez-Pérez, M.A. 10th International Conference on Foams and Foams Technology. FOAMS 2012. Barcelona, España.12-13 de Septiembre 2012. *Oral.*
3	**Nano-strategies applied to the production of cellular polymers with improved cellular structure and properties.** Rodríguez-Pérez, M.A.; Pardo-Alonso, S.; Estravis, S.; Saiz-Arroyo, C.; Solorzano-Quijano, E.; Escudero-Arconada, J.; Pinto-Sanz J.; López-Gil, A.; Rodríguez-Pérez, M.A. CellMat Conference. Dresden, Alemania. Noviembre 2012. *Key-note lecture.*
4	**Understanding the foamability of polypropylene blends and polypropylene nanocomposites by using extensional rheology.** Laguna-Gutiérrez, E.; Escudero, J.; López-Gil, A.; Rodríguez-Pérez, M.A.; AERC, 8thAnnualEuropeanRheologyConference. Lovaina, Belgica. 2-5 de Abril. 2013. *Oral.*
5	**AniCell. Low density and non-crosslinked polypropylene foams as a promising option to produce structural panels.** López-Gil, A.; Escudero, J.; Laguna-Gutierrez, E.; Saiz-Arroyo, C.; Rodríguez-Pérez, M.A.EUROTEC 2013. Lyon, Francia. 5 de Julio.2013. *Oral.*
6	**Production and cellular structure characterization of polypropylene foams: influence of the chain arquitecture, density and blowing agent.** Salmazo, L.O.; Bellucci, F.S.; López-Gil, A.; Rodríguez-Pérez, M.A.; Job, A.E.XIII. Encontro SBP Mat. João Pessoa, Brasil. 2014. *Oral.*
7	**Extensional rheology: a tool to predict the foamability of complex systems such as polymer blends and recycled polymers.** Laguna-Gutiérrez, E.; López-Gil, A.; Saiz-Arroyo, C.; Rodríguez-Pérez, M.A. FOAMS 2014. 10-11 de Septiembre. 2014. Nueva Jersey, Estados Unidos. *Oral.*

Tabla 0.2. Congresos y jornadas.

Finalmente, en la tabla0.3 se recogen las actividades adicionales desarrolladas durante la tesis, como estancias de investigación, publicación de capítulos en libros y elaboración de patentes así como trabajos desarrollados ajenos a la actividad principal de la misma, como es el caso de los trabajos desarrollados con espumas de caucho natural.

Artículos científicos y congresos.	
1	**Natural rubber foams with anisotropic cellular structures: mechanical properties and modelling.** Salmazo, L.O.; López-Gil,A.; Silva-Bellucci, F.;Job,A.E.; Rodríguez-Pérez, M.A. *Industrial Crops and Products*. *Submitido*
2	**Study of the concentration of ZnO in the production of vulcanized natural rubber foams.** Salmazo, L.O.; Bellucci, F.S.; Lopez-Gil, A.; Rodriguez-Perez, M.A.;Job, A.E. XI Encontro da SBP Mat-Brazilian MRS meeting. Florianópolis, Brazil. September 27th 2012. *Poster.*
2	**Mechanical compression tests of multifunctional vulcanized natural rubber nanocomposites.** Bellucci, F.S.; Salmazo, L.O.; Lopez-Gil, A.; Budemberg, E.R.; Nobre, M.A.L.; Rodriguez-Perez, M.A.; Job, A.E. XII Brazilian MRS Meeting -SBP Mat .2013. Campos do Jordão, Brasil. *Poster.*
3	**Cellular structure and mechanical properties of foams based on natural rubber and natural rubber/styrene butadiene rubber blends.** Salmazo, L.O.; Bellucci, F.S.; López-Gil, A.; Rodríguez-Perez, M.A.; Job, A.E.XII Brazilian MRS Meeting-SBP Mat. 2013. Campos do Jordão, Brasil. *Poster.*
4	**Estudo das propriedades morfológicas, estruturais e acústicas de espumas de borracha natural.** Salmazo, L.O.; Bellucci, F.S.; López-Gil, A.; Rodríguez-Pérez, M.A.; Job, A.E. 12 Congresso Brasileiro de Polímeros - CBPOL.2013. Florianópolis. Brasil. *Poster.*
5	**Correlation between mechanical properties and cellular structure of medium-density natural rubber foams with different anisotropy ratios.** Salmazo, L.O.; Bellucci, F.S.; López-Gil, A.; Rodriguez-Perez, M.A.; Job, A.E.XIII Encontro SBP Mat. 2014. João Pessoa, Brasil. *Poster.*
Estancias de investigación.	
1	**Universidade Estadual Paulista (UNESP).** Presidente Prudente. Brasil. Julio-Octubre de 2012.
2	**Universidade Federal do ABC(UFABC).**São Paulo. Brasil. 6-10 de Agosto de 2012.
Contribuciones en libros.	
1	**Natural Rubber Materials. Volume 2: Composites and Nanocomposites. Chapter 26:applicationsofnatural rubber composites and nanocomposites.** Job, A.E.; Cabrera, F.C.; Oliveira-Salmazo, L.; Rodriguez-Perez, M.A.; Lopez-Gil, A.; De Siqueira, A.F. and Bellucci, F.S. DOI:10.1039/9781849737654.

Patentes.	Capítulo.
1	**Method for producing cellular materials having a thermoplastic matrix.** Miguel Angel Rodríguez Pérez, José Antonio de Saja Sáez, Javier Escudero Arconada, Alberto López Gil. Número de patente:WO2014/009579 A1. 12.01.2014.	Annex

Tabla 0.3. Actividades adicionales.

0.6- Metodología de trabajo.

Esta tesis se ha desarrollado siguiendo una metodología de trabajo basada en una ***selección inicial de materias primas***, en el empleo de ***procesos de fabricación*** adecuados para los materiales seleccionados y en el uso de ***técnicas de caracterización*** capaces de contestar a los principales interrogantes abiertos al comienzo de la investigación. Estos tres tipos de actividades se detallan en los siguientes apartados:

0.6.1- Selección de materias primas.

Las materias primas seleccionadas se muestran en la tabla 0.4. Esta selección se ha realizado en función del tipo de matriz polimérica empleada: almidón y polipropileno.

Polímero	Plastificante	Espumante	Carga inorgánica	Compatibilizante	Sección
Almidón de patata	Glicerol	-	Fibras de paja de cebada y fibras de uva	-	4.2
Almidón de trigo (MERITENA 200)	Agua	Agua	Fibras de paja de cebada, fibras de uva y fibras de cardo	-	4.3
Polipropileno copolímero *random* (PP 200 CA10/Inneos)	-	Azodicarbonamida (LANXESS POROFOR MC-1)	-		5.2
Polipropileno ramificado homopolímero (PP Daploy WB135 HMS/Borealis)	-	Azodicarbonamida (POROFOR MC-1/Lanxess)	Nanoarcillas (CLOISITE C20-A/Southern Clay products)	Polipropileno modificado con anhídrido maleico (POLYBOND 3200/Chemtura)	5.3

Tabla 0.4. Materias primas

En el caso del almidón se utilizan dos tipos de plastificantes dependiendo del tipo de material que se quiere obtener finalmente. En el caso de fabricar materiales sólidos (sección 4.2) se utiliza glicerol ya que es un agente plastificante con una temperatura de volatilización alta (290ºC) y por tanto es estable (no volatiliza) durante el procesado del material. En el caso de fabricar materiales celulares (sección 4.3) se utiliza como agente plastificante agua ya que al mismo tiempo actúa como el agente espumante del proceso. La volatilización del agua durante la aplicación de la radiación microondas permite expandir la matriz polimérica y al mismo tiempo estabilizar la estructura celular por secado de la matriz polimérica. En el agua empleada para plastificar el almidón se disuelve una determinada cantidad de NaCl que actúa como potenciador de la absorción de radiación microondas. Además, se han utilizado tres tipos de fibras naturales obtenidas de residuos de la industria agrícola: fibras de paja de cebada, fibras de uva y fibras de cardo. Las fibras de paja de cebada fueron sometidas a tratamientos químicos adicionales con el objetivo de aislar su fracción celulósica (hidrolisis con agua caliente seguida de un tratamiento con una solución alcalina). Se han seleccionado estos tres tipos de fibras naturales porque presentan composiciones químicas diferentes entre ellas pero muy parecidas a la matriz polimérica de almidón y porque además, presentan morfologías muy diferente como se puede ver en la Figura 3.2. Este último factor puede repercutir en obtener biocomposites sólidos y celulares con propiedades mecánicas muy variadas por lo que constituye uno de los temas de estudio de esta tesis y que se desarrolla de forma extensa en el capítulo 4.

En el caso del polipropileno se utiliza una matriz ramificada (sección 5.3) por las razones expuestas anteriormente (mayor resistencia en fundido y por tanto, mayor capacidad de expansión volumétrica) pero además, se utiliza un copolímero *random* debido a que su resistencia en fundido es inferior y ha permitido estudiar como los parámetros de proceso en la ruta ICM afectan a las estructuras celulares y por tanto a las propiedades mecánicas de estos tipos de materiales celulares (sección 5.2). En ambos casos se ha utilizado azodicarbonamida como agente espumante por dos razones: primero porque descompone a temperaturas suficientemente altas (210ºC) como para fabricar un *compound* polipropileno-agente espumante suficientemente homogéneo mediante mezclado en fundido (extrusión) antes del proceso de

expansión. Segundo, porque es un agente espumante con un alto rendimiento en generación de gases (228 ml/g medidos a 210ºC) lo que permite la obtención de espumas con altos ratios de expansión. Como partícula de refuerzo se han utilizado nanoarcillas modificadas con sales cuaternarias de amonio ya que en primer lugar, son las que presentan un coste más bajo de entre las nanopartículas comerciales que actualmente se pueden encontrar en el mercado (nanotubos de carbono, nanofibras de carbona, etc.) y en segundo lugar porque la modificación química con sales cuaternarias de amonio (junto con el empleo de un agente compatibilizante basado en polipropileno modificado con anhídrido maleico) permite obtener una adecuada adhesión, exfoliación y distribución de la mismas a lo largo de la matriz polimérica.

0.6.2- Procesos de fabricación.

Se han utilizado varias rutas de fabricación en función de la matriz polimérica empleada y en función del tipo de material a desarrollar: sólido o espuma. Los métodos de fabricación empleados son los que se enumeran en la Tabla 0.5.

Método	Material	Equipo	Objetivo	Sección
Mezclado en fundido	Sólido	• Extrusora de doble husillo • Mezclador interno	Producción de biocomposites basados en almidón y fibras naturales	4.2 y 4.3
			Producción de nanocomposites basados en polipropileno y nanoarcillas	5.3
Termo-conformado	Sólido	• Prensa hidráulica de platos calientes • Moldes de aluminio y de acero inoxidable	Probetas para ensayos mecánicos	4.2
			Fabricación de precursores sólidos	4.2 y 5.2
			Fabricación de prototipos de bandejas de alimentación	6.2.1
Espumado mediante radiación microondas	Celular	• Horno microondas • Molde de teflón	Fabricación de espumas biodegradables basadas en almidón	4.3
Espumado mediante ICM	Celular	• Prensa hidráulica de platos calientes • Molde auto-expandible	Fabricación de espumas rígidas no reticuladas basadas en polipropileno	5.2 y 5.3

Tabla 0.5. Procesos de producción

En el caso de los materiales sólidos se han empleado procesos de mezclado en fundido (extrusora de doble husillo y mezclador interno) para poder incorporar de una forma homogénea tanto las fibras naturales (en el caso de los materiales basados en almidón) como las nanoarcillas (en el caso de los materiales basados en polipropileno). Además, se han utilizado prensas hidráulicas de platos calientes para poder termoconformar los biocomposites y de este modo fabricar probetas para ensayos mecánicos de tracción (sección 4.2) y compresión (sección 4.3). Este proceso de termoconformado también ha sido empleado para la fabricación de precursores sólidos cilíndricos basados en almidón previos al proceso de expansión por radiación microondas (sección 4.3), precursores sólidos basados en polipropileno previos al proceso de

espumado por ICM (sección 5.2)y además, para la fabricación de prototipos de bandejas de alimentación mediante el empleo de un molde especialmente diseñado para tal propósito (sección 6.2.1).

En el caso de los materiales celulares se han empleado métodos de fabricación novedosos en este campo como son el proceso de ***expansión por radiación microondas*** (materiales celulares basados en almidón) y el ***moldeo por compresión mejorado*** (materiales celulares basados en polipropileno).

0.6.2.1- Espumado por radiación microondas.

El proceso de espumado por radiación microondas de los materiales basados en almidón se puede dividir en tres etapas. En primer lugar, se produce el calentamiento del material por la interacción de las microondas con las moléculas de agua que inicialmente plastifican el almidón. En segundo lugar, las celdas nuclean y crecen debido a la generación de vapor de agua y en tercer lugar se produce la estabilización de la estructura celular por secado de la matriz polimérica. Este proceso se ilustra de forma esquemática en la Figura 2.37.

Este proceso ofrece muchas ventajas en materiales como el almidón plastificado con agua ya que en primer lugar, permite un calentamiento homogéneo de la matriz polimérica debido a que las moléculas de agua, que son las que interaccionan con la radiación microondas, se encuentran distribuidas en todo el volumen del precursor sólido. Por tanto se trata de un calentamiento volumétrico que es más homogéneo y rápido que el obtenido en procesos convencionales de calentamiento superficial (por conducción desde la superficie hasta el interior del material). En segundo lugar, el agente espumante empleado es agua y por tanto, no es necesario el uso de agente espumantes químicos o físicos que aumentarían de forma considerable el coste final del material.

El proceso se realizó en un horno microondas convencional y mediante el empleo de un molde de teflón (PTFE) especialmente mecanizado para la obtención de bloques espumados cilíndricos continuos (Figura 3.18). El empleo de moldes de teflón es importante por varias razones. En primer lugar, porque es un material que no absorbe la radiación microondas y por tanto, toda la energía del proceso es invertida en el calentamiento y expansión del precursor sólido de almidón. En segundo lugar, porque es un material que aguanta las temperaturas generadas durante el proceso en el material expandible y que se transmite por conducción a las paredes del molde. Por último, porque el almidón no se pega a las paredes del molde lo que permite que las espumas finalmente obtenidas se extraigan muy fácilmente.

0.6.2.2. Espumado mediante moldeo por compresión mejorado (ICM).

El moldeo por compresión mejorado (ICM) es un proceso de espumado que ha sido desarrollado por el propio grupo de investigación (*CellMat Laboratory*), y que ha sido empleado previamente en numerosos trabajos de investigación publicados por el grupo [19-26]. Su principal peculiaridad es el empleo de un molde auto-expandible que permite la generación de materiales celulares

con densidad constante y con distintas estructuras celulares mediante la modificación de parámetros de proceso (presión, temperatura, contenido de agente espumante etc.). Esto se debe en primer lugar, a que el molde permite el desplazamiento libre del pistón (en una única dirección) durante el proceso de expansión de la espuma y en segundo lugar, a que se diseñó un sistema de retención de la expansión. El ratio final de expansión de la espuma se puede alterar mediante el empleo de anillos exteriores(sobre los que se asienta el sistema de retención) con diferentes alturas. Las distintas partes de las que consta el proceso, el molde auto-expandible y sus diferentes componentes y un esquema del proceso de fabricación de la espuma se pueden ver en la Figura 3.24.

El proceso se puede dividir en tres etapas. En primer lugar, el material precursor (en forma de pellets o lámina termoconformada) con el agente espumante químico incorporado (en este caso azodicarbonamida) se introduce en la cavidad del molde. En segundo lugar, y tras el cerrado del molde, se aplica presión externa sobre el material precursor a través de un pistón y mediante el empleo de una prensa hidráulica de platos calientes. La temperatura de los platos de la prensa se sitúa por encima de la temperatura de descomposición del agente espumante. En tercer lugar, tras la fusión del polímero y la descomposición total del agente espumante se libera la presión ejercida por los platos de la prensa de tal manera que el gas inicialmente disuelto en el polímero forma celdas. Las celdas formadas crecen y provocan la expansión del polímero hasta el límite impuesto por el sistema de retención del molde auto-expandible. Por último, la estructura celular se estabiliza mediante enfriamiento del molde con la espuma en su interior en un baño de agua fría.

La principal ventaja del proceso ICM con respecto a procesos discontinuos convencionales de fabricación de espumas basadas en poliolefinas (como el moldeo por compresión en dos etapas [27]) es que es posible generar espumas de baja densidad y con forma definida sin el empleo de agentes reticulantes químicos. El molde es perfectamente estanco a la entrada de líquidos tras el proceso de expansión de la espuma lo cual permite la estabilización rápida de la estructura celular mediante enfriamientos con agua y por tanto, la formación de espumas con la forma de la cavidad del molde. Además, la expansión del polímero solo se puede producir de forma unidireccional lo que promueve la formación de estructuras celulares anisotropicas y por tanto con propiedades mecánicas diferentes en función de la dirección en la que se miden. Estas estructuras anisotrópicas se evalúan con detalle en el artículo incluido en la sección 5.3

0.6.3- Métodos de caracterización.

Las técnicas de caracterización que se han empleado en este trabajo se enumeran en la Tabla 0.6. En los capítulos 4 y 5 se ofrece una explicación más detallada de las mismas y de los resultados obtenidos con ellas que han permitido establecer relaciones entre las estructuras de los materiales desarrollados y sus propiedades mecánicas.

Técnicas de caracterización		Capítulos
Ensayos mecánicos a bajas velocidades de deformación Máquina de ensayos**.** Universal INSTRON modelo 5500R625.	Ensayos de compresión (ISO 604-2002)	4,5
	Ensayos de tracción (ISO 527).	4,5
	Ensayos de flexión (ISO 178).	5
Morfología de los gránulos de almidón, de los biocomposites sólidos basados en almidón termoplástico y de las estructuras celulares mediante microscopía electrónica de barrido (SEM) Microscopio electrónico de barrido JEOL modelo JSM-820.		4,5
Morfología de las fibras naturales mediante microscopía óptica Microscopio óptico LEICA modelo DM2500M.		4
Medida de densidad mediante el método volumétrico (ASTM D1622-08) Balanza de precisión METTLER modelo Toledo AT261.		4,5
Medida del contenido de celda abierta mediante picnometría de gases(ASTM D6226-10). Picnómetro de gases MICROMERITICS modelo AccuPyc II 1340		4,5
Evaluación de las propiedades térmicas de los polímeros y de los agentes espumantes empleados mediante análisis termogravimétrico (TGA) TGA/SDTA METTLER modelo 851e		4,5

Tabla 0.6. Técnicas de caracterización.

0.7- Principales resultados y conclusiones.

El principal objetivo establecido al comienzo de esta tesis se ha cumplido satisfactoriamente ya que se han desarrollado materiales sólidos y celulares medioambientalmente sostenibles gracias al empleo de matrices poliméricas bioderivadas y biodegradables como el almidón y de matrices poliméricas no reticuladas como el polipropileno ramificado. Los materiales desarrollados tienen un alto potencial para ser empleados en el sector de los envases de alimentos y embalaje de protección (almidón) y en el sector de los paneles estructurales ligeros (polipropileno). Los resultados específicos de la tesis se han dividido en dos secciones en función de la matriz polimérica empleada: almidón y polipropileno.

0.7.1- Almidón.

Para este tipo de matriz polimérica se han desarrollado dos tipos de formulaciones: las primeras para la fabricación de materiales sólidos flexibles capaces de sustituir a polímeros derivados del petróleo como el PP y el PET en aplicaciones de envasado de alimentos y las segundas para la fabricación de materiales celulares rígidos que se pueden emplear en aplicaciones de embalaje de protección sustituyendo al EPS.

En el caso particular de la investigación llevada a cabo con materiales sólidos flexibles basados en almidón (sección 4.2) los principales resultados obtenidos son:

- Se ha desarrollado un proceso de producción a escala de laboratorio que consiste en dos etapas: extrusión y termoconformado, para la producción de formulaciones basadas en almidón termoplástico (TPS) reforzado con fibras naturales.

- Se han producido y caracterizado varios tipos de formulaciones con el objetivo de estudiar el efecto del contenido de agente plastificante (glicerol) y el tipo y cantidad de fibras naturales empleadas como refuerzo (fibras de paja de cebada y fibras de orujo de uva).

- El rango de concentraciones de glicerol estudiado (20-30 wt%) ha hecho posible la obtención de formulaciones con propiedades mecánicas muy variadas. Por un lado, las formulaciones con un 20 wt% de glicerol se caracterizan por presentar alta rigidez y poca flexibilidad (modulo elástico>1600MPa; deformación a rotura< 5%). Por otro lado, las formulaciones con un 30 wt% de glicerol resultan en materiales muy flexibles (deformación a rotura>120%).

- Dos tipos de refuerzos naturales (fibras de paja de cebada y fibras de orujo de uva) fueron seleccionados para actuar como cargas en la matriz termoplástica de almidón debido a su diferente morfología. Los residuos de paja de cebada presentan una geometría fibrosa con elevadas relaciones de aspecto mientras que los residuos de uva presentan una geometría más irregular por lo que se les puede considerar como partículas sin forma definida.

- La adicción de estos refuerzos naturales supuso la obtención de biocomposites basados en TPS con importantes alteraciones estructurales con respecto a la matriz polimérica pura. Mediante imágenes de SEM ha sido posible observar como los dos tipos de fibras se distribuyen de forma homogénea a lo largo de la matriz polimérica lo que sugiere que las condiciones de fabricación fueron seleccionados de forma adecuada. Por el contrario, el grado de adhesión a la matriz varía en función del refuerzo considerado. En el caso de los residuos de uva se puede observar interfaces entre la matriz polimérica y las partículas mientras que las fibras de paja de cebada parecen adherirse de forma más íntima a la matriz. Esto puede ser debido a sus diferentes composiciones químicas (las fibras de paja de cebada fueron sometidas a tratamientos químicos para aislar su fracción celulósica).

- El uso de fibras de paja de cebada supuso la obtención de materiales sólidos con mejores propiedades mecánicas en tracción (rigidez y resistencia). El módulo elástico se incrementó más de 3 veces mientras que la resistencia a tracción 2.5 veces con respecto a la matriz pura. Por el contrario, la incorporación de partículas naturales basadas en residuos de uva no produjo resultados satisfactorios ya que no se registraron incrementos significativos en estas propiedades. Este resultado pudo ser debido a la presencia de interfases entre la partícula y la matriz y por tanto a un bajo grado de adhesión.

- Se emplearon varios modelos analíticos ampliamente conocidos en literatura para describir las propiedades mecánicas de los biocomposites sólidos desarrollados. En el caso del modelo de *Halpin* y *Tsai* las predicciones teóricas se ajustan bastante bien a los resultados experimentales obtenidos con los biocomposites basados en fibras de paja de cebada.

En el caso de la investigación realizada con materiales celulares rígidos basados en almidón reforzado con fibras naturales (sección 4.3) los principales resultados y conclusiones son los siguientes:

- Se ha desarrollado un método de fabricación a escala de laboratorio basado en el empleo de radiación microondas para la obtención de bloques espumados cohesionados de almidón. Este método se diferencia de los encontrados en literatura en que se parte como material precursor de un lámina termoconformada en vez de pellets lo que permite la obtención de bloques perfectamente cohesionados y con mejores propiedades mecánicas en cuanto a rigidez y resistencia.

- Se han producido y estudiado varias formulaciones basadas en almidón plastificado con agua y reforzado con distintos tipos de fibras naturales provenientes de residuos de la industria agrícola: paja de cebada, uva y cardo.

- En este caso se ha utilizado agua como plastificante porque actúa al mismo tiempo como el agente espumante en el proceso de espumado por radiación microondas. La menor temperatura de ebullición del agua (100 ºC) con respecto a la del glicerol (290 ºC) hizo necesario el empleo de temperaturas más bajas tanto en la extrusora como en la prensa hidráulica para evitar perder agua (por volatilización) previamente al proceso de espumado.

- Los tres tipos de biocomposites desarrollados se produjeron con la misma cantidad de fibras naturales (5 wt%) por lo que el objetivo en este caso fue determinar qué tipo de fibra natural es la que aportaba un mayor grado de refuerzo en la matriz polimérica tras el proceso de espumado. La morfología de las fibras fue evaluada de forma cualitativa mediante imágenes de microscopía óptica. Además, se cuantificaron ciertos parámetros morfológicos como la relación de aspecto (longitud/anchura) y el tamaño promedio (área) mediante análisis de imagen. Los resultados obtenidos muestran como las fibras de paja de cebada presentan relaciones de aspecto muy altas con valores cercanos incluso a 10. Por otro lado las partículas de residuos de uva presentan tamaños considerablemente mayores (en su mayoría por encima de4000 μm^2) que el resto de refuerzos aunque en todos los casos, la distribución de tamaños es muy ancha.

- La inclusión de refuerzos naturales produjo una ligera disminución de la capacidad de expansión del polímero que fue más acusada en el caso de las fibras de paja de cebada. En este caso, la densidad del biocomposite celular obtenido fue de 347 Kg/m^3 mientras que la de la espuma sin reforzar fue de 292 kg/m^3.

- Las estructuras celulares obtenidas son en general muy poco homogéneas lo que se comprueba mediante las distribuciones de tamaño de celda que son todas muy anchas (celdas con tamaños entre 100 y 1600 µm). Además, las espumas obtenidas presentan elevados grados de interconectividad entre celdas, factor que se cuantifico mediante medidas de picnometría de gases y en las que se observó como todas las espumas presentan altos contenidos de celda abierta (>95%). Debido a las pequeñas diferencias encontradas con los ratios de expansión alcanzados por cada espuma, el tamaño de celda promedio fue normalizado frente a la densidad de la espuma correspondiente con el objetivo de evitar la influencia de este parámetro en el análisis de las estructuras celulares obtenidas. Los valores

obtenidos muestran como las partículas de uva no alteran de forma significativa las estructuras celulares en cuanto al tamaño de celda promedio. Sin embargo, el resto de fibras han producido reducciones ostensibles del tamaño de celda lo que ha podido ser debido a fenómenos de nucleación heterogénea causados por las partículas de menor tamaño (mayor área superficial en contacto con el gas disuelto en el polímero y por tanto un mayor número de centros activos para la formación de núcleos).

- El comportamiento mecánico de las espumas producidas fue evaluado mediante ensayos de compresión. Los resultados obtenidos dentro de la región elástica lineal (módulo y resistencia a compresión) mostraron como en general todos los refuerzos naturales empleados mejoran la resistencia a compresión de las espumas. Sin embargo, solamente los residuos de uva incrementaron los valores del módulo de compresión (normalizados frente a la densidad). Este resultado puede tener relación con el hecho de que estas partículas fueron las únicas que no produjeron modificaciones apreciables de la estructura celular. Por otro lado, la capacidad de absorción de energía (W) de estas espumas se incrementa considerablemente cuando se añaden fibras en general, pero este incremento es más drástico con las fibras de paja de cebada pasando de valores de 1.91 MJ/m^3 para la espuma sin refuerzo a valores de 4.54 MJ/m^3 para la espuma con refuerzo.

- El mecanismo de estabilización de la estructura celular en estas espumas es promovido por un secado gradual de la matriz polimérica durante el proceso de expansión. Las propiedades de la matriz en las aristas y paredes de celda sufren una importante evolución de tal manera que el proceso comienza con un precursor sólido flexible y acaba con un material celular rígido. El módulo de compresión de las espumas obtenidas es incluso mayor que el de los sólidos de partida. En este caso concreto, el modelo analítico de *Gibson* y *Ashby* permitió únicamente predecir las propiedades del material sólido en las paredes y aristas de las celdas mediante la introducción en la ecuación que describe el modelo de los valores correspondientes de la espuma (densidad y módulo de compresión).

- La producción de bloques espumados continuos a partir de precursores sólidos basados en láminas termoconformadas permitió obtener materiales celulares basados en almidón con mejores propiedades en cuanto a rigidez y resistencia que los encontrados hasta el momento en literatura, los cuales parten de pellets como material precursor.

Los métodos de producción utilizados para la producción tanto de materiales sólidos como celulares basados en almidón, fueron optimizados para la producción de prototipos de bandejas de envasado de alimentos. Los principales resultados y conclusiones obtenidas en esta parte de la tesis son:

- Las formulaciones desarrolladas en etapas previas de la investigación (sección 4.2) permitieron la producción de prototipos de bandejas sólidas flexibles para envasado de alimentos (sección 6.2.1). Estas bandejas fueron testadas en condiciones de envasado reales (envasado de champiñón) en el marco del proyecto ACTIBIOPACK con resultados muy

satisfactorios. Además, el método de producción empleado es muy parecido al que habitualmente se emplea en la industria porque consiste de un proceso de extrusión seguido de un proceso de termoconformado. Por tanto, es posible afirmar que las formulaciones desarrolladas podrían ser utilizadas en procesos de producción industriales.

- Se produjeron también prototipos de bandejas espumadas de envasado de alimentos (sección 6.2.2) mediante el mismo proceso de expansión por radiación microondas empleado para la producción de bloques cilíndricos (sección 4.3). Sin embargo, las propiedades de estas bandejas (alta fragilidad) impedirían su uso en el mercado del envasado de alimentos donde se requieren productos con una mayor flexibilidad. Por el contrario, la producción de estas bandejas permitió demostrar que mediante este proceso de espumado es posible obtener espumas con formas definidas con alto potencial de aplicación en el mercado de los embalajes de protección ligeros (como los empleados para la protección de electrodomésticos).

- Se realizó una evaluación económica de las formulaciones desarrolladas en la tesis y aplicadas para la producción de bandejas (sección 6.2.3) que mostró de forma clara como estos materiales presentan costes competitivos frente a los polímeros derivados del petróleo que se emplean habitualmente en este sector como el PET y el PP. Este hecho representa un avance significativo en esta aplicación ya que hasta ahora el uso de biopolímeros estaba limitado por sus elevados precios.

- La capacidad de biodegradación del almidón no fue afectada de forma considerable tras la incorporación de plastificantes, refuerzos naturales y ayudantes de proceso, hecho que fue confirmado mediante ensayos de biodegradabilidad de formulaciones representativas desarrolladas durante la tesis (sección 6.2.4).

0.7.2- Polipropileno.

La investigación llevada a cabo en esta tesis ha permitido desarrollar paneles celulares rígidos no reticulados basados en polipropileno mediante la ruta ICM y en un amplio rango de densidades (desde 200 kg/m^3 hasta 600 kg/m^3). Este tipo de materiales celulares presentan un gran potencial para reemplazar a los materiales que actualmente se utilizan en este mercado y que están basados en polímeros reticulados como las espumas de PVC (no se pueden reciclar por técnicas de mezclado en fundido) y madera de balsa (material natural con propiedades no siempre reproducibles).

Los principales resultados y conclusiones obtenidos se van a presentar siguiendo la misma estructura del capítulo 5 de la tesis. Por tanto, en primer lugar se presentan los resultados y conclusiones obtenidos con la investigación desarrollada con espumas de media-alta densidad (densidad relativa>0.2) y que se encuentra en la sección 5.2

- El proceso ICM se ha optimizado satisfactoriamente para la producción de materiales celulares basados en PP de media-alta densidad. El proceso de optimización se centró

fundamentalmente en ajustar parámetros de proceso como la presión, la temperatura y el tiempo de espumado y en ajustar las formulaciones en base al contenido de agente espumante empleado.

- Se han obtenido materiales celulares con estructuras celulares muy variadas en cuanto al contenido de celda abierta y al tamaño de celda pero manteniendo constante el ratio de expansión del material. Esto ha sido posible principalmente por la variación del contenido de agente espumante en las formulaciones. Al mismo tiempo se ha estudiado el efecto del ratio de expansión final en la estructura celular. Estos estudios fueron posibles gracias a que el proceso ICM permite controlar de forma independiente la estructura celular y la densidad de los materiales celulares desarrollados mediante la utilización de un molde auto expandible con un sistema de retención de la expansión basado en la utilización de anillos exteriores con distintas alturas.

- El empleo de altas presiones externas y altos contenidos de agente espumante (15 wt%) resultó en la obtención de materiales celulares muy homogéneos (distribuciones de tamaño de celda estrechas), con altas densidades de población de celdas y por tanto, con tamaños de celda promedio muy bajos (Φ<100µm).

- Se ha demostrado que el contenido de celda abierta es un parámetro estructural que depende, en este tipo de materiales celulares basados en PP, tanto del ratio de expansión (ER) alcanzado como del contenido de agente espumante. Cuanto mayor es el ratio de expansión de la espuma mayor es también el contenido de celda abierta. Por ejemplo, las espumas producidas con un ER=3 presentaron valores del contenido de celda abierta muy altos (OC≅60%) con independencia del contenido de agente espumante empleado. Sin embargo, cuando se consideran ratios de expansión más bajos (ER=1.6) el contenido de agente espumante comienza a jugar un papel más determinante. En este caso, el grado de interconectividad de las espumas disminuyo de forma gradual con el contenido de agente espumante e incluso se obtuvieron materiales celulares de celda cerrada para contenidos de agente espumante del 1 wt%.

- Se midió el módulo elástico de los materiales celulares desarrollados mediante diferentes ensayos mecánicos: compresión, tracción y flexión, y los resultados obtenidos se analizaron mediante el modelo de *Gibson* y *Ashby* (exponente n). En el caso de los ensayos de tracción todos los materiales celulares siguen la misma tendencia con un exponente n=2. Sin embargo, cuando se consideran ensayos de compresión y flexión, la tendencia se sitúa entre n=1 y n=2 lo que puede ser debido a que la respuesta mecánica de estos materiales en estas configuraciones de carga es más sensible a cambios en la estructura celular. Este resultado confirma que el contenido de celda abierta (bajos contenidos de agente espumante) es un parámetro estructural que juega un papel más determinante que el tamaño de celda a la hora de definir la respuesta mecánica de materiales celulares basados en PP.

- La resistencia a colapso de los distintos materiales celulares desarrollados también se midió bajo distintas configuraciones de carga: compresión, tracción y flexión. En este caso, la mejor respuesta mecánica se obtuvo ante cargas de flexión ya que los valores del exponente n fueron todos cercanos a 1. Sin embargo, no se ha podido obtener una relación clara entre las estructuras celulares y los valores de resistencia a colapso. Este parámetro mecánico parece que depende en mayor medida del ratio de expansión de la espuma que de la estructura celular.

En el caso de los materiales celulares de baja densidad (densidades relativas < 0.2) que se han desarrollado en el marco del trabajo descrito en la sección 5.3 se han obtenido los siguientes resultados y conclusiones:

- El empleo de polipropilenos ramificados de alta resistencia en fundido y la ruta ICM han permitido la obtención de materiales celulares de baja densidad, con una forma definida y con estructuras celulares más homogéneas que las obtenidas hasta ahora por métodos de espumado por extrusión. Además, el material obtenido es completamente reciclable mediante métodos de mezclado en fundido por lo que se trata de un producto medioambientalmente más sostenible que los que actualmente se utilizan en el mercado de los paneles estructurales ligeros (espumas de PVC).

- Las estructuras celulares obtenidas se caracterizaron por presentar celdas alongadas en una única dirección como consecuencia de la restricción de la expansión del polímero dentro de la cavidad del molde. Este hecho repercutió en que las propiedades mecánicas del material celular resultante fuesen dependientes de la dirección de medida.

- El uso de nanoarcillas como refuerzo de la matriz polimérica indujo importantes alteraciones en las estructuras celulares obtenidas. Por ejemplo, se obtuvieron estructuras bimodales caracterizadas por la presencia de un pequeño grupo de celdas grandes y orientadas en la dirección de expansión de la espuma (celdas anisotrópicas) y un elevado número de celdas pequeñas e isotrópicas rodeando a las celdas grandes. Se han encontrado dos posibles razones que explican la obtención de este tipo de estructuras. En primer lugar, el posible efecto catalítico que las nanoarcillas tienen sobre la descomposición del agente espumante y en segundo lugar, la posible separación en dos etapas del proceso de nucleación de celdas.

- El posible efecto catalítico de las nanoarcillas sobre la descomposición de la azodicarbonamida (ADC) fue evaluado mediante análisis termogravimétrico (TGA). Las curvas de pérdida de masa registradas permitieron observar como la temperatura de descomposición de la ADC (onset de descomposición) disminuye desde 217,5 hasta 197,7 ºC. tras añadir nanoarcillas. Como el proceso de transferencia térmica en ambos tipos de materiales (espumas puras y espumas reforzadas con nanoarcillas) es el mismo, la cantidad de gas generado en los materiales con nanoarcillas es mayor por lo que estas espumas son más sensibles a los cambios de presión externa ejercidos.

- El empleo de bajas presiones externas en el proceso de espumado (<4MPa) y las altas cantidades de gas generadas tras añadir nanoarcillas han inducido la aparición de fenómenos de nucleación en dos etapas, que es otra de las causas por las que se forman las estructuras bimodales mencionadas anteriormente. Según esta teoría, las celdas grandes anisotrópicas se forman durante el tiempo en el que se retiene la expansión del polímero mediante presión externa (el polímero no es capaz de disolver el gas generado por la descomposición del agente espumante), mientras que las celdas pequeñas isotrópicas se forman en una segunda etapa tras liberar la presión ejercida sobre el molde. Las celdas formadas durante la primera etapa tienen más tiempo y espacio para crecer por lo que se forman celdas grandes y alongadas en la dirección de expansión.

- La presencia de nanoarcillas induce otro cambio estructural importante en las espumas de PP desarrolladas ya que aumenta de forma considerable el grado de interconexión entre las celdas. Este hecho fue observado de forma cualitativa mediante imágenes de SEM y de forma cuantitativa mediante picnometría de gases. Las espumas con nanoarcillas presentan contenidos de celda abierta (OC) superiores al 50% y en la mayor parte de los casos cercanos al 100% mientras que las espumas sin refuerzo presentan valores de OC inferiores al 35%. Estos resultados fueron posiblemente debidos al hecho de que las nanoarcillas modifican el comportamiento reológico del polímero durante el proceso de expansión de tal manera que su resistencia en fundido disminuye considerablemente. Cuando se alcanzan altos ratios de expansión las paredes con nanoarcillas son más susceptibles a sufrir roturas por las altas presiones ejercidas por los gases del agente espumante. Esto da lugar a materiales celulares con altos contenidos de celda abierta como los obtenidos en este trabajo.

- En esta tesis se ha establecido una nueva metodología para cuantificar el ratio de anisotropía (*R*)de las estructuras celulares obtenidas. Esta metodología surge de la clara relación que se estableció entre el grado de anisotropía y el tamaño de las celdas y que deriva de las estructuras bimodales obtenidas. En esta metodología, el ratio de anisotropía promedio de las celdas (medido como la relación entra la longitud de las celdas en la dirección de expansión y la longitud en la dirección perpendicular) se ponderó en relación al área de cada celda. Por tanto, se obtiene un nuevo ratio de anisotropía (R_w) que explica mejor los diferentes comportamientos mecánicos obtenidos.

- El módulo elástico de los materiales celulares desarrollados se evaluó mediante ensayos de compresión en los que la carga fue aplicada en la dirección de expansión. De entre los materiales reforzados con nanoarcillas, los que presentaron una mejor respuesta mecánica fueron precisamente aquellos producidos con bajas presiones externas (0.5 y 1.5 MPa) y por tanto, caracterizados por tener estructuras bimodales. Además, en las espumas con nanoarcillas se obtuvieron módulos mayores que en las espumas puras respectivas por lo que se puede concluir que las nanoarcillas están realmente reforzando las propiedades del polímero en las paredes y aristas de las celdas.

Con el objetivo de analizar con más detalle las propiedades mecánicas obtenidas experimentalmente se han utilizado modelos analíticos que describen el comportamiento mecánico de espumas anisotrópicas, como es el caso del modelo de celda prismática de *Huber* y *Gibson* y el modelo de celda tetradecaedrica de *Kelvin*. Estos modelos se ajustan bastante bien a los valores obtenidos experimentalmente cuando los valores de R_w se encuentran por debajo de 1.6. Sin embargo, cuando se consideran las espumas con valores de R_w mayores que 1.6 se empiezan a producir claros desajustes. Esto puede ser debido a la falta de homogeneidad de las estructuras con altos valores de R_w que son precisamente las espumas con estructuras bimodales. Este tipo de estructuras no cumplen con dos principios básicos de los modelos empleados como son: periodicidad de la estructura y celdas sin paredes (estructuras de celda abierta).

Las propiedades de los materiales celulares basados en PP obtenidos durante el desarrollo de esta tesis fueron muy prometedoras. Este hecho hizo pensar en su posible escalado a nivel industrial. Es por ello que la sección 6.3 se centró en evaluar las posibilidades de escalado de estos materiales. Los principales resultados y conclusiones obtenidos tras esta sección se muestran a continuación:

- El primer obstáculo que pueden presentar estos materiales a la hora de dar el salto a la escala industrial es por un lado, incrementar el tamaño de los paneles y por otro lado, cambiar su forma (en la tesis se han producido en forma de discos). En la industria, es habitual producir estos paneles con formas rectangulares de una gran superficie. Es por ello que se diseñó un nuevo molde con sección cuadrada y con mayor tamaño que los empleados en el capítulo 5 pero capaz de ser utilizado en la prensa hidráulica disponible en el laboratorio. Los resultados fueron bastante satisfactorios ya que se obtuvieron paneles prismáticos y de mayor tamaño con lo que se demostró que tanto el proceso (ICM) como las formulaciones desarrolladas son capaces de emplearse en equipos industriales.

- Las estructuras celulares obtenidas en las espumas desarrolladas así como sus altas prestaciones mecánicas en cuanto a rigidez y resistencia hacen de este tipo de materiales celulares un sustituto muy prometedor a los que habitualmente se emplean en el mercado de los paneles estructurales ligeros. Para demostrarlo se realizó un estudio comparando los módulos de compresión de las espumas de PP desarrolladas y los módulos de espumas de PVC reticuladas y de espumas de PET, materiales de uso habitual en esta aplicación (Figura 6.28).

- A las espumas desarrolladas en esta tesis en el marco del proyecto NANCORE se las denominó como ANICELL CC (espumas de celda cerrada) y ANICELL OC (espumas reforzadas con nanoarcillas de celda abierta). Además, los resultados obtenidos y el conocimiento generado se protegieron con una patente denominada "*Method for producing cellular materials having a thermoplastic matrix*" y que está incluido en un anexo de este tesis.

Referencias

[1] Saiz-Arroyo, C.; de Saja, J.A. and Rodríguez-Pérez. M.A. Production and characterization of crosslinked low-density polyethylene foams using waste of foams with the same composition. *Polymer Engineering and Science*. 52, 751-759. 2012.

[2] Obeso, C.G.; Song, W.; Rodríguez-Pérez, M.A. and Mano, J.F. Superhydrophobic to superhydrophylic biomimetic poly(3-Hydroxybutyrate) surfaces made by phase inversion. *Materials Science Forum*. 730-732, 44-49. 2013.

[3] Obeso, C.G.; Sousa, M.P.; Song, W.; Rodriguez-Pérez, M.A.; Bhushand, B. and Mano, J.F. Modification of paper using polyhydroxybutyrate to obtain biomimetic super hydrophobic substrates. *Colloids and Surfaces A: Physicochemical and Engineering Aspects*. 416, 51–55. 2013.

[4] Bellucci, F.S.; Salmazo, L.O.; Budemberg, E. R.; da Silva, M.R.; Rodríguez-Pérez, M.A.; Nobre, M.A.L. and Job, A.E. Preparation and structural characterization of vulcanized natural rubber nanocomposites containing nickel-zinc ferrite nanopowders. *Journal of Nanoscience and Nanotechnology*. 12, 2691-2699. 2012.

[5] Rodriguez-Perez, M.A.; Simoes, R.D.; Roman-Lorza, S.; Alvarez-Lainez, M.; Montoya-Mesa C.; Constantino, C.J.L.; de Saja. J.A. Foaming of EVA/Starch Blends: Characterization of the structure, physical properties, and biodegradability. *Polymer Engineering & Science*.52, 62-70. 2012.

[6] Rodriguez-Perez, M.A.; Simoes, R.D.; Constantino, C.J.L. and de Saja, J.A. Structure and physical Properties of EVA/Starch precursor materials for foaming applications. *Journal of Applied Polymer Science*. 121, 2324-2330. 2011.

[7] Simões, R.D.; Rodriguez-Perez, M.A.; de Saja, J.A. and Constantino, C.J.L. Thermomechanical characterization of PVDF and P(VDF-TrFE) blends containing corn starch and natural rubber. *Journal of Thermal Analysis and Calorimetry*. 99, 621-629. 2010.

[8] Simões, R.D.; Rodriguez-Perez, M.A.; de Saja, J.A.; Constantino, C.J.L. Tailoring the structural properties of PVDF and P(VDF-TrFE) by using natural polymers as additives. *Polymer Engineering & Science*.49, 2150-2157. 2009.

[9] Ghosh, S.; Gutierrez, V.; Fernandez, C.; Rodriguez-Perez, M.A.; Viana, J.C. Reis, R.L.; Mano, J.F. Dynamic mechanical behaviour of starch-based scaffolds in dry and physiologically simulated conditions: Effect of porosity and pore size. *Acta Biomaterialia*. 4, 950-959. 2008.

[10] Saiz-Arroyo, C.; Wang, Y.; Rodriguez-Perez, M.A.; Alves, M.; Mano, J.F. In vitro monitoring of surface mechanical properties of poly(L-Lactic Acid) using microhardness. *Journal of Applied Polymer Science*, 105, 3858-3864. 2007.

[11] Prabaharan, M.; Rodriguez-Perez, M.A.; de Saja, J.A.; Mano, J.F. Preparation and characterization of poly(L-lactic acid)-chitosan hybrid scaffolds with drug release capability. *Journal of Biomedical Materials Research Part B: Applied Biomaterials*. 81, 427-434. 2007.

[12] Alves, N.M.; Saiz-Arroyo, C.; Rodriguez-Perez , M.A.; Reis, R.L.; Mano, J.F. Microhardness of starch based biomaterials in simulated physiological conditions. *ActaBiomaterialia.*3, 69-76. 2007.

[13] Wang, Y.; Rodriguez-Perez, M.A.; Reis, R.L.; Mano. J.F. Thermal and thermomechanical behaviour of polycaprolactone and starch/polycaprolactone blends for biomedical applications. *Macromolecular Materials and Engineering*.290, 792-801. 2005.

[14] Gibson, L.J. and Ashby, M.F. Cellular solids: Structure and properties.2nd ed. Cambridge: UK, *Cambridge University Press*, 1997.

[15] Saiz-Arroyo, C.; Rodriguez-Perez, M.A.; Tirado, J.; Lopez-Gil, A. and de Saja, J.A. Structure-property relationships of medium-density polypropylene foams. *Polymer International.* 62, 1324-1333. 2013.

[16] Huber, A.T. and Gibson L.J. Anisotropy of polymer foams. *Journal of Materials Science.* 23, 3031-3040. 1988.

[17] Sullivan, R.M.; Ghosn, L.J. and Lerch, B.A.A. General tetrakaidecahedron model for open-celled foams. *International Journal of Solids and Structures.* 45, 1754-1765. 2008.

[18] Sullivan, R.M.; and Ghosn, L.J. Shear moduli for non-isotropic, open cell foams using a general elongated Kelvin foam model. *International Journal of Engineering Science***.** 47, 990-1001. 2009.

[19] Rodríguez-Pérez, M.A.; Lobos, J.; Pérez-Muñoz, C.A.; de Saja, J.A.; González, L.M. and del Carpio, M.A. Mechanical behaviour at low strains of LDPE foams with cell sizes in the microcellular range: advantages of using these materials in structural elements. *Cellular Polymers*. 27, 347-362. 2008.

[20] Rodríguez-Pérez, M.A.; Lobos, J.; Pérez-Muñoz, C.A. and de Saja. J.A. Mechanical response of polyolefin foams with high densities and cell sizes in the microcellular range. *Journal of Cellular Plastics*. 45, 389-403. 2009.

[21] Román-Lorza, S. Formulación y caracterización de materiales celulares retardantes de llama libres de halógenos basados en poliolefinas. *Tesis Doctoral*. Universidad de Valladolid. España. 2010.

[22] Román-Lorza, S.; Rodríguez-Pérez, M.A. and de Saja, J.A. Cellular Structure of halogen-free flame retardant foams based on LDPE. *Cellular Polymers*. 28, 249-268. 2009.

[23] Román-Lorza, S.; Rodríguez-Pérez, M.A.; de Saja, J.A. and Zurro, J. Cellular structure of EVA/ATH halogen-free flame retardant foams. *Journal of Cellular Plastics*. 10, 1-21. 2010.

[24] Román-Lorza, S.; Sabadell, J.; García-Ruiz, J.J.; Rodríguez-Pérez, M.A. and de Saja, J.A. Fabrication and characterization of halogen free flame retardant polyolefin foams. *Materials Science Forum*. 636/637, 98-205. 2010.

[25] Rodríguez-Pérez, M.A.; Simões, R.D.; Constantino, C.J.L. and de Saja, J.A. Structure and physical properties of EVA/Starch precursor materials for foaming applications. *Journal of Applied Polymer Science*. 212, 2324-2330.2011.

[26] Rodríguez-Pérez, M.A.; Simões, R.D.; Román-Lorza, S.; Álvarez-Laínez, M.; Montoya-Mesa, C.; Constantino, C.J.L. and de Saja, J.A. Foaming of EVA/Starch blends: Characterization of the structure, physical properties and biodegradability. *Polímer Engineering and Science*. 52, 62-70. 2012.

[27] Hidalgo, F. Diseño Optimizado de los Parámetros de Proceso en la Fabricación de Espumas de Poliolefina Reticulada mediante Moldeo por Compresión. *Tesis Doctoral*. Universidad de Valladolid. España. 2008.

CHAPTER 1:

INTRODUCTION

Contents

1.1- Introduction.

The polymer foam scientific and industrial communities are directing their efforts in the development of new processes and materials, which are more environmentally sustainable with the environment because nowadays, plastic waste represents an important source of pollution. Hence, this research work aimed at developing sustainable formulations and lab-scale production processes which could be applied to obtain foamed products such as food packaging trays and the core of sandwich panels. With regards to formulations, native starch and branched polypropylene were selected as the polymer matrixes because of their inherent eco-friendly properties. Starch because it is completely biodegradable under controlled conditions and branched polypropylene because of its good foaming performance without being cross-linked.

However, these two polymers still present some drawbacks, which have not been completely solved by scientists and engineers. On the one hand, starch needs to be plasticized in order to obtain a thermoplastic material able to be processed by the machinery commonly employed in the plastic industry. The mechanical properties of thermoplastic starch (TPS) are very low when compared to those of more common synthetic polymers employed in the food-packaging market such as PP and PET. Moreover, starch-based materials are highly susceptible to absorb water and environmental humidity, making their mechanical properties highly variable and the products obtained from them dimensionally unstable. Finally, the application of starch-based foams has been limited so far due to the poor cellular structures obtained from the foaming methods currently employed. On the other hand, the cellular structures of low-density foams produced from branched polypropylene are also very poor. As a consequence, these foams could not be employed up to now for structural applications such as in the core of sandwich panels where cellular structures with good mechanical performances (closed cellular structures for instance) are required

This piece work tries to contribute providing new insight not only in the development of solid formulations and foamed products based on these two polymers but also in understanding the relationship between their structures and mechanical properties. The employment of *natural fillers* and *nanoclays* to reinforce thermoplastic starch and branched polypropylene, respectively, and the production of foams from these composites were important challenges gradually overcome throughout the research. As far as production is concerned, on the one hand starch was expanded by an interesting process based on microwave radiation. This process offers unique features with respect to the conventional ones because of the low energy consumed and the volumetric heating of the sample. On the other hand, the virgin and nano-reinforced polypropylenes were foamed by the *improved compression moulding* (ICM) route, a process developed in our group (*CellMat Laboratory. University of Valladolid*), which allows low-density foams with defined shapes and varied cellular structures to be obtained, due to the use of specifically designed moulds (*self-expandable moulds*).

This introductory chapter will provide the reader firstly, with an overall and detailed frame work connected to the environmental damage caused by petroleum-based polymers with a special

focus on the polymer foam industry. Secondly, with the particular context of ***CellMat Laboratory*** and the projects developed surrounding this topic. Finally, with the specific objectives of this thesis, its contents and the scientific articles and conferences derived from it.

1.2- Framework and motivation.

1.2.1- Backgrounds of the polymer foam industry.

Nowadays, the consumption of plastic worldwide is growing increasingly due to the interesting properties of these materials such as ease of processing and unique property/weight ratio in comparison with traditional materials such as metal, wood and glass. It is difficult to imagine our society without plastics because we can find them in lots of applications such as household appliances, packaging, electronics etc. Plastics are mostly composed of synthetic polymers obtained through polymerization of petroleum-based monomers. Their industrial production on a large scale was boosted when *Ziegler* and *Natta* developed a titanium-based catalyst for the polymerization reaction of alkenes during the Second World War. This catalyst allowed polyolefins to be produced in softer conditions without needing elevated pressures and temperatures. They were awarded the Nobel Prize for Chemistry in 1963 for this discovery, which opened up the market for plastics [1]. The World and European plastic production has been rising constantly since then, with China and Europe being the largest producers worldwide as shown in Figure 1.1 [2].

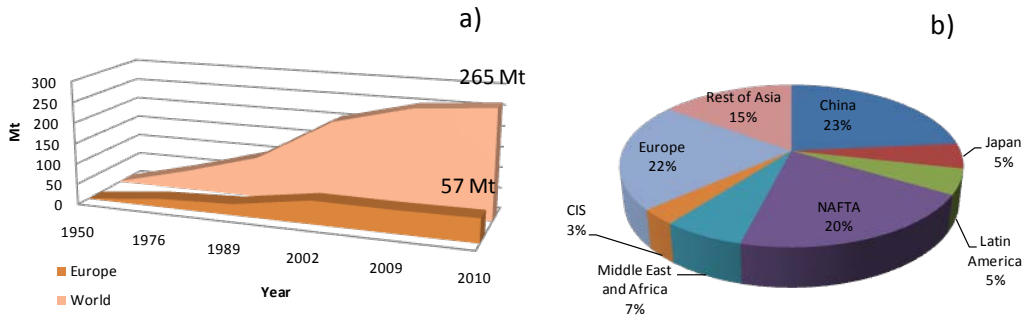

Figure 1.1. a) World and European production of plastics since 1950.(Mt: millions of tonnes). b) World plastic production by zones.

The extensive consumption of plastics, mainly thermoplastics, gave rise to the development of numerous industrial processes for transformation into consumer goods such as extrusion, thermoforming, injection etc. One of them was foaming in which the molten polymer is expanded by a gaseous phase to produce expanded beads, sheets, boards and shaped products of lower density. The first man-made polymer foams appeared during the first half of the 20th century. Concretely, in 1931,when the Swedish inventors *C.G Munters* and *J.G. Tandberg* launched the concept of cellular polystyrene and filed a patent (*U.S patent 2,023,204*) [3]. Later in 1941, the *Dow Chemical Company* developed an industrial process for the production of foamed polystyrene. *STYROFOAM* was the commercial name given to this foam and it was used by the U.S Coast Guard and Navy to produce floating devices for military equipment and antisubmarine nets during World War II [4].

Currently, the market of polymer foams is clearly dominated by polyurethane (PU) and polystyrene (PS) foams followed at a long distance by polyvinyl chloride (PVC) and polyolefin(PO) based foams as shown in Figure 1.2, in which the U.S market of polymer foams in 2010 is shown [5].

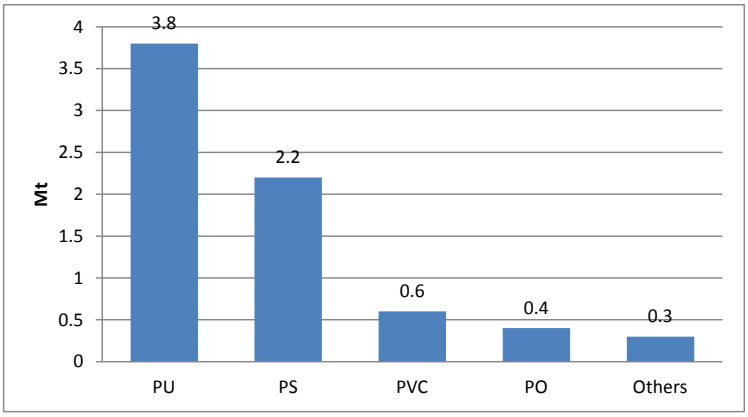

Figure 1.2. U.S production of polymer foams in 2010.(Mt: millions of tonnes).

The global market of polymer foams in 2014 is of approximately 20 Mt, which is about 10% of the overall plastic market in weight (Figure 1) and more than 50% of the overall market in volume. An AAGR (average annual growth rate) for this market higher than 4.5% is expected [6]. This data indicates that there is an increasing interest in developing new foamed products and technologies due to the reduction of weight involved and to their outstanding properties that broaden those usually covered by their solid counterparts [7].

1.2.2- Environmental concerns.

Throughout the 20th century, the development of the polymer foam industry was mainly directed at technological challenges established by the everyday more demanding applications of foamed products. Nevertheless, these technological challenges are currently giving way to those derived from environmental concerns. The polymer foam industry is used to them because one of its most important turnarounds was motivated by the chlorofluorocarbons (*CFCs*) banning after the Montreal Protocol in 1987 due to the ozone depletion problem [4]. This event led to the conversion of the polymer foam industry, which had to employ new processes and blowing agents more compatible with the environment. During the present century, the polymer foam industry is facing up to new environmental challenges due to the increasing global awareness caused by the huge amount of plastic waste generated daily.

Plastic residues are not easily attacked by microorganisms and remain in the environment for many years without being substantially degraded. The main degradation mechanisms of synthetic polymers such as photo-oxidative, thermal and ozone induced degradation only involve alterations of their properties [8,9].Hence, the formation of new fossil resources from them, such as natural gas or petroleum, is a slow process that requires millions of years. This fact avoids closing the plastics life- cycle and plastic waste ends up in landfills as shown in Figure 1.3.

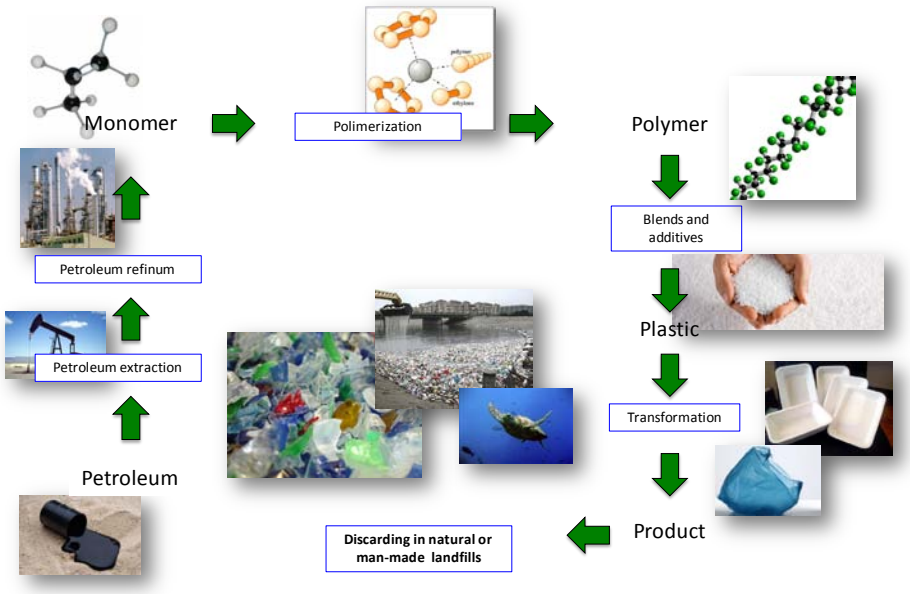

Figure 1.3.Life cycle of petroleum-based plastics.

The huge amount of plastic waste generated and its high bulk volume is shortening the lifespan of landfills. For instance, during the year 2010 in Europe approximately 10.4 Mt of plastics were discarded in landfills, which represents about 42.1% of the total plastic waste generated and almost 20% of the whole plastic production [2]. As a result a high amount of plastic waste is also discarded in natural landfills such as oceans which is bringing about the deterioration of these ecosystems as well as its ingestion by numerous animal species. At least 44% of marine bird species were reported to have ingested plastics and it is known the case of micro-plastic litter is known to be a means of transporting pollutants into living organisms by ingestion [10,11].

The recovery of plastic waste either by recycling or incineration represents the most important alternative to landfill [12,13]. In Europe during the year 2010, 24.1% of the total plastic waste generated was recycled while an even higher percentage, 33.8%, was recovered as energy. The European governments have made great efforts to launch policies and laws with the aim of potentiating the recovery of plastic waste [14]. Nevertheless, the rate of plastic recovery depends to a great extent on the infrastructures, technology available and strategies adopted in each country. For instance in Spain the rate of plastic recovery is 40%, which is still very low in comparison with that of countries such as Switzerland and Germany, where it is nearly 100% [2].

However, these approaches also present several drawbacks. On the one hand, effective recycling largely depends on the purity of the plastic products discarded. Virgin polymers are usually blended with other polymers, reinforced with inorganic fillers or additives and cross-linked to improve their properties. On the other hand the incineration of some plastic waste such as PVC could release hazardous chlorine compounds [12]. Moreover, investment required to set up the necessary infrastructure is very high and some countries are not well disposed to face it.

1.2.3- Towards the development of sustainable polymer foams

The polymer foam industry is not unaware of the damage caused by plastic materials to the environment. On the one hand, because most of the polymer foams produced are based on thermosetting resins such as polyurethane and cross-linked polyolefin foams (Figure1.2), which cannot be transformed again by melting processes. On the other hand, because a large part of the food-packages used are based on foams which are discarded shortly after being used by the consumer. The whole packaging market represents 39% of the total demand for plastic in Europe as shown in Figure 1.4, data that reflects the importance of this sector [2].

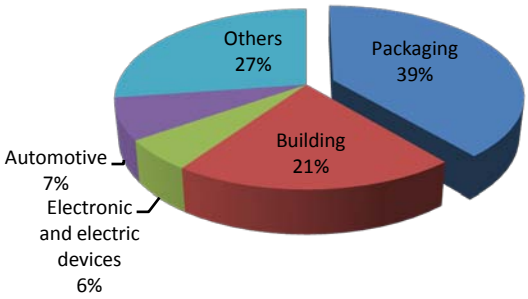

Figure 1.4.Plastic demand in Europe by industrial sectors in 2010.

Industry and science, in the face of these problems have been directing their efforts to the development of new foamed products and foaming processes based on more sustainable polymers. In this sense, the use of **bioplastics** and **non-crosslinked polymers** represent very interesting approaches.

1.2.3.1- Bioplastics.

Bioplastics represent a whole family of polymers that are bioderived and/or biodegradable. *Bioderived,* because they can be partly or completely obtained from biomass (plants) and *biodegradable* because they can be degraded under the action of microorganisms into natural substances such as water, carbon dioxide and biomass [15]. This fact is precisely the main advantage of *biodegradable* polymers because it allows them to be discarded, together with the organic waste stream being degraded under controlled conditions in a few months. The compost produced closes the bioplastic life-cycle because it is employed in agricultural fields for the growing of the same plants from which biopolymers were obtained. These processes take considerably less time (a few months) to be carried out than that required for the formation of petroleum. The starch life-cycle is represented in Figure 1.5 as a typical example of a biopolymer life-cycle. Starch is synthesized into the endosperm of cereals. Later, it is extracted from the grain and industrially processed to become a thermoplastic material. After end-use it is discarded in landfills and finally converted into compost.

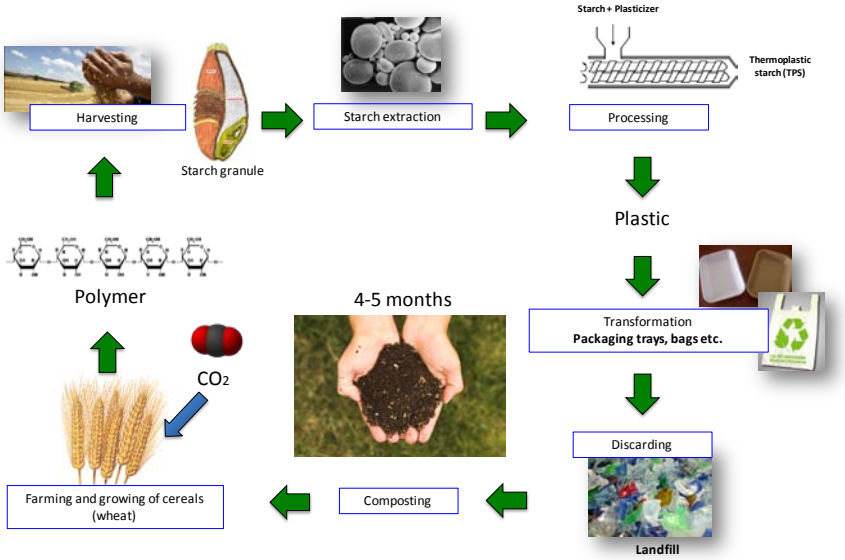

Figure 1.5. Life-cycle of starch.

There are several kinds of biopolymers which can be classified according to several criteria such as the biodegradability character or their basic components [16,17]. In this work a classification based on where the reaction of polymerization takes place has been used and represented in Figure 1.6. The first group gathers those biopolymers synthesized by the cells of the plants (cereals, tubers, algae and so on). Men only have to extract them. For this reason the price of these biopolymers is even lower than that of petroleum-based polymers. Among these biopolymers, starch [18,19] and cellulose [20] are the most widely employed. The biopolymers of the second group are generally known as polyhydroxyalkanoates (PHAs), which are microbial polyesters synthesized in fermentation vessels by a wide range of microorganisms as intracellular energy storage compounds [16]. After polymerization, PHAs are carefully extracted from the cells by solvents. In the third group, the monomers are extracted from plants but their polymerization undergoes through chemical reactions similar to those employed for synthetic polymers. In this case, two kinds of biopolymers can be found depending on their biodegradability. On the one hand, PLA is a bioderived and biodegradable aliphatic polyester synthesized from lactic acid, which in turn is obtained after the enzymatic hydrolysis of starch [17]. PLA is one of the most developed biopolymers due to its outstanding properties which make it a very promising replacement for petroleum-based polymers. Companies such as *NATURE WORKS*[21] are currently producing high amounts of PLA for several applications being the most important in the packaging sector. However, it is still very expensive due to its costly production route. On the other hand, bio-polyethylene, bio-polypropylene and bio-PET are bioderived polymers but non-biodegradable. For instance, bio-polyethylene is obtained from the alcoholic fermentation of sugar cane. The petrochemical company *BRASKEM* [22] in Brazil is one of the world largest producers of these biopolymers due to the high amount of sugar cane available in the country.

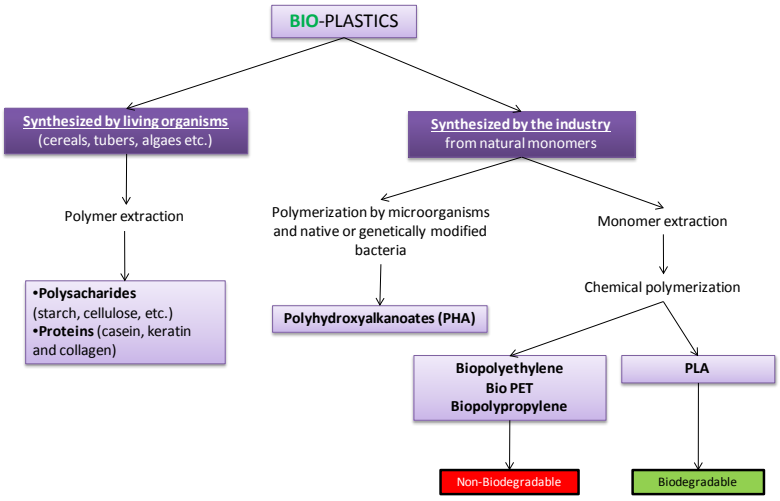

Figure 1.6.Biopolymers classification.

Biopolymers are starting to play an important role in our daily lives and it is possible to find them in products such as plastic bottles, bags, cups and so on. For instance, *COCA-COLA* is currently producing bottles (*Plant-bottle*) whose composition is mostly Bio-Pet [23]. Nevertheless, their properties are still far from those of synthetic polymers and therefore, there is still a gap to be bridged by scientists in this field. Figure 1.7 shows the world production of bio plastics since 2010 to 2012 and the estimated production for 2017. Despite the increasing demand of these biopolymers whose production increased from 1 Mt in 2010 to 1.4 Mt in 2012 there is still an enormous difference with respect to the world production of synthetic plastics which was of265 Mt in 2010 (Figure 1.1). An exponential growth has been predicted for 2017 and around 6Mt are expected to be produced [15].

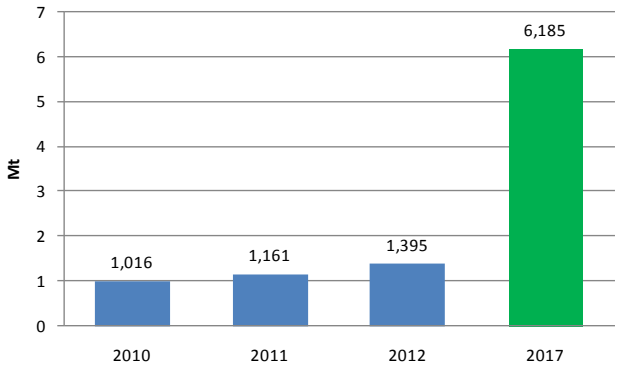

Figure 1.7. World plastic production of bioplastics.

With regards to foams, there are few products in the market based on biopolymers and all of them are used for packaging applications such as PLA foamed trays [24] and starch loose fill chips. However, the production of biopolymer foams for other applications apart from packaging is difficult because of their poor foaming performance and poor final properties in comparison with conventional polymer foams. Further research is still necessary to obtain biodegradable

polymers with similar properties to those of synthetic ones regarding foaming applications and achieving the desired purpose of entirely replacing them.

1.2.3.2- Non cross-linked polymers

Another important approach towards the production of more sustainable foams is the development of new foaming processes and foams able to replace traditional routes in which the polymer matrix is cross-linked. Nowadays, thermosetting resins like polyurethane and cross-linked PVC are used in a broad bracket of applications different from those related to foams, such as in polymer composites, electrical insulation and printed circuit boards. Nevertheless, their chemical nature makes them non-recoverable by melting and reshaping because heating leads to their decomposition and degradation [25]. An alternative way is mechanical recycling in which plastic scrap is reduced in size by shredders and hammer mills. These grinded recyclates could be used as fillers in substitution for calcium carbonate although the processing of these powders is very expensive [26].

Specifically speaking about foams, one of the principal methods to achieve a good balance between the viscosity of a molten polymer and the capacity to be expanded by gases is cross-linking. In the case of polyolefin-based foams, this production method dates back to the mid-1960s in the Japanese market and in principle, that development was an alternative process to that developed by the *Dow Chemical Company* in 1958 for the production of low density foamed boards by extrusion with volatile blowing agents (*VOBA*) based on CFCs [4]. Nevertheless, the banning of *CFCs* after the Montreal Protocol in 1987 brought about their replacement by other physical blowing agents of lower performance and by chemical blowing agents (CBA) [4]. The temperatures required for the decomposition of *CBA* are usually very high. At such high temperatures the viscosity of the molten polymer would not be adequate to withstand the pressure of the gas generated and cross-linking the polymer matrix prior to being expanded becomes essential to achieve the adequate viscosity. The cross-linking of polyolefins can be produced either by chemical reactions with peroxides or physically through high energy irradiation [3,4,27,28]. In both cases the thermoplastic polymer turns while cross-linked into a thermoset and hence, the foam produced becomes non-recyclable by melting procedures. An interesting approach reported in literature to mitigate the environmental impact caused by cross-linked foams was using the foam scraps as fillers in polyethylene foams [29] or using them directly for thermoforming new items [30].There are several industrial routes for the production of cross-linked polyolefin foams based on low-density polyethylene (LDPE), high-density polyethylene (HDPE), ethylene vinyl acetate (EVA) and mixtures of them. Companies such as *TROCELLEN*, *SEKISUI ALVEO*, *OK COMPANY, PALZIV and ZOTEFOAM* are known to use using these processes [31-35].Nevertheless, their main field of application is the production of flexible foams for non-structural applications.

When considering structural applications, the most employed rigid foams in the market are also based on cross-linked resins such as PVC and PU. The production of rigid closed cell PVC foams with excellent mechanical performance is only possible when the polymer matrix is cross-linked.

There are two methods to produce these foams. The first one is based on a *PVC grafting reaction* and the second one on the formation of a *semi-IPN* (interpenetrating polymer network) structure [36]. This last method is very similar to that employed by the company *DIAB* for the production of closed cell PVC foams (*Dyvinicell*) [37]and consists of the steps shown in the scheme of Figure 1.8.

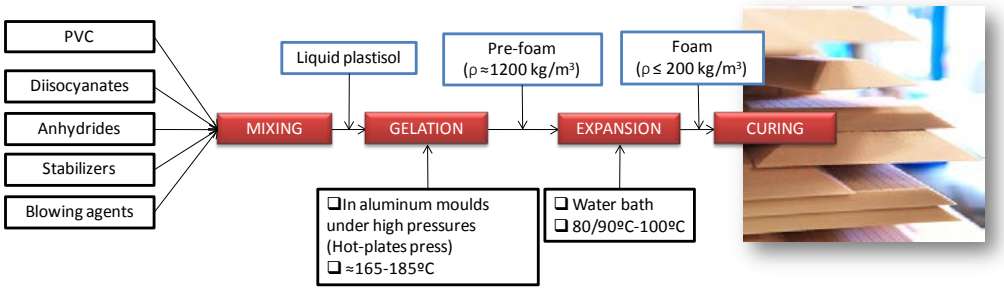

Figure 1.8. Rigid closed PVC foam production.

In this process, the liquid formed (*plastisol*) after mixing all the components is poured into an aluminium mould in which temperature and pressure are applied by a hot plates press in order to produce the *gelation* of the mixture. After gelation, a pre-expanded block is formed due to the nitrogen generated during the decomposition of the blowing agent. The expansion process is carried out inside a water bath whose temperature is set above the glass transition temperature (T_g) of PVC. Water diffuses into the softened material reacting with diisocyanates. The CO_2 generated in this reaction goes into the cells already created during the gelation step expanding the soft polymer matrix. The previous reaction also generates amines, which in turn react with still free isocyanates and anydrides creating a polyurea/imide/amide network. This network embraces the PVC macromolecules in the cell walls and struts resulting in an entangled or crosslinked structure called interpenetrating polymer network (IPN). Finally, during the curing step all the non-reacted isocyantes presented in the final foam are consumed [38].

Rigid polyurethane (PU) foams are produced in a similar way because the formation of cross-linked network during the expansion process allows the viscosity of the polymer matrix to be increased, producing the stabilization of the cellular structure.

There are many applications in which the cross-linking of the polymer is the only way of achieving the optimum combination of low density and fine closed microcellular structures, such as in the aforementioned processes for polyolefins, PVC and PU. However, the recent development of branched polypropylenes [39] allowed low-density polypropylene foams for structural applications to be produced without being cross-linked. Polypropylene has been considered a polyolefin with low foaming performances due to its linear architecture, hence, low melt strength. The formation of branches along its chain by synthesis, melt grafting or electron beam irradiation increases its extensional viscosity substantially in the molten state due to a phenomenon called strain hardening which will be explained in more detail in *section 2.5.2*

[40,41,42]. This phenomenon permits widen the range of densities for the production of non-crosslinked polypropylene foams.

1.2.4- CellMat Laboratory research

This PhD thesis presents the investigations carried out at *CellMat Laboratory* facilities (University of Valladolid) during the last four years in order to develop sustainable solid and foamed materials for their application as food packaging trays and the core of sandwich panels. *CellMat Laboratory* is a research group founded in 1999 by the Professor Dr. D Jose Antonio de Saja and the Professor Dr. D. Miguel Ángel Rodríguez Pérez with the purpose of developing new scientific knowledge in the area of Cellular Materials. At the beginning, it was focused on the structure-properties relationship but as time went by several research lines were set up concerning the development of advanced cellular materials. One of its aims is to provide the polymer foam industry with new formulations and processes able to improve the current foamed products found in the market and at the same time, contributing to create new scientific knowledge on the foaming mechanisms involved in these processes and on the processing-structure-properties relationship for these materials. The research lines currently addressed by *CellMat Laboratory* in the area of polymer foams are shown in Figure 1.9. This PhD thesis is included in two of the research topics: *cellular nanocomposites* and *biopolymer based cellular materials.*

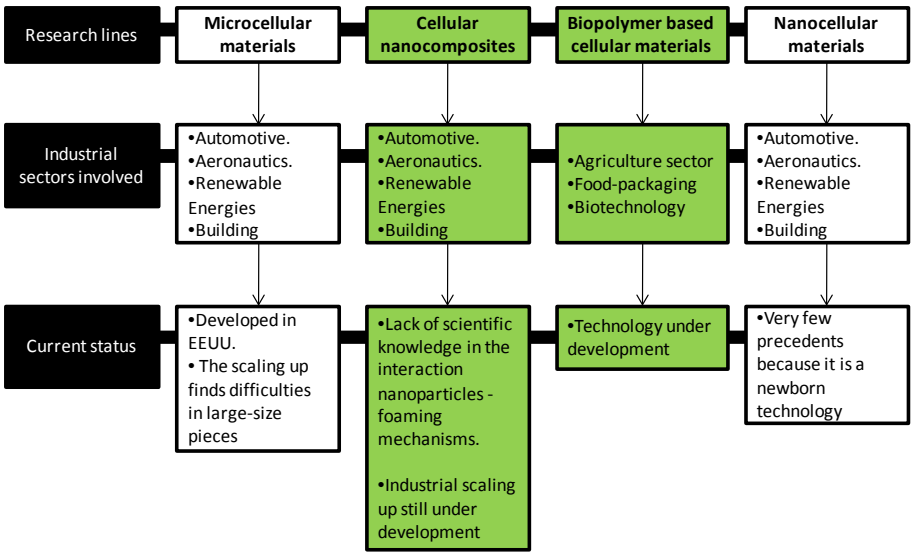

Figure1.9.CellMat Laboratory research lines

Due to an increasing environmental awareness caused by the use of plastic materials one of the research lines set up by *CellMat Laboratory* was the development of polymer foams based on bioplastics and more sustainable polymers. In this sense, some of the scientific papers published by the group in the recent years have dealt with this topic [30, 43-54]. Moreover, the research group has been also involved in public-funded projects for the development of foams based on sustainable polymers for food packaging, *ACTIBIOPACK* [55], or structural applications, *NANCORE*

[56]. Most of the scientific work developed in this thesis was also conducted in the framework of these two projects and for this reason, they are explained in more detail in the next sections.

Figure 1.10.The research was conducted in the framework of two research projects:a)***Actibiopack.***b) ***Nancore.***

1.2.4.1- Actbiopack.

ACTIBIOPACK was a research project funded by the Spanish government (INNPACTO program 2011) constituted by a consortium of public research groups and industries related to the food packaging market. The organisations involved and their main roles within the project are briefly described in Table 1.1.

NAME	ORGANIZATION	ROLE
Bandesur Alcala S.A. (BANDESUR)	Private	Trays development
WP División Transformados S.L. (WPDT)	Private	Films development
Aragonesa de Tintas, Barnices Y Lacas, S.A. (ARTIBAL)	Private	Active coatings development
Asociación para la investigación de la industria cárnica de La Rioja (CITA)	Private	Mushrooms packaging optimization at a lab scale.
Asociación para la investigación de la industria cárnica de la Rioja (CTIC)	Private	Fresh meat packaging optimization at a lab scale.
Riberebro Integral S.A. (RIBEREBRO)	Private	Mushrooms packaging optimization at a lab scale.
Profesionales de la Carne (PROFECARNE)	Private	Fresh meat packaging optimization at a lab scale.
University of Valladolid (UVA). *CellMat Laboratory.*	Public	Research on bioplastics and foaming techniques for the production of food packaging trays.
University of Zaragoza (UNIZAR)	Public	Active compounds selection and safety tests for the packages.

Table 1.1.Actibiopack consortium.

The general purpose of this project was the development of biodegradable food-packaging trays and films with active compounds to increase the shelf-life of food products such as meat and mushrooms. The University of Valladolid (*CellMat Laboratory*) was specifically focused on the development of formulations based on biopolymers and natural reinforcements for the production of solid and foamed food-packaging trays. Starch was chosen as the polymer matrix

because it is completely biodegradable and cheap in comparison with XPS, PET and PP, polymers traditionally employed for the production of such trays.

Nevertheless, starch in the form of powder is a material which is difficult to process using industrial plastic equipment such as presses, extruders and injection machines and for this reason, it was plasticized with glycerol and/or water to turn it into thermoplastic starch (TPS) [57], material with better processability and similar properties to those of thermoplastic petroleum-based polymers. In spite of the similarities to other thermoplastics commonly employed for the production of solid food-packaging trays such as PET and PP, TPS still represents a scientific challenge for this application due to the fact that its mechanical properties are very dependent on the degree of plasticization and on its hydrophilic character. Moreover, these properties evolve with time because of ageing (crystallization) [58-61].

Moreover, the replacement of XPS trays for TPS foamed trays seems to be very difficult because they become very dry after foaming and thus, brittle. Food-packaging trays require certain flexibility. For this reason, starch foams are more suitable for *protective-packaging* applications. In this project, a new process was employed for the production of homogeneous starch foamed blocks based on the interaction of water and microwave radiation. This process allowed a more efficient and homogeneous heating of the samples to be produced, which results in more homogeneous foams with regard to cellular structure. This work is explained in *chapter 4* of this thesis.

1.2.4.2- Nancore.

Nancore was a project funded by the *Seventh Framework Programme* of the European Union whose main goal was to develop novel microcellular nanocomposite foams able to be employed as the core of sandwich panels for structural purposes, such as in the hull of yachts and in wind turbine blades. Several public research organisations and industries around Europe were involved in the project. They are listed in Table 1.2 together with their roles within the project.

NAME	ORGANIZATION	ROLE
LM Glass fiber A/S (Denmark)	Private	Requirement specification with regards to process, production and mechanical characteristics; demonstration and full scale testing; Consortium Management; integration of microcellular polymer nanocomposite (MNPC) into a sandwich structure.
Aalborg University (Denmark)	Public	Multi-scale modelling and simulations of microcellular nanocomposites; integration of MNPC into a sandwich structure; selection of functionalized components of polymer nanocomposites.
Recticel polyurethanes (Belgium)	Private	Development of PU formulations. Fabrication of PU foams on an industrial scale.
Katholieke Universiteit Leuven (Belgium)	Public	Rheological characterization of nanocomposites; multi-scale modelling and simulations of microcellular nano-composites; integration of MNPC into a sandwich structure.

Universität Kassel (Germany)	Public	Industrial processing of microcellular nanocomposites; mechanical characterization of foamed sandwich panels
University of Valladolid (Spain). ***CellMat Laboratory.***	Public	Production and characterization of foams at lab-scale
Azimut-Benetti S.P.A. (Italy)	Private	Requirement specification with regards to process, integration of MNPC into a sandwich structure; demonstration and full-scale testing.
Centre of Molecular and Macromolecular Studies (Poland)	Public	Selection of functionalized components of polymer nanocomposites and elements of foaming processes, production and characterization of solids PP nanocomposites for foaming applications
Institute of Occupational Medicine (United Kingdom)	Public	Safety issues of nanoparticles from nanocomposites
Technical University of Denmark (Denmark)	Private	Life Cycle Assessment of new core material
EconCore N.V. (Belgium)	Private	Integration of MNPC into a sandwich structure
FOCAL limited (United Kingdom)	Private	Requirement specification with regard to process; integration of MNPC into a sandwich structure; demonstration and full-scale testing.
Sekisui Alveo AG (Switzerland)	Private	Production of PP foamed nanocomposite on an industrial scale.

Table1.2. Nancore consortium.

The materials currently employed in the aforementioned applications are usually Balsa Wood and PVC foams. Balsa Wood is a natural cellular solid with excellent mechanical properties due to its unique structure composed of highly elongated cells as shown in Figure 1.11 [62]. However, homogeneity in properties is not always guaranteed, due to its natural origin. PVC foams, on the other hand, present a high structural homogeneity although their price is usually high because of complex foaming technology (briefly explained in section 1.2.3.2) only available at two companies around the world: *DIAB* [63]and*3A COMPOSITES* [64]. In addition, the PVC polymer matrix is cross-linked in order to obtain low density foams with closed cellular structures. This makes this foam non-recoverable by recycling after end-use [65].

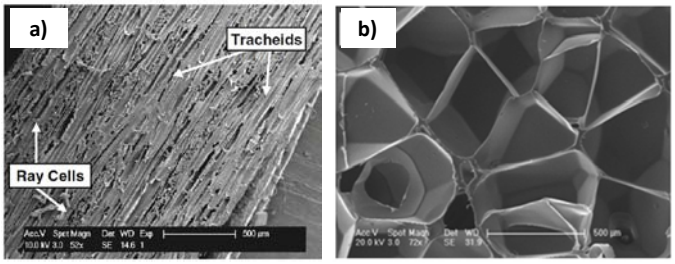

Figure 1.11. a) Cellular structure of Balsa Wood[62].b) Cellular structure of a rigid PVC foam[65].

The project aimed at developing new rigid microcellular foams based on polypropylene and polyurethane because they are cost-effective materials. This work is focused especially on the polypropylene part of the project due to the fact that this polymer was non cross-linked and

therefore, represents a sustainable alternative to cross-linked PVC foams. The work developed with PU foams within this project can be found in a previous thesis of the group [66]. The scientific and technical challenges of the project are connected to the inherent difficulties in foaming polypropylene to low densities [4,40,41,42], the necessity of reinforcing it with nanoparticles and the development of additional strategies with the aim of obtaining PP foams with comparable mechanical properties to those based on PVC [67].

1.3- Objectives.

The main objective of this work is the development of production routes and solid and foamed materials based on sustainable polymers that could contribute to mitigating the damage that common synthetic polymers are causing in the environment. This is a common aim of all the research performed but some other specific objectives were set regarding the specific applications of each polymer: starch and polypropylene.

1.3.1- Starch.

The use of starch as a biopolymer for the production of food-packaging trays and protective packaging foams requires solving several challenges related to its poor foaming behaviour and poor mechanical properties after being plasticized and foamed. One of the strategies that can be adopted to increase the strength of TPS is the reinforcement with natural fillers, which seems in principle the best choice due to their bioderived and biodegradable character and to their chemical compatibility with starch. However, after revising the existing literature related to the production and characterization of starch-based biocomposites (*Section 2.3.2.2*) and starch-based foams (*Section 2.4*), it has been detected that there is a general lack of knowledge concerning how natural fillers influence the foaming behaviour of starch and the final cellular structures and mechanical properties obtained. As far as processing is concerned, there are few studies dealing with the production of starch-based foams by microwave radiation for packaging applications. Indeed, the reinforcement of these foams with natural fillers is a topic which has not been addressed so far. Taking all these considerations into account several objectives were established:

1. Developing biobased and biodegradable formulations based on thermoplastic starch (TPS) and optimizing the lab-scale production routes such as thermoforming and microwave foaming to obtain solid and foamed materials.
2. Improving the mechanical properties of solid and foamed TPS-based materials by the reinforcement with natural fillers.
3. Studying the effect that natural fillers have on the mechanical properties of the materials developed. In the case of foamed materials the analyses will be extended to understanding their effect on foaming mechanisms and on the final cellular structures obtained.
4. To analyse the structure-properties relationship in these materials.
5. Describing the mechanical results obtained by using analytical models found in literature such as the cubic cell model of *Gibson* and *Ashby* [7].
6. Evaluating if the developed processing routes and formulations can be used to produce food packaging trays and shaped-foams for protective packaging applications.

1.3.2- Polypropylene.

The use of PP foams for structural applications has always been restricted because of its poor foamability and low mechanical properties. In spite of the recent improvements achieved in the development of branched polypropylenes, the cellular structures and mechanical properties obtained with these foams are still far from those of Balsa Wood and closed cell PVC foams. The use of nanoclays, which in principle should have represented a promising strategy to solve these matters, has not produced all the expected results so far. A revision of literature in this field (*section 2.5.3*) showed us that there is still a lack of understanding of the processing-structure-properties relationship in these heterogeneous foamed systems. This work aimed at solving these challenges by setting the following objectives:

1. Developing formulations and optimizing the lab-scale production routes such as the improved compression moulding route (ICM), a foaming process previously developed at CellMat Laboratory [68] for the production of medium and low-density polypropylene based foams.
2. Evaluating the influence that processing parameters such as pressure, temperature/time and blowing agent content have on the cellular structure and hence, on the mechanical properties of medium-density polypropylene foams.
3. Evaluating the influence of nanoclays on the cellular structure and mechanical properties of low-density polypropylene based foams produced under different foaming pressures.
4. To analyse the relationship structure-properties in these materials.
5. To use analytical models found in literature to describe the mechanical behaviour of the rigid cellular materials obtained [69-71].
6. To evaluate if the PP foams produced could replace cross-linked PVC foams as the core of sandwich panels.

1.4- Contents.

This work is presented in the form of *articles compendium*. Three articles already published in international journals and one more submitted for publication are presented. The general structure of the work consisted of seven chapters in which the articles published are included.

- ***Chapter 1. Introduction:*** the framework of the research is presented in this chapter, which accounts for the environmental concerns caused by the huge increment of petroleum-based plastics production and the strategies employed to mitigate them, all these aspects analysed from the point of view of the polymer foam industry. Moreover, the specific objectives, the contents of the work and the scientific articles and conferences derived from it are listed.

- ***Chapter 2. Background and State of the art:*** this chapter deals with a revision of the main concepts related to polymer foams, such as those derived from the cellular structure and mechanical properties, and with a description of the most used analytical models found in literature to explain their mechanical behaviour. Moreover, a description of the previous works found in the field of starch-based biocomposites, nanocomposites, starch-based foams and polypropylene-based foams have also been included.

- ***Chapter 3. Materials, production methods and characterization techniques:*** the materials employed in this work such as polymers, micro and nano-fillers and blowing agents will be described. The production methods used will be presented and analysed. The use of microwaves represents a promising way of transferring heat to a polymer matrix such as starch in order to be foamed and the *improved compression moulding route(ICM)* is a process developed in *CellMat Laboratory* in which the pressure applied to the molten polymer and the use of *self-expandable moulds* plays a fundamental role for obtaining varied cellular structures.

- ***Chapter 4. Development of starch-based materials:*** in this chapter the research carried out with starch isdescribed, which consists of two parts. The first one corresponds to the research performed with solid biocomposites. A scientific article is included addressing the research performed with TPS reinforced with natural fillers [72]. The second one deals with the development of starch foamed blocks reinforced with natural fillers produced by microwave radiation. The results are also shown by means of a published scientific article [73].

- ***Chapter 5. Development of polypropylene foams:*** in this chapter the attention is focused on the research developed with polypropylene foams produced by *ICM*. It is also split up into two parts, the first one dedicated to medium-density polypropylene foams and the second one to low-density polypropylene foams (<200 kg/m^3) reinforced with nanoclays and produced by varying the pressure applied to the molten polymer during foaming. The results will be shown as well in the form of published or submitted articles to international scientific journals [74,75].

- ***Chapter 6. Production of prototypes:*** all the previous research led to the development of prototypes of food packaging trays and structural foamed panels. Due to the high industrial applicability of this research, a chapter dealing with the methodology and main production steps of each prototype are included. In the case of the PP foams the properties of the foamed panels produced were found to be similar to those of foamed panels habitually used in the market.

- ***Chapter 7. Conclusions and Future work:*** although the results obtained increased the knowledge in the field of starch and PP-based foams, some questions have not yet been answered and some others arise from them. Currently, new research lines are under development in the group with regards to these topics. This chapter summarizes the main conclusions obtained and the future work.

1.5- Publications and Conferences

The work developed during this thesis resulted in the publication of several scientific articles, some of which have already been published in international journals and others have been submitted. They are listed in table 1.3. The section in which the articles are included is specified in the third column. Some of the works appearing in this table were not included in this thesis in spite of being related to the fields studied.

Starch-based materials.		Section
1	**Almidón termoplástico celular reforzado con fibras naturales. Una opción bioderivada y biodegradable para el envasado de alimentos.** López-Gil, A.; Bellucci, F.S.; Ardanuy, M.; Rodríguez-Pérez, M.A.; de Saja, J.A. *Revista de plásticos modernos*. Num. 671. January 2013.	-
2	**Strategies to improve the mechanical properties of starch-based materials: plasticization and natural fibres reinforcement.** López-Gil, A.; Bellucci, F.S.; Ardanuy, M.; Rodríguez-Pérez, M.A.; de Saja, J.A. *Polímeros. Ciência e Tecnologia.* vol. 24, n. Especial, 36-42. 2014.	4.2
3	**Cellular structure and mechanical properties of starch-based foamed blocks reinforced with natural fibres and produced by microwave heating.** Lopez-Gil A., Silva-Bellucci, F., Velasco D., Ardanuy, M., Rodriguez-Perez, M.A. *Industrial Crops and Products*. 66, 194–205. 2015.	4.3
Polypropylene-based materials.		Section
1	**Structure property relationships of medium-density polypropylene foams.** Saiz-Arroyo, C.; Rodríguez-Pérez, M.A.; Tirado, J.; López-Gil, A.; de Saja, J.A.; *Polymer International*. 62, 1324-1333. 2013.	-
2	**Production of non-crosslinked thermoplastic foams with a controlled density and a wide range of cellular structures.** Lopez-Gil, A.; Saiz-Arroyo, C.; Tirado, J.; Rodríguez-Pérez, M.A. *Journal of Applied Polymer Science*. 132, 2015.	5.2
3	**Anisotropic polypropylene foams filled with nanoclays: microstructure and properties.** Lopez-Gil, A.; Benanti, M.; Lopez-Gonzalez, E.; Ruiz-Herrero, J.L.; Briatico, F.; Rodriguez-Perez, M.A. *Submitted.*	5.3

Table1.3. Scientific articles.

In addition, this work was presented in national and international conferences. These presentations are included in Table 1.4.

Starch-based materials.	
1	**Mechanical properties of biocomposites based on thermoplastic starch and cellulosic fibres from agricultural residues.** Ardanuy, M.; Algaba, I.; García-Hortal, J.A.; López-Gil, A.; Rodríguez-Pérez, M.A. 4th International Textiles Congress. Istanbul, Turkey. 16-18 May. 2010. *Oral.*
2	**Development of starch biobased and biodegradable plastics for their use in trays for food-packaging.** López-Gil, A.; Rodríguez-Pérez M.A.; de Saja, J.A.; Bellucci, F.S.; Ardanuy. M.EUROTEC 2011. Barcelona. Spain. 14-15 November2011. *Oral.*
3	**Productos bioderivados y biodegradables de bajo coste basados en almidón. Aplicación en bandejas para alimentación.** López-Gil, A.; Rodríguez-Pérez, M.A.; de Saja, J.A.; V Jornadas de Innovación y Tecnología Alimentaria CTIC-CITA. Calahorra, Spain. April 25th 2012. *Oral.*
4	**Development of low density starch-biobased and biodegradable plastics reinforced with natural fibers.** López-Gil, A.; Silva-Bellucci F.; Ardanuy, M.; Rodríguez-Pérez, M.A.; de Saja, J.A. XI Brazilian MRS Meeting (SBP mat). Florianópolis, Brazil. September 27th 2012.*Oral.*
Polypropylene-based materials.	
1	**Multi-level characterization of the compressive behaviour of novel cellular nanocomposites.** Shishkina, O.; Zhu, Y.; Escudero, J.; Lopez-Gil, A.; Rodriguez Perez, M.A.; Gorbatikh, L.; Lomov, S.V.; Verpoest, I. European Conference on Composite Materials. ECCM15. Venice, Italy 24-28 June 2012. *Oral.*
2	**Production of non-crosslinked polyolefin foams with controlled density and tailored cellular structure and physical properties.** Saiz-Arroyo, C.; Escudero, J.; López-Gil, A.; Rodríguez-Pérez, M.A. 10th International Conference on Foams and Foams Technology. FOAMS 2012. Barcelona, Spain.12-13 September 2012. *Oral.*
3	**Nano-strategies applied to the production of cellular polymers with improved cellular structure and properties.** Rodríguez-Pérez, M.A.; Pardo-Alonso, S.; Estravis, S.; Saiz-Arroyo, C.; Solorzano-Quijano, E.; Escudero-Arconada, J.; Pinto-Sanz J.; López-Gil, A.; Rodríguez-Pérez, M.A. CellMat Conference. Dresden, Germany. November 2012. *Key-note lecture.*
4	**Understanding the foamability of polypropylene blends and polypropylene nanocomposites by using extensional rheology.** Laguna-Gutiérrez, E.; Escudero, J.; López-Gil, A.; Rodríguez-Pérez, M.A.; AERC, 8thAnnualEuropeanRheologyConference. Leuven, Belgium. April 2-5 2013. *Oral.*
5	**AniCell. Low density and non-crosslinked polypropylene foams as a promising option to produce structural panels.** López-Gil, A.; Escudero, J.; Laguna-Gutiérrez, E.; Saiz-Arroyo, C.; Rodríguez-Pérez, M.A.EUROTEC 2013. Lyon, France. July5th2013. *Oral.*
6	**Production and cellular structure characterization of polypropylene foams: influence of the chain arquitecture, density and blowing agent.** Salmazo, L.O.; Bellucci, F.S.; López-Gil, A.; Rodríguez-Pérez, M.A.; Job, A.E.XIII Encontro SBPMat. João Pessoa, Brazil. 2014. *Oral.*
7	**Extensional rheology: a tool to predict the foamability of complex systems such as polymer blends and recycled polymers.** Laguna-Gutiérrez, E.; López-Gil, A.; Saiz-Arroyo, C.; Rodríguez-Pérez, M.A. FOAMS 2014. September 10-11 2014. New Jersey, United States.*Oral.*

Table 1.4. Scientific conferences.

Finally, Table 1.5 shows additional activities developed during this thesis related to other materials, such as natural rubber foams, and research stays, contributions in books and patents.

Scientific articles and conferences.	
1	**Natural rubber foams with anisotropic cellular structures: mechanical properties and modelling.** Salmazo, L.O.; López-Gil, A.; Silva-Bellucci, F.; Job, A.E.; Rodríguez-Pérez, M.A. *Industrial Crops and Products*. *Submitted*
2	**Study of the concentration of ZnO in the production of vulcanized natural rubber foams.** Salmazo, L.O.; Bellucci, F.S.; Lopez-Gil, A.; Rodriguez-Perez, M.A.;Job, A.E. XI Encontro da SBPMat-Brazilian MRS meeting. Florianópolis, Brazil. September 27th 2012.*Poster.*
2	**Mechanical compression tests of multifunctional vulcanized natural rubber nanocomposites.** Bellucci, F.S.; Salmazo, L.O.; Lopez-Gil, A.; Budemberg, E.R.; Nobre, M.A.L.; Rodriguez-Perez, M.A.; Job, A.E. XII Brazilian MRS Meeting -SBPMat .2013. Campos do Jordão, Brazil. *Poster.*
3	**Cellular structure and mechanical properties of foams based on natural rubber and natural rubber/styrene butadiene rubber blends.** Salmazo, L.O.; Bellucci, F.S.; López-Gil, A.; Rodríguez-Perez, M.A.; Job, A.E.XII Brazilian MRS Meeting-SBPMat. 2013. Campos do Jordão, Brazil. *Poster.*
4	**Estudo das propriedades morfológicas, estruturais e acústicas de espumas de borracha natural.** Salmazo, L.O.; Bellucci, F.S.; López-Gil, A.; Rodríguez-Pérez, M.A.; Job, A.E. 12 Congresso Brasileiro de Polímeros - CBPOL. 2013. Florianópolis. Brazil. *Poster.*
5	**Correlation between mechanical properties and cellular structure of medium-density natural rubber foams with different anisotropy ratios.** Salmazo, L.O.; Bellucci, F.S.; López-Gil, A.; Rodriguez-Perez, M.A.; Job, A.E.XIII EncontroSBPMat.2014. João Pessoa, Brazil. *Poster.*
Research stays.	
1	**Universidade Estadual Paulista (UNESP).** Presidente Prudente. Brazil. July-October 2012.
2	**Universidade Federal do ABC(UFABC).**São Paulo. Brazil. 6-10 August 2012.
Contribution in books.	
1	**Natural Rubber Materials. Volume 2: Composites and Nanocomposites. Chapter 26:applicationsof natural rubber composites and nanocomposites.** Job, A.E.; Cabrera, F.C.; Oliveira-Salmazo, L.; Rodriguez-Perez, M.A.; Lopez-Gil, A.; De Siqueira, A.F. and Bellucci, F.S.DOI:10.1039/9781849737654.
Patents.	Chapter
1	**Method for producing cellular materials having a thermoplastic matrix.** Miguel Angel Rodriguez Perez, José Antonio de Saja Saez, Javier Escudero Arconada, Alberto López Gil. Patent number:WO2014/009579 A1. 12.01.2014 — Annex

Table1.5. Additional activities

References

[1] Eduardo, P. Y. Química Orgánica básica y aplicada. *Editorial Reverté. S.A.* 1995.

[2] Plastic Europe. Association of Plastic Manufacturers. www.plasticseurope.es.

[3] Lee, S.T.; Park, C.B. and Ramesh, N.S. Polymeric Foams. Science and Technology. *Taylor and Francis Group*.2007.

[4] Klempner, D. and Frisch, K.C. Handbook of polymeric foams and foam technology. *Hanser Publishers.*1991.

[5] www.bccresearch.com/market-research/plastics/polymeric-foams-pls008g.html

[6] Löffler, A. and Däschlein, C. The future of polymer foams. A matter of sustainability. *BASF. The Chemical Company*. Polymer Foam 2014.Cologne-Germany. 2-4 November **2014.**

[7] Gibson, L.J. and Ashby, M.F. Cellular solids: Structure and properties. 2nd ed. Cambridge: UK, *Cambridge University Press*, 1997.

[8] Singh, B. and Sharma, N. Mechanistic implications of plastic degradation. *Polymer Degradation and Stability*. 93, 561-584. 2008.

[9] Shah, A.A.; Hasan, F.; Hameed, A. and Ahmed, S. Biological degradation of plastics: A comprehensive review. *Biotechnology Advances*. 26, 246-265. 2008.

[10] Andrady, A.L. Microplastics in the marine environment. *Marine Pollution Bulletin*. 62, 1596-1605. 2011.

[11] Moore, C.J. Synthetic polymers in the marine environment: A rapidly increasing, long-term threat. *Environmental Research*. 108, 131-139. 2008.

[12] Davis, G. and Song. J.H. Biodegradable packaging based on raw materials from crops and their impact on waste management. *Industrial Crops and Products*. 23, 147-161. 2006.

[13] Hamad, K.; Kaseem, M. and Deri, F. Recycling of waste from polymer materials: An overview of the recent works. *Polymer Degradation and Stability*. 98, 2801-2812. 2013.

[14] http://europa.eu/legislation_summaries/environment/waste_management/index_en.htm

[15] http://en.european-bioplastics.org

[16] Chanprateep S. Current trends in biodegradable polyhydroxyalkanoates. *Journal of Bioscience and Bioengineering*.110, 621–632, 2010.

[17] Nampoothiri, K.M.; Nair, N.R. and John, R.P. An overview of the recent developments in polylactide (PLA) research. *Bioresource Technology.* 101. 8493-8501. 2010.

[18] James, B. and Roy, W. Starch: Chemistry and Technology.*3th ed. Elsevier*.2009.

[19] Bertolini, A.C. Starches. Characterization, properties and applications. *Taylor and Francis Group*.2010.

[20] Kalia, S.; Kaith, B.S. and Kaur, l. Cellulose fibers: bio and nano-polymer composite. *Springer.*2011.

[21] http://www.natureworksllc.com/

[22] http://www.braskem.com.br/site.aspx/plasticoverde

[23] http://www.cocacola.es/compromiso/medio-ambiente/envases-sostenibles#.VGkE8fmG8mt

[24] http://www.coopbox.it/portal/page?_pageid=896,6266577&_dad=portal&_schema=PORTAL

[25] Zhang, Y.; Broekhuis, A.A. and Picchioni, F. Thermally self-healing polymeric materials: the next step to recycling thermoset polymers. *Macromolecules.* 42, 1906-1912. 2009.

[26] Pickering, S.J. Recycling technologies for thermoset composite materials-current status. *Composites: Part A.* 37, 1206-1215. 2006.

[27] Rodriguez-Perez, M.A. Crosslinked polyolefin foams: Production, structure, properties and applications. *Advances in Polymer Science*. 184, 97-126. 2005.

[28] Rodriguez-Perez, M.A. Propiedades térmicas y mecánicas de espumas de poliolefinas. *Tesis doctoral.* Universidad de Valladolid. España.1998.

[29] Tamboli, S.M.; Mhaske, S.T. and Kale, D.D. Properties of high-density polyethylene filled with waste crosslinked foam. *Journal of Applied Polymer Science*. 91,110–114. 2004.

[30] Saiz-Arroyo, C.; de Saja, J.A. and Rodríguez-Pérez. M.A. Production and characterization of crosslinked low-density polyethylene foams using waste of foams with the same composition. *Polymer Engineering and Science*. 52, 751-759. 2012.

[31] http://www.trocellen.com./

[32] http://www.sekisuialveo.com/nc/es/pagina-de-inicio.html

[33 http://www.okcompanysa.com./

[34] http://www.palziv.com/

[35] http://www.zotefoams.com/

[36] Jiang, Z.; Yao, K.; Dua, Z.; Xue, J.; Tang T. and Liu, W. Rigid cross-linked PVC foams with high shear properties: the relationship between mechanical properties and chemical structure of the matrix. *Composites Science and Technology.* 97, 74-80. 2014.

[37] http://www.diabgroup.com/en-GB/Products-and-services.

[38] Danielsson, M. and Grenestedt. J.L. Gradient foam core materials for sandwich structures: preparation and characterization. *Composites Part A*.29, 981-988. 1998.

[39] http://www.borealisgroup.com/en/polyolefins/new-business-development/Foam-and-HMS/

[40] Spitael, P. and Macosko.C.W. Strain hardening in polypropylenes and its role in extrusion foaming. *Polymer Engineering and Science*. 44, 2090-2100. 2004.

[41] Stange J. and Münstedt, H. Rheological properties and foaming behaviour of polypropylenes with different molecular structures. *Journal of Rheology*.50, 907-923. 2006.

[42] Gotsis, A.D. and Zeevenhoven, B.L.F. Effect of long branches on the rheology of polypropylene. *Journal of Rheology*. 48, 895-914. 2004.

[43] Obeso, C.G.; Song, W.; Rodríguez-Pérez, M.A. and Mano, J.F. Superhydrophobic to super hydrophylic biomimetic poly(3-Hydroxybutyrate) surfaces made by phase inversion. *Materials Science Forum*. 730-732,44-49. 2013.

[44] Obeso, C.G.; Sousa, M.P.; Song, W.; Rodriguez-Pérez, M.A.; Bhushand, B. and Mano, J.F. Modification of paper using polyhydroxybutyrate to obtain biomimetic super hydrophobic substrates. *Colloids and Surfaces A: Physicochemical and Engineering Aspects*. 416, 51–55.2013.

[45] Bellucci, F.S.; Salmazo, L.O.; Budemberg, E. R.; da Silva, M.R.; Rodríguez-Pérez, M.A.; Nobre, M.A.L. and Job, A.E. Preparation and structural characterization of vulcanized natural rubber nanocomposites containing nickel-zinc ferrite nanopowders. *Journal of Nanoscience and Nanotechnology*. 12, 2691-2699. 2012.

[46] Rodriguez-Perez, M.A.; Simoes, R.D.; Roman-Lorza, S.; Alvarez-Lainez, M.; Montoya-Mesa, C.; Constantino, C.J.L.; de Saja. J.A. Foaming of EVA/Starch Blends: Characterization of the structure, physical properties, and biodegradability. *Polymer Engineering & Science*.52, 62-70. 2012.

[47] Rodriguez-Perez, M.A.; Simoes, R.D.; Constantino, C.J.L. and de Saja. J.A. Structure and physical Properties of EVA/Starch precursor materials for foaming applications. *Journal of Applied Polymer Science*.121, 2324-2330. 2011.

[48] Simões, R.D.; Rodriguez-Perez, M.A.; de Saja, J.A. and Constantino, C.J.L. Thermo mechanical characterization of PVDF and P(VDF-TrFE) blends containing corn starch and natural rubber. *Journal of Thermal Analysis and Calorimetry*. 99, 621-629. 2010.

[49] Simões, R.D.; Rodriguez-Perez, M.A.; de Saja, J.A.; Constantino, C.J.L. Tailoring the structural properties of PVDF and P(VDF-TrFE) by using natural polymers as additives. *Polymer Engineering & Science*. 49, 2150-2157. 2009.

[50] Ghosh, S.; Gutierrez, V.; Fernandez, C.; Rodriguez-Perez, M.A.; Viana, J.C. Reis, R.L.; Mano, J.F. Dynamic mechanical behaviour of starch-based scaffolds in dry and physiologically simulated conditions: Effect of porosity and pore size. *ActaBiomaterialia*. 4, 950-959. 2008.

[51] Saiz-Arroyo, C.; Wang, Y.; Rodriguez-Perez, M.A.; Alves, M.; Mano, J.F. In vitro monitoring of surface mechanical properties of poly(L-Lactic Acid) using microhardness. *Journal of Applied Polymer Science*, 105, 3858-3864. 2007.

[52] Prabaharan, M.; Rodriguez-Perez, M.A.; de Saja, J.A.; Mano, J.F. Preparation and characterization of poly(L-lactic acid)-chitosan hybrid scaffolds with drug release capability. *Journal of Biomedical Materials Research Part B: Applied Biomaterials*. 81, 427-434. 2007.

[53] Alves, N.M.; Saiz-Arroyo, C.; Rodriguez-Perez , M.A.; Reis, R.L.; Mano, J.F. Microhardness of starch based biomaterials in simulated physiological conditions. *ActaBiomaterialia.* 3, 69-76. 2007.

[54] Wang, Y.; Rodriguez-Perez, M.A.; Reis, R.L.; Mano. J.F. Thermal and thermo mechanical behaviour of polycaprolactone and starch/polycaprolactone blends for biomedical applications. *Macromolecular Materials and Engineering*. 290, 792-801. 2005.

[55] http://clusterfoodmasi.es/proyectos/actibiopack.

[56] http://cordis.europa.eu/result/rcn/45930_en.html.

[57] Leon, J. and Leszek, M. Thermoplastic starch. A green material for various industries.*Wiley-VCH.*2009.

[58] Avérous, L.; Fringant, C. and Moro, L. Starch-based biodegradable materials suitable for thermoforming packaging. *Starch/Stärke*. 53, 368-371. 2001.

[59] Hulleman, S.H.D.; Janssen, F.H.P.; and Feii, H. The role of water during plasticization of native starches.*Polymer.*39. 2043-2048. 1998.

[60] Myllärinen, P.; Partaken, R.; Seppälä, J. and Forssella, P. Effect of glycerol on behaviour of amylose and amylopectin films. *Carbohydrate Polymers*. 50, 355-361. 2002.

[61] Van Soest, J.J.G.; Hulleman, S.H.D.; De Wit, D. and Vliegenthart, J.F.G. Changes in the mechanical properties of thermoplastic potato starch in relation with changes in B-type crystallinity. *Carbohydrate Polymers*. 29, 225-232. 1996.

[62] Shishkina, O.; Lomov, S.V.; Verpoest, I. and Gorbatikh, L. Structure–property relations for balsa wood as a function of density: modelling approach. *Archive of Applied Mechanics*. 84, 789-805, 2014.

[63] http://www.diabgroup.com.

[64] http://www.3acomposites.com.

[65] Jiang, Z.; Yao, K.; Du, Z.; Xue, J.; Tang, T. and Liu, W. Rigid cross-linked PVC foams with high shear properties: the relationship between mechanical properties and chemical structure of the matrix. *Composites Science and Technology*. 97, 74-80. 2014.

[66] Estravís, S. Cellular nanocomposites based on rigid polyurethane and nanoclays: Fabrication, characterization and modelling of the mechanical properties and thermal properties. PhD Thesis. University of Valladolid. Spain. 2014.

[67] Lee, L.J.; Zeng, C.; Cao, X.; Han, X.; Shen, J. and Xu, G. Polymer nanocomposite foams. *Composites Science and Technology*. 65, 2344-2363. 2005.

[68] Saiz-Arroyo, C.; Rodriguez-Perez, M.A.; Tirado, J.; Lopez-Gil, A. and de Saja, J.A. Structure-property relationships of medium-density polypropylene foams. *Polymer International.* 62, 1324-1333. 2013.

[69] Huber, A.T. and Gibson L.J. Anisotropy of polymer foams. *Journal of Materials Science.* 23, 3031-3040. 1988.

[70] Sullivan, R.M.; Ghosn, L.J. and Lerch, B.A.A. General tetrakaidecahedron model for open-celled foams. *International Journal of Solids and Structures.* 45, 1754-1765. 2008.

[71] Sullivan, R.M.; and Ghosn, L.J. Shear moduli for non-isotropic, open cell foams using a general elongated Kelvin foam model. *International Journal of Engineering Science***.** 47, 990-1001. 2009.

[72] Lopez-Gil, A.; Bellucci, F.S.; Ardanuy, M.; Rodriguez-Perez, M.A. and de Saja, J.A. Strategies to improve the mechanical properties of starch-based materials: plasticization and natural fibres reinforcement. *Polímeros: Ciência e Tecnologia*. 24, 36-42. 2014.

[73] Lopez-Gil, A.; Bellucci, F.S.; Velasco, D.; Ardanuy, M.; Rodriguez-Perez, M.A. Cellular structure and mechanical properties of starch-based foamed blocks reinforced with natural fibres and produced by microwave heating. *Industrial Crops and Products*. 66, 194-205. 2015.

[74] Lopez-Gil, A.; Saiz-Arroyo, C.; Tirado, J.; Rodriguez-Perez, M.A. Production of non-crosslinked thermoplastic foams with a controlled density and a wide range of cellular structures. *Journal of Applied Polymer Science*. 132, 42324.2015.

[75] Lopez-Gil, A.; Benanti, M.; Lopez-Gonzalez, E.; Ruiz-Herrero J.L.; Briatico, F.; Rodriguez-Perez, M.A. Anisotropic polypropylene foams filled with nanoclays: microstructure and properties. *Submitted*. 2015.

CHAPTER 2:

BACKGROUND AND STATE OF THE ART

Contents

2.1- Introduction.

This chapter deals with the revision of the main concepts related to cellular materials (*section 2.2*) being more focused on those specifically used for polymer foams (*section 2.3*). The sustainable foams developed in this thesis, based on biodegradable thermoplastic starch and non-crosslinked polypropylene, belong to this family of cellular materials. The principal mechanisms constituting a foaming process (nucleation, expansion and stabilization) will be also dealt with in *section 2.3.* Among them, the *stabilization of the cellular structure* will receive special attention because its understanding is a key factor for the production of starch-based foams by microwave radiation (*chapter 4*). *Section 2.4* will address the relationship between *cellular structure* and *mechanical properties* in polymer foams focusing the subject on the mechanical behaviour of anisotropic cellular structures. This issue will be treated specifically in *chapter 5* because some of the PP-based foams produced in this thesis present this particular structure. The reinforcement of the polymer matrix with fillers was a common strategy employed throughout the thesis in order to increase the mechanical properties of solid and foamed materials. *Section 2.4.2* will address the main concepts related to the production of starch-based biocomposites reinforced with natural fibres and to the production of polymer nanocomposites reinforced with nanoclays. Finally, in *sections 2.5* and *2.6* an exhaustive revision of the works found in literature dealing with the production of solid and foamed starch-based materials and the production of polypropylene foams is included. This revision was of paramount importance in order to settle the objectives of the thesis, which were listed in *chapter 1*.

2.2- Cellular materials.

Cellular materials have become a fundamental part of our daily lives because we can find them everywhere: within house walls, inside car seats and in food-packaging trays to name but a few applications. They are called cellular materials or "cellular solids" because they are composed of two different phases: a solid phase and a gaseous phase. This combination brings about a reduction of density and a widening of the solid properties that makes cellular materials useful in applications in which for instance, high energy absorption in impacts and/or thermal insulation are required. Moreover, the inherent reduction of density allows cellular materials to be used in buoyancy applications. Last but not least, reducing density is a key issue for industries from an economical and environmental point of view because they are constantly striving to reduce weight and in this way, cut down on raw materials and costs [1].

These kinds of materials are found in nature such as in wood, corals, cork, tree trunks, honeycombs, marine organisms etc. or are produced by men. They can be classified according to several criteria. Density (ρ) is one of them. In the case of cellular materials this property is usually expressed as the ratio between the density of the foam (ρ_f) and that of the solid (ρ_s). This ratio is called *relative density* (ρ_f/ρ_s) and there are three kinds of cellular materials according to it: high-density ($\rho_f/\rho_s \geq 0.7$), medium-density ($0.7 > \rho_f/\rho_s \geq 0.2$) and low-density cellular materials ($\rho_f/\rho_s < 0.2$). High-density cellular materials are more frequently denominated as *porous solids*(Figure 2.1a).Another criterion used to classify them is connected with the organization of cells in space. There are two options: periodic or random. A honeycomb is a typical example of a *periodic cellular solid* because hexagonal cells are periodically organised in a two-dimensional array (Figure 2.1b). On the other hand, in *random cellular solids* polyhedron cells are organised without hierarchy in a three-dimensional array (Figure 2.1c).

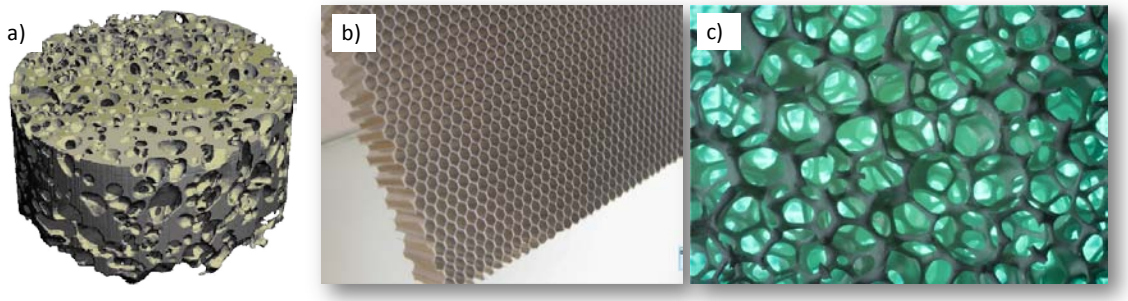

Figure 2.1. Different kinds of cellular solids. a) Porous solid. b) Periodic aluminium honeycomb. c)Random ceramic foam.

2.3- Polymer foams: fundamentals of foaming.

The three-dimensional random structure of some cellular materials is a direct consequence of the production process. Cells are formed after the anarchic dispersion of gas molecules within a molten material. This production method is usually referred to as *foaming* and the cellular materials obtained from it are called *foams.* A foaming process can be split up in several steps, all of which are schematically shown in Figure 2.2: first of all, the formation of a *polymer/blowing agent system* in which both phases, gas and molten material, are completely miscible. Secondly, *cells nucleation*, which is a response of gas molecules towards the change in surrounding conditions (pressure and/or temperature) that involves their diffusion into clusters to form spherical nuclei. Thirdly, the *expansion* of the molten material due to gas diffusion from the molten phase to the interior of the cells, and finally, the *stabilization* of the cellular structure by increasing the melt strength up to solidification [2].

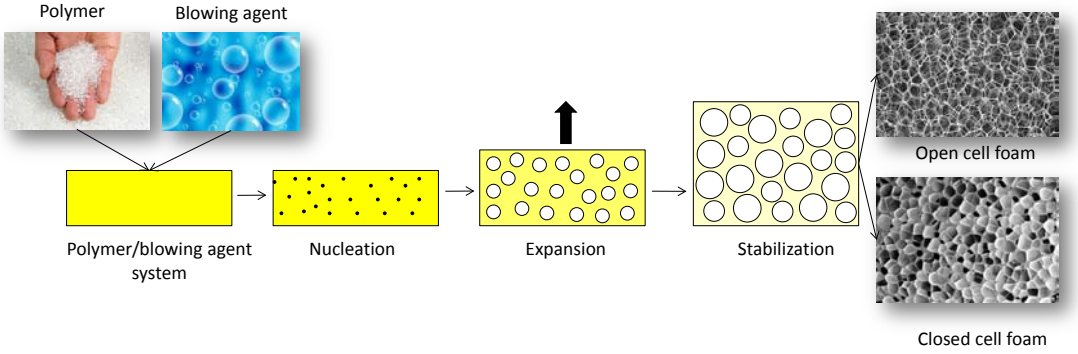

Figure 2.2.Foaming stages.

Once the foam is stable, the gas phase can be isolated in specific domains or can be interconnected resulting in a new classification of cellular materials: *closed cell foams* and *open cell foams*. In *closed cell foams* the solid material in each cell is distributed along the vertexes, edges and walls enclosing the gaseous phase inside. On the contrary, in *open cell foams,* cells are interconnected forming a continuous gas phase [1,2].

The classifications described previously are based on the structures obtained but foams can be also classified in terms of the material constituting the solid phase: metals, ceramics, glass or polymers. In this work the thermoplastic starch and polypropylene foams developed belong to the family of polymer foams. Polymers are materials with unique features in the molten state. When they melt they do not become a liquid such as in soap foams (Figure 2.3) or metallic foams. Instead, they become a viscous fluid, which is more stable and has a broader temperature/time *foaming window*. However, this stability is limited in time and it depends on the rheological behaviour of the polymer and on the expansion ratio of the foam. The expansion ratio (*ER*) is defined as the ratio between the density of the solid and that of the foam: ρ_s/ρ_f. When *ER* is very high (above four times) the contact between neighbouring cells is more frequent which results in cell wall sharing (Figure 2.3) [2].

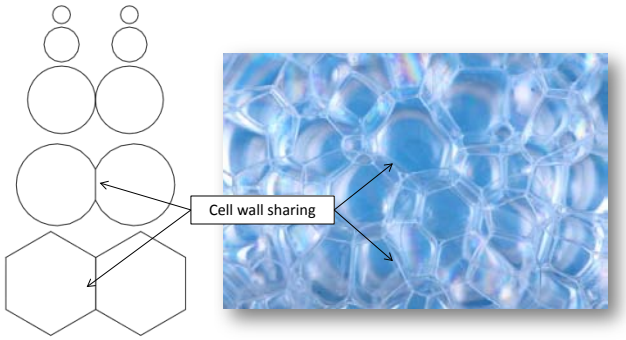

Figure 2.3.Evolution of cells during foam expansion and analogy with a soap foam.

Cell wall sharing is the phenomenon that triggers the degeneration* of the cellular structure which is mainly caused by three mechanisms: *drainage*, *coalescence* and *coarsening. Drainage* could be microscopically described as the transport of the molten polymer from the cell walls to the edges and vertexes due to *capillary forces*. It is a phenomenon which is more pronounced in soap and metallic foams because they have lower viscosities in the molten state. In the case of polymer foams the extent to which this phenomenon occurs depends on the viscosity of the molten polymer. *Drainage* can also be induced by *gravity forces* producing in this case macroscopic density gradients along the foam. The main consequence of an excessive drainage of the molten polymer, either micro or macroscopically, is the thinning of the cell walls, which in turn leads to cell wall rupture and the joining of the two cells sharing the cell wall. This new phenomenon is called *coalescence*. Finally, *coarsening* is the result of a pressure difference produced between two adjacent cells, which creates the diffusion of gas molecules from the smaller to the larger cells through the molten material constituting cell walls, edges and struts. This results in degenerated cellular structures composed of large cells surrounded by packs of smaller cells.

The stabilization of the cellular structure is necessary in any foaming process to mitigate the adverse effects caused by the degeneration mechanisms previously described. A new classification of polymer foams arises from how the cellular structure becomes stable after expansion. This classification is shown in Figure 2.4.

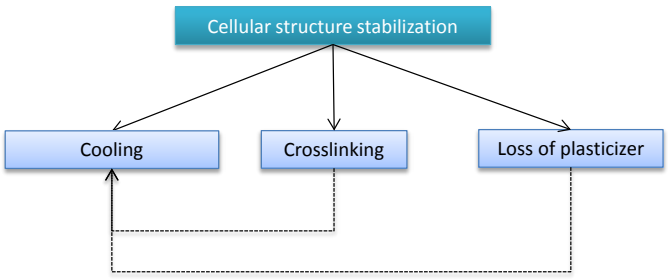

Figure 2.4.Classification of polymer foams based on the stabilization mechanisms taking place during foaming.

*The word degeneration is used here to describe all the processes that cause an increase of cell size and a widening of the cell size distribution.

All the mechanisms shown in Figure 4 have something in common: the viscosity of the molten polymer gradually increases during stabilization so as to increase the melt strength. The difference between them is the way of producing this increment.

Cooling the polymer below its crystallization temperature (if it is a crystalline polymer) or below its glass transition temperature (if it is an amorphous polymer) is the natural way to stabilize the cellular structure. The other mechanisms usually act in combination with cooling. This mechanism is especially important in polymer foams because of the inherent poor thermal conductivity of both, the polymer and the gaseous phase located inside the cells [2]. It is especially controlled in chemical foaming processes in which temperatures well above the melting temperature of the polymer are employed in order to decompose the blowing agent. The viscosity of the polymer at these high temperatures is very low and therefore, the cooling rate plays a very determining role in the final foam structure.

Other mechanism is the ***crosslinking*** of the polymer matrix, which is based on forming an interconnected network of covalent bonds between polymer chains. Crosslinking can be achieved either by chemical reactions with peroxides (for polyolefins) or by irradiation (for instance with high energy electrons). In some cases, the crosslinking process is carried out before expansion because the main purpose is providing the polymer with the required viscosity to be highly expanded. This is the case of thermoplastics such as polyethylene. In other cases, the crosslinking reaction and the expansion process take place simultaneously such as in polyurethane foams and when a certain viscosity is reached the foam is stabilized. Figure 5 shows a plot in which the viscosity in the molten state of virgin and crosslinked polymers are presented versus temperature. T_m represents the melting temperature of the polymer. There is a range of temperatures, called *foaming window*, in which the polymer is able to be expanded providing good cellular structures. After crosslinking the *foaming window* of a given polymer broadens, hence, its stability in the molten state[3].

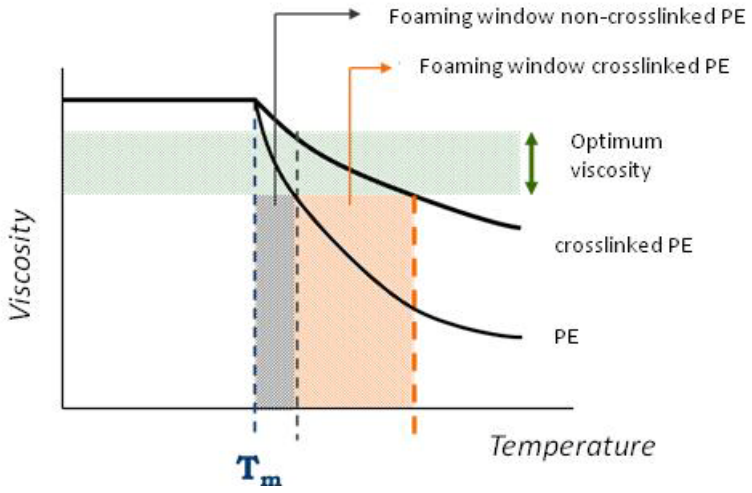

Figure 2.5.Foaming window comparison between crosslinked PE and non-crosslinked PE.

Finally, the ***loss of plasticizer*** from the polymer during the expansion stage is another interesting mechanism to stabilize the cellular structure. This phenomenon usually takes place in foaming processes carried out under supercritical conditions in which gases such as $CO_2$are able to diffuse and dissolve into the polymer due to the high pressure applied (100 to 300 bars)[4].The gas molecules occupy the free space between the polymer chains in the amorphous regions. As a result, the distance between polymer chains increases. In other words, the gas molecules plasticized the polymer matrix resulting in a reduction of its glass transition temperature (T_g). This phenomenon has been studied in detail and even theoretical models have been proposed with the aim of predicting the depression of the T_g suffered by the polymer during the formation of the polymer/CO_2 system [5].Figure 2.6 represents a plot extracted from the work of *Chow T.S* [5] in which T_g/T_{go} is plotted versus ϑ for polystyrene. T_{go} is the initial glass transition temperature of the polymer and ϑ is a factor that depends on the number of diluent molecules and on the number of lattice sites. The higher the number of diluent molecules, the higher the T_g drop.

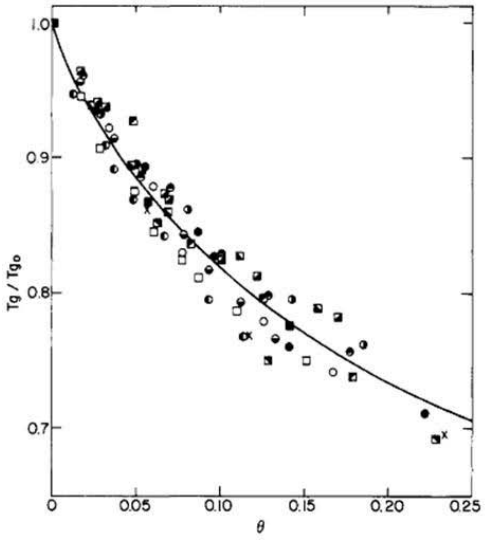

Table I
Various Diluents in Polystyrene

diluent	M_d, g/mol	V_d, cm³/mol	symbol in Figure 1
methyl acetate	74.08	79.30	○
CS_2	76.14	60.28	◒
C_6H_6	78.12	88.87	◓
CH_2Cl_2	84.93	64.20	◑
ethyl acetate	88.11	98.34	◐
$C_6H_5CH_3$	92.14	106.03	●
n-butyl acetate	116.16	131.70	○
$CHCl_3$	119.38	80.94	◪
$C_6H_5NO_2$	123.11	102.28	◧
methyl salicylate	152.15	128.95	◨
CCl_4	153.82	96.49	◘
phenyl salicylate	214.22	171.38	×
β-naphthyl salicylate	264.22	214.00	■

Figure2.6.Glass transition temperature depression of polystyrene by diluents of different molecular weight [5].

To promote the foaming process of these systems the pressure is released and as a consequence the cells are created. When gas diffuses out of the polymer, the T_g of the polymer increases and when it reaches a value equal to the temperature of the foam the cellular structure is stabilized. This phenomenon is very similar to the effect that takes place when foaming starch-based materials plasticized with water, an issue which will be explained in more detail in *section 2.5*.

2.4- Cellular structure-mechanical properties relationship in polymer foams.

The stabilization of polymer foams after expansion involves the formation of a cellular structure, which is composed of a three-dimensional, range of randomly distributed cells. A cell is a single entity within the cellular structure, which is composed of gas molecules surrounded by solid vertexes, edges and walls. The three elements are presented in *closed cell foams* while in *open cell foams* cell walls they disappear totally or partially (presence of holes or ruptures within the cell walls). These structures are shown in Figure 2.7.

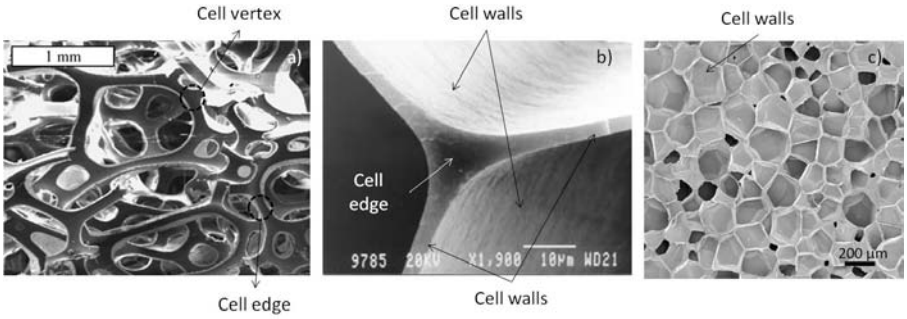

Figure2.7.Typical cellular structures showing the main structural components of the solid phase in a foam: vertexes, edges and walls. a) Edges and vertexes in an open cell polyurethane foam [6]. b) Edges and walls in a cross-linked polyethylene foam [7]. c) Cell walls in a closed-cell polyethylene foam [8].

The mechanical behaviour of cellular structures under external loads depends on the foam density, the properties of the solid material within the cell walls, edges and vertexes and on several morphological parameters of the constituent cells such as their shape, size, distribution of cell sizes, the degree of interconnection, the fraction of material in the struts and their anisotropy. The use of analytical models is a common approach used by polymer foam engineers and scientist to relate cellular structure with mechanical properties and in this way, predict the mechanical behaviour of polymer foams. Several analytical models have been reported in literature but all of them have something in common that simplifies the cellular structure in order to make easier the analyses of the results [9,10,11]. Hence, the cell shape is usually defined by simple geometries such as the ones shown in Figure 2.8 which are periodically distributed to fill the space [12].

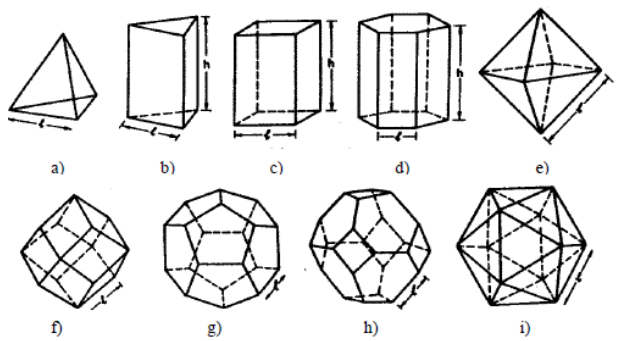

Figure 2.8.Three dimensional cells: a) Tetrahedron. b) Triangular prism. c) Rectangular prism. d) Hexagonal prism. e) Octahedron. f) Rombidodecahedron. g) Pentagonal dodecahedron. h) Tetrakaidecahedron. i) Icosahedron.

Despite the great simplicity of these models, they proved to work well, but only under specific conditions. *Gibson* &*Ashby* [1], for instance, developed one of the simplest models found in literature but at the same time one of the most frequently employed. It is the cubic cell model in which the cells are assumed to be cubes whose edges, of length *l*, are formed by squared-cross section beams, of side t_e and cell walls of thickness t_f (Figure2.9).

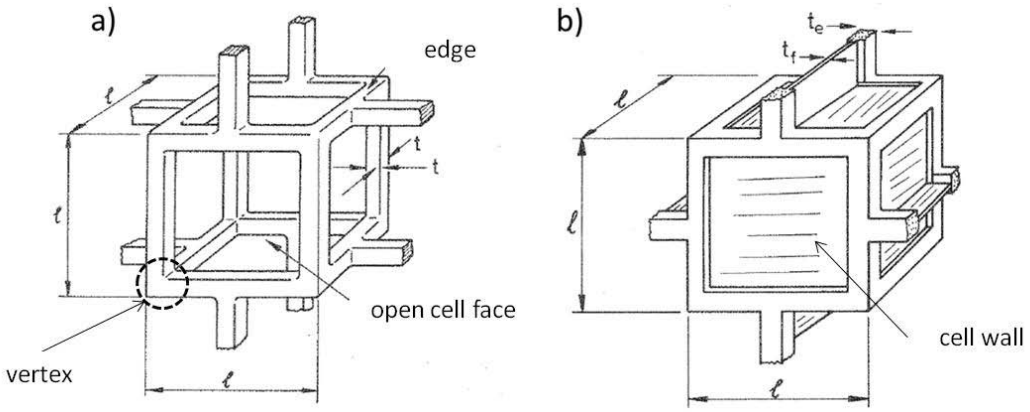

Figure 2.9.Cubic cell representation of *Gibson* and *Ashby*. a) Open cell material. b) Closed cell material.

In the particular case of applying an *uniaxial compression* the behaviour is similar to the one represented in Figure 2.10 in which typical stress-strain curves of the thermoplastic starch (TPS) and the polypropylene foams (PP) produced in this work are plotted.

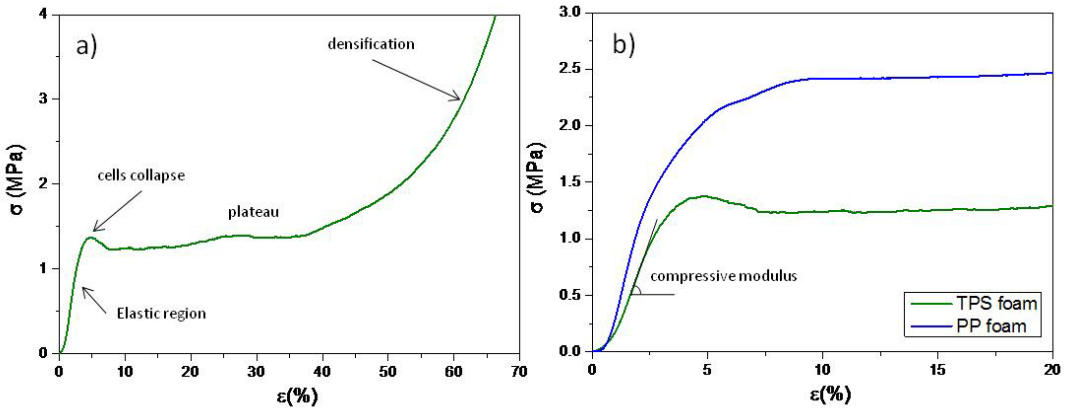

Figure 2.10. a) TPS foam stress-strain curve up to high strains. b) Stress-strain curves of TPS and PP foams at low strains (below 20%).

These curves, regardless of the polymer employed, share three common regions: the ***linear elastic region***, the ***plateau*** and the ***densification region***. In the *linear elastic region* as the stress grows linearly so does the strain, the deformation induced in the foam is almost entirely recoverable. Figure 2.11 shows the main deformation mechanisms of cells under uniaxial compression, which are bending and *axial deformation* of the edges, cell wall *stretching* and *gas compression*. The contribution of the last two mechanisms is only significant in the case of closed cell foams. In the case of open cell foams the gas flows between cells and its contribution is

scarce. Only when filling the foam with fluids of high viscosity can this contribution be significant[1].

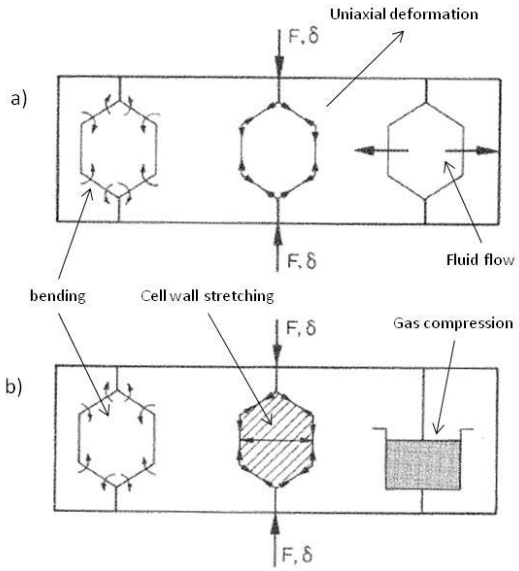

Figure 2.11. Linear elastic deformation mechanisms of a) open cell foams and b) closed cell foams.

The foam stiffness is quantified by the ***compressive modulus***, which is calculated as the slope of the curve in the linear elastic region. *Stiffness* is a very important parameter used to design foams for structural elements. For instance, stiff foamed panels are employed as the core of sandwich panels in structural applications in which lightness is also required, such as in the hull of yachts. A more detailed explanation about how the foamed core stiffness influences the general behaviour of a sandwich panel is found in *section2.6.4* because it is one of the main applications of the non-crosslinked PP foams developed in this work.

Once the stress reaches a certain level the cellular structure collapses and the foam deforms without opposing any additional resistance. This region, in which the strain increases at constant stress, is called *plateau*. The border between the linear elastic region and the plateau is marked by a stress which quantifies the ***collapse strength*** of the foam. The collapse mechanisms are usually attributed to *elastic buckling* for elastomeric foams, to the formation of *plastic hinges* for rigid polymers such as PP, and to *brittle crushing* such as in the case of the starch-based foams produced in this work (Figure 2.12). The reason why starch based foams are considered brittle will be discussed in *section 2.5* and in *chapter 4*. The collapse strength is an important parameter in structural applications (accounts for the maximum stress that can be applied to the foam without failure) and the area under the stress-strain curve in the long plateau region is used for designing crash protection and *protective-packaging* because it determines the energy absorbed by the foam during the load [1].

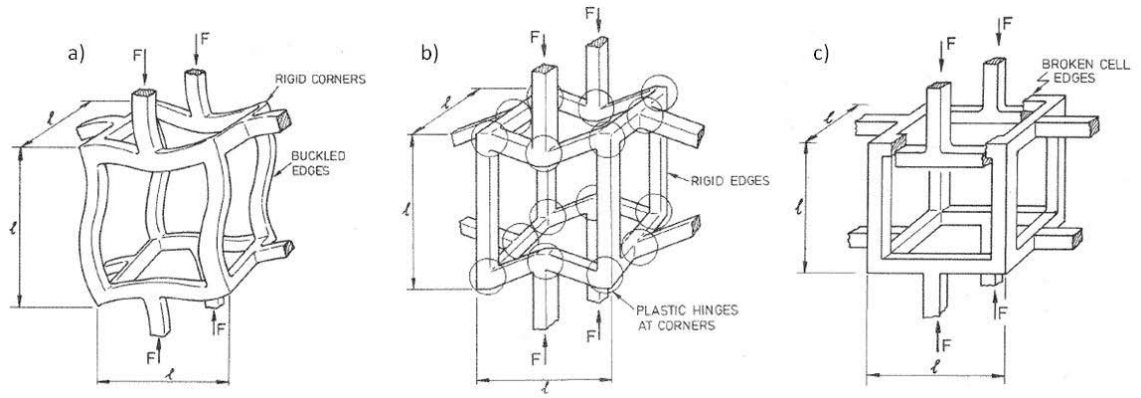

Figure 2.12. Cell collapse mechanisms: a) elastic buckling, b) plastic hinges and c) brittle crushing.

Finally, the foam deforms to such extent that opposing cell walls and edges touch and the foam density increases. This is why this region is usually referred to as ***densification*** region (Figure 13). As a result the stress grows abruptly. The different stages of a uniaxial compression test performed in an open cell polyurethane foam can be measured by means of X-ray tomography in Figure 2.13.

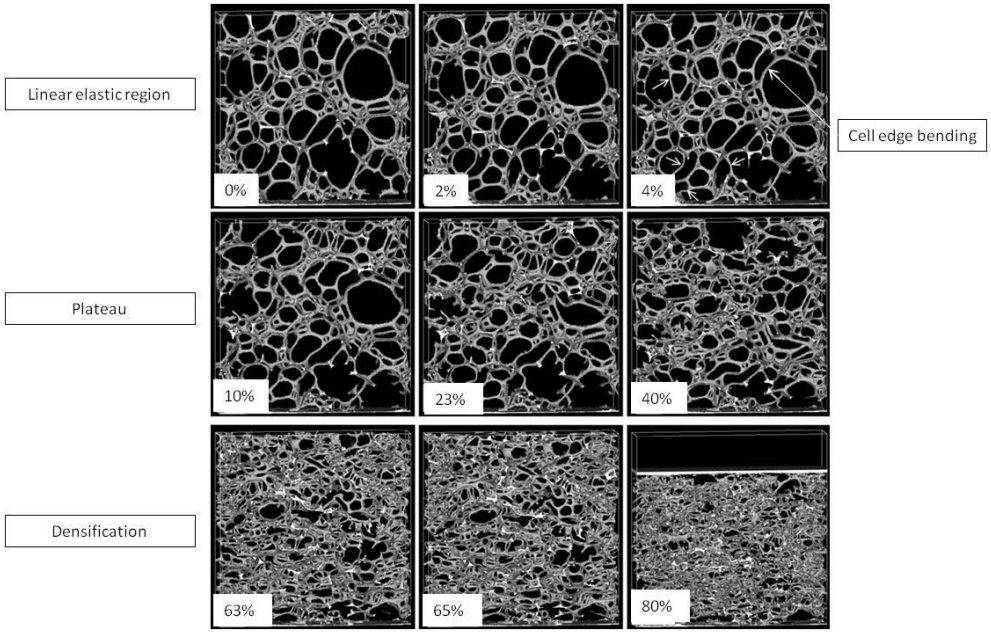

Figure 2.13. X-ray tomography images of a polyurethane foam as a function of the compressive strain (white boxes). These images have been taken in the three regions[6].

Equation 2.1 describes the *Gibson & Ashby* model within the linear elastic region taking an open cell foam subjected to uniaxial compression into account and supposing *bending* as the deformation mechanism of the edges. This equation is obtained by using the standard beam theory of *Timoshenko & Godier* [13].

$$\frac{E_f}{E_s} = C\left(\frac{\rho_f}{\rho_s}\right)^n \tag{2.1}$$

In equation 2.1 the compressive modulus of the foam (E_f) depends on the compressive modulus of the solid polymer (E_s), on the relative density (ρ_f/ρ_s) and on the cellular structure. The influence of the cellular structure is mainly included in the exponent *n*. Experimental results obtained for low-density open cell polymer foams fit well with the previous equation if *n* is estimated as 2 [1]. For this reason, it is generally assumed that the compressive modulus of a foam decreases quadratically with the density. Figure 14 shows a plot in which the compressive modulus of a foamed polymer is represented versus density. The blue line represents a linear decrease (*n=1*) of the compressive modulus while the red line (*n=2*) represents a quadratic reduction.

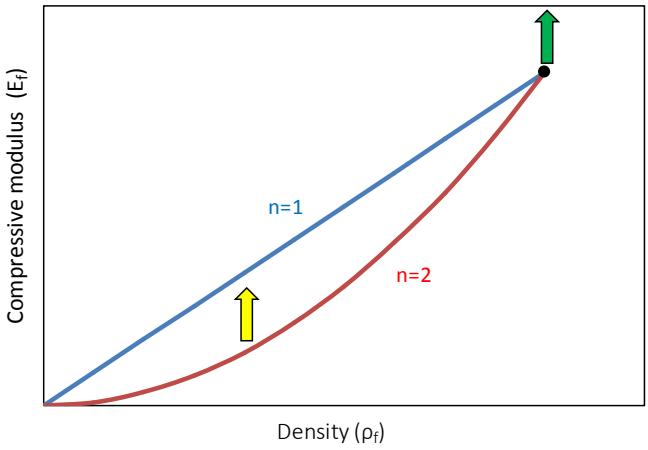

Figure 2.14.Compressive modulus versus density of a foamed material in terms of the cubic cell model.

From this model it is obvious that density is the main factor determining the mechanical properties of polymer foams. However, several strategies can be used to reduce the strong effect of density. One of them is improving the properties of the solid polymer matrix before the foaming process as pointed out by the green arrow in Figure 2.14. In this sense, the reinforcement with fillers, crosslinking and the blending with other polymers are typical approaches. The other one is improving the cellular structure to shift the exponent *n* from 2 up to values between 1 and 2 as marked by the yellow arrow. The improvement of the cellular structure can be carried out, for instance, by obtaining closed cell foams, reducing the width of the cell size distribution, increasing cell density and modifying the anisotropy ratio.

In the following sections (*2.4.1* and *2.4.2*) the previous strategies proposed to improve the mechanical properties of a polymer foam are tackled in more detail but being more focused on the production of *anisotropic cellular structures* and on the reinforcement of the polymer matrix with *natural fibres* and *nanoclays*. In principle, the use of *natural fibres* seems to be an ideal reinforcement strategy for starch-based materials with the aim of maintaining their bioderived and biodegradable character. Therefore, this strategy could be employed for the development of eco-friendly *food-packaging* trays as stated in *Chapter 1*. On the other hand, the development of polypropylene foams reinforced with nanoclays and with anisotropic cellular structures is also a

very interesting approach to increase the properties of the foam without crosslinking the polymer and hence, producing rigid foamed materials which can be recycled after end-use.

2.4.1- Improving the cellular structure: the role of Anisotropy.

There are several ways of improving the cellular structure of polymer foams in order to enhance their mechanical performance. *Decreasing cell size* in foams of the same density, as observed in Figure 15,could be one of them, but previous works reported a scarce influence of cell size in the mechanical properties measured at low strains [14,15,16]. On the other hand, *narrowing the cell size distribution* implies a homogeneous distribution of the solid polymer within the walls and struts along the foam volume resulting in better mechanical properties[2,3]. The performance of *closed cell foams* is undoubtedly greater than that of *open cell foams* because the faces can contribute to the overall mechanical response [1]. The gas contribution is generally negligible except for flexible polymers.

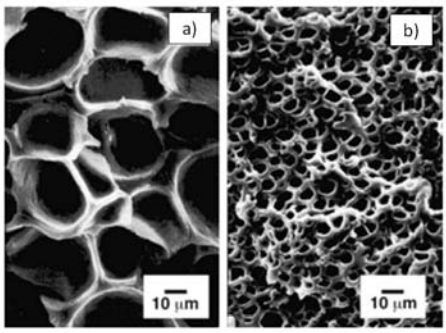

Figure 2.15.Policarbonate foams of the same density: 0.6 g/cm^3 and very different cell sizes: a) 21.5 µm. b) 4.9µm [14].

The production of anisotropic cellular structures (Figure 2.16) in a controlled way is still a challenge for scientists and industry. Anisotropic cellular structures are characterized as being composed of elongated cells and they can be found in nature, such as in Balsa wood, whose structure was previously shown in *chapter 1* (Figure 1.11). This kind of structure makes the mechanical response anisotropic. Several analytical models have been developed to describe the mechanical behaviour of foams with elongated cells, which are explained in the following sections.

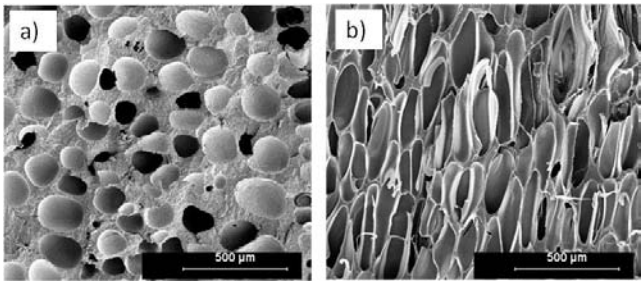

Figure 2.16. Polymer foams with different structures: a) isotropic cellular structure and b) anisotropic cellular structure.

2.4.1.1- Rectangular cell model.

Huber & Gibson [17] modified the cubic cell model with the aim of describing the mechanical properties of anisotropic polymer foams in terms of an idealized elongated cell. The concept is the same because the cell is held by squared cross-section beams of the same dimensions and is periodically distributed to fill the space. Nevertheless, the cubic cell turns into a rectangular prismatic cell in which the struts in the *z* direction are larger than those in the *x* and *y* directions as shown in Figure 17. The *z* direction usually coincides with the foam expansion direction. For this reason, this axis will be frequently denominated as the expansion direction throughout the work.

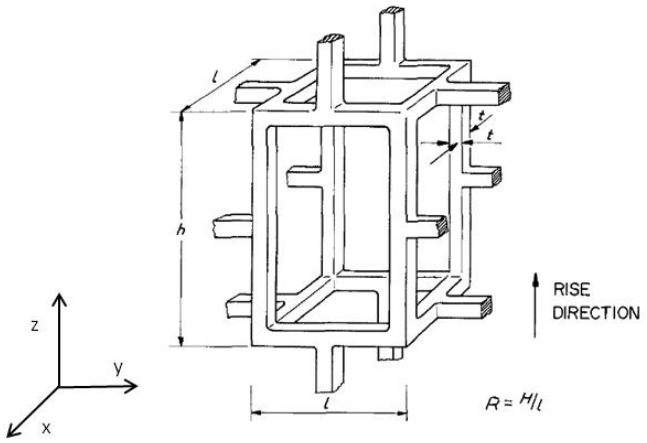

Figure 2.17. Rectangular cell used by *Huber* and *Gibson*.

The idealized *axysimmetric* cell represented in Figure 17 allows a morphological parameter to be defined called *shape anisotropy ratio* or *anisotropy ratio* (***R***) which is calculated by equation 2.2, that is, by dividing the length of the struts (*h*) in the expansion direction and the length in any of the other two perpendicular directions (*l*). Nevertheless, it is possible to find *orthotropic* foams in which the cell dimensions vary in the three directions(z≠x≠y) and therefore, the shape anisotropy ratio should be defined at least in two planes.

$$R = \frac{h}{l} \tag{2.2}$$

Elongated cells result in different mechanical properties depending on the loading direction. The compressive modulus of the cell represented in Figure 2.17, loaded in the expansion direction (z)and assuming bending as the deformation mode,is inversely proportional to the length of the beams, as shown in equation 2.3. Hence, the foam is weaker when loaded over the parallel planes to the expansion direction because their edges are larger.

$$E_f = CE_s\left(\frac{t}{l}\right)^4 \frac{h}{l} \tag{2.3}$$

The model of *Gibson & Ashby* can be modified by simply introducing the shape *anisotropy ratio* as shown in equation 2.4. This means that the modulus is proportional to the shape anisotropy ratio.

$$\frac{E_f}{E_s} = C\left(\frac{\rho_f}{\rho_s}\right)^n R \tag{2.4}$$

In addition, the ratio between modulus: $\boldsymbol{E_z/E_{x,y}}$, or in other words the *mechanical anisotropy* of the foam, is solely a function of ***R***, as described by equation 5.

$$\frac{E_z}{E_{x,y}} = \frac{2R^2}{1+\left(\frac{1}{R^3}\right)} \tag{2.5}$$

After observing equation2.5, it is clear that increments in the anisotropy ratio of the cells should lead to significant increments of the ratio between modulus. When considering anisotropic foams with closed cellular structures, equation 2.5 turns into equation 2.6, in which a new parameter (f_s) is included. This parameter represents the mass fraction in the struts (edges+ vertexes). The f_s of a completely open cellular structure, such as that of an open cell PU foam (Figure 7.a), is equal to one because there are no walls and hence, the entire solid polymer is found in the struts. f_s values lower than one indicates the presence of cell walls in the structure, which contribute to the overall stress of the foam.

$$\frac{E_{exp}}{E_{transv}} = f_s\frac{2R^2}{1+\left(\frac{1}{R^3}\right)} + (1-f_s)\frac{2R^2}{1+(1/R)} \tag{2.6}$$

The rectangular cell model of *Huber & Gibson* for open cell foams, in which f_s=1 (continuous line) and for closed cell foams (values of f_s lower than one) has been represented in Figure 2.18 together with experimental results found in literature in order to appreciate the important increment of the mechanical anisotropy with the shape anisotropy ratio better.

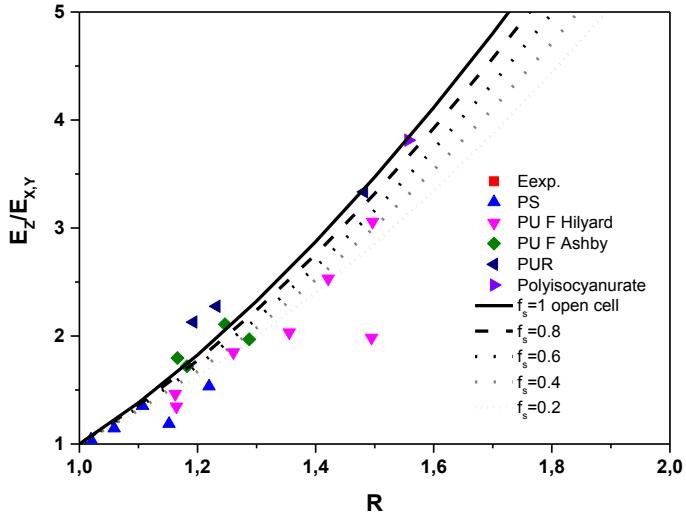

Figure 2.18.Compressive modulus ratio versus the shape anisotropy ratio. Theoretical model and experimental values for low-density polymer foams:(◀) PU(R), (♦) PU(F) [18], (▶) polyisocyanurate [19], (▼) PU(F), Hilyard [20] and (▲) PS [18].

2.4.1.2- Tetrakaidecahedron cell model.

A tetrakaidecahedron is a cell geometry which has been extensively used in literature because it is more similar to the real shape of cells in low density foams than the previous rectangular cell. Moreover, it also packs to fill the space. This geometry was originally employed by *Thomson* in 1887 to define what is called today the *Kelvin cell model* [21].

More recently, *Sullivan et al.* developed a general model also based on an elongated tetrakaidecahedron cell to calculate the foam stiffness [22,23]. This elongated tetrakaidecahedron contains eight hexagonal faces, two horizontal square faces and four vertical diamond faces as shown in Figure 19. The model was only developed for open cell foams (i.e foam without cell walls).

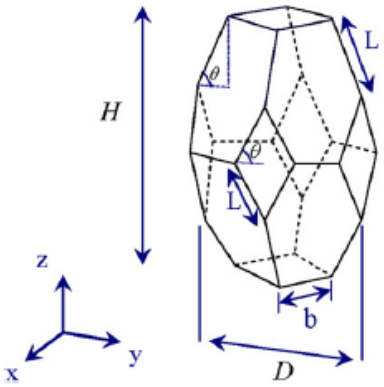

Figure 2.19. Elongated tetrakaidecahedron cell represented by *Sullivan et al* [22].

The size and shape of this cell can be defined by specifying three of the cell dimensions: *b*, *L*, *θ*, *H* and *D*. In this way, two morphological parameters arise: one is ***R*** or ***anisotropy ratio*** (equation 7)

and the other is ***Q*** (equation 2.8). Both of them can vary independently as specified in Figure 2.20 in which two elongated tetrakaidecahedron cells with the same *R* and different values of *Q* are shown.

$$R = \frac{H}{D} = \frac{4L\ sin\vartheta}{2Lcos\vartheta + 2\sqrt{b}} \tag{2.7}$$

$$Q = \frac{b}{L\cos\vartheta} \tag{2.8}$$

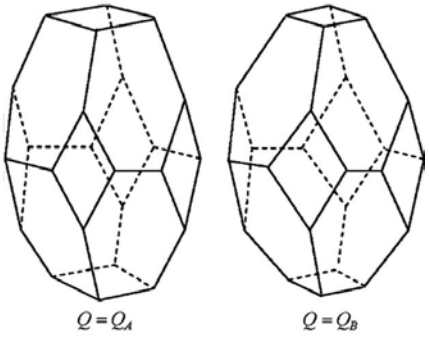

Figure 2.20.Tetrakaidecahedron cells with the same R but different values of Q.

Other authors, such as *Gong et al* [24], also employed an elongated tetrakaidecahedron cell to describe the mechanical behaviour of open cell foams but they restricted the shape of the cell to be exclusively function of θ because they assumed that $b/L=\cos\theta$. Nevertheless, there is no apparent reason to make such a restriction as these parameters can vary independently for simple geometrical reasons. Equation 2.9 was developed by *Sullivan* to describe the mechanical anisotropy of foams and it is written in terms of the cell dimensions (b, L and ϑ) and the relative density of the foam (ρ_f/ρ_s).

$$\frac{E_z}{E_{x,y}} = \frac{R^2}{4}\left[\frac{\left(2\widetilde{Q}^{\,2}R^2 + \frac{64Q^3}{\sqrt{16+\widetilde{Q}^{\,2}R^2}}\right)C_1 + \frac{8RC_2\widetilde{Q}^{\,3}\left(32+4Q\sqrt{16+\widetilde{Q}^{\,2}R^2}\right)}{\left(4Q+2\sqrt{16+\widetilde{Q}^{\,2}R^2}\right)(16+\widetilde{Q}^{\,2}R^2)}\left(\frac{\rho_f}{\rho_s}\right)}{16\,C_1 + \frac{8R^3C_2\widetilde{Q}^{\,5}}{\left(4Q+2\sqrt{16+\widetilde{Q}^{\,2}R^2}\right)(16+\widetilde{Q}^{\,2}R^2)}\left(\frac{\rho_f}{\rho_s}\right)}\right] \tag{2.9}$$

This model also predicts that the modulus in the direction in which the cells are elongated is much higher than the modulus in the perpendicular direction. The models presented in these last sections will be employed in *chapter 5* in order to analyse the mechanical behaviour of the PP based foams developed in this thesis.

2.4.2- Reinforcement with fillers: polymer composites.

The reinforcement of the polymer matrix with fillers represents another strategy to improve the mechanical performance of foams as denoted in Figure 14. In this way, the solid phase in the cell walls and edges becomes a composite. A biocomposite in the case of the TPS-based foams developed in this research because they are reinforced with *natural fibres* and a *nanocomposite* in the case of the PP-based foams investigated in this research because they are reinforced with *nanoclays*. In an ideal situation the polymer matrix acts not only as the fillers binder but also as the medium to transmit the external forces to them, while fillers are the component which truly supports the structure because their stiffness and strength are considerably greater than those of the matrix. Both components not only preserve their chemical and physical identities but also act together to improve the foam mechanical performance [2].

The mechanical properties of polymer composite-based foams cannot be exclusively evaluated in terms of how the solid phases involved, polymer and fillers, interact with each other. The effect of the fillers during the foaming process has also to be taken into account and this fact adds a great deal of complexity in these systems. For instance, it is known that fillers promote heterogeneous nucleation mechanisms during the first stages of foaming because the nuclei formation is favoured in the liquid-solid interface. As a consequence, the number of potential nucleating sites could be increased as shown in Figure 2.21 in which the fillers are represented by orange symbols and the cell nuclei by black circles. Theoretically, this fact should bring about the generation of more homogeneous cellular structures with higher cell densities and therefore, lower cell sizes. Moreover, a good adhesion between the solid phases causes variations of the polymer matrix viscosity, which in turn could affect other foaming stages such as the expansion stage and stabilization process.

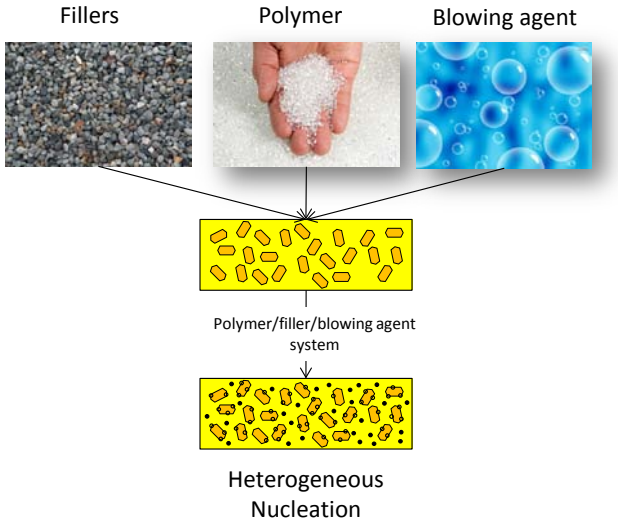

Figure 2.21.Heterogeneous nucleation of cells with fillers.

The fillers usually employed to reinforce polymers are classified according to several criteria as shown in the scheme of Figure 2.22. With regards to shape, they can be considered as *particles* or *fibres*. In terms of their chemical composition they can be *mineral* or *organic* fillers. Mineral

fillers such as calcium carbonate, talc, silica, clay, etc. have been used in the plastic industry for many decades with the main purpose of decreasing cost. On the other hand, functional mineral fillers, or *synthetic fillers* such as glass fibres, glass spheres and carbon fibres were developed with the aim of improving the performance of the polymer for structural applications. The main drawback associated with mineral fillers is their relatively high density [2]. Last but not least, fillers can be also classified in relation to their size: from micrometric fillers to nanometric fillers. This last classification will be dealt with in more detail in *section 2.4.2.3*.

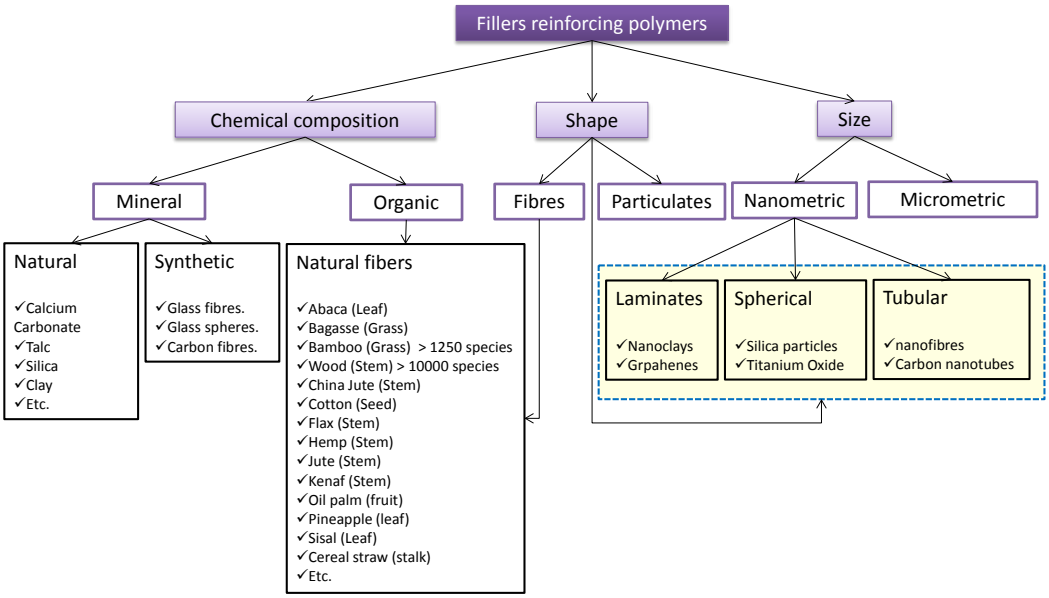

Figure 2.22. Fillers classification according to their chemistry, shape and size.

2.4.2.1- Natural fibres.

Organic fillers such as *natural fibres* are naturally occurring composites because they are composed of cellulose fibrils embedded in a lignin matrix, among other minor components such as hemicelluloses, pectin and waxes. This is the case of the natural fibres obtained from plants which have been used in the preparation of composites since historical times. At the beginning of the 20th century, they were principally used in aircraft applications but were progressively replaced by *synthetic fillers* due to the lack of data about their properties and to their lower mechanical performance. Their reinforcing effect lies in the cristallinity of cellulose. Cellulose is a natural linear polymer with a degree of polymerization about 10000 consisting of D-anhydroglucose ($C_6H_{11}O_5$) repeating units joined by 1,4-β-D-glycosidic linkages at C_1 and C_4position [25] (Figure 2.23).

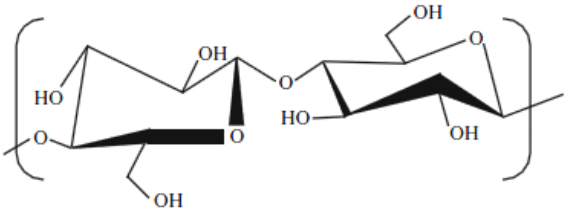

Figure 2.23.Chemical structure of cellulose.

Each repeating unit contains about three hydroxyl groups which are prone to establish hydrogen bonds. This fact decisively contributes to the crystalline nature of cellulose and finally, to its strength and stiffness. On the other hand, lignin is a complex hydrocarbon polymer with both aliphatic and aromatic constituents. It is hydrophobic in nature and it is considered to be a thermoplastic polymer with a glass transition temperature of 90ºCand a melting temperature of 170ºC. The mechanical properties of lignin are lower than those of cellulose [26,27].

Each one of the single fibrils composing natural fibres has a hollowed and complex layered structure such as the one shown in Figure 2.24. Within the layers, cellulose fibrils are arranged helically along the amorphous matrix composed of lignin and hemicellulose.

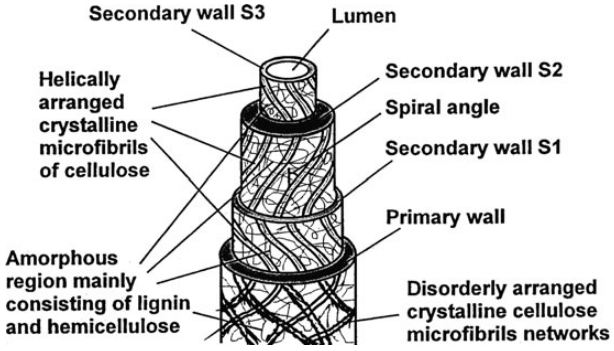

Figure 2.24.Layered structure of natural fibres [26].

The main advantages of *natural fibres* with respect to *mineral fillers* such as glass fibre are their lower cost, lower density and higher specific stiffness and strength. Table 2.1 shows a comparison between the properties of common natural fibres obtained from plants and those of the most representative fibres employed in the market such as glass fibre, carbon fibre and Kevlar.

Fiber	Density (g/cm^3)	Specific Tensile strength ($GPa\ cm^3/g$)	Specific Tensile modulus ($GPa\ cm^3/g$)	Cost (US dollar/tonnes)	Energy content (GJ/tonnes)
Plant fiber	0.6-1.2	1.60-2.95	10-130	200-1000	4
Glass	2.6	1.35	30	1200-1800	30
Kevlar	1.4	2.71	90	7500	25
Carbon	1.8	1.71	130	12500	130

Table 2.1.Comparison of properties and energy content, density and cost of lignocellulosic fibres and synthetic fibres [28].

Moreover, handling natural fibres is safer because dermal and respiratory irritations, normally produced when using mineral fibres, are reduced. They are non-abrasive for the machinery employed in their processing, thus the costs associated with machine maintenance are reduced. They are good thermal and acoustic insulators because of their hollowed structure. Last but not least, the environmental impact associated with their use is lower because they are a renewable resource available worldwide and their production requires little energy. In this way, agricultural industry is favoured because the value of this natural product is increased, which otherwise would be a residue.

On the other hand, they also present some drawbacks. *Natural fibres* have a polar chemical nature which makes their mixing with non-polar thermoplastics obtained from fossil-resources very difficult. This fact also contributes to high moisture absorption leading to swelling and to the presence of voids in the interface between the fibres and the polymer. The processing temperature of the resultant composites is restricted to 200ºC as fibres undergo degradation at higher temperatures. Their microbial resistance is very low making the composites produced susceptible to rooting. Moreover, their properties are not as homogenous as those of *synthetic fillers* because of their natural origin. These drawbacks make the replacement of *mineral fibres* such as *glass fibres* for *natural fibres* for the reinforcement of synthetic polymers challenging.

2.4.2.2-Starch-based biocomposites.

The inherent polarity of *natural fibres* makes them ideal fillers when used as reinforcement for starch-based materials because both, starch and cellulose, share the same repeating unit: glucose. In fact, starch is a polysaccharide composed of two polymers: *amylose* and *amylopectin*. *Amylose* is a primarily linear polymer with (1→4) li nked α-glucosyl units whereas *amylopectine* presents multiple branches joined to the main chain by (1→6) linkages. Minor components are also found in starch such as lipids, proteins, fatty acids and phosphate ester groups. Starch is synthesized in the *amyloplast* of plant cells where it is densely packed in the form of semicrystalline granules (Figure 2.25) with a density of around 1.5 g/cm^3. Starch can be found in seeds, roots, tubers, stems and leaves representing their main source of energy during germination or whenever energy is needed for the plant.

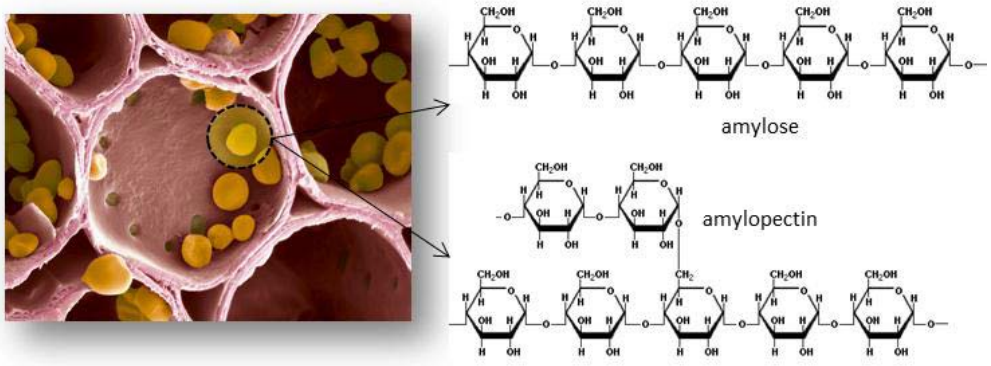

Figure 2.25.Starch granules in the amyloplast. Amylose and amylopectine chemical structure.

Starch is extracted from the plants by gravity sedimentation, centrifugation and filtration [29]. Depending on the botanical origin, starch granules have different shapes: spherical, oval, polygonal, disk and elongated to name but a few, and different sizes: from less than 1 μm to 100 μm in diameter[29]. The granule morphology of the two starches employed in this work is shown in Figure 2.26. Potato starch granules can be either oval or spherical while wheat starch presents a bimodal distribution of sizes in which the large granules have a disk shape and the small granules have a spherical shape.

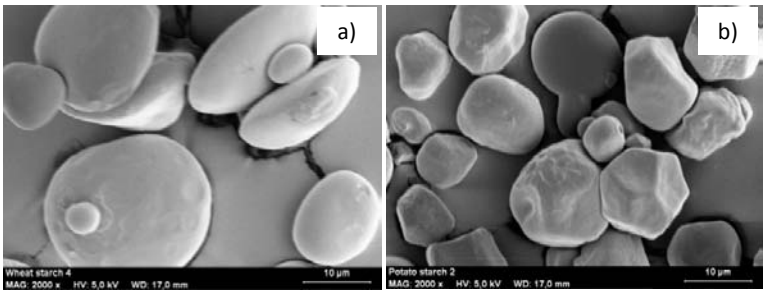

Figure 2.26. Starch granules used in this research: a) Wheat starch. b) Potato starch.

Starch is a semicrystalline polymer with crystalline contents varying from 15 to 45% [29].The model that describes the inner structure of starch granules is shown in Figure 2.27. In this model the granule consists of 120 to 400 nm thick concentric shells, which alternates between low-density semicrystalline and high-density crystalline shells. These shells in turn, are made of approximately 10 nm thick lamellae which are believed to be organized into pseudo-spherical structures called *blockets*.The pores present on the surface of the granules are the external openings of interior channels located within the starch granule [30].

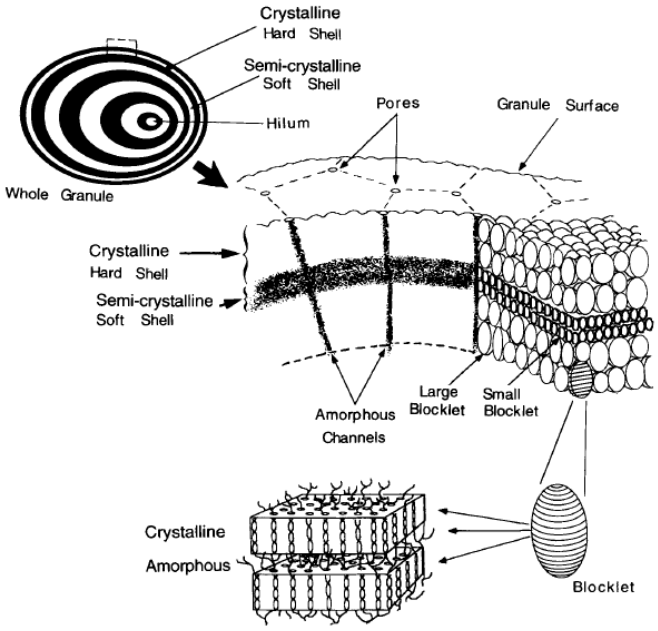

Figure 2.27.Organization model of the starch granule structure.

The processing of starch granules by common plastic industrial equipment such as extruders, injection machines and presses is very difficult because they only melt after being degraded. Some works reported that the *glass transition temperature* (T_g) of dry amylose and amylopectin is 227 °C, whereas others determined that the T_g of dry starch is 332 °C [31]. For this reason, starch in the form of granules was originally employed as natural filler in synthetic polymers so as to decrease the final cost of the composite and at the same providing it with certain biodegradability [32-34]. However, only a limited amount of starch, around 30 % in weight, could be added. The plasticization of starch allowed it to be blended with other polymers in greater amounts. Moreover, the processing of starch itself improved because granules turn while plasticized into *thermoplastic starch* (TPS) which is a material mostly amorphous material with a lower glass transition temperature. Nowadays, TPS is commercially available [35] and used for certain applications such as plastic bags [36].

The plasticization process is called *gelatinization* when starch is diluted with water and heated. The process is split up into several stages: diffusion of water into the starch granule, water uptake by the amorphous regions, loss of crystalline order, radial swelling of the granules, and amylose leaching. Finally, starch granules completely disintegrate and form a viscous batter [37].This process is shown by light microscopy in the images of Figure 2.28.

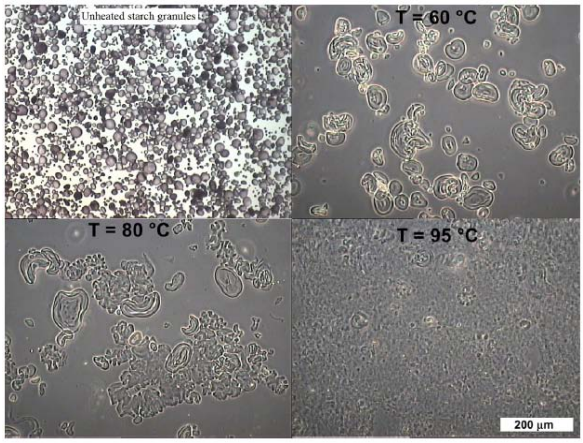

Figure 2.28. Light micrographs of wheat starch gelatinization under microwave radiation [37].

Plasticization can be carried out not only under heat but also under shear forces in *twin screw extruders* or *internal mixers*. Figure 2.29 shows pellets obtained after plasticizing starch in a twin-screw extruder and a SEM image showing the continuous morphology of TPS, similar to that of other synthetic thermoplastics.

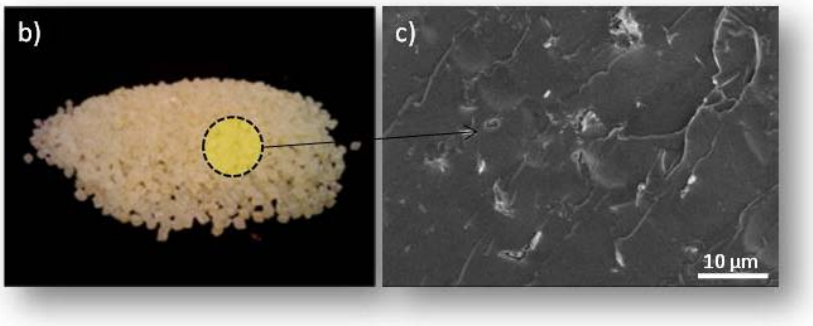

Figure 2.29. a)Thermoplastic starch pellets. b)SEM micrograph of a plasticized starch produced during this thesis.

Efficient plasticizers are generally molecules or polymers with low molar mass and therefore, with low viscosities. The mechanism of plasticization is mainly based on the formation of hydrogen bonds between the plasticizer and starch. Common plasticizers are water, glycerol, sorbitol, urea and formamide but water and glycerol are the most frequently employed [38,39]. Water, because it is widely available and cheap. Nevertheless, the processing conditions are very stringent because of its low volatilization temperature (100ºC) and because the composites obtained are less durable, prone to rooting and more sensitive to environmental conditions. Water is usually employed when TPS is subsequently foamed because it could also acts as the blowing agent. On the other hand, glycerol is a better alternative when solid composites are to be produced. Its volatilization temperature is higher (≈290ºC) and hence, the range of processing temperatures increase substantially. Moreover, the TPS materials obtained with glycerol are more durable. However, TPS plasticized with glycerol during storing suffers from aging or retrogradation, which is a recrystallization phenomenon that makes TPS brittle at ambient temperature in time. Urea is a plasticizer that acting alone avoids aging but the resultant TPS is brittle itself and mixtures with other plasticizers are required [38-39].

The plasticization process of starch involves a drastic change of its physical properties. One of which is the reduction of mechanical properties due to the loss of crystalline order. The degree of mechanical property reduction depends on the kind and amount of plasticizer employed although the degree of plasticization is the factor with the greater influence. An optimum content of glycerol was found to be in the range of 20-35 wt% (percentage in weight). Lower amounts result in brittle TPS and higher amounts lead to glycerol exudation.

Starch plasticized with high contents of glycerol (about 35 wt%) is a material with an adequate viscosity to be processed in plastic equipment and it is soft and ductile at ambient temperature. Nevertheless, its stiffness and strength are low in comparison with most of synthetic polymers. The reinforcement with natural fibres represents a good approach to increase these mechanical properties and at the same time to maintain the bioderivability and biodegradability of starch. There are several works in literature dealing with the reinforcement of TPS with natural fibres. In most of them the plasticizer contents are about 30wt%andglycerol is the plasticizer employed. Table 2.2 shows a list of the main works on the topic specifying the kind of starch, plasticizer and natural fibre employed, the production route followed and the conditioning of the sample

carried out prior to the mechanical tests which is very important due to the water sensitivity of starch.

Author	Starch	Plasticizer	Natural fiber	Production method	Conditioning
Averous[40]	Wheat	Glycerol and water	Leafwood[a]	Single screw extruder+ injection	23ºC. 54%HR. 42 days
Curvelo[41]	Corn	Glycerol	Eucalyptus urograndis	Internal mixer+ thermoforming	22-25ºC. 43%HR. 14 days.
López[42]	Corn	Glycerol	Recovered newspaper	Internal mixer+ thermoforming	Drying to 70ºC for 120 hours/ 53%HR. 20 days.
Martins[43]	Corn	Glycerol	Bacterial cellulose[a]	Internal mixer+ injection	25ºC. 50%HR.
			Eucalyptus globulus[a]		
Belhassen[44]	Starch-based biopolymer blended with biodegradable polyester		Esparto *Alfa* fibres[a]	Internal mixer+ injection	23ºC. 50%HR. 3 days
Gironés[45]	Corn	Glycerol	Sisal	Internal mixer+ thermoforming	Drying to 70ºC for 120 hours/ 53%HR. 20 days.
			Hemp		
Wattanakornsiri[46]	Tapioca	Glycerol	Office paper[a]	Internal mixer+ thermoforming	23-25ºC. 44-55%HR. 14 days.
			Newspaper[a]		
Teixeira[47]	Corn	Glycerol	Cotton nanofibres	Twin screw extruder+ thermoforming	Drying to 70ºC until constant weight/ 23ºC. 53%HR. 30 days.
Müller 1[48]	Cassava	Glycerol	Eucalyptus	Casting	25ºC. 58%HR.
Müller 2[49]	Cassava	Glycerol	Softwood short fibres	Casting	25ºC. 58%HR. 2 days
Ma[50]	Corn	Formamide+Urea	Micro winceyette fibre	Single screw extruder+ injection	1 week in plastic bags
[a]Chemically treated to isolate the cellulose fraction.					

Table 2.2. Biocomposites based on TPS reinforced with natural fibres reported in literature.

Several natural fibres of different botanical origins were used in these works such as sisal, hemp and eucalyptus. The final properties of these biocomposites were determined by the chemical composition of the fibres and compatibility with the polymer matrix, the fibres volume fraction, their shape and aspect ratio, their size and finally to the degree of distribution throughout the matrix. The morphology of some of the fibres employed in these works is shown in Figure 2.30, which also includes a SEM micrograph showing how natural fibres are distributed along a thermoplastic starch matrix (Figure 2.30d).

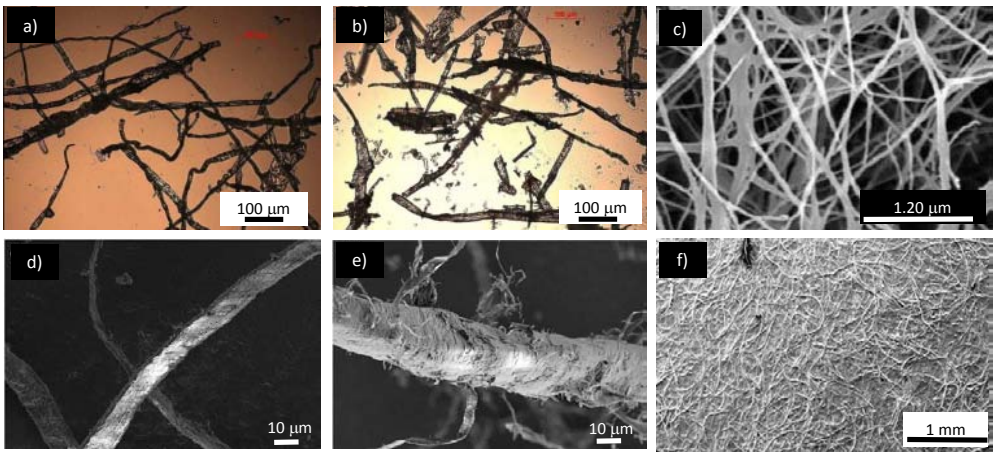

Figure 2.30. Optic micrographs and SEM micrographs of different fibres: a) leafwood cellulose fibres [40]. b) paper pulp fibres [40], c) bacterial cellulose fibres [43],d) office paper fibres [46], e) newspaper fibres [46],f) cassava starch film reinforced with eucalyptus cellulose fibres [48].

Figure 2.31 shows plots representing mechanical properties of the TPS-based composites listed in Table 2.2relative to those of the corresponding TPS without fibres: *relative tensile modulus*(E_c/E),*relative tensile strength* (σ_c/σ) and *relative elongation at break* ($\varepsilon_{bc}/\varepsilon$) versus the natural fibre loading.

These plots will be very useful to evaluate the reinforcement efficiency of the natural fibres used in this work (*chapter 4*) which would be key taking into account that their botanical origin: *barley*, *grape* and *cardoon*, are very different to those of the natural fibres traditionally employed in literature (Table 2.2).

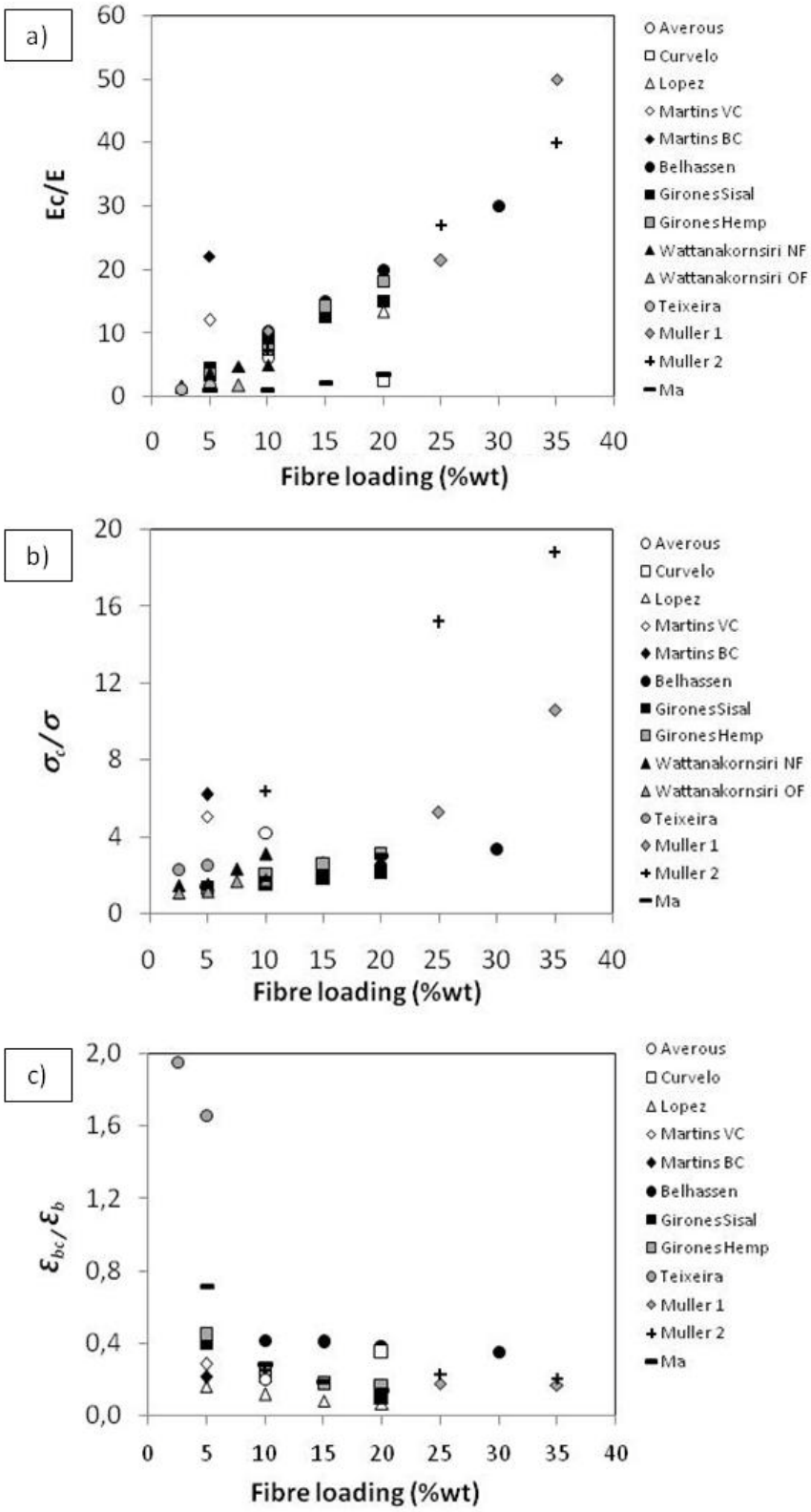

Figure 2.31.Variation of properties with the addition of natural fibres for the systems of table 2. a) Relative tensile modulus. b) Relative tensile strength. c) Relative elongation at break.

In all these works tensile modulus and strength increases with the addition of natural fibres while the elongation at break decreases. The principal reason found for such improvement is the chemical compatibility between both materials, as the tensile load is effectively transferred from the matrix to the fibres due to H-bonding between the hydroxyl groups of starch and cellulose [42].On the contrary, the strengthening of the TPS matrix implies a reduction of elasticity and ductility. This effect is expected considering that fibres imparts rigidity and restrains the deformation of the matrix [45].

The ***chemical composition*** of these fibres differs because some of them were chemically treated to isolate the cellulose fraction and increase their reinforcing effect. The reason given is that cellulose is composed of glucose as the polymer chain repeating unit, which is polar and therefore, with a high chemical affinity with starch whose polymer backbone is composed of glucose as well. On the contrary, lignocellulose fibres have lignin on their surface, which is a less polar component [40]. Figures 2.30a and b show two kinds of fibres with apparently similar morphology but with different chemical composition. The *cellulose* based fibre (Figure 30.a) displayed better mechanical properties than the *lignocellulose* based fibre (Figure 30.b) However, other works stated the opposite claiming that lignin could act as an interfacial compatibilizer between fibres and starch. Lignin, due to its constituent hydroxyl groups and to its location on the surface of the fibres, is able to establish on the one hand, covalent bonds with cellulose and on the other hand, with glycerol and starch [48].

Fibre morphology is usually specified by its ***aspect ratio*** which is the ratio between its length and its diameter. It is generally assumed that fibres with high aspect ratios produce larger reinforcements in the polymer matrix than short fibres with low aspect ratios[51]but at the same time, they are more susceptible to damage during the composite production in the sense that fibres are shortened[44]. The level of damage increases with the amount of fibres added due to the increased probability of fibre-fibre and fibre-machine interaction and to the higher melt viscosity of the composite, resulting in higher bending forces during compounding and moulding.

Size is another important morphological parameter. For instance, the mechanical performance of *Bacterial cellulose fibres,* composed of a tri-dimensional network of nano and microfibrils (Figure2.30c) is higher than that of conventional vegetable fibres at the same loading level [43].*Nanocellulose* is produced by acid hydrolysis of cellulose under controlled temperature conditions. After this process, a suspension of needle-like particles with lengths and diameters of the order of nanometres are obtained. *Cotton cellulose nanofibres* and *Cassava bagasse cellulose nanofibrils* were employed to reinforce TPS with very interesting results because the usual increase in tensile modulus and strength obtained with the addition of natural fibres did not involve in this case a loss of elasticity. On the contrary, elongation at break increased with the addition of *cellulose nanofibres* [47,52].

The influence of the fibres ***surface*** was also considered. Figure 2.30e shows cellulosic fibres obtained from newspaper with a hair follicle and rough surface. These fibres, after being mixed with TPS, resulted in higher tensile strengths and modulus than composites produced with

cellulose fibres obtained from office paper whose surface is smother (Figure2.30d). The first surface could provide stronger intrinsic adhesion between the fibres and the matrix [46].

Not only the mechanical properties of TPS are affected by the addition of fibres but also its characteristic thermal transitions such as the glass transition temperature (T_g). Taking the high chemical affinity of both materials into account a restriction of the polymer chains mobility in the vicinity of the fibre phase is expected, resulting in an increase of the overall T_g. This increment can also be due to the interaction between the fibres and the plasticizer that makes the polymer matrix less plasticized than the pure sample. This fact has been reported in literature by means of differential scanning calorimetric measurements (DSC) and by dynamic mechanical thermal analyses (DMTA) [40-46].

TPS is very sensitive to the environmental humidity because of its hydrophilic character. This fact is an advantage when the degradation of the polymer after end-use is studied. Composting conditions usually involve wet environments and therefore, the degradation process of TPS is accelerated. On the other hand, it is a drawback during the service period of the polymer because mechanical properties and dimensional stability are clearly influenced by the absorption of water due to the plasticizing effect of water. The incorporation of *natural fibres* could reduce the water sensitivity of TPS because of fibre-matrix interactions and due to the hydrophobic character of cellulose. However, there is not a full agreement in this respect. In some cases the results reveal a clear reduction of the water absorption with the addition of fibres [41-46,49,53,54].In others, the results are not so conclusive [42,45]. In any case, the absorption of water seems to be more dependent on the relative humidity of the atmosphere to which TPS is exposed than on the incorporation of natural fibres.

One of the reasons for selecting three kinds of natural fibres in this work (*barley*, *grape* and *cardoon*) is that they present very different morphology in terms of shape, size and aspect ratio. These morphological parameters have been found to be very important when determining the final properties of starch-based composites as this brief description of the literature has proved.

2.4.2.3- Polymer nanonocomposites: nanoclays.

Explaining the chemistry and structure of nanoclays and how they interact with the polymer in which they are embedded is one of the objectives of this section. During the last 25 years the development and synthesis of nanoparticles has brought about a new class of materials with multifunctional properties called *polymeric nanocomposites.* Their origin dates back to the early 1990s when the *Toyota Central Research Laboratories* in Japan produced a nanocomposite based on Nylon-6 in which small amounts of nanofillers enhanced substantially the thermal and mechanical properties of the original polymer [55].They are called nanoparticles because at least one of their dimensions is in the range of nanometers and can be classified according to their shape (Figure 2.32). They can be considered as ***laminates***, with a platelet-like structure, in which only one of their dimensions is in the range of nanometres (*nanoclays* and *graphene*), ***tubulars*** in which two of their dimensions are in the range of nanometres while the third is larger, even in the micron scale, resulting in elongated structures (*carbon nanotubes* and *nanofibres*) and finally

spherical in which all the dimensions are in the nanometric scale (*silica particles, nanocrystals, gold and other metal nanoparticles and titanium oxide*) [56].

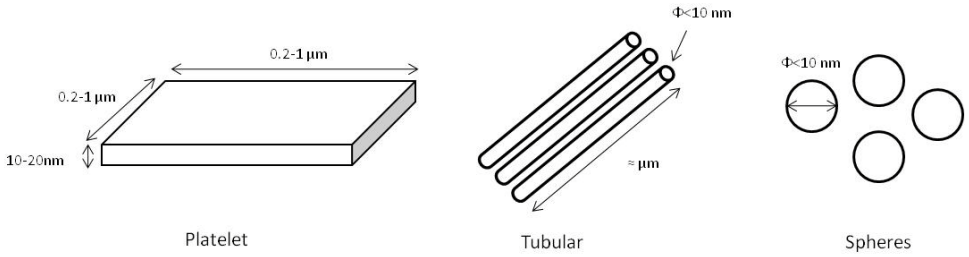

Figure 2.32.Nanoparticles classification as a function of their shape.

An interesting example of tubular nanoparticle is *vapour grown carbon nanofibres* (*VGCNF*) which are hollow cylinders with diameters of around 100 nm and lengths of few microns resulting in high aspect ratios (length/diameter≥100). They posse ss very high mechanical properties having Young´s modulus in the range 100-1000 GPa and tensile strength between 2.5 and 3.5 GPa and very high electrical conductivities (10^3 S/cm). Figure 2.33 shows a TEM image of VGCNF and a SEM image of a VGCNF/epoxi nanocomposite [57].

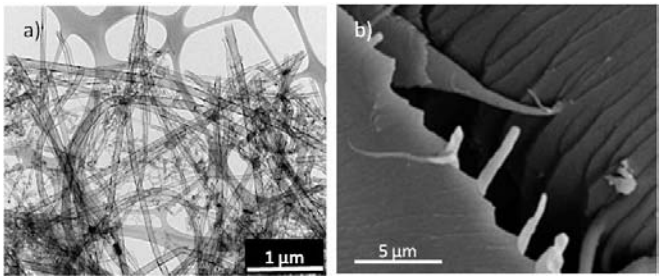

Figure 2.33.a) TEM image of VGCNF. b) SEM image of VGCNF/epoxy nanocomposite.

The reason why the range of properties is substantially wider with respect to their micrometric counterparts resides in the higher *surface/volume* ratio of nanoparticles. With regards to mechanical properties, the load transfer surface from the polymer to the filler is increased. From another point of view, it is possible to load the polymer with lowers amounts of fillers than with microparticles to produce the same effect because the reinforcement with nanoparticles is more effective. The works of *Kojima et al* based on the reinforcement of Nilon-6 with modified nanoclays and that of *Zohu et al* in which polyester-based polyurethanes films were reinforced with nanosilica particles are clear examples of how mechanical properties such as hardness, abrasion resistance and tensile properties are enhanced by the addition of low amounts of nanoparticles [58,59]. The improvement of mechanical properties is conditioned to an effective degree of adhesion and dispersion [60].Nanoparticles, precisely due to their elevated *surface/volume* ratio tend to agglomerate more easily than microparticles.

A good dispersion is dependent on the nanocomposite production method. Three approaches have been usually adopted: ***solution-blending***, ***melt-blending*** and ***in-situ polymerization***. In the case of *solution-blending* a solvent mixture is used to dissolve the polymer and at the same time to disperse nanoparticles. It is a very attractive method when it comes to water-soluble

polymers. On the contrary, when considering hydrophobic polymers, large amounts of non-water based solvents are required and hence, the product cost becomes very high. Nanoparticles tend to re-agglomerate upon solvent removal and moreover, the selection of the proper solvent for each kind of polymer is critical. In the *in-situ polymerization* method, nanoparticles are mixed with the monomer prior to polymerization. The dispersion degree is typically enhanced with respect to the other methods because of the low monomer viscosity. Finally, *melt- blending* processes are preferred because the use of expensive solvents is avoided and it is compatible with industrial polymer extrusion and blending processes. It represents a cost-effective processing route of polymer nanocomposites. For instance, the clay and the polymer can be fed together into a twin- screw extruder at high temperatures, usually above the melting temperature of the polymer. They are held at this temperature for a period of time and put under shear to encourage intercalation and exfoliation of the clay. Most of the works reported so far in relation to polypropylene based naocomposites employed this technique. The processing conditions, especially the shear rate, have important effects on the dispersion degree and on the final structure [56].

The degree of adhesion depends on the chemistry of both polymer and nanoparticles. There are several kinds of nanoparticles employed for the development of polymer nanocomposites but *layered silicates* are the most widely studied because of their unique features and lower cost with respect to carbon nanotubes, carbon nanofibres etc. They have a platelet-like geometry with distances between the platelets about 1 nanometre as shown in Figure 2.34.These platelets are assembled as a gallery of parallel layers packed together by dipolar and Van der Waal forces between each single layer and Na^+ and Ca^{2+}cationslocated in the interlayer space. The lateral dimension of these galleries (or primary particles) may vary from 30 nanometres to several micrometres. Their aspect ratio is between 100 and 1000 and the surface area is about 750 m^2/g [61,62].

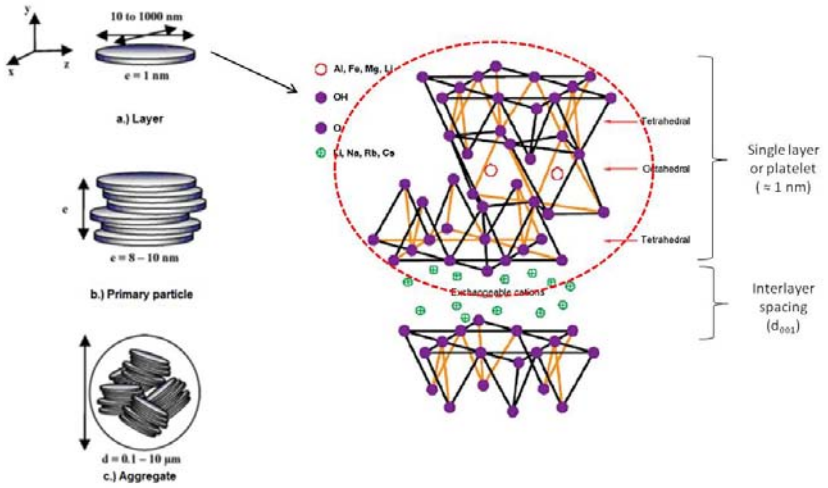

Figure 2.34.Multilayer structure of layered silicates.

Among the general family of 2:1 layered silicates, *montomorillonite* has received a great deal of attention because of the weak dipolar and Van deer Waal forces that join the platelets together.

Each individual platelet is composed of a tetrahedral and octahedral range of oxygen and hydrogen atoms with central silicon atoms in the case of the tetrahedrons and central aluminium atoms in the case of the octahedrons. The Na^{+} and Ca^{2+}cations residing in the interlayer spacing can be easily replaced by organic cations such as *alkyl ammonium ions* via an ion-exchange reaction. This organic cations due to their long non-polar alkyl groups turn the silicate layer into organophilic and therefore, the compatibilization with organic polymers such as polypropylene is easier. Moreover, the organic cations increase the interlayer spacing and during the production of the nanocomposites, the polymer chains are able to penetrate between the layers more easily producing their effective exfoliation and dispersion throughout the whole polymer matrix.

The exfoliation and dispersion degree sets the morphology of the polymer nanocomposite obtained, as observed in Figure 2.35. A *phase-separated microcomposite* is produced when the polymer is unable to penetrate between the clay platelets. It is called microcomposite because the platelets form microscopic agglomerates. An *Intercalated nanocomposite* occurs when there is a partial intercalation of the polymer chains between the platelets. Finally, when the individual layers are completely separated by the polymer chains and are uniformly dispersed within the polymer matrix, an *exfoliated structure* is obtained. The degree of exfoliation is usually evaluated by means of X-ray diffraction. Pure nanoclays usually exhibits a single peak linked to the interlayer spacing (d_{001}), which can be calculated by Bragg´s law. When nanoclays are intercalated by the polymer, the interlayer spacing increases and when they are exfoliated, the peak disappears (Figure 2.35).

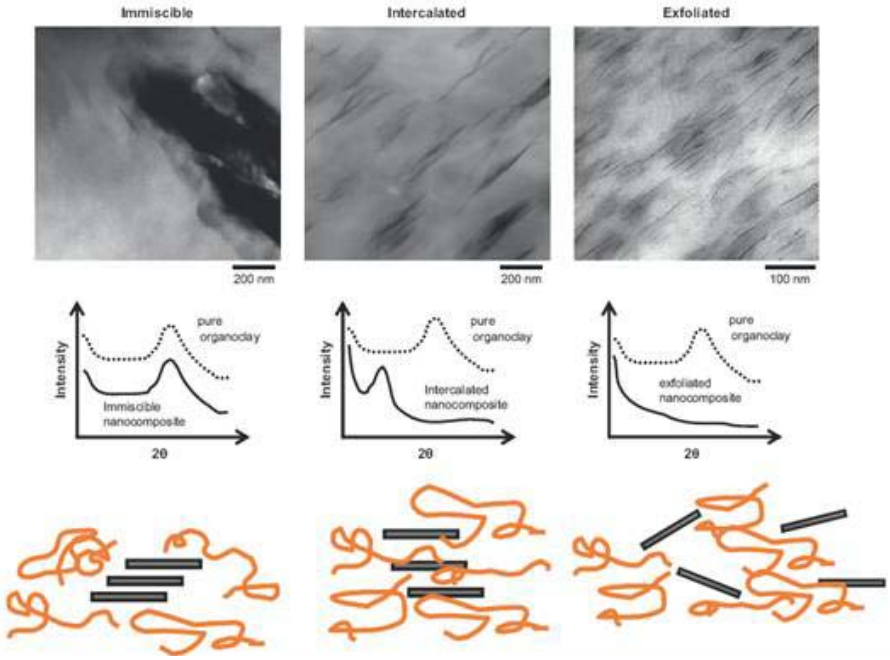

Figure 2.35.Types of polymer nanocomposites depending on the degree of exfoliation.

Many research works in literature address the production of polypropylene-based nanocomposites reinforced with nanoclays in order to increase the mechanical properties of the pure polymer. These materials are gaining special attention due to the industrial interest in

using PP for automotive applications in which lightweight materials with high stiffness and strengths are required [63,64,65]. The mechanical property improvement is not only associated with the intrinsic reinforcing effect of nanofillers but also with the morphological changes induced in the polymer because nanoparticles can act as nucleating agents during the crystallization process [66,67,68].

This thesis has been mainly focused on how the cellular structure and consequently, the mechanical properties of PP-based foams are modified by the presence of nanoclays within their cell walls, edges and vertexes, which is a very complex task due to the multifunctional effect of nanoparticles during the foaming process. More details about these aspects will be given in *section 2.6.3*.

2.5- Starch-based foams.

Starch-based foams were originally produced to obtain cereal snacks because foaming alters their texture and make them appetizing and crisp (Figure 2.36). Starch, as the dominant polymer in cereal composition, plays a major role in their expansion, although there are other components such as proteins, sugars, fats and fibres that could also bear a certain influence. This fact adds a great deal of complexity to the understanding of the expansion of starch-based food. There are few works in literature dealing with the topic [69,70].

Figure 2.36. Expanded cereal snacks.

Nowadays, starch is finding new market niches as a bioderived and biodegradable polymer due to the rising environmental awareness caused by the huge amount of plastic waste which is being generated as commented in *Chapter 1*. In this sense, starch is starting to be employed for the production of packaging products such as plastic bags and trays. The Spanish national project *ACTIBIOPACK,* which represents the framework of this investigation*,* is a clear example of this general trend (*section 1.2.4.1*) because its principal target was the development of biodegradable food-packaging trays based on solid and foamed starch.

Several processes such as *extrusion*, *baking* and more recently *microwave heating* have been used to produce foamed starch. In spite of the differences found in the machinery employed and the source of heat, the expansion of starch-based materials always follows a similar pattern which is not very different from the one explained in *section 2.2*. Nevertheless, there are certain differences that make this foaming process peculiar, the most important being how the cellular structure is stabilized. In fact, the viscosity increase required to stabilize the cellular structure is achieved by other means different to crosslinking or cooling. In most of the technologies employed to foam starch water plays a key role because it acts not only as the plasticizer of starch but also as the blowing agent. Figure 37 shows a plot which explains the foaming process of starch from a state in which it is a solid precursor with a determined height ($h_{precursor}$) to a final state in which it becomes a foam with a higher height (h_{foam}). In this plot the temperature of the sample subjected to foaming is presented versus the moisture content of the polymer. This plot was drawn up with the aim of describing a microwave foaming process but most of its fundamentals can also be applied to other foaming processes of starch.

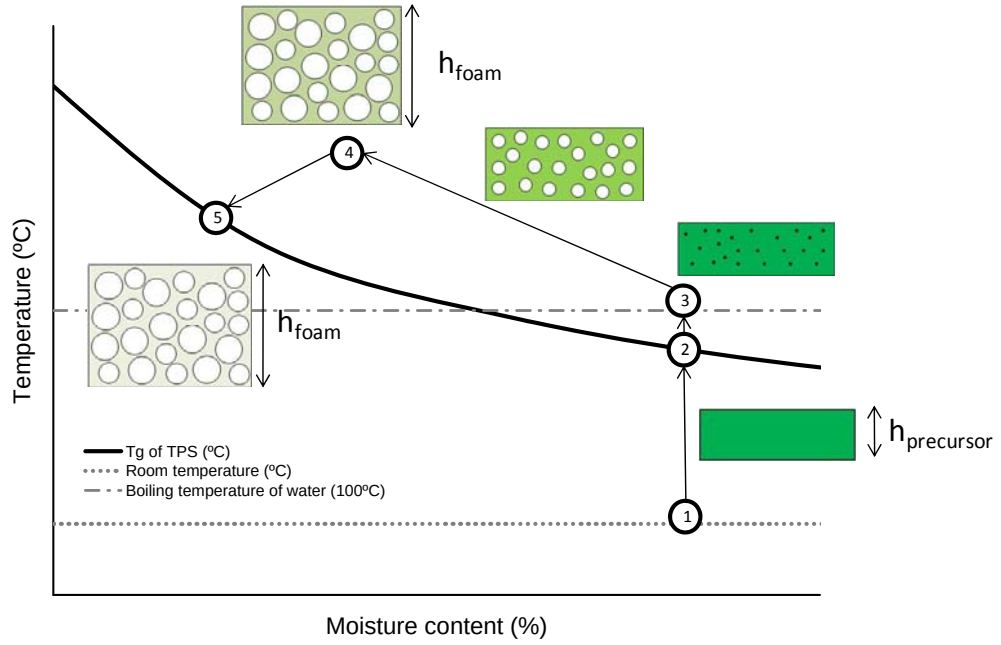

Figure 2.37. Diagram for microwave expansion of starch plasticized with water [70].

First of all, starch granules are plasticized with water. In this process, the semicrystalline granules turn while being plasticized into a rubber-like material (TPS) in which water molecules are dissolved into the polymer matrix. Depending on the level of plasticization, the TPS obtained could be in a rubbery state at ambient temperature (above its T_g)or in a glassy state as represented in the plot (stage 1). The T_g of the TPS sample is represented by the black solid line which shows the high dependency of the T_g with the moisture content. During the whole foaming process, the temperature of the sample is constantly rising. Between 1 and 2, the sample is in the glassy state but after undergoing stage 2, the precursor becomes rubbery because its temperature is higher than the T_g of the polymer. Then, when reaching boiling point (stage 3), cells nuclei appear and water goes from the polymer matrix to the cells as steam expanding the polymer melt (between 3 and 4).The polymer matrix is gradually losing water during this process and hence, its T_g increases. At the same time, the water volatilization contributes to cooling down the foam due to the enthalpy exchanged. Once the microwave radiation supply ceases (4), the temperature of the foam decreases. Finally, when the T_g of the polymer matrix becomes higher than the foam temperature, the polymer matrix undergoes a new transition but in the opposite direction, that is, from rubbery to glassy and then the cells are not able to continue growing and the foam is stabilized.

Therefore, in the case of starch foams in which water acts as the plasticizer and the blowing agent at the same time, the cellular structure is stabilized due to physical changes of the polymer induced, in this case, by the loss of plasticizer and not by crosslinking or by cooling as is the normal approach in common polyolefin foaming processes.

Moreover, the use of water as the blowing agent represents an additional contribution to the general aim of this thesis of producing more sustainable foams (*Chapter 1*) because it is very

abundant and renewable and in this way, more common *physical* and *chemical blowing agents* are avoided which on some occasions, release toxic substances to the atmosphere or remain in the final foam which is produced.

2.5.1- Starch foaming processes.

The foaming of starch-based materials by water always follows a similar pattern when it comes to the mechanisms involved although several differences can be found regarding the source of heat employed and the way of transferring it, the pressure applied to the system (*P*) and the equipment employed. Figure 2.38 shows an scheme in which the three main processes used to foam starch with water are classified according to the previous criteria.

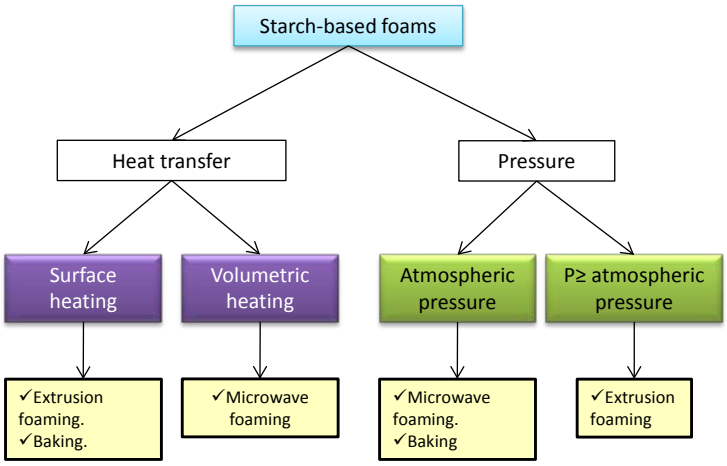

Figure 2.38. Classification of starch-based foaming processes based on the pressure applied and the heat transfer.

2.5.1.1- Extrusion foaming.

This section is especially dedicated to the main parameters influencing the production of starch-based foams by *extrusion foaming*. However, a more detailed explanation of this process and its fundamentals will be found in *section 2.6.1.1*, which is more focused on the production of polyolefin foams. The most important parameter to control cell size in this process is pressure. Most of the industrial foaming processes employ high pressures to produce foams with fine microcellular structures and with homogeneous cell size distributions. The high pressures applied over the *polymer-blowing agent* system allow gas molecules to remain dissolved in the polymer melt. This equilibrium is altered by a sudden depressurization. Trying to find a new equilibrium at atmospheric pressure, gas molecules escape from the polymer, forming cells. In *extrusion foaming* the depressurization of the system takes place at the exit of the die.

In the case of starch-based foams the plasticized batter formed along the extruder length face up to atmospheric pressures at the exit of the die and the steam generated expand the polymer matrix. Figure 2.39 shows schematically how the cellular structure evolves from the moment in which the *polymer/blowing agent* system exits the die: nucleation, bubble growth and degeneration of the cellular structure that promotes some contraction of the material.

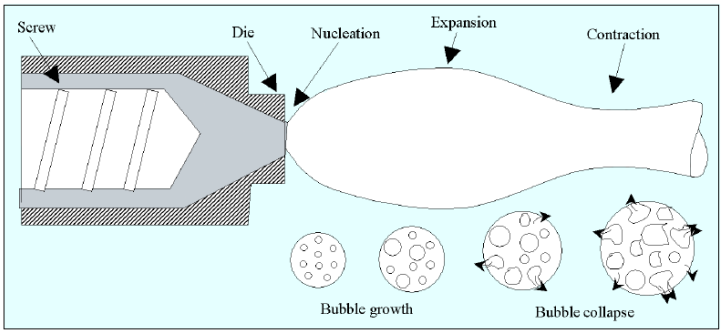

Figure 2.39.Extrusion foaming of starch[70].

Extrusion foaming has been one of the main methods employed to foam starch-based materials because it is a continuous process with high output rates. Nevertheless, as far as packaging applications are concerned this process has an important drawback that lies precisely in the cellular structure stabilization mechanism. It is not possible to mould or re-shaped the foams obtained at the exit of the die because they become almost completely dry and brittle. This fact has restricted the use of starch-based foams obtained from extrusion to the production of *loose-fill chips* (Figure 2.40a) for *cushion-packaging* [71,72]. Recently, the use of extrusion foaming for the production of starch-based foam planks has been reported (Figure 2.40b). They are joined to corrugated boards in order to obtain sandwich panels which can be used as *protective-packaging* [73].

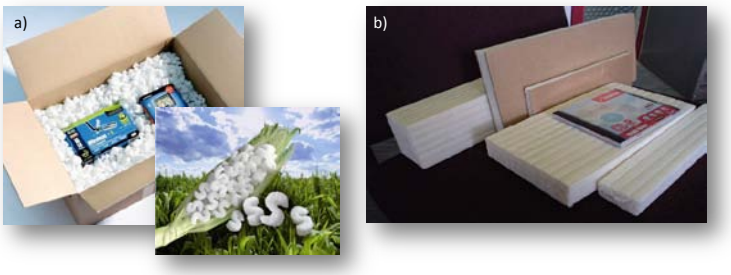

Figure 2.40.a) Loose-fill chips based on starch [74].b) Starch-based sandwich panels [73].

2.5.1.2- Baking.

Baking is a *batch* foaming process closely related to the baking of waffles and wafer cookies which allows foamed products with a defined shape such as cups, plates, trays, bowls and clam-shells to be obtained. A mixture of starch and water, together with other additives, is placed inside a mould, which is then heated. Firstly, starch gelatinizes under the action of water and temperature forming a viscous batter. Secondly, the steam generated expands the viscous batter until it fills the mould. Once the mould is filled, the shaped product dries acquiring enough consistency. In many cases a special laboratory-baking machine is employed to produce baked-starch trays, which has two heated steel moulds. The upper one is hydraulically lowered to meet the bottom mould during foaming [75,76,77]. The pressure applied in this machine only serves to transmit the required heat for the process. Hence, the foaming process evolves under atmospheric pressure. This is one of the reasons why the homogeneity of the cellular structures

obtained by this method are generally poor (wide cell size distributions) and with large cell sizes, even larger than 1000μm. Figure 2.41 shows atypical cellular structure of foamed starch trays produced by using this method. An outer skin denser than the interior is produced due to the contact with the hot upper and bottom parts of the mould that dries the foam and avoids further expansion.

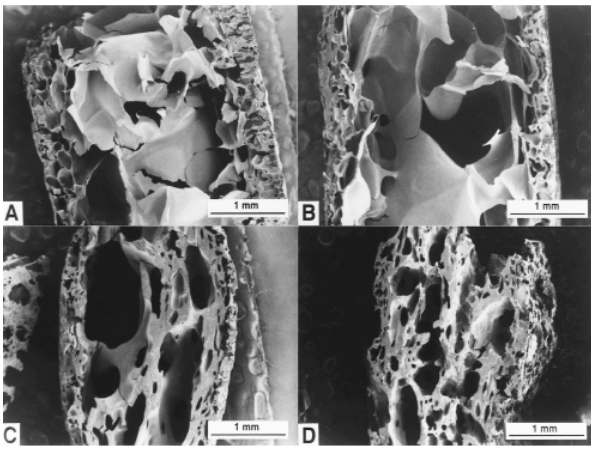

Figure 2.41.Cellular structure of baked foamed plates made from: a) waxy maize starch, b) normal corn starch, c) high amylose (50%) corn starch and d) high amylose (70%) corn starch [75]

2.5.1.3- Microwave foaming

Starch foaming processes can also be classified with regards to the way in which heat is transferred. In *Surface heating* the heat is firstly transferred to the surface of the sample and later to the interior by conduction. This means that there is a temperature gradient along the sample thickness and therefore, the homogeneity of the resultant cellular structures could be poor, as in the baking process (Figure 2.41). On the other hand, in *volumetric heating* the formation of temperature gradients is less likely because heat transfer mainly depends on how water molecules are distributed along the sample. This is the case of the ***microwave foaming*** of starch-based materials. Microwaves applied over the sample interact with water molecules because of their intrinsic polarity that makes them vibrate and/or re-orientate under the frequency of the radiation. This vibration is restrained by the surrounding polymer and the energy generated is dissipated as heat, which is then transferred to the whole sample by conduction. Both heating processes have been schematically represented in Figure 2.42.

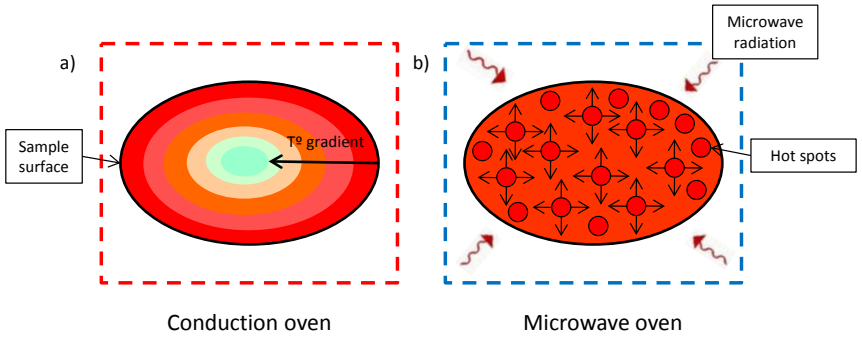

Figure 2.42. Heat transfer mechanisms: a) surface heating and b) volumetric heating.

Microwave radiation has been traditionally employed for heating liquids and cooking wet-food products but nowadays it is also being used for foaming food products. The case of *popcorns* (Figure 2.43) is especially well known. The corn kernel is composed of three main structural parts: germ, endosperm and pericarp. The endosperm contains starch granules and the pericarp is a tough protective layer that covers the whole kernel. The water trapped inside the kernel turns into steam during microwave radiation but instead of leaking out from the kernel it is dissolved into the starch polymer matrix due to the action of pericarp, which acts as a pressure vessel. Meanwhile, pressure grows up to a point in which the pericarp is not able to contain the pressure anymore and finally breaks letting the starch-based kernel expands or pop [78].

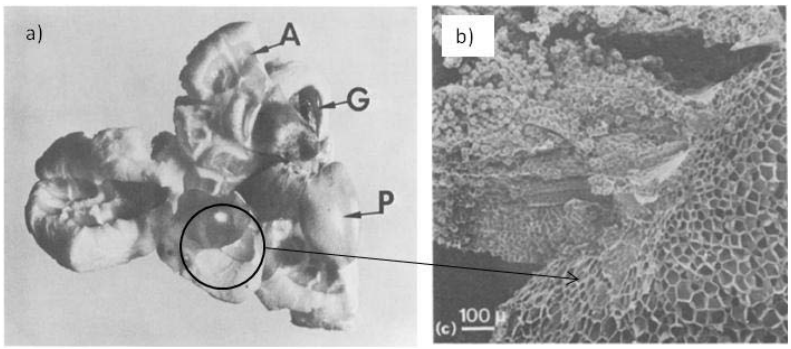

Figure 2.43.Popped kernel. a) G is the germ, P is the broken pericarp after popping and A is the aleurone. b) Cellular structure of a popped kernel [78].

More recently, microwave heating has been employed for manufacturing a 3rd generation of snacks because in this way, it is possible to create snacks of various biological origins in any desirable shape. They are obtained from non-expanded starch-based pellets produced by extrusion at high moisture contents (30-35%) and moderate shear and temperatures (below 100ºC) [70].

The challenge that scientists and engineers are currently facing up to is the use of microwave radiation for the development of foamed starch-based materials, either for *protective* or *food-packaging* applications, because this process would consume less energy and would be cheaper than existing technologies such as thermoforming and injection moulding. The Italian company *NOVAMONT* [79]has recently made great efforts in this sense. They filled several patents [80,81] and have been in charge of a European project dealing with the topic: *REBIOFAM*[82]. However, it is a foaming process which is not industrially scaled-up so far. Several scientific works can be found in literature addressing the issue. The processing route is very similar to the one employed for the manufacturing of 3rd-generation snacks because starch is firstly plasticized by water in extruders and later foamed by microwave radiation. In some of these works, the starch-based pellets obtained are simply placed inside a microwave oven chamber and foamed freely [69,83-85]. An interesting approach to obtain foamed starch blocks was reported by *Zhou et al*[86]. They placed a certain amount of pellets inside the cavity of a PTFE mould, expanding them by microwave radiation to obtain a foamed block with the desired shape. They tried to simulate the process of obtaining shaped packages from expanded polystyrene beads (EPS).However, the compressive modulus and strength of these foamed blocks were very low due to poor interfacial adhesion between the expanded pellets. Lack of adhesion is likely caused by the loss of water at

the surface of the pellets. On some occasions, the foamed sample burnt in the middle due to the non-homogeneity distribution of microwaves along the oven chamber and because of the temperature gradient between the sample and the mould. A foamed block produced in the paper of *Zhou et al* is shown in Figure 2.44b.

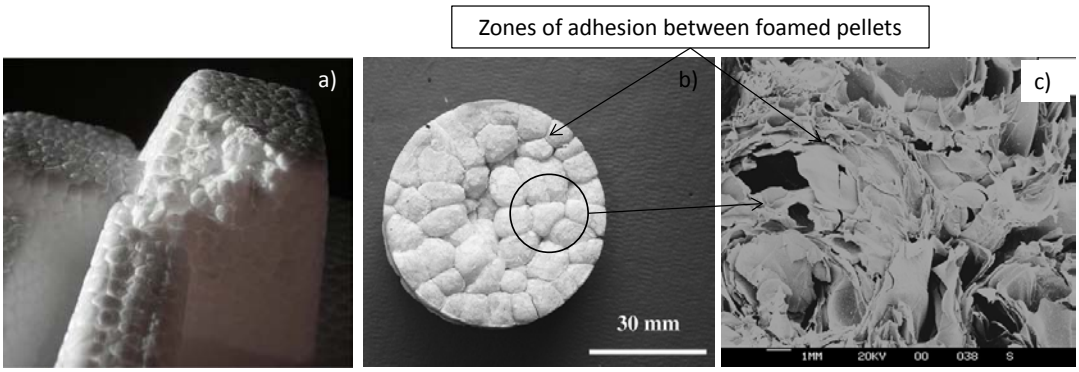

Figure 2.44.a) Expanded polystyrene (EPS).b) Starch-based foamed block produced by microwave radiation.c) Cellular structure of the foamed block [86].

Finally, it is fair to point out that an interesting attempt was made by *Sjöqvist et al* to foam batters of starch mixed with water by microwave radiation without previously producing starch-based pellets by extrusion. In this way, a production step is taken out of the production process [87].

2.5.2- Starch foams reinforced with natural fibres.

Natural fibres proved to reinforce solid starch-based materials as stated in *section 2.4.2.2* where a more detailed description of the production and characterization of starch-based biocomposites was reported. Nevertheless, their effect on starch-based foams is still a matter of scientific debate. It is clear that good compatibility exists between cellulose and starch but the high diversity of natural fibres employed in terms of composition and morphology and the different ways of producing and characterizing foams creates certain contradictory results in the topic. This section is focused on describing the main works in literature related to the topic and will give some clues about why there are still doubts about the reinforcement effect of fibres when employed for the production of starch-based foams.

Table 2.3 shows a list of the most representative scientific works addressing the production of starch-based foams reinforced with natural fibres in which it is possible to see the great diversity of production routes, natural fibres, and mechanical tests employed to characterize them.

Author	Starch	Plasticizer	Natural fibre	Production method	Mechanical tests
Shogren [77]	Corn	Water	Softwood	Baking	Bending
Kaisangsri [88]	Cassava	Water	Kraft fibre	Baking	Tensile
Soykeabkaew [89]	Tapioca	Water	Jute	Baking	Bending
			Flax		
Bénézet [90,91]	Potato	Water	Cellulose	Extrusion	Bending
			Hemp		
			Linter cotton		
			Wheat straw		
Lawton [92]	Corn	Water	Aspen	Baking	Bending
Glenn [93]	Wheat	Water	Softwood	Baking	Bending and Tensile
	Corn				
	Tapioca				
	Potato				
Cinelli [94]	Potato	Water	Corn	Baking	Bending
Carr [95]	Cassava	Water	Cassava	Baking	Bending
			Wheat		
Salgado [96]	Cassava	Water	Softwood (Eucalypt)	Baking	Tensile
Mali [97]	Cassava	Water	Sugarcane bagasse	Extrusion	Compression

Table 2.3.Starch-based foams reinforced with natural fibres reported in literature

In most of these works the matter has not been tackled properly because the inclusion of fibres not only affects the properties of the solid material but also influences the foaming process. The different foaming stages, from nucleation to degeneration of the cellular structure can be affected by their presence. For instance, fibres could induce a heterogeneous nucleation of cells because the available nucleation sites could increase substantially with respect to the pure polymer. This effect can be clearly seen in the work of *Soykeabkaew et al* in which tapioca starch-based foams produced by baking are reinforced with different amounts of jute and flax fibre [89].Figure 2.45 shows SEM micrographs of the foams reinforced with different amounts of

flax-fibres. Increasing the amount of fibres resulted in higher populations of cells and hence, in lower cell sizes, a phenomenon usually linked to heterogeneous nucleation mechanisms.

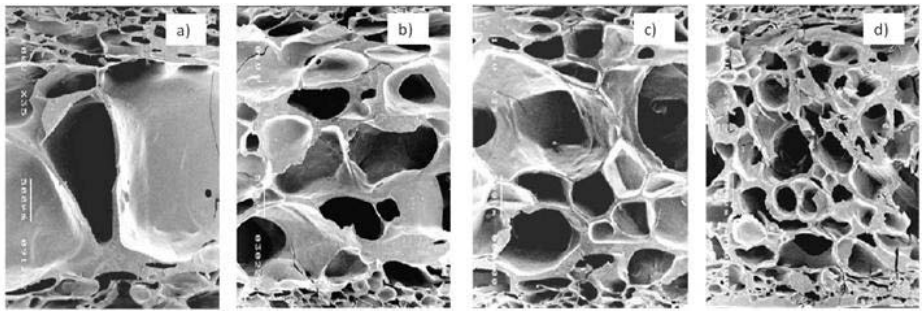

Figure 2.45. Starch foams produced by baking and reinforced with different amounts of flax-fibres: a) 0 wt%. b) 1 wt%. c) 5 wt%. d) 10 wt% [89].

Well-adhered fibres are also able to induce changes in the viscosity and rheological behaviour of the polymer matrix and as a result, in its capability of expansion. Some of the works listed in Table 2.3 could not be analysed exclusively in terms of the reinforcing effect of fibres because the density of the foams produced also varied. For instance, in the previous work of *Soykeabkaew et al* the density increased from 0,2 g/cm^{3}up to more than 0.3 g/cm^{3}when the material was reinforced with a 10 %wt of both, jute and flax fibres. This could be the principal reason behind the improvement in mechanical properties obtained by adding fibres.

On the other hand, in the work of *Kaisangsri et al*, the reinforcement with 40 %wt of Kraft fibres produced slight increments of the density, from 0.12 to 0.15 g/cm^3, while the tensile strength shifted up from 302 MPa to 1170 MPa. This drastic increment of strength cannot be explained exclusively in terms of the density variation. Nevertheless, an additional explanation arose from this work which is based on the lower absorption of water of the samples reinforced with fibres. It is known that the presence of water plasticizes the starch polymer matrix resulting in a loss of strength [88].

When the foams are produced by *extrusion foaming* the density seems to decrease as the fibre content increases although no consistent explanation was found for this result [90]. On the contrary, density usually increases with fibre content in *baking* processes. In this case, there are not shear effects as in *extrusion foaming* and it seems that the only possible explanation is that cell growth was avoided by higher viscosities of the polymer matrix.

Some works reported that there is an optimum in the amount of fibres used. Beyond this value, they start to agglomerate and mechanical properties decrease due to the appearance of areas without fibres that represent weak points under mechanical loads[92].This phenomenon is observed in Figure 2.46 in which baked starch trays reinforced with different amount of aspen fibres are observed. The tray reinforced with 40wt% of fibres present regions of higher clarity due to the agglomeration of fibres.

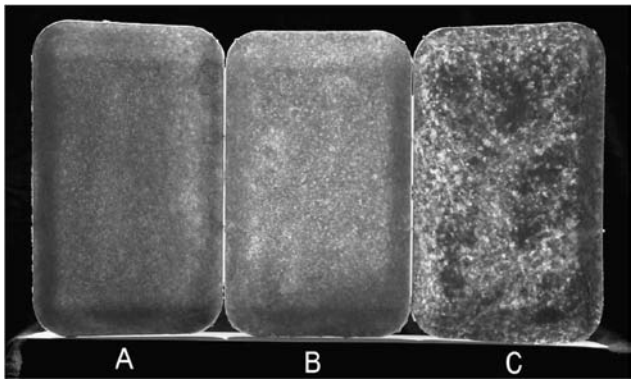

Figure 2.46. Baked starch trays reinforced with different amounts of aspen-fibres: a) 5 %wt. b) 20 wt%. c) 40 wt% [92].

In other works the analyses of the results is not clear simply because the ratio *starch/water* was not kept constant [93,94,96]. The fact of keeping this ratio constant is important because water, as was mentioned previously, is the blowing agent and at the same time the plasticizer of the polymer matrix. Hence, varying this ratio could affect on the one hand, the amount of gas available to expand the polymer matrix and on the other hand, the viscosity of the polymer matrix and its capability of supporting the pressure generated by steam without collapsing.

In addition, few works performed a detailed characterization of the cellular structure probably due to the poor homogeneity of the structures obtained. Moreover, an important factor determining the mechanical properties of cellular materials such as the open cell content is not considered in most of the papers. Another important aspect is that finding scientific papers dealing with starch reinforced with fibres foamed using microwave heating has not been possible. This is one of the areas explored in this research.

2.5.3- Summary.

The first parts of *section 2.5* dealt with the fundamentals of foaming starch, especially focused on those mechanisms which are mainly affected by the properties of starch. This is the case of the stabilization mechanism which depends on the fact that water plays a dual role as the plasticizer and the blowing agent. The following section (*2.5.1*) describes the main production processes of starch-based materials: *extrusion foaming*, *baking* and *microwave foaming*. The only application found for foams produced from *extrusion foaming*(*section 2.5.1.1*) is *protective-packaging* (loose-fill chips) because they cannot be reshaped after foaming. Shaped products such as plates and trays can be produced by *baking* (*section 2.5.1.2*) but the cellular structures obtained are very inhomogeneous. Hence, the production of starch-based foams with greater mechanical performances than the existing ones depends on the development of more efficient foaming processes. In this sense, *microwave foaming* (*section 2.5.1.3*) represents the best approach because it is based on a *volumetric heating* of the sample. Moreover, energy consumption is lower than with traditional foaming routes such as *extrusion foaming* and *baking*. Some works reported the production of starch foams by microwave radiation to be used for *packaging* applications but the mechanical properties obtained were poor. One possible

reason is that these foams were obtained from solid TPS pellets which did not adhere properly after their expansion[86].

One of the works included in this thesis (*chapter 4*) proposes an interesting alternative based on the production of foamed blocks by microwave radiation from thermoformed sheets. Moreover, natural fibres were employed to increase the mechanical properties of the foams produced regarding stiffness and strength. In spite of having found a significant amount of works in which starch-based foams are reinforced with natural fibres (*section 2.5.2*), there are not many pieces of work reporting on this kind of reinforcement in microwave foaming processes.

The revision of the state of the art carried out in this section helps to set the objectives of the thesis regarding the development of starch-based foams(*section 1.3.1*).Moreover, this revision has been very useful in order to detect which points require further research in order to develop these materials for the production of more sustainable foams. A more detailed description of the state of the art concerning this topic will be found in the works included in this thesis (*chapter 4*).

2.6- Polypropylene-based foams.

The production of polypropylene foams has been somewhat limited due to the poor foaming performance of this polymer. However, the research conducted during the last few years and the synthesis of new polypropylene grades permitted the appearance of some interesting developments in this field without the necessity of crosslinking the polymer. The research performed during this thesis constitutes one of them. In order to understand the novelty of this research, this section will provide the reader with the main concepts related to polypropylene foams: from the basics of the polymer to the application of PP foams as a recyclable lightweight core in sandwich panels.

Despite the few applications of polypropylene (PP) as a foam, it is one of the most widely employed polymers in the market due to its outstanding properties and low price. It belongs to the polyolefin group of polymers because propylene, an unsaturated alkene or olefin obtained as a derivative of the petroleum fractionation, is the constituent monomer of the polymer chain. The polymerization reaction is carried out by *Ziegler* and *Natta* catalyst at low pressures (1-5 bar) and temperatures between 30 and 80 ºC. The side methyl groups (Figure 2.47) provide polypropylene with several steric configurations depending on their position in the polymer chain. When they are randomly distributed, ***atactic polypropylene*** is obtained. On the other hand, when they are distributed in an orderly way ***isotactic*** and ***sindiotactic polypropylene*** are obtained. In the first case the methyl groups are placed in the same side of the chain while in the second case, they are alternatively placed on both sides.

The *isotactic* version of the PP polymer chain increased its cristallinity substantially and the use of PP extended worldwide because it was a cheap thermoplastic, electric insulator and chemical resistant, as well as PE, but with better mechanical properties regarding strength and stiffness and proved to have greater thermal stability. Moreover, its density is even lower than that of low-density polyethylene (LDPE).

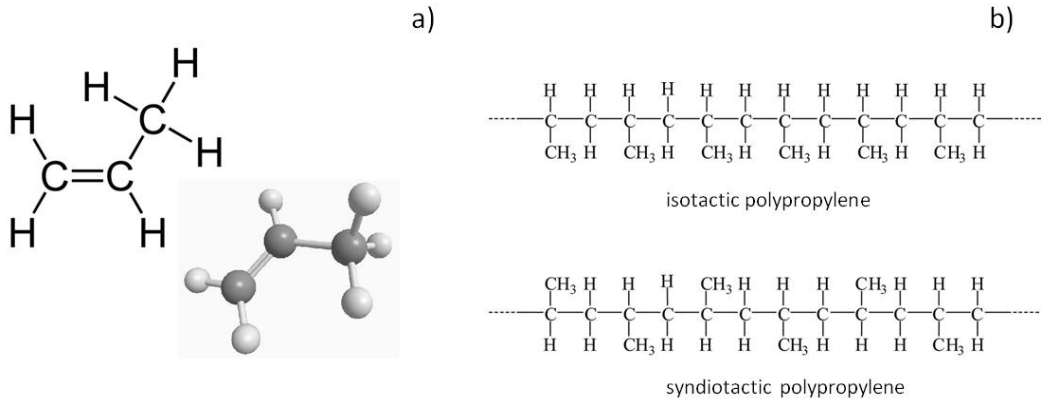

Figure2.47. a) Propylene monomer. b) Isotactic polypropylene and syndiotactic copolymer.

The main drawback of *isotactic* PP is its low ductility which prevents it being used in applications where high impact strengths are required. The introduction of ethylene monomers in the polymer chain brought about the development of PP-based copolymers which in turn are

denominated as ***random copolymers***, when the ethylene monomer is randomly located along the chain, or ***block copolymers***, when they are placed in an orderly way.

2.6.1- Polypropylene foaming processes.

The production of polyolefin foams, such as those based on PP, is conditioned by the kind of polymer employed, by the density and properties required for the final application and by the shape of the product [3]. Most of these foaming processes employ technology, which is very similar to that used for the production of solid parts but differ in the fact that a gas phase is introduced into the system making the control of parameters more complex [2]. The gas phase can be introduced either by thermal decomposition of solid particulates(*chemical blowing agents*) or by directly dissolving a gas or a low boiling point liquid (*physical blowing agents*) into the molten polymer.

There are lot of thermoplastic foaming processes such as *rotomolding*, *injection molding*, *bead foaming*, *extrusion foaming*, *compression moulding* and *batch-foaming processes* based on gas dissolution [98]. Some of them are focused on the production of medium-high density foams, such as *rotomolding* and *injection moulding*, which are mainly used for applications where the objective is to reduce weight and at the same time to maintain a certain level of the mechanical properties. This section is especially focused on those processes commonly used for the production of medium and low density PP foams such as *extrusion foaming*, *compression moulding* and *bead foaming*.

2.6.1.1- Extrusion foaming.

Extrusion foaming is technology that possesses several advantages, the principal one being that it is a cost-effective and continuous process with high output rates. In terms of processing, the screws are deliberately designed to have a large surface-to-volume ratio allowing heat to be transferred to the polymer rapidly, which melts only a few seconds after being fed into the extruder. Moreover, the pressure of the *polymer/blowing agent* system increases substantially from the entrance to the exit due to the screw design which can be controlled by the flight and shaft dimensions [2]. The main disadvantage of the process is that only simple geometries can be obtained such as sheets, profiles and tubes as shown in Figure 2.48.

Figure 2.48. Foamed products obtained by extrusion foaming.

The common stages in extrusion foaming are polymer ***melting***, polymer-gas ***mixing***, ***cooling*** and ***shaping (foaming)***. The polymer-gas mixing stage differs depending on the kind of blowing agent employed. In the case of *physical blowing agents* the gas is fed in the middle of the extruder barrel through a pump and mixed with the molten polymer. In the case of *chemical blowing agents*, the blowing agent is mixed with the polymer at the entrance of the extruder and the temperature is raised enough to decompose the blowing agent and generate gases. The main drawback of extrusion foaming is how to dissipate the heat from the molten polymer to reduce its viscosity and make it adequate for foaming. This process is challenging because the screw continues transferring heat to the system until the end of the barrel. In the case of using one single extruder machine, the length of the extruder barrel has to be very high (high L/D ratios) in order to give enough time to the *polymer/blowing* agent mixture to dissipate heat before foaming. For this reason, it is usually preferable to use tandem equipment (Figure 2.49) which allows the first extruder to be employed to mix the polymer with the blowing agent at high temperatures and the second one, set at low temperatures to cool the mixture before foaming. After cooling, the stabilized gas/melt system is pumped into a shaping unit for foaming [2,99,100].

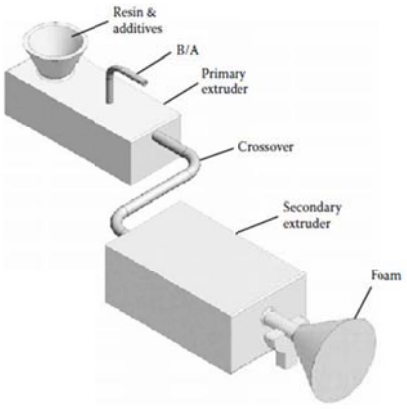

Figure 2.49.Tandem extrusion system.

This process was also explained in *section 2.5.1.1*focussing on what happens to starch based materials, especially in the last stages (expansion and stabilization) in which the polymer expands after exiting the die. Figure 2.39 shows an evolution of the cellular structure which can also be applied for polyolefin foams.

2.6.1.2- Compression moulding.

This is a batch-foaming process whose main feature is the use of chemical blowing agents that have previously been dispersed throughout the polymer in a melt-blending step as shown in Figure 50. Hence, in this process pressure is not needed for diffusing the gas into the polymer and it is only applied ($P_0 \rightarrow P$)with the purpose of transferring heat to the compound, decomposing the blowing agent ($T \geq T_d$) and holding all the gas produced into the molten polymer until the moment in which pressure is released ($P \rightarrow P_0$) and expansion takes place. The effective time in which pressure is applied is considerably shorter than in batch foaming processes based

on gas dissolution of physical blowing agents making the process less costly. Moreover, hot-plate presses are used to apply pressure. In fact, this is common plastic equipment found in industry (Figure2.50) making no additional investments in machinery necessary. This technique is mainly used today for the production of cross-linked polyolefin foams.

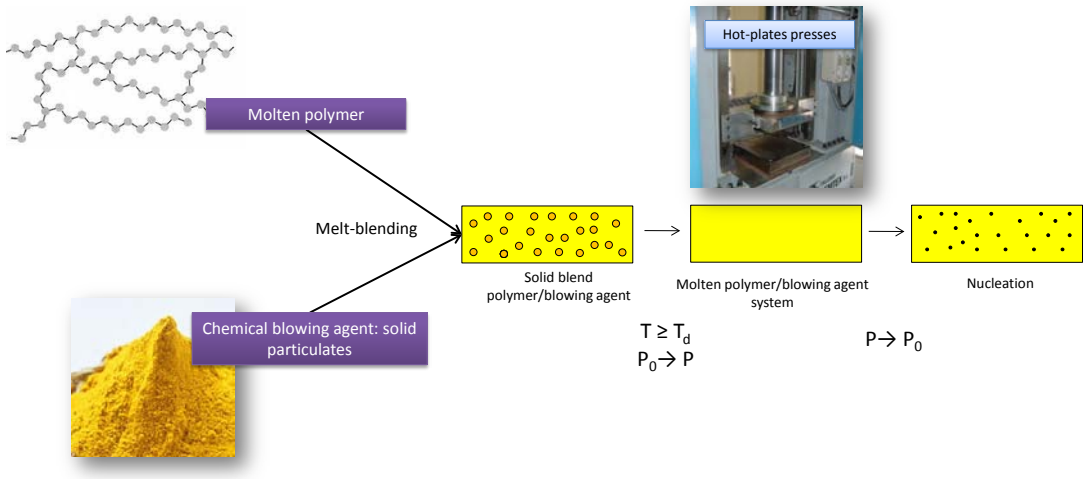

Figure 2.50.Formation of the polymer/chemical blowing agent system in compression moulding.

A exothermic blowing agent such as azodicarbonamide is usually employed because its decomposition temperature (between 200 and 220ºC) is higher than the melting temperature of the polymer, even in the case of foaming polypropylene. Moreover, the amount of gas liberated in its decomposition is very high (gas yields between 240 and 270 cm^3/g), which is a fact that permits higher density reductions to be obtained. *Azodicarbonamide* is the chemical blowing agent which is widely used throughout the world and is presented in the form of a yellow powder (Figure 2.50). Its decomposition liberates N_2(about 65%) and minor quantities of CO, CO_2 and NH_3[8,100].

There are two kinds of processes based on this methodology. The first one is usually known as ***single-step compression moulding*** and the second one is the ***two-stages compression moulding process***. In both cases the blowing agent is compounded with the polymer at a previous stage. The main difference resides in the final density obtained. When the target density is higher than 100 kg/m^3 (ER≤9)the single-step process is preferred. On the other hand, when densities lower than 100 kg/m^3 are required, the process is split up into two stages. One of them, crosslinking the polymer matrix and the other one, producing the final expansion. Crosslinking is required because the polymer matrix is subjected to expansion ratios up to 40. Figure 2.51 shows the main steps of the two-stage foaming process[8].

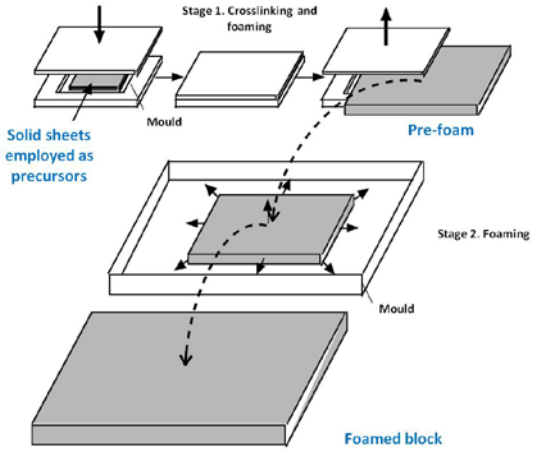

Figure 2.51. Two-stage foaming process[8].

2.6.1.3- Bead-foaming.

The bead-foaming process has been traditionally employed for the production of expanded polypropylene (EPP). In this process, polypropylene beads, previously impregnated with the liquid blowing agent, are later expanded by heating with steam. The final shape of the foamed product is obtained inside moulds where the expanded beads are fused together. The main difference with respect to the process with PS is that PP beads have to be expanded just after being impregnated with the blowing agent because of the high diffusion rate of the blowing agent in PP under atmospheric pressure. Moreover, high steam temperatures and pressures are needed due to the high melting temperature of PP, generally between 150 and 170ºC. These facts make EPP foams more expensive than EPS [101].

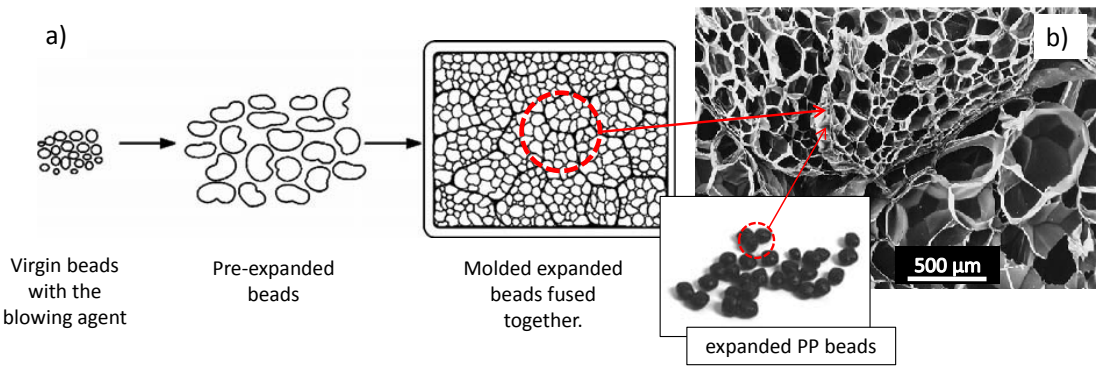

Figure 2.52. a) Moulded-bead process. b) Moulded expanded beads (EPP) and SEM image of their structure [102].

Polypropylene copolymers are employed in this process because they present two melting temperatures. The lower one corresponds to the melting of ethylene monomers and the higher one to the melting of propylene monomers. The foaming temperature is set up between these two temperatures. In this way, one part of the PP beads are melted allowing not only their expansion but also their adhesion while the other part is not melted, which is the key to obtaining a certain degree of melt strength during expansion.

2.6.2- Polypropylene foams in the market: development of branched polypropylenes.

Polypropylene has been considered for foaming applications because it is an ideal candidate to replace more common thermoplastics used in this field such as polystyrene (PS) and polyethylene (PE). The reasons are mainly two. Firstly, the higher stiffness and strength of PP with respect to PE and secondly, the higher impact strength with respect to PS. This is because PP at ambient temperature is rubbery while PS is glassy (The T_g of PS is 105ºC). Moreover, the low heat-deflection temperatures of PE and PS makes their foamed counterparts non suitable in high-service temperature applications. For instance, PS foams when heated above its T_g soften and deform.

Several foamed products based on conventional grades of PP have been developed and launched on the market. The main example is ***expanded polypropyl*ene** (EPP), which is used as a shock energy absorber in automotive applications [103]. It is produced by the *bead foaming process* previously explained in *section 2.6.1.3*. The stiffness of the final foamed parts produced from EPP is low in comparison with other materials employed for structural applications such as PVC and PET. There are several reasons for this but the principal one is that polypropylene copolymers are usually employed in this foaming process because they are tough rather than stiff. EPP is currently being produced by companies such as *BASF* [104] and *JSP* [105].

The production of polypropylene foams from isotactic grades is a challenging task because of their low melt strength linked to their linear architecture and low viscosity in the molten state. Branching is another interesting alteration of the PP chain architecture that allows this polymer to be used for foaming applications. In 1990, *BASELL* launched the first grade of high melt strength (HMS)PP which was based on a branched PP. This alteration of the chain architecture is generally achieved by subjecting the polymer to electron irradiation under a poor O_2atmosphere[3]. Branched PPs are able to reach higher expansion than linear PPs due to the *strain hardening* phenomenon which is based on a sudden increase of the extensional viscosity produced by the entanglement of the polymer chains when they are subjected to high strains as in a foaming process. Extensional viscosity measurements are usually performed in order to quantify the strain hardening phenomenon. Typical extensional viscosity curves are shown in Figure 2.53 in which the different behaviours of a linear PP and a branched PP are clearly observed. In the case of the branched PP the extensional viscosity (η_E) is drastically increased even at the highest strain rate (1.0 s^{-1}).

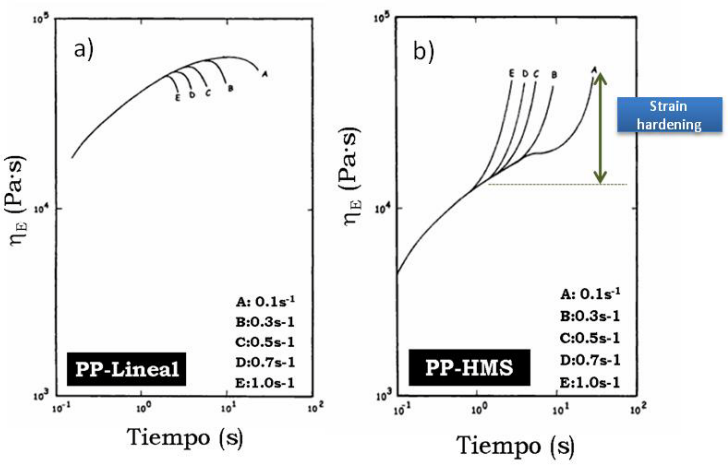

Figure 2.53.Extensional viscosity curves. a) Linear PP. b) Branched PP.

The first foamed sheet based on a branched polypropylene was produced by DOW in 1994[106]. Since then, the production of PP foams obtained from branched PP or mixtures with linear PP has spread worldwide. However, the foamed sheets produced by extrusion foaming present poor cellular structures of large cell sizes with cells typically oriented in the extrusion direction which also reduces the stiffness and strength in the thickness direction [107-109].

2.6.3- Foamed polypropylene nanocomposites.

The combination of foaming technology and polymer nanocomposites gave place to a new class of cellular materials: ***polymer nanocomposite foams***, in which nanoparticles play a multifunctional role because they not only enhance the properties of the solid material but are also able to promote significant alterations of the foaming process. The different foaming stages: nucleation, expansion and stabilization can be affected by their presence. In this way, the properties of the foams produced are subjected to changes induced in the cellular structure, which in turn are dependent on the degree of polymer-nanoparticle adhesion and the dispersions along the polymer matrix as mentioned in *section 2.4.2.3* [56].

The nucleation of cells during the first stages of foaming could be influenced by the presence of nanoclays. The heterogeneous nucleation mechanisms usually associated with the use of fillers are more pronounced with nanoparticles than with their micrometric counterparts due to their higher *surface/volume* ratio. Equation2.10 shows how to calculate the available nucleating sites in polymers reinforced with fillers [110].

$$\frac{Nucleants}{cm^3} = \frac{w}{\rho_p}\frac{\rho_{blend}}{V_p} \qquad (2.10)$$

where *w* is the weight fraction of the particle in the composite, ρ_p is the density of the particle, ρ_{blend} is the density of the polymer containing the particle and V_p is the volume of the individual particle. This last term accounts for the influence of the filler size. When decreasing the filler size the number of potential nucleating sites increases. The same thing happens when increasing the concentration of nanoparticles (*w*).

What happens during the nucleation stage should be reflected in the cellular structure morphology. Normally, the population of cells increases on adding nanofillers. For instance, the cell density (cells/cm^3) of polypropylene based foams reinforced with nanoclays strongly increased with the addition of 7.5 wt% of nanoclays [111]. For this reason, the use of nanofillers is also implemented as a common strategy for the production of microcellular foams. Moreover, the nanoparticle dispersion influences to a great extent the cellular structure morphology. The nucleation rates of exfoliated nanocomposites proved to be higher than those of intercalated nanocomposites, which is attributed to the fact that at the same nominal particle concentration, the effective particle concentration is higher for well dispersed nanoparticles [112].

The expansion process is also affected by the presence of nanoclays because the elongational viscosity of the polymer matrix can be increased. Even in some cases, nanoclays induce the presence of strain-hardening phenomenon [113-115]. In addition, nanofillers based on platelet geometries such as nanoclays act as a barrier against gas diffusion avoiding blowing agent loses during the expansion process [112].The fire retardant properties of polymer foams are also improved by incorporating nanofillers due to the formation of a char during burning, which avoids further propagation of flames [112].

The cell wall thickness of microcellular polymer foams is in the range of microns or even submicrons. This fact makes nanofillers an ideal reinforcement because they can be allocated within the cell walls, edges and struts without breaking them during the expansion process. This reinforcing effect has been proved in several publications [112,116].

In the particular case of polypropylene, the research currently being conducted is especially focused on the effect that nanoclays have on the branched structure of HMS polypropylenes. When linear polypropylenes are employed the cellular structure homogeneity tends to increase due to a higher nucleation rate and to the appearance of strain hardening in some cases. On the contrary, when using branched polypropylenes these effects are not so clear and it was even stated that branches avoid an effective intercalation of the polymer between the clay layers [117]. Despite the unclear results, some works reported improvements in the cellular structure and enhancements in the mechanical properties by the addition of nanoclays to blends of HMS PPs and linear PPs [118]. These kinds of blends are usually produced for foaming applications of PP due to the higher cost of HMS PPs with respect to linear PPs. Moreover, the addition of nanoclays to the same kind of blends proved to broaden their foaming window due to an increase of their thermal resistance in the molten state [119].

2.6.4- Practical use of polypropylene foams as the core of sandwich panels.

Low-density PP foams could be used as the core of sandwich panels due to the high stiffness and strength of the solid matrix but their cellular structure has to be improved in order to reach the performance of common foamed cores employed in the market such as PVC foams. Sandwich panels are light structural materials composed of thin solid skins separated by a thicker lightweight rigid core. The role of the core is to increase the inertia moment of the panel without substantially increasing the weight. Figure 2.54 shows an analogy between a sandwich panel

with a foamed core and a metallic l-beam because both behave in a similar way under bending loads. In the metallic l-beam the flanges are subjected to in-plane compression and tension loads, in the same way as the skins of the sandwich panel are. However, the web is subjected to shear loads, as the foamed core is [120].

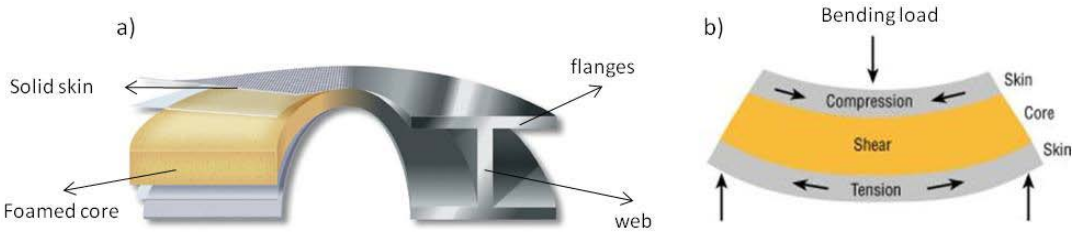

Figure 2.54.a) Analogy between sandwich panel and l-beam. b) Sandwich panel behaviour under three-point bending load.

The mechanical behaviour of a sandwich panel depends on the properties of the solid skins and core material and on its geometry. The design of a sandwich panel can be formulated as an optimization problem in which the goal is to design the panel with the minimum weight fulfilling at the same time the constraints imposed by stiffness and strength. Considering a sandwich panel under a load P in three point bending (Figure 2.55), its mechanical behaviour is given by equation 11 in which δ/P represents the deflection of the beam (δ)divided by the applied load (P) [1].

$$\frac{\delta}{P} = \frac{2l^3}{B_1 E_f b t c^2} + \frac{l}{B_2 b c G_c} \qquad (11)$$

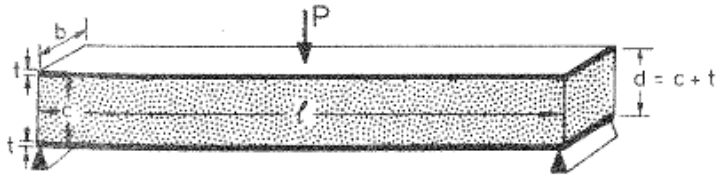

Figure 2.55. Sandwich panel dimensions.

The second term of equation 10 accounts for the contribution of the foamed core to the overall response of the panel. It is possible to see how the shear modulus of the foamed core (G_c) is the parameter that mainly influences its response. The compressive modulus of the skin (E_f)appears in the first term. However, in both terms the core thickness appears(c). Indeed, the dependency of the first term is quadratic with the core thickness. This fact reflects the importance of the foamed core in the sandwich panel behaviour [1].

Currently, the core of sandwich panels are made of PVC, SAN, PET and PU foams, balsa wood and honeycombs (Figure 56). PVC foams, for instance, are frequently used in marine applications such as in the hulls of yachts or boats where apart from mechanical properties, buoyancy and hydrophobicity are important requirements. The PVC foams present closed cellular structures that prevent the entrance of water to the structure. The main drawback of rigid PVC foams is

that they are crosslinked and therefore, non-recyclable after end-use (*section 1.2.3.2*). Moreover, few companies around the world: *DIAB*[121]and*A3 COMPOSITES*[122], produce these foams and hence, they are very expensive.

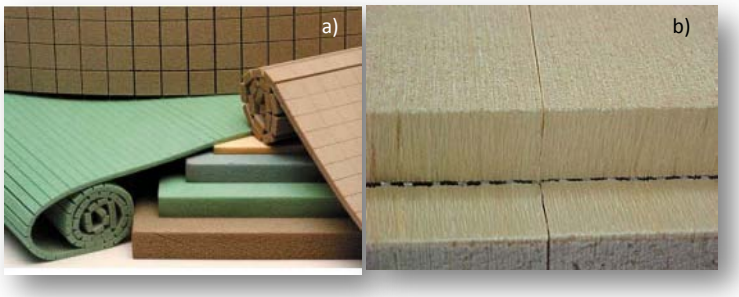

Figure 56.a) PVC foamed panels. b) Balsa Wood.

A cheaper and more sustainable alternative would be PET foams, which indeed are produced from a cost-effective production method based on extrusion foaming, although it presents some peculiarities. This process is commonly known as *strand foaming* because the extruder possesses a multi-orifice die from which several PET strands expand at the same time. They fuse together when reaching a certain expansion. A mould is placed at the exit of the die making the fused strands pack together resulting in foamed blocks with very peculiar structures such as those shown in Figure 2.57.

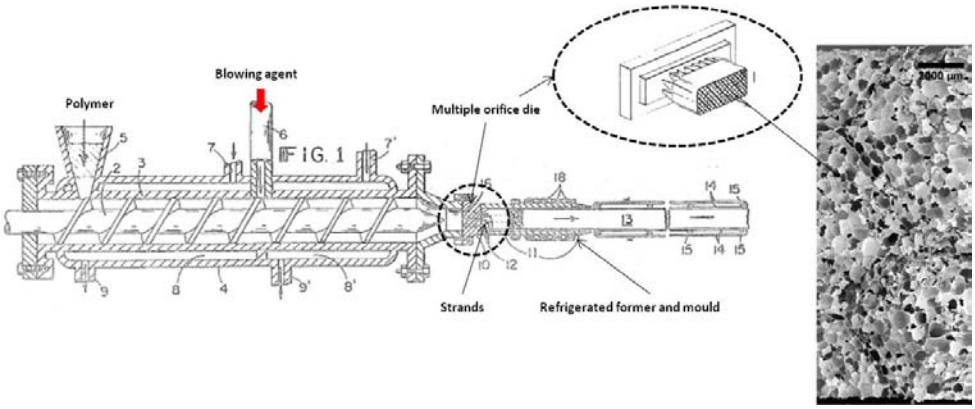

Figure 2.57. Strand foaming technology.

2.6.5- Summary

This part of the thesis is focused on the development of PP-based foams able to be used as the core of sandwich panels (*section 2.6.4*). The development of branched polypropylenes allowed obtaining foams with similar expansion ratios to those of PVC foams but without being crosslinked and therefore, enabling recycling after end-use. For this reason, these foams fulfil one of the main objectives of this thesis: the development of sustainable and environmentally-friendly polymer foams (*chapter 1*). Nevertheless, the cellular structures of the foams obtained by using conventional foaming processes, such as *extrusion foaming*, are not ideal for this application (*section 2.6.1.1*). The *moulded-bead process* requires the use of copolymers grades

which are not as stiff nor strong as conventional photopolymers (*section 2.6.1.3*) and the *compression moulding* route requires crosslinking the polymer matrix with the aim of achieving foams with high expansion ratios and with a defined shape (*section 2.6.1.2*). All these facts make the *improved compression moulding* (*ICM*) route developed at *CellMat Laboratory* and described in *chapter 3*, a promising foaming process to be employed for the production of rigid low-density PP foams. *Chapter 5* will show results confirming that the cellular structures and the mechanical properties obtained from this process are at least comparable to those of the PVC and PET foams currently employed in the market. In addition, *Chapter 6* will show a comparison between these materials and the PP foams developed in this thesis.

Last but not least, the use of nanoclays could represent an additional contribution to the target of obtaining PP foams with better cellular structures. There are some works in literature dealing with this topic (*section 2.6.3*) whose results suggest that both the cellular structure and the mechanical properties of PP foams can be improved with their addition. Nevertheless, there are lot of doubts still remaining about how nanofillers interact with the foaming process of polymers. One of the works carried out (*chapter 5*)shows some interesting results which can contribute to increasing the knowledge existing so far about the effect of nanoclays on the production and properties of polymer foams.

The state of the art performed here settled the objectives of the thesis in this topic. They were listed in *section 1.3.2*. Besides, a more detailed description of the state of the art will be found in each one of the works based on the development of PP foams included in this thesis (*chapter 5).*

References.

[1] Gibson, L.J. and Ashby, M.F. Cellular Solids: Structure and Properties. 2th ed. *Cambridge University Press*, Cambridge. 1997.

[2] Lee, S.T.; Park, C.B. and Rajesh, N.S. PolymericFoams. Science and Technology. *Taylor and Francis Group*. 2007.

[3] Klempner, D. and Frisch, K.C. Handbook of polymeric foams and foam technology. *Hanser Publishers*. 1991.

[4] Reglero-Ruiz, J.A.; Viot, P. and Dumon, M. Foaming behaviour and compressive properties of microcellular nanostructured polystyrene. *Cellular polymers*. 28, 363-386. 2009.

[5] Chow, T.S. Molecular interpretation of the glass transition temperature of polymer-diluent systems. *Macromolecules*. 13, 362-364. 1980.

[6] Elliott, J.A.; Windle, A.H.; Hobdell, J.R.; Eeckhaut, G.; Oldman, R.J.; Ludwig, W.; Boller, E.; Cloetens, P. and Baruchel, J. In-situ deformation of an open-cell flexible polyurethane foam characterised by 3D computed microtomography. *Journal of Materials Science*.37, 1547-1555. 2002.

[7] Rodriguez-Perez, M.A. Crosslinked polyolefin foams: Production, structure, properties and applications. *Advances in Polymer Science*. 184, 97-126. 2005.

[8] Hidalgo, F. Diseño Optimizado de los Parámetros de Proceso en la Fabricación de Espumas de Poliolefina Reticulada mediante Moldeo por Compresión. *Tesis Doctoral*. Universidad de Valladolid. España.2008.

[9] Christensen, R.M. Mechanics of low density materials. *Journal of the Mechanics and Physics of Solids*.34, 563-578. 1986.

[10] Zhu, H.X.; Knott, J.F.; and Mills, N.J. Analysis of the elastic properties of open-cell foams with tetrakaidecahedral cells. *Journal of the Mechanics and Physics of Solids*. 45, 319-343. 1997.

[11] Warren, W.E.; Kraynik A.M. Foam mechanics: The linear elastic response of two dimensional spatially periodic cellular materials. *Mechanics of Materials*.6, 27-37. 1987.

[12] Rodriguez-Perez, M.A. Propiedades térmicas y mecánicas de espumas de poliolefina.*Tesis Doctoral*. Universidad de Valladolid. 1998.

[13] Timoshenko, S. and Goodier, J.N. Theory of elasticity. *Mc-Graw Hill*. 1951.

[14] Weller, J.E. and Kumar, V. Solid-State Microcellular Polycarbonate Foams. II. The Effect of Cell Size on Tensile Properties. *Polymer Engineering and Science*.50, 2170-2175. 2010.

[15] Rodriguez-Perez, M.A.; Lobos, J.; Pérez-Muñoz, C.A. and de Saja, J.A. Mechanical response of polyethylene foams with high densities and cell sizes in the microcellular range. *Journal of Cellular Plastics*.45, 389-403. 2009.

[16] Rodriguez-Perez, M.A.; Lobos, J.; Pérez-Muñoz, C.A. and de Saja, J.A. Mechanical behaviour at low strains of LDPE foams with cell sizes in the Microcellular range. Advantages of using these materials in structural elements. *Cellular Polymers*. 27, 347-362. 2008.

[17] Huber, A.T. and Gibson, L.J. Anisotropy of polymer foams. *Journal of Materials Science*.23, 3031-3040. 1988.

[18] Mehta, B.S. and Colombo, E.A. Mechanical properties of foamed thermoplastics. *Journal of Cellular Plastics.*12, 59-66. 1976.

[19] Gupta, S; Watson, B.; Beaumont, P.W.R. and Ashby, M.F. *Final Year Project*. Cambridge University Engineering Department. Cambridge. UK. 1986.

[20] Hilyard, N.C. Mechanics of Cellular Plastics. *McMillan Publishing CO*.London. 1982.

[21] Thomson, W. (Lord Kelvin).On the division of space with minimum partitionalarea. *Philosphical Magazine.*24, 503-514. 1887.

[22] Sullivan, R.M.; Ghosn. L.J. and Lerch, B.A.A. General tetrakaidecahedron model for open-celled foams. *International Journal of Solids and Structures.*45, 1754-1765. 2008.

[23] Sullivan, R.M. and Ghosn, L.J. Shear moduli for non-isotropic, open cell foams using a general elongated Kelvin foam model. *International Journal of Engineering Science.*47, 990-1001. 2009.

[24] Gong, L.; Kyriakides, S; and Jang, W.Y. Compressive response of open cell foams. Part I: Morphology and elastic properties*. International Journal of Solids and Structures.*42, 1355-1379. 2005.

[25] Kalia, S.; Kaith, B.S. and Kaur, I. Cellulose fibres: bio- and nano-polymer composites. Green Chemistry and Technology. *Springer*. Berlin. 2011.

[26] Maya, J.J. and Sabu, T. Biofibres and biocomposites. *Carbohydrate Polymers*. 71, 343-364.2008.

[27] Bledzki, A.K. and Gassan, J. Composites reinforced with cellulose based fibres. *Progress in Polymer Science*.24, 221-274. 1999.

[28] Satyanarayana, K.G.; Arizaga, G.G.C. and Wypych, F. Biodegradable composites based on lignocellulosic fibres- An overview. *Progress in PolymerScience*.34, 982-1021. 2009.

[29] James, B. and Roy, W. Starch: Chemistry and Technology.*3th ed. Elsevier*. 2009.

[30] Gallant, D.J.; Bouchet, B. and Baldwin, P.M. Microscopy of starch: evidence of a new level of granule organization. *Carbohydrate Polymers*.32, 177-191. 1997.

[31] Bizot, H.; Le Bail, P.; Leroux, B.; Davy, J.; Roger, P. and Buleon, A. Calorimetric evaluation of the glass transition in hydrated, linear and branched polyanhydroglucose compounds. *CarbohydratePolymers*.32, 33-50. 1997.

[32] Thakore, I.M.; Sonal, D. and Sarawade, B.D. Studies on biodegradability, morphology and thermomechanical properties of LDPE/modified starch blends. *European Polymer Journal*.37, 151-160. 2001.

[33] Park, H.M.; Lee, S.R.; Chowdhury, S.R.; Kang, T.K.; Kim, H.K.; Park, S.H. and Ha, C.S. Tensile properties, morphology, and biodegradability of blends of starch with various thermoplastics. *Journal of Applied Polymer Science*.86, 2907-2915. 2002.

[34] Pedroso, A.G. and Rosa, D.S. Mechanical, thermal and morphological characterization of recycled LDPE/corn starch blends. *Carbohydrate Polymers*.59, 1-9. 2005.

[35] http://www.novamont.com/Products/default.asp?id=505

[36] http://www.sphere-spain.es/

[37] Bilbao-Sáinz, C.; Butler, M.; Weaver, T.; and Bent, J. Wheat starch gelatinization under microwave irradiation and conduction heating. *Carbohydrate Polymers*. 69, 224-232. 2007.

[38] Ma, X. and Yu, J. The plasticizers containing amide groups for thermoplastic starch. *Carbohydrate Polymers*. 57, 197-203. 2004.

[39] Da Róz, A.L.; Carvalho, A.J.F.; Gandini, A. and Curvelo, A.A.S. The effect of plasticizers on thermoplastic starch compositions obtained by melt processing. *Carbohydrate Polymers*. 63, 417–424. 2006.

[40] Averous, L. and Boquillon, N.; Biocomposites based on plasticized starch: thermal and mechanical behaviours. *Carbohydrate Polymers*. 56, 111-112. 2004.

[41] Curvelo, A.A.S.; de Carvalho, A.J.F.; Agnelli, J.A.M. Thermoplastic starch-cellulosic fibres composites: preliminary results. *Carbohydrate Polymers*. 45, 183-188. 2001.

[42] López, J.P.; Mutjé, P.; Carvalho, A.J.F.; Curvelo, A.A.S. and Gironés, J. Newspaper fibre- reinforced thermoplastic starch biocomposites obtained by melt processing: Evaluation of the mechanical, thermal and water sorption properties. *Industrial Crops and Products*. 44, 300-305. 2013.

[43] Martins,I.M.G.; Magina, S.P.; Oliveira, L.; Freire, C.S.R.; Silvestre, A.J.D.; Neto, C.P. and Gandini, A. New biocomposites based on thermoplastic starch and bacterial cellulose. *Composites science and technology*.69, 2163-2168. 2009.

[44] Belhassen, R.; Boufi, S.; Vilaseca, F.; López, J.P.; Méndez, J.A.; Franco, E.; Pèlach, M.A. and Mutjé, P. Biocomposites based on Alfa fibres and starch-basedbiopolymer. *Polymer Advanced Technologies*.20, 1068-1075. 2009.

[45] Gironés, J.; López, J.P.; Mutjé, P.; Carvalho, A.J.F.; Curvelo, A.A.S. and Vilaseca, F. Natural fibre-reinforced thermoplastic starch composites obtained by melt processing. *Composites Science and Technology*. 72, 858-863. 2012.

[46] Wattanakornsiri, A.; Pachana, K.; Kaewpirom, S.; Traina, M. and Migliaresi, C. Preparation and properties of green composites based on tapioca starch and differently recycled paper cellulose fibers. *Journal of Polymers and theEnvironment*.20, 801-809.2012.

[47] Teixeira, E.M.; Cybele, L.; Corrêa, A.C.; Teodoro, K.B.R.; Marconcini, J.M. and Mattoso, L.H.C. Thermoplastic corn starch reinforced with cotton cellulose nanofibres. *Journal of Applied Polymer Science*.120, 2428-2433.2011.

[48] Müller, C.M.O.; Laurindo, J.B. and Yamashita, F. Effect of cellulose fibres on the cristallinity and mechanical properties of starch-based films at different relative humidity values. *Carbohydrate Polymers*. 77, 293-299. 2009.

[49] Müller, C.M.O.; Laurindo, J.B. and Yamashita, F. Effect of cellulose fibres addition on the mechanical properties and water vapour barrier of starch- based films. *FoodHydrocolloids.*23, 1328-1333. 2009.

[50] Ma, X.; Yu, J. and Kennedy, J.F. Studies on the properties of natural fibres-reinforced thermoplastic starch composites. *Carbohyhdrate Polymers*. 62, 19-24.2005.

[51] Averous, L.; Fringant, C. and Moro, L. Plasticized starch-cellulose interactions in polysaccharide composites. *Polymer.*42, 6565-6572. 2001.

[52] Teixeira, E.M.; Pasquini, D.; Curvelo, A.A.S.; Corradini, E.; Belgacem, M.N. and Dufresne, A. Cassava bagasse cellulose nanofibrils reinforced thermoplastic cassava starch. *Carbohydrate Polymers*. 78,422-431.2009.

[53] Funke, U.; Bergthaller, W. and Lindhauer, M. G. Processing and characterization of biodegradable products based on starch. *Polymer Degradation and Stability*.59, 293-296.1998.

[54] Dufresne, A.; Dupeyre, D.; Vignon, M.R. Cellulose microfibrils from potato tuber cells: Processing and characterization of starch–cellulose microfibril composites. *Journal of Applied Polymer Science*. 76, 2080-2092.2000.

[55] Usuki, A.; Kawasumi, M.; Kojima, Y.; Okada, A.; Kurauchi, T. and Kamigaito, O.J. Swelling behaviour of montmorillonite cation exchanged for V-amino acids by E-caprolactam. *Journal of Materials Research*.8, 1174-1178.1993.

[56] Lee, L.J.; Zeng, C.; Cao, X.; Han, X.; Shen, J. and Xu, G. Polymer nanocomposite foams. *Composites Science and Technology*. 65, 2344-2363.2005.

[57] Ardanuy, M.; Rodríguez-Perez, M.A. and Algaba, I. Electrical conductivity and mechanical properties of vapour-grown carbon nanofibers/trifunctional epoxy composites prepared by direct mixing. *Composites: Part B*. 42, 675-681. 2011.

[58] Kojima, Y.; Usuki, A.; Kawasumi, M.; Okada, A.; Fukushima, Y.; Kurauchi, T. and Kamigaito, O.J. Mechanical properties of nylon 6-clay hybrid. *Journal of Materials Research*.8, 1185-1189.1993.

[59] Manias, E.; Touny, L.; Wu, K.; Strawhecker, B.; Lu, T. and Chung, C. Polypropylene/montmorillonite nanocomposites. Review of the synthetic routes and material properties. *Chemistry of Materials*.13, 3516-3523.2001.

[60] Tjong, S.C. Structural and mechanical properties of polymer nanocomposites. *Materials Science and Engineering*. 53, 73-197. 2006.

[61] Estravís, S. Cellular nanocomposites based on rigid polyurethane and nanoclays: Fabrication, characterization and modelling of the mechanical properties and thermal properties. *PhD Thesis*. University of Valladolid. Spain. 2014.

[62] Manias, E.; Touny, A.; Wu, L.; Strawhecker, K.; Lu, B. and Chung T.C. Polypropylene/montmorillonite nanocomposites. Review of the synthetic routes and materials properties. *Chemistry of Materials*.13, 3516-3523.2001.

[63] Pascual, J.; Fages, E.; Fenollar, O.; Garcıa, D. and Balart. R. Influence of the compatibilizer/nanoclay ratio on final properties of polypropylene matrix modified with montmorillonite-based organoclay. *Polymer Bulletin*. 62, 367-380.2009.

[64] Rama, M.S.; Neppalli, R.; Chellaswamy, R. and Swaminathan, S. Exfoliation of clay layers in polypropylene matrix using potassium succinate-g-polypropylene as compatibilizer. *Composites Science and Technology*.70, 1550-1556. 2010.

[65] Ferreira, J.A.M.; Reis P.N.B.; Costa, J.D.M.; Richardson, B.C.H. and Richardson M.O.W. A study of the mechanical properties on polypropylene enhanced by surface treated nanoclays. *Composites: Part B*. 42, 1366-1372. 2011.

[66] Bikiaris, D.N.; Papageorgiou, G.Z.; Pavlidou, E.; Vouroutzis. N.; Palatzglou, P. andKarayannidis, G.P. Preparation by melt mixing and characterization of isotactic polypropylene/SiO_2 nanocomposites containing untreated and surface-treated nanoparticles. *Journal of AppliedPolymer Science*. 100, 2648-2696. 2006.

[67] Jacob, S.; Suma, K.K.; Mendez, J.M. and George, K.E. Reinforcing effect of nanosilica on polypropylene-nylon fibre composite. *Materials Science and Engineering B.* 168, 245-249. 2010.

[68] Lai, S.M.; Huang, C.Y.; Li, S.C.; Chen, Y.H.; Hsu, H.C.; Yu, Y.F. and Hsiou, Y.F. Preparation and properties of melt-mixed metallocene polyethylene/silica nanocomposites. *Polymer Engineering and Science*. 51, 434-444.2010.

[69] Boischot, C.; Moraru, C.I. and Kokini. J.L. Factors that influence the microwave expansion of glassy amylopectin extrudates. *Cereal Chemistry*. 80, 56-61. 2002.

[70] Moraru, C.I. and Kokini, J.L. Nucleation and expansion during extrusion and microwave heating of cereal foods. *Comprehensive Reviews in Food Science and Food Safety*. 2, 147-165. 2003.

[71] Pushpadass, H.A.; Babu, G.S.; Weber R.W. and Hanna, M.A. Extrusion of starch-based loose-fill packaging foams. Effects of temperature, moisture and talc on physical properties. *Packaging technology and science*.21, 171-183. 2008.

[72] Pushpadass, H.A.; Weber, R.W.; Dumais, J.J. and Hanna, M.A. Biodegradation characteristics of starch-polystyrene loose-fill foams in a composting medium. *Bioresource Technology*. 101, 7258-7264. 2010.

[73] Wang, B.Y.; Gao, Y.X.; Song, J.; Bonin, M.; Guo, M. and Murphy, R. Assessment of technical and environmental performances of wheat-based foams in thermal packaging applications. *Packaging technology and Science.*23, 363-382. 2010.

[74] http://www.storopack.com/en/products-solutions/flexible-protective-packaging/packaging-chips-loose-fill-packaging.html

[75] Shogren, R.L.; Lawton, J.W. and Doane, W.M. Structure and morphology of baked starch foams. *Polymer*. 39, 6649-6655. 1998.

[76] Shogren, R.L.; Lawton, J.W. and Tiefenbacher, K.F. Starch–Poly(vinyl alcohol) foamed articles prepared by a baking process. *Journal of Applied Polymer Science*.68, 2129-2140. 1998.

[77] Shogren, R.L.; Lawton, J.W. and Tiefenbacher, K.F. Baked starch foams: starch modifications and additives improve process parameters, structure and properties. *Industrial crops and products*.16, 69-79. 2002.

[78] Hoseney, R.C.; Zeleznak, K. and Abdelrahman, A. Mechanism of popcorn popping. *Journal of Cereal Science*.1, 43-52. 1983.

[79] http://www.novamont.com/

[80] Errington, J.G.; Hornsey, A.J.; Chapman, T.J.; Quinn, P.J. and Wake, M.L. US7393492 B2.2008.

[81] Errington, J.G.; Hornsey, A.J.; Chapman, T.J.; Quinn, P.J. and Wake, M.L. EP1691962 B1. 2014.

[82] http://www.rebiofoam.eu/home.php

[83] Zhou, J.; Song, J. and Parker, R. Structure and properties of starch-based foams prepared by microwave heating from extruded pellets. *Carbohydrate Polymers*. 63, 466-475.2006.

[84] Peng, X.; Song, J. and Nesbitt, A. Microwave foaming of starch-based materials. Dielectric performance (I).Journal of Cellular Plastics. 49, 245-258. 2013.

[85] Peng, X.; Song, J. and Nesbitt, A. Microwave foaming of starch-based materials. Thermomechanical performance (II). *Journal of Cellular Plastics*. 49, 147-160. 2013.

[86] Zhou, J.; Song, J. and Parker, R. Microwave-assisted moulding using expandable extruded pellets from wheat flours and starch. *Carbohydrate Polymers*. 69, 445-454. 2007.

[87] Sjöqvist, M. and Gatenholm, P. The effect of starch composition on structure of foams prepared by microwave treatment. *Journal of polymers and the environment*.13, 29-37. 2005.

[88] Kaisangsri, N.; Kerdchoechuen, O. and Laokakunjit. N. Biodegradable foam tray from cassava starch blended with natural fibres and chitosan. *Industrial crops and products*. 37. 542-546. 2012.

[89] Soykeabkaew, N.; Supaphol, P. and Rujiravanit, R. Preparation and characterization of jute- and flax- reinforced starch-based composite foams. *Carbohydrate Polymers.* 58, 53-63. 2004.

[90] Bénézet, J.C.; Stanojlovic-Davidovic, A.; Bergeret, A.; Ferry, L. and Crespy, A. Mechanical and physical properties of expanded starch, reinforced by natural fibres. *Industrial crops and products*. 37.435-440. 2012.

[91] Bergeret, A. and Bénézet, J.C. Natural fibre-reinforced biofoams. *International Journal of Polymer Science*.2011.

[92] Lawton, J.W.; Shogren, R.L. and Tiefenbacher, K.F. Aspen fibre addition improves the mechanical properties of baked corn starch foams. *Industrial Crops and Products.*19, 41-48. 2004.

[93] Glenn, G.M.; Orts, W.J. and Nobes, G.A.R. Starch, fibre and $CaCO_3$ effects in the physical properties of foams made by a baking process. *Industrial Crops and products.*14, 201-212. 2001.

[94] Cinelly, P.; Chiellini, E.; Lawton, J.W.; Imam, S.H. Foamed articles based on potato starch, corn fibres and poly (vinyl alcohol). *Polymer degradation and stability*.91, 1147-1155. 2006.

[95] Carr, L.G.; Parra, D.F.; Ponce, P.; Lugão, A.B. and Buchler, P.M. Influence of fibres on the mechanical properties of cassava starch foams. *Journal of polymers and theenvironment*.14, 179-183.2006.

[96] Salgado, P.R.; Schmidt, V.C.; Molina Ortiz, S.E.; Mauri, A.N. and Laurindo, J.B. Biodegradable foams based on cassava starch, sunflower proteins and cellulose fibres obtained by a baking process. *Journal of Food Engineering.*85, 435-443. 2008.

[97] Mali, S.; Debiagi, F.; Grossmann, M.V.E. and Yamashita, F. Starch, sugarcane bagasse fibre, and polyvinil alcohol effects on extruded foam properties: a mixture design approach. *Industrial Crops and Products.* 32, 353-35. 2010.

[98] Saiz-Arroyo, C. Fabricación de materiales celulares mejorados basados en poliolefinas. Relación procesado-composición-estructura-propiedades. *Tesis Doctoral*. Universidad de Valladolid.España. 2012.

[99] Throne, J.L. Thermoplastic foam extrusion. An introductionon. *Hanser publishers,* Munich. 2004.

[100] Lee, S.T. Foam Extrusion: Principles and Practice. *Technomic Publishing Company*. Lancaster-Pennsylvania.2000.

[101] Zhai, W.; Kim, Y.W. and Park, C.B. Steam-Chest Molding of Expanded Polypropylene Foams. 1. DSC Simulation of Bead Foam Processing. *Industrial and Engineering Chemistry Research*.49, 9822-9829. 2010.

[102] Mills, N.J. and Gilchrist. A. Properties of bonded-polypropylene-bead foams: data and modelling. *Journal of materials science*.42, 3177-3189. 2007.

[103] Bouix, R.; Viot, P. and Lataillade. J.L. Polypropylene foam behaviour under dynamic loadings: Strain rate, density and microstructure effects. *International Journal of Impact Engineering*.39, 329-342. 2009.

[104] http://www.plasticsportal.net/wa/plasticsEU/portal/show/content/products/foams/neopolen_p/

[105] http://www.jsp.com/sp/products/beads

[106] Suh, K.W.; Park, C.P.; Maurer, M.J.; Tusim, M.H.; Genova, R.; Broos, R. and Sophiea, D.P. Lightweight Cellular Plastics. *Advanced Materials*.12, 1779-1789. 2000.

[107] Stange, J.; Münstedt, H. Effect of long-chain branching on the foaming of polypropylene with azodicarbonamide. *Journal of Cellular Plastics.*42, 445-467. 2006.

[108] Naguib, H.E. and Park, C.B. Strategies for achieving ultra low-density polypropylene foams. *Polymer Engineering and Science.* 42, 1481-1492. 2002.

[109] Nam, G.J.; Yoo, J.H. and Lee, J.W. Effect of long-chain branches of polypropylene on rheological properties and foam-extrusion performances. *Journal of Applied Polymer Science.*96, 1793-1800. 2005.

[110] Saiz-Arroyo, C.; Rodriguez-Perez, M.A.; Tirado, J.; Lopez-Gil, A and de Saja J.A. Structure–property relationships of medium-density polypropylene foams. *Polymer International.* 62, 1324-1333. **2013.**

[111] Nam, P.H.; Maiti, P.; Okamoto, M.; Kotaka, T.; Nakayama, T.; Takada, M. Ohshima, M.; Usuki, A.; Hasegawa, N. and Okamato, H. Foam processing and cellular structure of polypropylene/clay nanocomposites. *Polymer Engineering & Science.* 42, 1907-1918. 2002.

[112] Han, X.; Zeng, C.; Lee, L.J.; Koelling, K.W. and Tomasko, D.L. Extrusion of polystyrene nanocomposite foams with supercritical CO_2. *Polymer Engineering & Science.* 43, 1261-1275.2003.

[113] Zhai, W.; Park, C.B. and Kontopoulou, M. Nanosilica addition dramatically improves the cell morphology and expansion ratio of polypropylene heterophasic copolymer foams blown in continuous extrusion. *Industrial& Engineering Chemistry Research.*50, 7282-7289. 2011.

[114] Okamoto, M.; Nam, P.H.;Maiti, P.; Kotaka, T.; Nakayama, T.; Takada, M.; Ohshima, M.; Usuki, A.; Hasegawa, N. and Okamoto. H. Biaxial flow-induced alignment of silicate layers in polypropylene/clay nanocomposite foam. *Nano Letters.* 1, 503-505. 2001.

[115] Chaudhary, A.K and Jayaraman. K. Extrusion of linear polypropylene–clay nanocomposite foams. *Polymer Engineering & Science*. 51, 1749-1756. 2011.

[116] Shen, J.; Han, X. and Lee, L.J. Nucleation and reinforcement of carbon nanofibers on polystyrene nanocomposite foam.63rd ed. *Annual technical conference. Society of Plastics Engineers*. p.1896. 2005.

[117] Guo, M.C.; Heuzey, M.C. and Carreau, P.J. Cell Structure and Dynamic Properties of Injection Molded Polypropylene Foams. *Polymer Engineering & Science.*47, 1070-1081. 2007.

[118] Antunes, M.; Realinho, V. and Velasco J.I. Foaming behaviour, structure, and properties of polypropylene nanocomposites foams. *Journal of nanomaterials*. 2010.

[119] Antunes, M.; Velasco, J.I.; Realinho, V. and Solorzano, E. Study of the cellular structure heterogeneity and anisotropy of polypropylene and polypropylene nanocomposite foams. *Polymer Engineering & Science.*49, 2400-2413. 2009.

[120] http://www.diabgroup.com/en-GB/Sandwich-technology/Introduction/The-DIAB-sandwich-principle.

[121] http://www.diabgroup.com/Products-and-services/Core-Material.

[122] http://www.3accorematerials.com/airex.html.

CHAPTER 3:

MATERIALS, PRODUCTION PROCESSES AND CHARACTERIZATION TECHNIQUES

Contents

3.1-Materials.

The properties of the solid and foamed materials produced in this work depend on the polymer matrix employed and on the additives used to modify them such as fillers, plasticizers and blowing agents. All of them are described in detail in this section.

3.1.1- Starch based materials.

The materials employed for the production of starch-based materials are grouped into three kinds depending on their function: the polymer matrix, in this case starch, the plasticizers used to produce thermoplastic starch (TPS) and the natural fibres employed to enhance the mechanical properties of the virgin polymer matrix. In addition, NaCl was also used in the production of foams by microwave heating.

3.1.1.1- Polymer matrix: starch.

Two kinds of native starches have been employed: ***potato and wheat starch***. The denomination "native" is due to the fact that they were not chemically modified after extraction and isolation from the plant. Potato starch and wheat starch (*MERITENA 200*) were supplied by *TATE &LYLE* and *TEREOS SYRAL,* respectively. Both starches were provided in the form of fine white powders and their morphology was characterized by means of SEM micrographs as exemplified in Figure 3.1 in which the granular morphology of wheat starch is shown. The morphology of the granules differs depending on the botanical source as described in Figure 2.26.

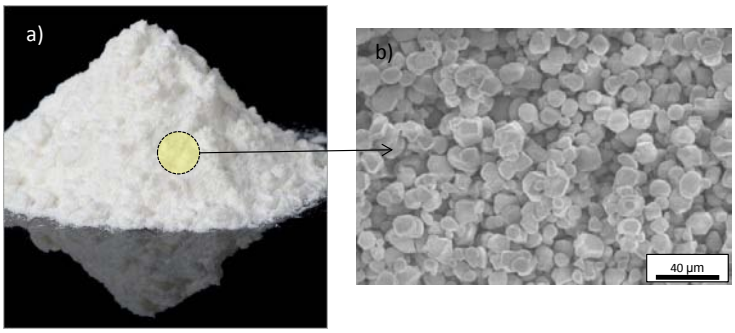

Figure 3.1.a) Starch fine white powders. b)SEM image of wheat starch.

3.1.1.2- Plasticizers.

Two kinds of plasticizers have been employed in this work, the selection of which was based on the final application of the starch-based material produced. When producing solid biocomposites, ***glycerol*** was used due to its high boiling point (290ºC) that allowed thermoplastic starch (TPS) to be processed at high temperatures without losing the plasticizer through evaporation. On the other hand, when starch-based foams were produced, ***water*** was employed because it also acts as the blowing agent in the process. The processing conditions to produce thermoplastic starch with water as the plasticizer prior to the expansion stage, taking the low boiling point of water into account (100ºC), must be softer than with glycerol in order to avoid excessive water loses. Water was simply obtained from the tap of the lab and

Glycerol was supplied by *VWR INTERNATIONAL* as a viscous liquid contained in 5l.glass bottles. The main properties of the glycerol employed are specified in Table 3.1.

Product	Properties and features	
Glycerol AnalaR NORMAPUR	Formula	$HOCH_2CH(OH)CH_2OH$
	Molecular weight (g/mol)	92,09
	Boiling point (ºC)	290
	Density- 20ºC (g/cm^3)	1,26

Table 3.1.Glycerol properties.

3.1.1.3- Natural Fillers.

Three kinds of natural fillers were selected: ***barley straw fibres***(supplied by the Universitat Politècnica of Catalunya), ***grape particle***(supplied by Matarromera Group) and ***cardoon particles***(supplied by Riberebro group).The reasons why they were selected are:

Firstly, because of their *lignocellulosic character* that makes them chemically compatible with the TPS matrix. In the case of the barley straw fibres the cellulose content is even higher because they were chemically treated prior to being mixed with TPS in order to isolate their cellulose fraction. This chemical treatment consisted of an hydrolysis with hot water followed by a treatment with an alkaline solution. Barley straw, without treatment, possesses cellulose and lignin contents of 33-44-5 wt% and 10-21 wt%, respectively, while after being treated the cellulose content was shifted up to 96.7%, the lignin content being clearly reduced to 1.51 wt% (these data were specified by the supplier).

Secondly, because of their *different morphology* (Figure 3.2). Barley straw fillers are fibres with high aspect ratios while grape an cardoon fillers are particulates of larger size. A more detailed characterization of their morphology will be shown in *chapter 4*.

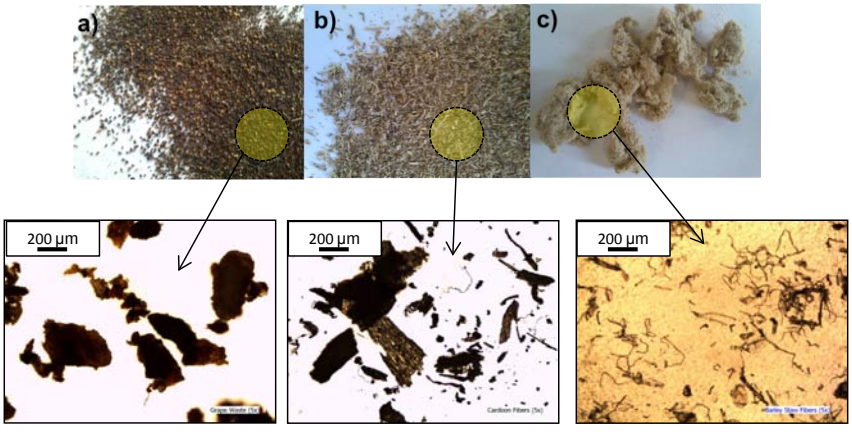

Figure 3.2.Pictures and optical micrographs of the natural fillers. a) Grape particles. b) Cardoon particles. c) Barley straw fibres.

Finally, they are obtained from *agriculture residues* which mean that their cost is negligible in comparison with the cost of the polymer matrix.

3.1.2.4- Blowing agent: water.

Water was employed not only as the plasticizer but also as the blowing agent of the microwave foaming process. It was obtained from the tap of the lab.

3.1.2.5- Salt (NaCl).

Salt (*Sodium chloride*) was provided by *SIGMA-ALDRICH* in the form of white crystalline powders with a *purity* ≥99%, a *particle size* of +80mesh (about 180 μm) and a *molecular weight* of 58.44 g/mol. This salt was employed as a microwave energy absorber for the production of the starch-based foams.

3.1.2- Polypropylene based materials.

The materials employed for the production of the polypropylene (PP) based foams are split up into different categories. The polymer matrix can be either virgin polypropylene or nanoreinforced polypropylene. In the latter case, nanoclays were the reinforcements employed and compatibilizers were used to improve the adhesion between the nanoclays and the polymer matrix. In both cases, azodicarbonamide was employed as the blowing agent and antioxidants were added with the aim of avoiding thermal degradation of the polymer during processing.

3.1.2.1- Polymer matrix: polypropylene.

Two kind of polypropylenes have been selected for the production of PP foams. On the one hand, a high melt strength (HMS) PP homopolymer provided by *BOREALIS* (PP Daploy WB 135 HMS) was used when the goal the production of foamed panels with densities below 200 kg/m^3 and at the same time, with high stiffness and strength. This grade of PP presents an excellent foaming performance due to its branched architecture. On the other hand, a random PP copolymer supplied by *INNEOS* (PP 200 CA10) was selected when the purpose was the evaluation of how the different foaming parameters in the *ICM* route influence the structure and properties of medium-density foams (relative density>0.2). The reason for selecting this PP is its low stability in the molten state during the foaming process, which makes it more sensitive to processing parameters such as blowing agent content, pressure and temperature/time. The main properties of the PPs selected are summarized in Table 3.2. Some of these data were taken from the technical data sheets of the polymers and others were measured at CellMat Laboratory as specified in the third column.

Product	Properties and features		
PP Daploy WB135 HMS	Structure	Long chain branched homopolymer.	
	Melt flow index	2,4 g/10 min (230ºC/2,16 kg)	ISO 1133
	Tensile modulus	2000 MPa	ISO 527-2
	Melt strength	32 cN	Borealis method
	Melt extensibility	250 mm/sec	Borealis method
	Melting temperature (DSC)	162 ºC	CellMat method
	Cristallinity (DSC)	46.5%	CellMat method
	Density	890 kg/m^3	CellMat method
PP 200 CA10	Structure	Random copolymer	
	Melt flow index	10 g/10 min (230ºC/2,16 kg)	ISO 1133
	Melting temperature (DSC)	150.4ºC	CellMat method
	Cristallinity(DSC)	44.4%	CellMat method
	Density	900 kg/m^3	CellMat method

Table 3.2. Properties of the polypropylenes employed.

3.1.2.2- Compatibilizer.

The compatibilizer used to adhere and disperse nanoclays within the polymer matrix was a linear PP homopolymer functionalized with maleic anhyhdride supplied by *CHEMTURA* (Polybond 3200). Its main properties are summarized in Table3.3. Maleic anhydride (Figure 3.3) is an organic compound suitable for compatibilization reactions between polymers due to the reactivity of its double bound in the presence of carbonyl groups.

Product	Properties and features		
Polybond 3200	Structure	Linear homopolymer functionalized with maleic anhydride	
	Melt flow index	115 g/10 min (190ºC/2,16 kg)	ASTM D-1238
	Melting temperature	157 ºC	Inneos method (DSC)
	Maleic anhydride level	1.0 wt%.	Inneos method
	Density	910 kg/m^3	ASTM D-792

Table 3.3.Polybond properties.

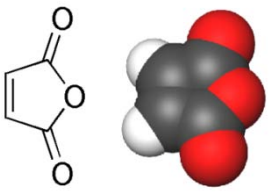

Figure 3.3.Maleic anhydride molecule.

3.1.2.3- Fillers.

The reinforcement employed for the production of nanocomposite foams is a natural montmorillonite modified with quaternary ammonium salts (Figure 3.4) provided by *SOUTHERN CLAY PRODUCTS* (Cloisite C20A). In the molecule shown in Figure 3.4 the groups denominated as **HT** are hydrogenated tails with these approximate compositions: ~65% C18; ~30% C16; ~5% C14. Table 3.4 lists the principal properties of the montmorillonite employed which were obtained from the technical data sheet.

Product	Properties and features	
Closite C20A	Organic modifier	2M2HT (dimethyl, dihydrogenatedtallow, quaternary ammonium).
	Modifier concentration	95 meq/100g clay
	Humidity (weight %)	≤ 2%
	Weight loss after ignition	38%
	Density	1770 kg/m^3
	d001 (Interlayer distance)	2.42 nm
	Particle size	90% less than 13 µm

Table 3.4.Cloisite C20A properties.

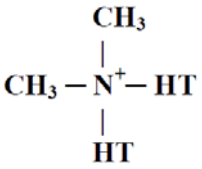

Figure 3.4.Quaternary ammonium salt.

3.1.2.4- Blowing agent.

Azodicarbonamide (ADC) was selected as the chemical blowing agent for several reasons. Firstly, because it is an exothermic blowing agent with a high gas yield. Secondly, because of its high decomposition temperature, which allows it to be blended with polypropylene without premature decompositions and last but not least, because of its low price in comparison with other chemical blowing agents which makes azodicarbonamide one of the most widely employed in industry. The azodicarbonamide employed in this work was supplied by *LANXESS* (Porofor M-C1) in the form of yellow powders. The properties obtained from the technical data sheet are shown in Table 3.5.

Product	Properties and features		
Porofor M-C1	Decomposition temperature	210 ºC	KA 13 p
	Density	1650 kg/m^3	DIN ISO 787
	Gas yield (volumetric at 210ºC)	228 ml/g	PAD 14
	Particle size	3.9 ± 0.6 µm	POR 41b

Table 3.5.Azodicarbonamide properties.

3.1.2.5- Antioxidants.

Antioxidants were employed in order to prevent thermal degradation of the polymer during processing due to the high temperatures and long time periods employed. A mixture of two antioxidants, Irganox 1010 and Irgafos 168, were employed both provided by *CIBA*.

3.2- Production processes.

Two foaming processes have been employed in this work. A *microwave foaming* process for the production of starch-based foams and the *improved compression moulding* route (ICM) when foaming polypropylene. A preliminary compounding process, based on melt-blending techniques such as extrusion, is necessary to disperse the required additives and fillers throughout the polymer. All these production processes will be explained in the following sections.

3.2.1- Bio and nanocomposites production by melt-blending.

The production of composites either biocomposites or nanocomposites, were performed in a *COLLIN* twin-screw extruder model *TEACH LINE ZK 25 T* (Figures3.5 and 3.6) and in a *HAAKE* internal mixer model *RHEODRIVE 5000* (Figure 3.7).

The twin-screw extruder is composed of two co-rotating screws of the same diameter which rotate inside a barrel, as shown in Figure 3.5, externally heated by five resistances. The fillers are dispersed throughout the molten polymer due to the high temperatures and shear force applied by the screws. Moreover, this equipment allows continuous production with high output rates. The main technical features of the twin- screw extruder employed are shown in Table 3.6.

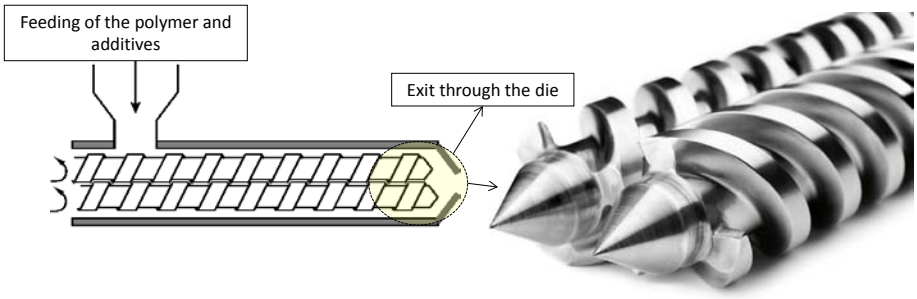

Figure 3.5.Scheme of a twin-screw extruder and picture of the end part of the screws.

Parameters	Units	Values
Diameter.	[mm]	2×25
Length.	[L/D]	24
Power.	[Kw]	2,2 (87 Hz)
Screw revolutions per minute.	[min^{-1}]	210 (87 Hz)
Torque	[Nm]	244
Output rate (LDPE).	[Kg/h]	4
Maximum melt temperature.	[ºC]	300
Maximum melt pressure.	[bar]	250

Table 3.6.Main characteristics of the twin-screw extruder employed.

The production of composites when using a twin-screw extruder always follows a similar pattern, regardless of the polymer employed. First of all, the polymer, the additives and the fillers are manually mixed. The mixture obtained is then fed into the extruder barrel by an automatic hopper located at the beginning of the extruder (Figure 3.6). The polymer melts shortly after being fed into the barrel because the extruder temperature is set higher than the melting temperature of the polymer. The molten polymer blended with the fillers moves forward through the extruder barrel pushed by the co-rotating movement of the screws. Finally, the composite produced comes out from the extruder die in the form of a circular strand. The molten strand, in the case of hydrophobic polymers, cools down and crystallizes in a water tank equipped with rollers with the aim of giving continuity to the process whereas cooling is performed in air in the case of hydrophilic polymers such as thermoplastic starch. At the end of the water tank there is an automatic pelletizer which cuts the solid strands into cylindrical pellets.

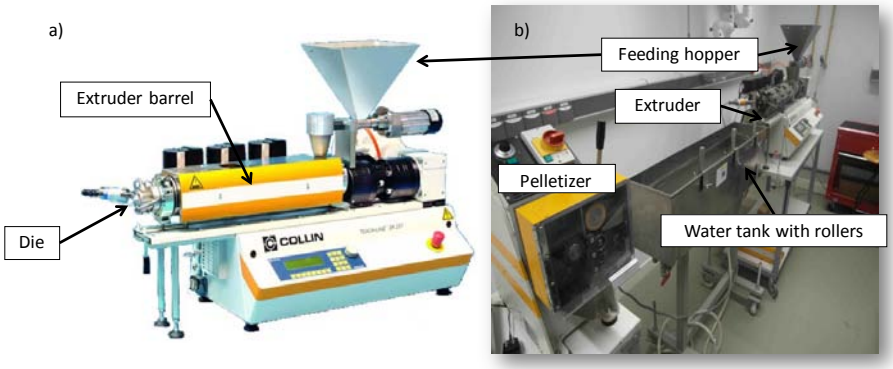

Figure 3.6.a) Extruder employed for the production of the composites. b) Complete extrusion system with the water tank and the pelletizer.

The production of composites in the internal mixer differs with respect to the production in the extruder because it is a batch process in which only a certain amount of material is fed into a chamber of known volume electrically heated by resistances. Inside the chamber, there are two screws that rotate in different directions, applying the required mechanical energy to the polymer and the fillers to produce proper blending. The main components of the internal mixer used in this work are shown in Figure 3.7.The temperature is set above the melting temperature of the polymer allowing the fibres to be homogeneously dispersed throughout the polymer by the action of the screws. Once optimum dispersion has been achieved, the composite is released from the chamber and cooled down by water or air, depending on its affinity with water.

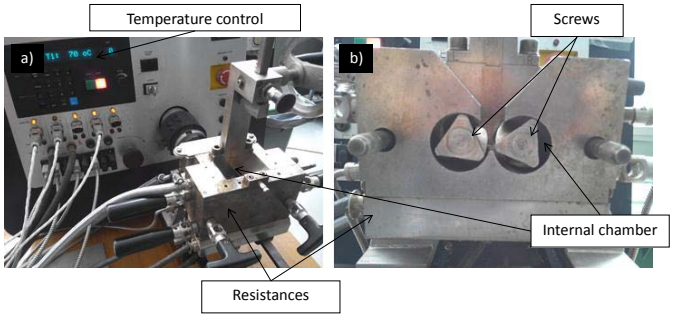

Figure 3.7.Internal mixer. a) General view. b) Internal chamber with the screws.

The equipment and production parameters employed were different depending on the polymer employed. These differences are presented in the next sections.

3.2.1.1- Starch-based biocomposites.

Two kinds of biocomposites were produced in this work. In the first one, starch was plasticized with glycerol because the objective was the production of solid biocomposites. In the second one, starch was plasticized with water with the aim of producing foams using microwave radiation. A common goal in both cases is to evaluate the degree of reinforcement of the polymer matrix with the addition of fillers.

✓ TPS plasticized with glycerol:

The complete production route followed when plasticizing starch with glycerol is schematically shown in Figure 3.8.

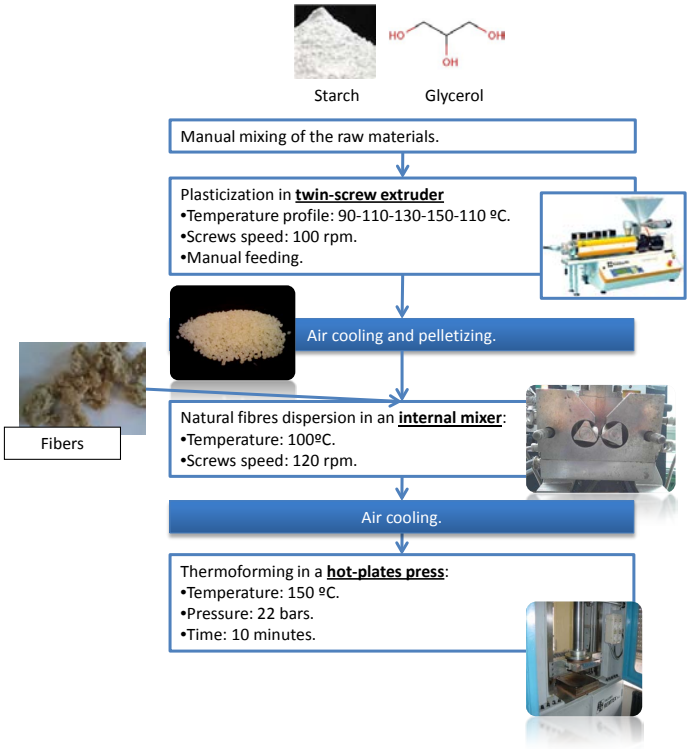

Figure 3.8. Production route of biocomposites plasticized with glycerol.

In this case starch is firstly plasticized with glycerol in the extruder. The plasticization of starch involves the complete disruption of the starch granules and the formation of a thermoplastic material with a smooth and continuous morphology. This morphological change produced during plasticization is observed in Figure 3.9 by means of SEM images.

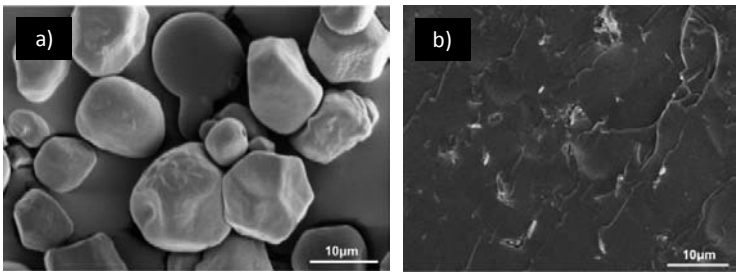

Figure 3.9. a) Starch granules. b) Thermoplastic starch.

Later, fillers are mixed with TPS in the internal mixer. Finally, tensile specimens (Figure 3.10)are produced by thermoforming so as to evaluate the reinforcement degree of the fillers by mechanical tests. The production process would differ on an industrial scale because the addition of fibres to the polymer matrix could be performed in a second extruder with the aim of giving continuity to the production and the thermoforming step would serve to provide the starch-based biocomposite with the final shape of the product. At the end of this work, in *chapter 6*, a lab-scale production route of flexible TPS-based trays developed in *Cellmat Laboratory* will be further described.

Figure 3.10. Tensile specimens of the starch-based biocomposites produced with different contents of barley straw fibres.

- ✓ TPS plasticized with water:

The process is very similar when water is employed as the plasticizer (Figure 3.11). However, the processing parameters were softer than when using glycerol. Especially as far as temperature is concerned, due to the low boiling point of water (100ºC). Water loses during the processing steps prior to foaming would result in poor foaming performances.

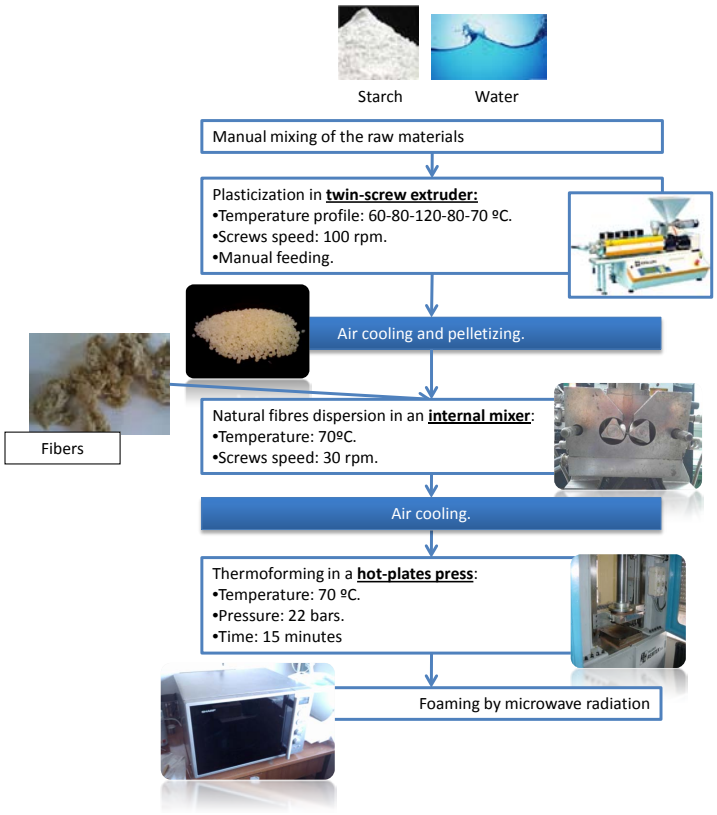

Figure3.11.Production route of foamed biocomposites.

The purpose of the thermoforming process is the production of cylindrical solid precursors with the shape of the foaming mould cavity as shown in Figure 3.12. The end of the process is the production of foams by microwave radiation although this step will be explained in more detail in *section 3.2.2*.

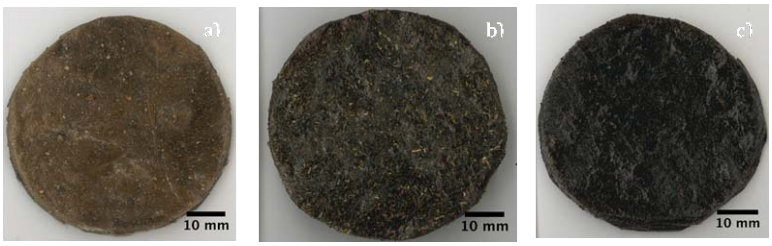

Figure 3.12.TPSsolid precursors for the production of foams by microwave radiation reinforced with: a) barley straw fibres, b) cardoon fillers and c) grape fillers.

The detailed chemical compositions of the starch-based composites produced, plasticized either with glycerol or water, are included in the articles of *chapter 4*.

3.2.1.2- Polypropylene-based nanocomposites.

The production of nanocomposites based on polypropylene as the polymer matrix and natural montomorillonites as the fillers is conditioned by the poor chemical compatibility between both materials. Polypropylene is an organic hydrophobic polymer while montmorillonite is an inorganic reinforcement that can only be compatibilized with the polymer by using compatibilizers and *melt-grafting compounding* routes.

With this purpose in mind, the natural montmorillonite employed (CLOSITE C20A) was functionalized (by the supplier)with quaternary alkyl ammonium salts composed of two long hydrogenated tails as shown in Figure 4. These salts replace the Na^{+} and Ca^{2+}cations(Figure 34 of *chapter 2*) increasing the interlayer distance. Moreover, montmorillonite becomes partially organophilic and more compatible with the chemistry of the polymer because the hydrogenated tails are mainly composed of carbon atoms. Nevertheless, its whole chemistry is still polar and an additional compatibilization step is necessary. This compatibilization was achieved by using a polypropylene modified with maleic anhydride (POLYBOND 3200) which easily intercalates within the montmorillonite interlayer. The driving force of the intercalation arises from the strong hydrogen bonding interaction between the maleic anhydride group (or COOH group generated from the hydrolysis of the maleic group) and the oxygen groups of the silicates present in the montmorillonite structure [1]. To make all these interactions possible it is necessary to blend the three components involved homogeneously (PP matrix, PP-based compatibilizer and montmorillonite) by using extruders or internal mixers. This is the reason why these compatibilization techniques are usually referred to as *melt-grafting compounding.*

Figure 3.13 shows a scheme of the *melt-compounding process* carried out in this work to obtain polypropylene nanocomposites.

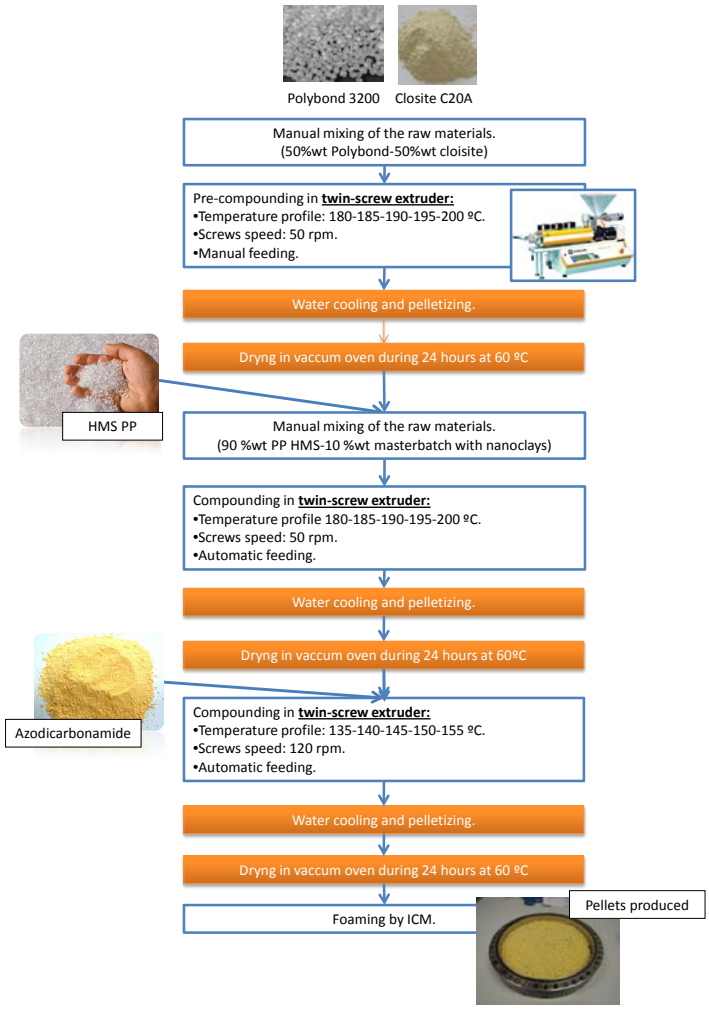

Figure 3.13.Production route of the PP-based nanocomposites.

The compounding process starts with the production of a *masterbatch* composed of compatibilizer (50 wt%) and montomorillonite (50 wt%).The temperatures employed in the extruder are high enough to melt polypropylene and disperse nanoclays effectively throughout the molten polymer. Once the *masterbatch* obtained at the exit of the die has been cooled and pelletized, it is dried in a vacuum oven with the aim of removing the water absorbed during cooling due to the hydrophilic character of montmorillonite. After drying, the masterbatch is diluted in the extruder again with the main polymer matrix (HMS PP) in such way that the final concentration of nanoclays in the nanocomposite is 5 wt%. The same process of cooling, cutting and drying is performed before using the materials to prepare a foamable composite.

Finally, azodicarbonamide is added to the nanocomposite in a new compounding stage performed at lower temperatures (135-140-145-150-155 ºC) and higher screw speeds (120 rpm) with the aim of avoiding premature thermal decomposition of the blowing agent. The material is then cooled, pelletized and dried to be used for the production of the foams (*section 3.2.3*).

3.2.2- Microwave foaming of starch.

The high interaction of microwave radiation with water molecules makes starch-based materials plasticized with water suitable for microwave heating applications. In addition, the high distribution of water along the polymer matrix allows heating the sample or *workload* homogeneously from the beginning of the process because each water molecule represents a hot spot from which the heat generated is subsequently transferred to the rest of the sample by conduction. A scheme showing this heating mechanism was previously shown in Figure 2.42.

3.2.2.1- The interaction of water with microwaves.

Water interacts with microwave radiation because it is a dielectric material composed of polar molecules. These molecules, when subjected to the electric field of microwaves, are reoriented as shown in Figure 3.14. This reorientation movement produces an alternating electric field (P) that lags behind the one generated by the microwaves (E) due to frictional forces of the water molecules. The different oscillating phase (δ) of both electric fields results in polarization loss and consequently, in the generation of heat(Figure3.14).This is a common feature of *dielectric lossy materials* such as water [2].

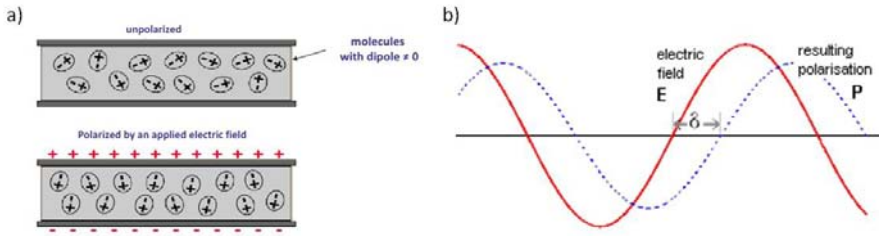

Figure 3.14.a) Polarization of water molecules by the electric field of microwaves. b) Phase difference between the electric field of microwaves (E) and that generated by the polarization of water molecules (P).

The *loss angle* δ, which represents the phase difference between both electric fields, is a parameter usually employed to quantify the *lossyness* of a dielectric material and hence, its ability to generate heat under microwave radiation. The loss angle is calculated by equation 1.

$$\tan \delta = \frac{\varepsilon''}{\varepsilon'} \tag{3.1}$$

In this equation, ε' represents the *permeability* of the material and its ability to be polarized by the electric field and thus, the ability of microwaves to propagate into it. On the other hand, ε'' is usually called the *loss factor* and indicates the ability of the material to dissipate the energy, that is, the efficiency of converting electromagnetic radiation into heat. This last parameter depends on the molecular structure of the material, the frequency of the radiation and the temperature [2].

Therefore, knowing the dielectric properties of the *workload* is of paramount importance in order to properly design a microwave heating process. The loss factor values of some materials are listed in Table 3.7 together with other important parameters considered when designing moulds for microwave processes (*section 3.2.2.2*) [3]. In this table it is possible to see how the loss factor of water is considerably higher than that of other materials such as PTFE and glass.

Materials	Loss factor (ε'')[a]	Max. service temperature (ºC)	Tensile strength (MPa)	Processability	Adhesion to molten starch
Glass (96% SiO_2)	0,00023	897-1397	45-155	Poor	High
Wood/paper	0,22[b]	117-137	60-100	Medium	Medium/High
Polyethylene	0,0024	125-132	21-45	Good	Low
PTFE	0,0003	250-271	20-30	Good	Very low
Water (distilled)	1,2	-	-	-	-
0.5 M NaCl	269	-	-	-	-

[a] Measured at 25ºC and 109 Hz [4]

[b] Estimated from data extracted from *Meredith* [4]

Table 3.7. Important properties of materials when subjected to microwave radiation

Conventional foaming processes based on *surface heating* such as *baking* (*section 2.4.1.2*) produce temperature gradients along the *workload*. The structures produced are usually characterized for presenting outer skins denser than the rest of the foam as shown in Figure 3.15. This is because the heat transfer starts at the surface of the batter and is later transferred to the rest of the sample by conduction. The water on the surface is the first to volatilize and as a result, most of it diffuses outside instead of forming cells. Moreover, the interior of the sample expands later than the exterior smashing the cells on the surface and producing a densification of this zone.

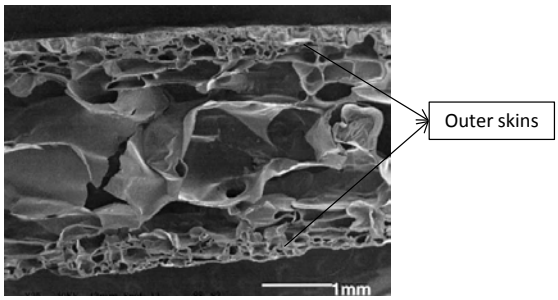

Figure 3.15. Starch foam produced by a *surface heating* method such as baking [5].

Volumetric heating methods such as microwave radiation could represent an alternative to processes such as baking for several reasons: first of all, during microwave heating the temperature of the dry and passive *workload* (passive refers to a material that does not change its state during heating) rises linearly and continuously as long as power is applied. On the contrary, in a *surface heating* method the *workload* temperature rises asymptotically until it reaches the oven temperature and does not continue rising above it. Secondly, microwave ovens are very efficient when converting energy into heat in the workload. In large industrial ovens as those shown in Figure 3.16 which operate continuously, the *microwave efficiency*, defined as the percentage of the applied microwave energy which is dissipated as heat in the workload, can be in the region of 95% and the *conversion efficiency* of electrical power into microwave power is about 85%. Thirdly, a conventional oven has to be heated at a temperature which is higher than that specified for the process, while in microwave ovens the temperature of the oven rarely reaches the surface temperature of the sample. Therefore, the radiation and convection loss from the microwave oven to the exterior is lower. Last but not least, the control of power with microwaves is instantaneous. This means that the equilibrium conditions are reached shortly after a change is produced. The start-up of the process is very rapid resulting in energy saving [4].

Figure 3.16.Industrial continuous microwave ovens for drying products.

The microwave foaming process of starch employed in this work is a batch process, like that produced in normal kitchen microwave ovens for heating or cooking food. In this kind of batch process the amount of energy injected into the *workload* can be calculated by equation 3.2.

$$E = \int_0^t p dt \tag{3.2}$$

where *E* is the total energy injected into the workload (Joules or watt seconds), *p* is the power applied to the workload (watts) and *t* is the total time of the process. This energy can be used to calculate the thermal change in the workload.

Under the assumption that the workload is dry and passive, which is not the case of starch plasticized with water, and that it is a batch process, the rate of temperature rise (*dT/dt*) is related to the power dissipation in the workload *p* (watts), the mass of the workload *M* (grams) and its mass specific heat *s* (joules per gram per degree Celsius) and can be calculated by equation 3.3.

$$P = M\frac{dT}{dt}s \tag{3.3}$$

From this equation it is clear that the increase in temperature produced in a dry passive workload while subjected to microwave radiation is linear as previously stated. This equation provides engineers with the possibility of designing a microwave heating process by simply setting the power required to increase the temperature of a determined mass of *workload* to a certain level.

In the particular case of foaming starch the matter varies substantially because one of the substances composing the *workload*, water, changes its state during foaming. Therefore, a latent heat of evaporation must be added to the heat balance previously shown in equation 3.3In the case of water, the latent heat of fusion (L_f) is 80 kcal/kg and the latent heat of evaporation (L_e) is 540 kcal/kg at 0ºC and 100ºC, respectively. Not only foaming but also many other industrial applications of microwave heating involve the presence of latent heat such as thawing, tempering, and drying. The process of foaming starch can be considered very similar to that of drying materials by microwaves. When considering the heat balance of a microwave forced-drying system in which all the energy is provided by microwaves the equation 3.3 turns into equation 3.4.

$$E = \frac{4.2}{60}\left\{s_d(T_b - T_0) + \frac{m_l}{100}s_1(T_b - T_0) + \frac{(m_1 - m_2)}{100}L\right\} \tag{3.4}$$

where:

- E= total energy required (kW/minkg).
- s_d= the specific heat of the dry matter (kcal/ºC kg).
- s_l= the specific heat of the liquid. For water: 1,00 kcal/ºC kg.
- m_1= initial moisture content % (dry-weight basis).
- m_2= final moisture content % (dry-weight basis).
- L= latent heat of evaporation of liquid (kcal/kg).
- T_0= initial temperature (ºC).
- T_b= boiling temperature of liquid (ºC).

The first term of the equation represents the sensible heat required to raise the temperature of the dry matter fraction of the *workload* up to 100ºC (T_b). The second term is the sensible heat required to raise the temperature of the water fraction to 100ºC (T_b). The third term accounts for the latent heat of evaporation of the water fraction. This equation gives the total heat input required to completely dry (m_2=0) a *workload* but it could be used either for designing a foaming process because in both cases the material is subjected to drying. During foaming the thermoplastic starch matrix is being dried because the water molecules go from the molten polymer to the cells, which are created after nucleation in the form of gas. In other words, the cell walls, edges and struts are being drying during expansion [4].

Not only for drying processes but also for foaming starch is very important to control the water content of the solid precursor prior to being foamed because it is the driving force of the process. The above treatment assumes that water molecules are in no way chemically attached by molecular forces to the dry matter. Nevertheless, the case of thermoplastic starch is different because the starch polymer chains are joined to the water molecules by intermolecular bonds or Van deer Waal forces. Hence, the total amount of energy required to release the molecules of water is greater than the normal latent heat of free water. In addition, the microwave absorption rate of the bound water is much less than that of the free water.

3.2.2.2- Production of starch foamed blocks by microwave radiation.

One of the principal novelties of the process developed in this work is the possibility of producing foamed blocks with a defined shape inside moulds. In the case of microwave heating the selection of the material to produce the mould is critical because the economy and performance of the process depends on the microwave absorption level of the mould. Some materials are transparent to microwave radiation because their constituent molecules do not suffer any kind of molecular reorientation during the application of microwaves. This is the case of *insulators* in which the microwaves penetrate the material without any absorption, loss or heat generation. Apart from not absorbing the microwave radiation (materials with low loss factors as shown in Table 3.7), the material of the mould has to fulfil other requirements: it must maintain its consistency at the foaming temperature of the process because the heat is transferred from the sample to the mould by conduction. It should have low adhesion with starch in order to demould the foamed block properly at the end of the process and finally, the processability of the material by machining must be good so as to produce the mould with the required shape and dimensions. The material which best fitted in with the previous requirements turned out to be PTFE (polytetrafluoroethylene). Figure 3.17 shows several PTFE pieces of different shapes and an example of PTFE machining.

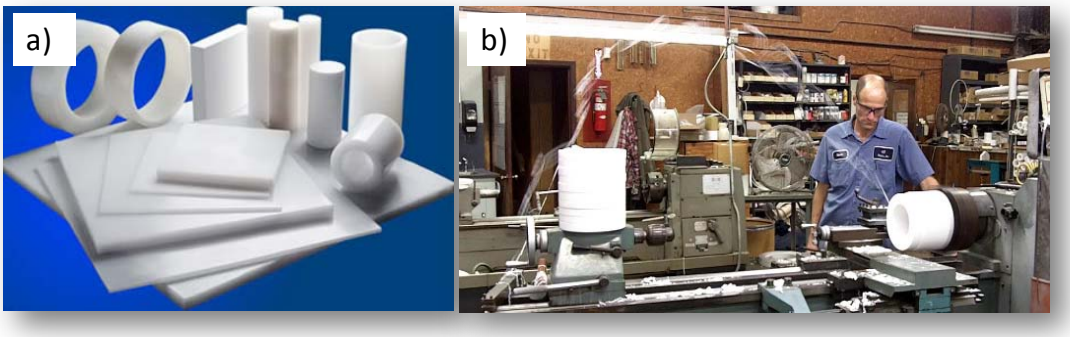

Figure 3.17. a) Machined PTFE pieces. b) Process of machining a pipe made of PTFE.

In this work, specially designed PTFE moulds were made with the aim of producing starch foamed blocks reinforced with natural fillers for *protective-packaging* applications and starch foamed trays for *food-packaging* applications. The production route employed for the production of the trays will be explained in *chapter6*. The aim of producing cylindrical foamed blocks was to perform mechanical compressive tests over foamed samples with the same density In this way, we were able to evaluate the reinforcement degree of natural fillers without the influence of the expansion ratio. Figure 3.18 shows the PTFE mould and the microwave oven model *SHARP R-939* employed in this work.

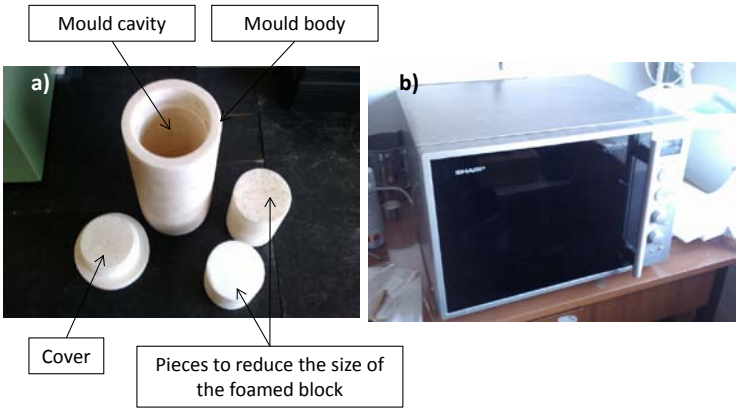

Figure 3.18. a) Principal parts of the PTFE mould. b) Microwave oven.

The procedure which was followed to produce the starch foamed blocks was: first of all, the PTFE mould was preheated to 160ºC for at least 30 minutes inside a conventional oven with the aim of avoiding excessive temperature gradients between the foamed sample and the mould which could lead to foam burning as shown in Figure 3.19c [3].The foamed material located on the surface of the sample transfers heat by conduction to the cold interior surfaces of the mould cavity. Hence, there is a decreasing temperature gradient from the interior of the sample to the exterior (Figure 3.19a). On the contrary, when the mould is preheated the temperature gradient becomes negligible (Figure 3.19b) and burning is avoided.

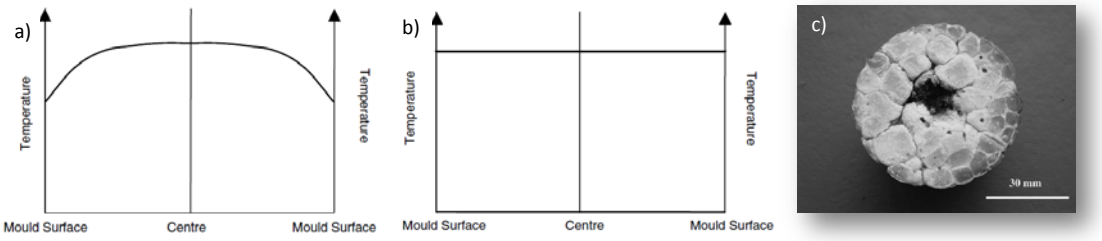

Figure 3.19. Temperature distribution of the foamed sample when: a) the mould was not pre-heated and b) the mould was pre-heated. c) Burning of the foam in the middle when the mould was not preheated [3].

During preliminary tests performed in our laboratory the temperature distribution of the PTFE mould after being preheated was evaluated by means of an infrared camera (model *Hotfind-L* from *SATIR*). This evaluation can be observed in Figure 3.20. Several points along the mould were evaluated to check the temperature distribution. The temperature in the interior of the mould was practically equal to that set in the oven (160ºC) while the temperature outside decreased substantially to values even below 130ºC. This is because several seconds elapsed from the moment in which the mould was taken out of the oven to the moment in which the image was taken; hence, heat was lost especially from the exterior part of the mould.

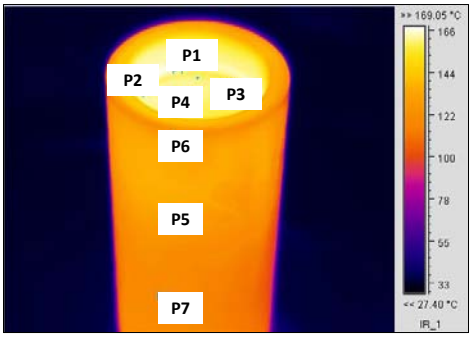

LOCATION	T (ºC)
P1	161
P2	163
P3	161
P4	161
P5	136
P6	137
P7	124

Figure 3.20.Temperature distribution of the mould after being pre-heated.

Once the mould was preheated, a solid precursor was placed into the mould cavity which was then rapidly closed and placed into the microwave oven chamber. This step must be carried out quickly enough to prevent the sample from being partially dried due to the high pre-heating temperatures of the mould.

In this precise moment microwave radiation, with a power of 900 watts, was applied to the *workload* (in this case the solid precursor) for 50 seconds. Once the microwave radiation ceased, the mould was removed from the oven and the foamed sample demoulded. Figure 3.21 shows a solid precursor prior to foaming and a foamed block after the process. The foamed block on the right had its surfaces polished so as to appreciate its cellular structure better.

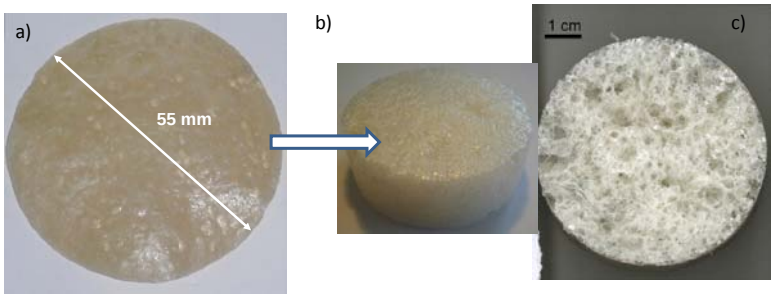

Figure 3.21. a) Solid precursor before the foaming process. b) Foamed blocks after microwave foaming. c) Foamed block after polishing.

During the application of microwave radiation the solid precursor is gradually heated until it becomes soft. Once the volatilization temperature of water is reached (100ºC) the soften polymer matrix is able to expand due to the sudden generation of steam which forms individual cells. An important part of the steam generated diffuses outside the polymer matrix and it is accumulated in the mould cavity. In order to evacuate this steam, several holes of 2mm in diameter were drilled in the mould cover. Figure 3.22 shows a schematic representation of the process in which the holes drilled to evacuate steam are also observed.

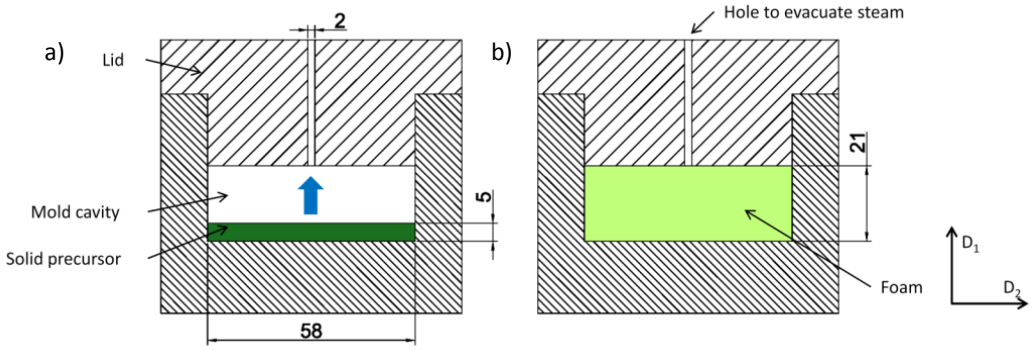

Figure 3.22. Scheme of the microwave foaming process of starch foamed blocks. a)Before foaming. b) When the foam fills the mould cavity.

One of the most challenging aspects of a microwave foaming process is how to monitor the temperature of the sample during the process. In a conventional heating process it is easy to place metallic thermocouples on the mould or even in contact with the molten material. However, the use of these metallic sensors as well as fibre optics inside microwave ovens is not possible. The use of Infrared (IR) cameras could be an option but in-situ monitoring the temperature of the sample through the screen door of the microwave oven is difficult because the screen in itself absorbs heat thus distorting the measurement[6]. In the work of *Boischot et al*[7], the IR measurement was performed after opening the oven door. The results were not very accurate in quantitative terms but some temperature differences along the foamed sample could be qualitatively appreciated.

In this work, infrared images of the empty mould cavity before the foaming process, the mould filled with the foamed sample and the foamed block shortly after being released from the mould are shown in Figure 3.23. It is possible to see how the temperature of the mould

decreases after the foaming process (Figure 3.23b) with respect to that of the pre-heated mould (Figure 3.23a) because it does not interact with the microwave radiation and only absorbs heat from the foamed sample. In addition, it has been observed that the temperature distribution along the foamed sample is very homogeneous as shown in Figures 3.23b and c.

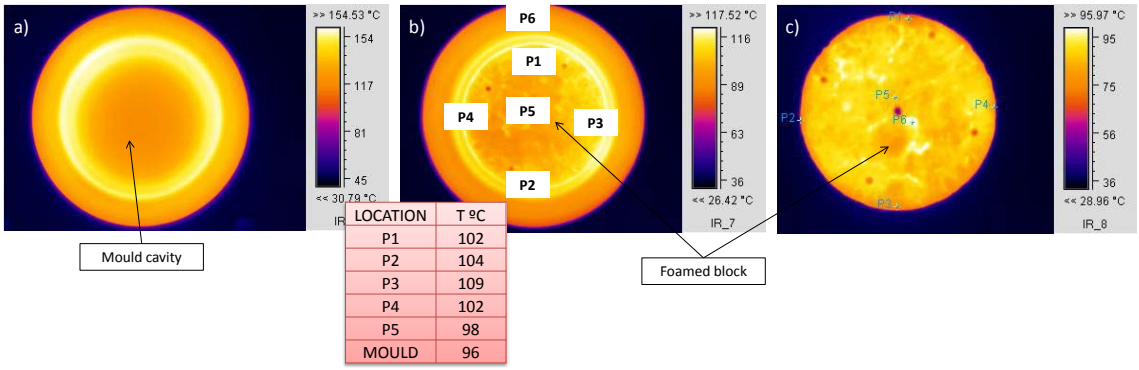

Figure 3.23. a) Mould after being pre-heated. b) Mould with the foamed block inside. c) Foamed block after being released from the mould.

Specific details of this process will be found in *chapter 4*in which starch-based foamed blocks reinforced with natural fillers with a cylindrical shape were produced by microwave radiation to evaluate the degree of reinforcement of these fibres.

3.2.3- Improved compression moulding

Among the foaming processes in which applying pressure is key to obtaining foams with high expansion ratios and fine cellular structures, ***compression moulding*** is one of the most widely employed in industry (*section 2.6.1.2*). Its main peculiarity, with respect to others such as *extrusion foaming* and *batch foaming processes based on gas dissolution,* is the use of chemical blowing agents which allows on the one hand, pressure to be applied to the polymer/blowing agent system by equipment which is not excessively sophisticated such as presses and on the other hand, high-thickness foamed blocks to be produced. There are two processes based on compression moulding: the *one-stage process* and the *two-stage process*. Nevertheless, crosslinking the polymer matrix is required in both cases. In the *two-stage process*, to obtain high expansion ratios during the second stage and in the *one-stage process,* to prevent the foamed polymer leaking out of the mould when producing low-density foams. Focusing on the *one-stage process*, the control of the density by this process is a very difficult task because it depends on the chemical composition and the processing parameters. There is no mechanical limitation for the polymer to expand once the pressure is released. Hence, the obtaining of defined shapes such as blocks and boards requires an additional cutting step resulting in material loss.

In an effort to overcome these drawbacks, the *Cellular Materials Laboratory*(*CellMat*) developed an alternative process called ***improved compression moulding***(*ICM*) which is mainly based on the use of specifically designed moulds called *self-expandable moulds*(Figure 3.24). These moulds allow heat and pressure to be transmitted simultaneously to the molten polymer and once pressure is released, the mould cavity is able to change its volume to let the

polymer expand. Moreover, they are able to control the expansion ratio regardless of the amount of blowing agent added. In this way, it is possible to obtain foams of the same density and with varied cellular structures by simply modifying processing parameters such as pressure, temperature/time and the chemical composition, like for instance the blowing agent content. In addition, the moulds are able to keep the foamable system inside the cavity even in the case of low viscosity non-crosslinked polymers which contains a gas dissolved and the stabilization of the cellular structure can be performed by cooling with water because the mould is hermetically sealed to prevent the entrance of liquids. Last but not least, it is possible to obtain foams of a defined shape: disks, cylinders, prisms etc.

The main steps of the ICM route are shown in Figure 3.24 in which the temperature evolution during the process is represented versus time. Moreover, schemes of the mould with the material inside are also presented in order to better understand the relation between each foaming step with the changes produced in the mould. In these schemes all the mould parts are included.

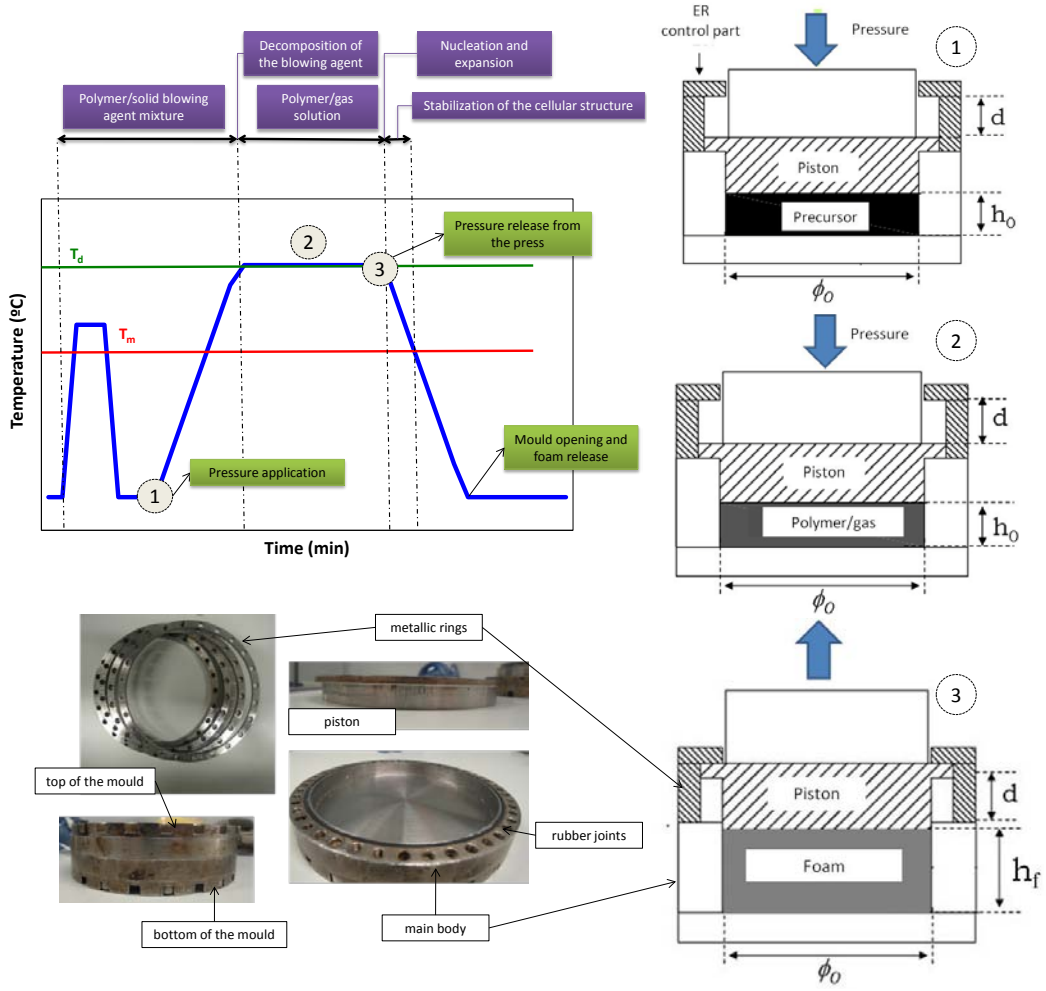

Figure 3.24. Stages of the improved compression moulding route (ICM).

Prior to the foaming stage it is necessary to produce a homogeneous blend *polymer-chemical blowing agent* by melt-blending (*section 3.2.1.2*) The first temperature cycle shown in the plot

of Figure 3.25 represents the compounding process in which temperature rises only above the melting temperature (T_m) of the polymer and below the decomposition temperature (T_d) of the blowing agent ($T_m<T<T_d$).

The initial mould cavity can be filled with expandable pellets or with thermoformed sheets. Then, it is closed by screws and sealed by rubber joints which are placed between the main body and the upper and bottom parts of the mould. At this moment, the mould is placed between the hot-plates of an automatic hydraulic press as shown in Figure 3.25and pressure and temperature are applied simultaneously (1). The temperatures used in this process are usually in the range of 190-200ºC while the pressures employed varied between 5 bars to 80 bars. Temperature rises up to the decomposition temperature of the blowing agent and the gas produced is dissolved into the polymer due to the high pressures applied (2) which result in the formation of the molten *polymer/gas* system. Once the pressure is released (3), cell nuclei appear and gas diffuses from the molten polymer to the cells created. Then, the pressure inside the cells becomes high enough to expand the molten polymer and to push the piston of the mould up to the maximum height allowed by the mould cavity.

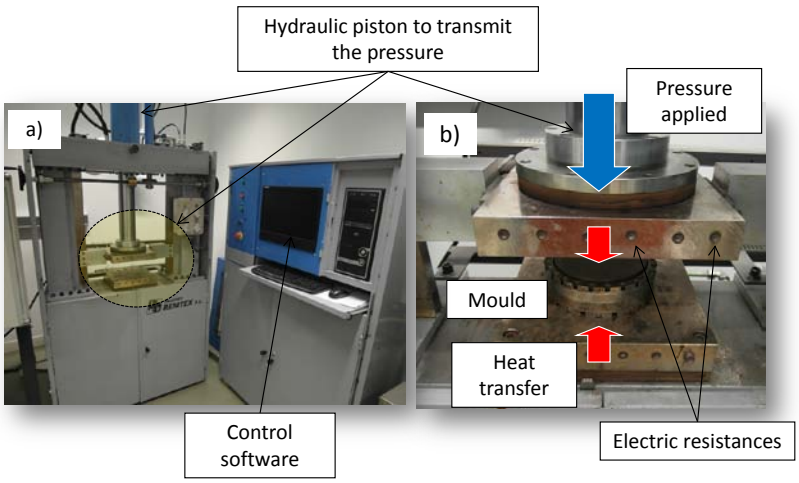

Figure 3.25.a) Automatic hydraulic press. b) Cylindrical mould between the hot-plates press.

The main feature of this foaming process is the ability of the mould cavity to change its dimensions, concretely its height, during the expansion of the polymer. The movement of the piston is free allowing the molten polymer to expand in one specific direction. This is why the mould is called *self-expandable mould*. This is possible because of the employment of metallic rings (Figure 3.24) with different heights placed between the main body and the top of the mould. The piston is displaced up to the height established by the ring. The relative expansion (ER) of the final foam is therefore, the ratio between the height of the mould cavity at the end of the process and the height of the mould cavity at the beginning ($ER=h_f/h_0$). Finally, the mould containing the foam inside is cooled down and stabilized by water.

An interesting characteristic of this process is that the molten polymer expands under the pressure exerted by the weight of the stainless-steel piston. How this fact influences the expansion process and hence, the cellular structures obtained is a matter which has not been

exhaustively studied so far. However, it is clear that it constitutes a remarkable difference with respect to other processes in which pressure is only applied in order to obtain a homogeneous solution polymer/gas prior to expansion, such as in *extrusion foaming* and *compression moulding*.

In this work, we have used the ICM route to produce polypropylene based foams in a density range between 150 kg/m^3 and 600 kg/m^3. The influence that production parameters such as pressure and blowing agent content have over the final cellular structures and the mechanical properties obtained, have been studied in detail. As the density range of the foams produced was very wide, the influence of the expansion ratio in structural parameters such as cell size and cell density has also been studied. On the other hand, the ICM route was also used to produce PP foamed panels reinforced with nanoclays. In this particular case, the study is focused on the influence that the nanoclay reinforcement and the use of different foaming pressures have on certain cellular structure parameters such as the anisotropy ratio and on the mechanical properties. All the foams were produced with the same expansion ratio and hence, this parameter did not influence the analysis of results. These studies will be explained in more detail in *chapter 5*.

Figure3.27 shows the different kind of polypropylene-based foamed panels obtained with this foaming process throughout this work, which were based on cylinders and disks.

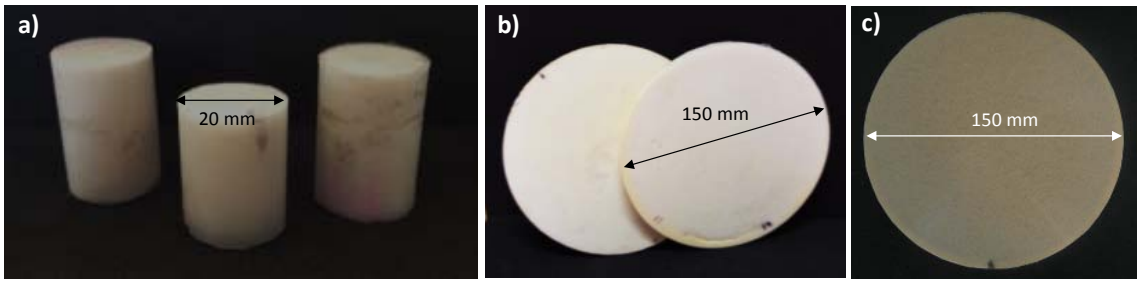

Figure 3.27. Shape of the foams produced in this work: a) PP foamed cylinders. b) PP foamed disks. c) PP nanocomposite foamed disk.

Although this work has been focused on foaming polypropylene based materials, the ICM route can be employed to foam any other thermoplastic polymer. In this sense, this process has been used for the production of LDPE foams, EVA foams and composites based on these polymers reinforced with aluminium and magnesium hydroxide and starch granules [8-15].

3.3- Characterization techniques.

The characterization techniques employed in this work are listed in Table 3.8. A more detailed explanation of how the samples which were produced were characterized by these techniques will be found in the chapters containing the experimental results. These techniques were mainly focused on studying the relationship between the cellular structure and the mechanical properties.

Characterization techniques.		Chapters
Mechanical tests to low strain rates. Universal machine INSTRON model 5500R625.	Compressive tests. (ISO 604-2002)	4,5
	Tensile tests(ISO 527).	4,5
	Bending tests. (ISO 178).	5
Starch morphology and cellular structure characterization by scanning electron microscopy (SEM) Electronic Microscope JEOL JSM-820.		4,5
Natural fibres morphology by optical microscopy. Optic microscope LEICA mo Del DM2500M.		4
Density measurement by the volumetric method.(ASTM D1622-08). Weighing scale METTLER Toledo AT261.		4,5
Open cell content measurement. Gas pycnometer model AccuPyc II 1340 Micromeritics. (ASTM D6226-10).		4,5
Evaluation of the thermal properties of the polymers and blowing agent content by thermogravimetric analyses (TGA) TGA/SDTA Mettler 851e		4,5

Table 3.8.Characterization techniques.

References

[1] Liu, X. and Wu, Q. PP/clay nanocomposites prepared by grafting/melt intercalation. *Polymer*. 42, 10013-10019. 2001.

[2] Bogdat, D. and Prociak, A. Microwave-enhanced polymer chemistry and technology. *Blackwell Publishing*. 2007.

[3] Zhou, J.; Song, J. and Parker, R. Microwave-assisted moulding using expandable extruded pellets from wheat flours and starch. *Carbohydrate Polymers*. 69, 445-454. 2007.

[4] Meredith, R. Engineers handbook of industrial microwave heating. *The institution of electrical engineers*. London. 1998.

[5] Shogren, R.L.; Lawton J.W. and Tiefenbacher, K.F. Baked starch foams: starch modifications and additives improve process parameters, structure and properties. *Industrial Crops and Products*. 16, 69-79. 2002.

[6] Tong, C.H.; Sheen, S.A.; Fu, Y.H.; Goedken, D.L. and Lund, D.B. Microwave heat transfer in food. 149-163. in: Advances in Food Engineering. Singh, P. and Wirakartakusumah, M.A. *CRC Press: Boca Raton, FL*.1992.

[7] Boischot, C.; Moraru, C.I.; and Kokini, J.L. Factors that influence the microwave expansion of glassy amylopectin extrudates. *Cereal Chemistry*.80, 56-61. 2002.

[8] Rodríguez-Pérez, M.A.; Lobos, J.; Pérez-Muñoz, C.A.; de Saja, J.A.; González, L.M. and del Carpio, M.A. Mechanical behaviour at low strains of LDPE foams with cell sizes in the microcellular range: advantages of using these materials in structural elements. *Cellular Polymers*. 27, 347-362. 2008.

[9] Rodríguez-Pérez, M.A.; Lobos, J.; Pérez-Muñoz, C.A. and de Saja. J.A. Mechanical response of polyolefin foams with high densities and cell sizes in the microcellular range. *Journal of Cellular Plastics*. 45, 389-403. 2009.

[10] Román-Lorza, S. Formulación y caracterización de materiales celulares retardantes de llama libres de halógenos basados en poliolefinas. *Tesis Doctoral*. Universidad de Valladolid. España. 2010.

[11] Román-Lorza, S.; Rodríguez-Pérez, M.A. and de Saja, J.A. Cellular Structure of halogen-free flame retardant foams based on LDPE. *Cellular Polymers*. 28, 249-268. 2009.

[12] Román-Lorza, S.; Rodríguez-Pérez, M.A.; de Saja, J.A. and Zurro, J. Cellular structure of EVA/ATH halogen-free flame retardant foams. *Journal of Cellular Plastics*. 10, 1-21. 2010.

[13] Román-Lorza, S.; Sabadell, J.; García-Ruiz, J.J.; Rodríguez-Pérez, M.A. and de Saja, J.A. Fabrication and characterization of halogen free flame retardant polyolefin foams. *Materials Science Forum*. 636/637, 98-205. 2010.

[14] Rodríguez-Pérez, M.A.; Simões, R.D.; Constantino, C.J.L. and de Saja, J.A. Structure and physical properties of EVA/Starch precursor materials for foaming applications. *Journal of Applied Polymer Science*. 212, 2324-2330. 2011.

[15] Rodríguez-Pérez, M.A.; Simões, R.D.; Román-Lorza, S.; Álvarez-Laínez, M.; Montoya-Mesa, C.; Constantino, C.J.L. and de Saja, J.A. Foaming of EVA/Starch blends: Characterization of the structure, physical properties and biodegradability. *Polymer Engineering and Science*. 52, 62-70. 2012.

CHAPTER 4:

DEVELOPMENT OF STARCH-BASED MATERIALS

Contents

4.1- Introduction.

Starch possesses numerous advantages that make it a very promising polymer especially for packaging applications: it is widely available and renewable, its price is very low in comparison with common synthetic polymers employed in this market such as PP, PET, XPS and EPS and finally, it is bioderived and biodegradable. However, the processing and transformation of starch granules, which are extracted from plants is difficult. The development of *thermoplastic starch* (TPS) drastically broadened the application of starch in the plastic market as previously mentioned in *chapter 2*. After plasticization, starch turns into a thermoplastic polymer which can be processed by conventional equipment employed in the plastic industry. This flexible material is adequate for use in the production of biodegradable food-packaging trays, which is the objective of the *ACTIBIOPACK* project in which the main part of this research was conducted. On the other hand, thermoplastic starch can be employed for foaming applications when it has been previously plasticized with water. However, the foamed product which is obtained is usually dry and brittle because water is lost during the expansion process. This fact restricts its application for *food-packaging* applications because these products (trays, films, etc.) require a certain degree of flexibility. On the contrary, these kinds of starch foams are very interesting materials for *protective-packaging* applications.

Unfortunately, these materials also present several drawbacks that make its use for the production of food-packaging trays and protective-packaging foams difficult. The most important drawbacks are related to their poor mechanical properties and their great affinity with water. In this thesis, research has been focused on the improvement of the mechanical properties as shown in the scheme of Figure 4.1.

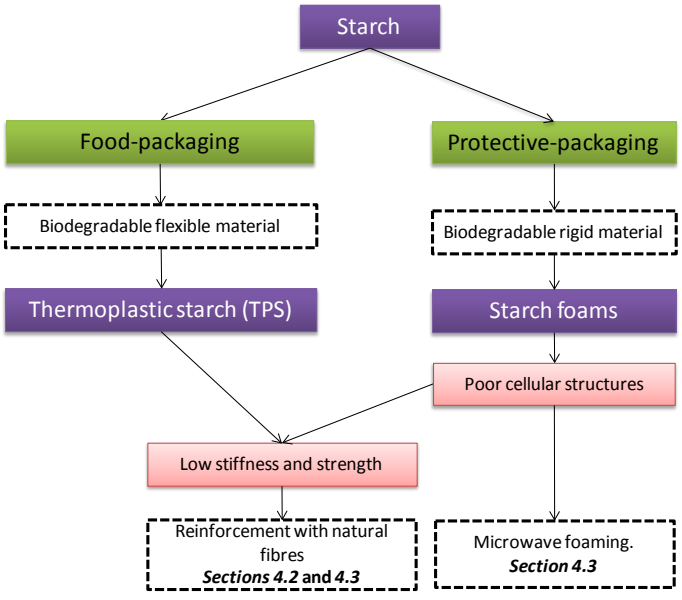

Figure 4.1. Drawbacks of starch and strategies used to overcome them in this thesis

On the one hand, the plasticization process involves a drastic reduction of mechanical properties because during this process starch becomes a mostly amorphous material which is frequently rubbery at ambient temperature. The reinforcement with lignocellulose-based

natural fibres represents an interesting strategy to overcome this problem because they are widely available (their main source being from agricultural and forest plants) and their chemical compatibility with starch is very high. There are lot of pieces of work in literature reporting the production of starch-based biocomposites with very promising results. These works were described in *section 2.4.2.2.* One of the works included in this chapter(*section4.2*) describes the production of biocomposites based on thermoplastic starch reinforced with *barley straw* and *grape* fillers. The main objective is to improve the mechanical properties of TPS and obtaining a bioderived and biodegradable material able to be used for the production of flexible food-packaging trays.

The use of starch foams for protective packaging applications has been limited due to their poor cellular structures and mechanical properties mainly derived from the production process employed (generally *extrusion foaming* and *baking*).The production of starch-based foams with higher mechanical performances from more efficient foaming routes is one of the aims of this thesis. In this sense, a microwave foaming process was employed due to the low energy consumption and to the heating transfer, which is more homogeneous (*volumetric heating*). Moreover, natural fibres were employed in order to increase the strength of the foams and to study their effect in the foaming mechanisms of this process in which the use of natural fibres have not been reported so far. The research conducted on this topic is presented in section 4.3.

4.2- Solid starch-based biocomposites.

The production of biocomposites based on TPS reinforced with natural fibres brought about the elaboration of a scientific article. This article was published in a scientific journal called: "*Polímeros: Ciência e Tecnologia*", which is included in this section and whose title is: *Strategies to improve the mechanical properties of starch-based materials: plasticization and natural fibre reinforcement.*

In spite of the fact that the materials developed in this section are solid, some of the results obtained can be extrapolated to what would happen with foamed materials. For instance the reinforcement of TPS with natural fibres was carried out not only on solid materials but also on foamed materials produced by microwave foaming. The comparison between both systems will be one of the issues discussed at the end of this chapter (*section 4.4)*

The methodology employed to evaluate the degree of the reinforcement of natural fibres in the solid TPS was: firstly, studying the adhesion and dispersion degree along the polymer matrix by means of SEM micrographs and secondly, studying the mechanical properties of the materials produced by tensile tests. The influence of the plasticizer content was also evaluated prior to the biocomposites production. Thus, TPS with different amounts of glycerol were produced and mechanically characterized.

Barley straw and grape fibres were selected because they represent an important source of lignocellulose wastes from the agricultural industry in Spain. Moreover, their morphology is very different which allowed the influence of fibre morphology on the mechanical properties of TPS to be studied. The results obtained will be analysed by the comparison with analytical models found in literature that describes the mechanical response of composites: the *law of mixtures*, the *Halpin & Tsay* model and the *Kerner & Nielsen* model. They were chosen for this study because they described the reinforcement degree of particles of different geometry (spherical particles and long fibres) and different orientations along the matrix.

Finally, a comparison between the properties of the materials developed in this article and those of synthetic polymers employed in the market of food-packaging trays is shown. In this comparison a biodegradable polymer such as PLA is also included.

http://dx.doi.org/10.4322/polimeros.2014.054

Strategies to Improve the Mechanical Properties of Starch-based Materials: Plasticization and Natural Fibers Reinforcement

A. Lopez-Gil, M.A. Rodriguez-Perez, J.A. De Saja
CellMat Laboratory, Department of Condensed Matter Physics, University of Valladolid, Valladolid, Spain

F.S. Bellucci
Department of Physics, Chemistry and Biology, São Paulo State University - UNESP, Presidente Prudente, Brasil

M. Ardanuy
Department of Textile and Paper Engineering, Universitat Politècnica de Catalunya, Terrassa, Spain

Abstract: Biodegradable polymers are starting to be introduced as raw materials in the food-packaging market. Nevertheless, their price is very high. Starch, a fully biodegradable and bioderived polymer is a very interesting alternative due to its very low price. However, the use of starch as the polymer matrix for the production of rigid food packaging, such as trays, is limited due to its poor mechanical properties, high hidrophilicity and high density. This work presents two strategies to overcome the poor mechanical properties of starch. First, the plasticization of starch with several amounts of glycerol to produce thermoplastic starch (TPS) and second, the production of biocomposites by reinforcing TPS with promising fibers, such as barley straw and grape waste. The mechanical properties obtained are compared with the values predicted by models used in the field of composites; *law of mixtures*, *Kerner-Nielsen* and *Halpin-Tsai*. To evaluate if the materials developed are suitable for the production of food-packaging trays, the TPS-based materials with better mechanical properties were compared with commercial grades of oil-based polymers, polypropylene (PP) and polyethylene-terphthalate (PET), and a biodegradable polymer, polylactic acid (PLA).

Keywords: *Biodegradable, starch, thermoplastic starch, biocomposites, food packaging, natural fibers, barley, grape.*

Introduction

The packaging market has commonly employed materials such as paper, glass and metals to produce packages for several applications. Nevertheless, these materials have been progressively substituted over the last fifty years by plastic, which is lightweight, resistant to corrosion, presents excellent mechanical properties relative to density, is easy to process by common industrial equipment and last but not least, is cheap. For instance, almost 40% of the plastic consumed worldwide in 2010 belonged to the packaging market [Source: Plastics Europe].

Plastics, in general, are mainly composed of an oil-based polymer matrix mixed with additives such as fillers, plasticizers, lubricants etc., which improve its processability and properties. Such a high diversity in composition makes the recycling of plastics very difficult and the few recycled products obtained are generally of poor quality. For these reasons, plastic waste is usually discarded and accumulated in landfill sites. The high volume of this waste and its slow-rate of degradation, which takes at least 400 years, are dramatically shortening the useful-life of the landfill sites. Several strategies have been set up during the last few years in order to overcome this problem like the incineration and energy recovery of plastic waste and the development of new recycling methods[1]. However, all of them require high investments. Last but not least, petroleum prices have been increased mainly because it is becoming a scarce natural resource, which only few countries possess worldwide. As a result, oil-based resin prices have also been raised.

All these environmental and economic problems are promoting the development of **biodegradable polymers** whose degradation scarcely takes a few weeks and can be employed for the production of compost[2]. Nevertheless, some of these biopolymers such as PLA, polycaprolactone (PCL) and polyhydroxyalkanoates (PHA) are produced by means of high-cost processes of extraction, fermentation, condensation etc. resulting in very expensive polymers in comparison with oil-based polymers employed in the packaging market such as PP and PET[3-6]. On the contrary, polysaccharides such as starch are directly extracted from cereals, tubers etc. without the need of being synthesized. This fact makes starch even cheaper than oil-based polymers and therefore, an ideal candidate to replace them in applications such as

***Corresponding author: Alberto López Gil**, Cellular Materials Laboratory – CellMat, Condensed Matter Physics Department, Faculty of Sciences, University of Valladolid – UVa, Paseo de Belen, 7, 47011, Valladolid, Spain, e-mail: alopgi@fmc.uva.es*

food packaging, a sector that is currently demanding this kind of biodegradable polymers. For all these reasons, the development of a fully biodegradable starch-based material for the production of rigid-food packaging such as trays is currently a challenge not only for scientist but also for industry[7].

Nevertheless, starch also presents several drawbacks, which are preventing the employment of this material for the production of food-packaging trays. These drawbacks are: poor processability in common industrial equipment such as extruders and thermoforming presses, high density (1400 kg/m^3), poor mechanical properties after being thermoformed (brittleness) and finally, it is hydrophilic and therefore, wet products cannot be packed.

The rigid packaging market usually employs polymers with high rigidity and strength such as high-density polyethylene HDPE, PP and PET. The high rigidity of these polymers allows the production of trays of low thickness and at the same time, able to support the weight of the food products and other requirements during transport and storage. The low amount of polymer employed for the production of one-single packaging due to its low thickness, results in a drastic reduction of raw-material costs. Nevertheless, native starch by itself is not able to fulfill these mechanical requirements because as was previously mentioned, after being thermoformed, it results in a brittle product, which breaks easily under any loading or impact. Two interesting approaches have been adopted by scientists with the aim of overcoming the poor mechanical properties of starch: first of all, the production of thermoplastic starch (TPS) by the plasticization of native starch with polyols or water[8] and secondly, the production of TPS composites reinforced with natural fibres[9,10]. Several fibres have been traditionally employed such as flax, jute, oil palm to name but a few[11,12]. However, blends of TPS with fibres such as barley straw and grape waste have not been studied in detail yet.

The purpose of this work is the production of materials based on thermoplastic starch able to be employed as the polymer matrix for the production of food-packaging trays. In this sense, two strategies have been developed: on the one hand, the production of TPS with different amounts of glycerol and on the other hand, the production of biocomposites of TPS with natural fibres such as barley straw and grape waste. Models found in literature such as the *law of mixtures*, *Kerner-Nielsen* and *Halpin-Tsai* will be employed in order to evaluate if the fibres are closely adhered and homogeneously orientated and distributed along the TPS matrix and if they fit closely to the experimental results. Finally, the materials produced will be compared, as far as mechanical properties are concerned, with the polymers currently employed in the rigid food-packaging market in order to evaluate if they are suitable to replace the oil-based polymers.

Materials

Wheat starch (*Meritena 200*) and potato starch were provided by *Syral* and *Tate & Lyle*, respectively. Glycerol was supplied by *Analar Normapur* (99,5% of purity). The barley straw fibers were provided by the department of textiles of the *Universitat Politècnica de Catalunya* and the grape waste by *Matarromera Group*.

Production

Thermoplastic starch is obtained by using plasticizers at high temperatures and shear forces. The high temperatures and shear applied by extruders help the plasticizer to penetrate into the granules of starch and break them resulting in a material with smooth and continuous morphology characteristic of thermoplastics. Apart from morphology, the plasticization of starch also involves changes in its characteristic thermal transitions such as the glass transition temperature, which is shifted from values above 200 °C in the case of native starch to values below 100 °C in the case of TPS. As a result, starch becomes a material, which is easy to process by industrial plastic equipment and with mechanical properties similar to those of oil-based polymers[13].

In this research work a Twin Screw Extruder model *Collin Teach Line ZK 25 T SCD 15* was used to plasticize starch and the plasticizer employed was glycerol. The reason for using glycerol was mainly because of its high boiling point (290 °C), which avoided the expansion of TPS by gases at the exit of the extruder. The temperature profile and the screw speed were set to 90-110-130-150-110 °C and 100 rpm respectively. Once thermoplastic starch (TPS) had come out of the die, it was air dried, and later cut into cylindrical pellets. When it comes to the production of biocomposites, the TPS pellets were mixed with natural fibres in a rheometer model *Haake 5000*. The temperature was set up to 100 °C and the screws speed to 120 rpm. All the materials were thermoformed in a hot-plates press in order to obtain tensile tests specimens. The temperature was set to 150 °C and the pressure applied was 11 MPa.

Three TPS-based formulations with different amounts of glycerol were produced. Wheat Starch (*Meritena 200*) was employed as the polymer matrix. Table 1 shows these formulations.

Eight biocomposites were produced mixing TPS (30% of glycerol) with different contents of barley straw fibres and grape waste. These formulations are shown in Table 2. In this case, potato starch was employed as the polymer matrix. The reason for using different starches, wheat and potato starch was to study the influence of the botanical origin over the mechanical properties of the final TPS produced.

Characterization

All the materials produced were mechanically and morphologically characterized. A Stereoscopic zoom microscope model *SMZ-U Nikon* was employed in order to evaluate morphological aspects of the natural fibres such as shape, size and aspect ratio. A Scanning electron microscope model *JSM -820 Jeol* was employed in order to evaluate the morphology of the TPS samples produced and in the case of the biocomposites, the adhesion degree between the natural fibres and the polymer matrix and its distribution and orientation. Tensile tests were carried out with the aim of evaluating mechanical properties

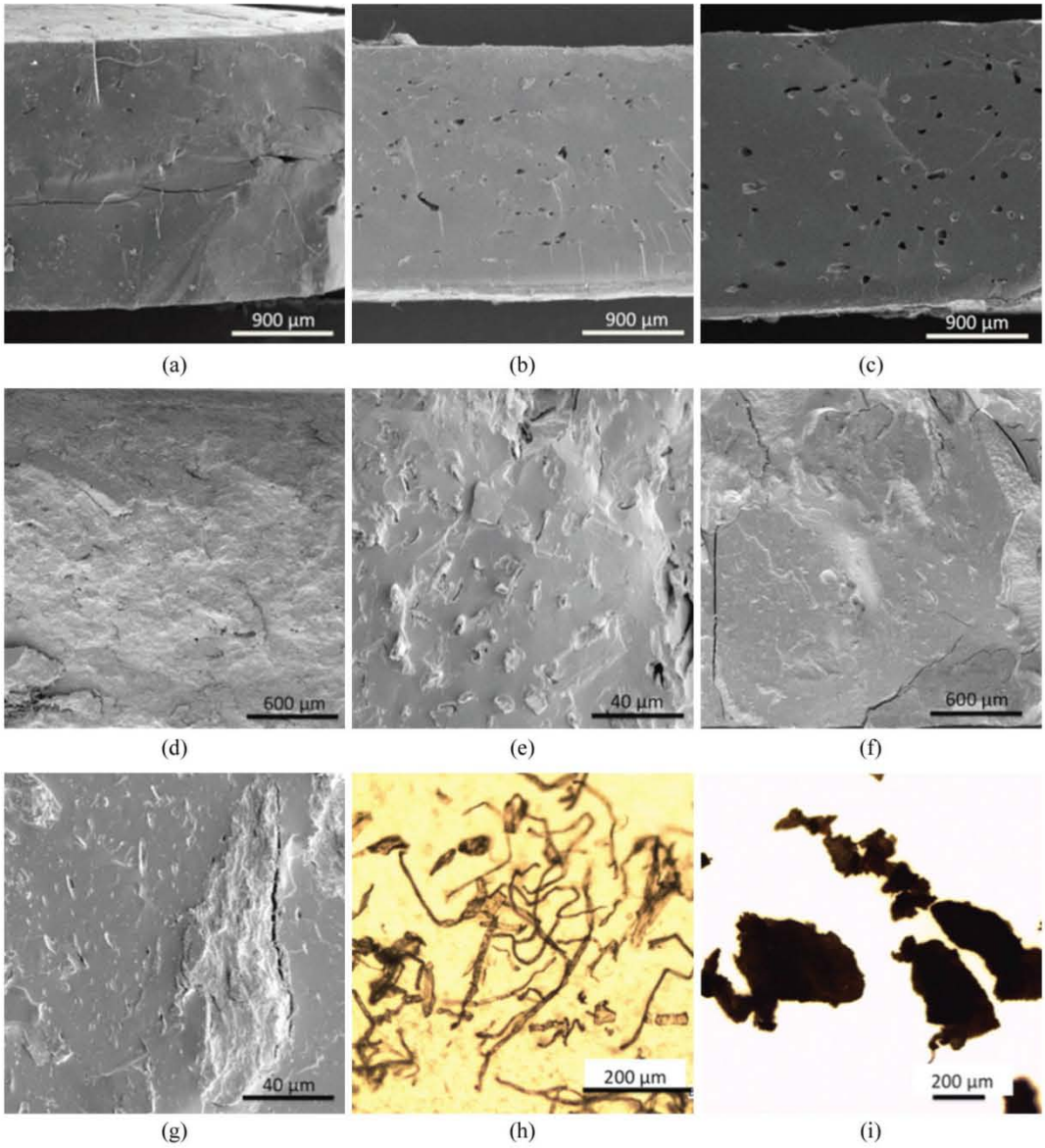

Figure 1. a) WS20 b) WS25 c) WS30 d) PS30B15 (mag35X) e) PS30B15 (mag500X) f) PS30G15 (mag35X) g) PS30G15 (mag500X) h) Barley Straw Fibres i) Grape fibres.

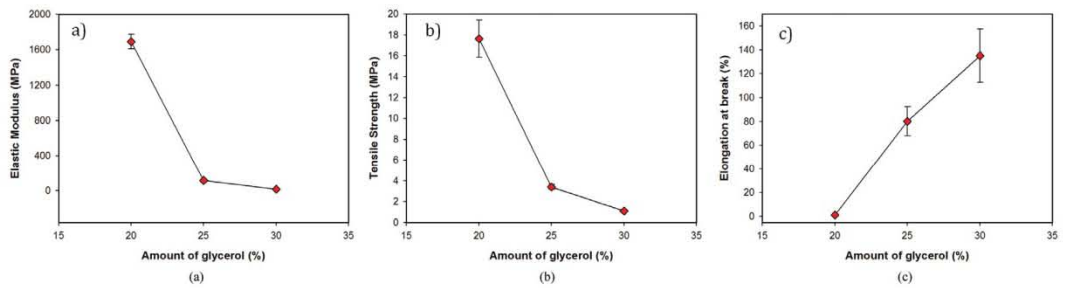

Figure 2. Mechanical properties of the TPS with different amounts of plasticizer: a) Elastic Modulus b) Tensile Strength c) Elongation at break.

instance, is very different for both fibres. In the case of the barley straw fibres the cellulose content is 97% while in the case of the grape fibres is 29%.

With regards to the orientation of the fibres, the SEM images do not clarify if they were oriented in a preferential direction. For this reason, a comparison between the experimental results and models found in literature was performed. The model commonly employed for the prediction of the elastic properties of composites is the **basic law of mixtures**. This law considers that the properties of a composite are between the responses of two basic models: a model in *parallel* and a model in *series*, and therefore both phases are under the same strain or stress conditions (Figure 4). The expressions that result for the Young's modulus are shown in Equations 1 and 2. Equation 1 represents the upper limit or the most optimistic prediction (plane strain) while the bottom limit is defined by Equation 2 (plane stress). E_c, E_m and E_p are the Young's modulus of the composite, polymer matrix (TPS in this case) and the filler (natural fibres in this case). V_p is the filler volumetric fraction.

$$E_c = E_m\left(1-V_p\right)+E_pV_p \quad (1)$$

$$E_C = \frac{E_PE_m}{E_P\left(1-V_p\right)+E_mV_p} \quad (2)$$

This model was applied only for the TPS-based biocomposite reinforced with barley straw fibres because of the poor results obtained with the grape fibers. Figure 4c shows the real behaviour of the TPS reinforced with barley straw fibres and the results obtained by the **law of mixtures model**. The Young's modulus of the barley straw fibres was calculated taking into account the cellulose and lignin content of this fiber, 96.7% and 1.5% respectively, and typical Young's modulus values found for them in literature[16].

As shown in Figure 4, both limits are far away from each other and the real behaviour is nearer the bottom than the upper limit and therefore, a plane-stress model is predicted by this law. Nevertheless, because of the long distance between both limits, this model has scarce utility in common composites systems. This model is more suitable for polymer blends than for filler-reinforced polymers.

Kerner developed one of the most widely accepted theories for the prediction of the Young's modulus of composites reinforced with **spherical particles**. His model is based on spherical particles dispersed and closely adhered to a polymer matrix. **Nielsen** adapted this model in order to simplify it and make the application in practical situations easier. **Kerner-Nielsen model**[17] is represented by the Equations 3, 4 and 5.

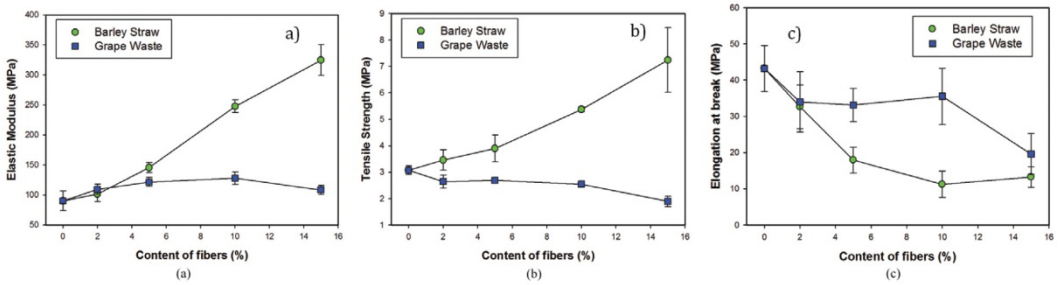

Figure 3. Mechanical properties of the TPS-natural fibre composites. a) Elastic modulus b) Tensile strength c) Elongation at break.

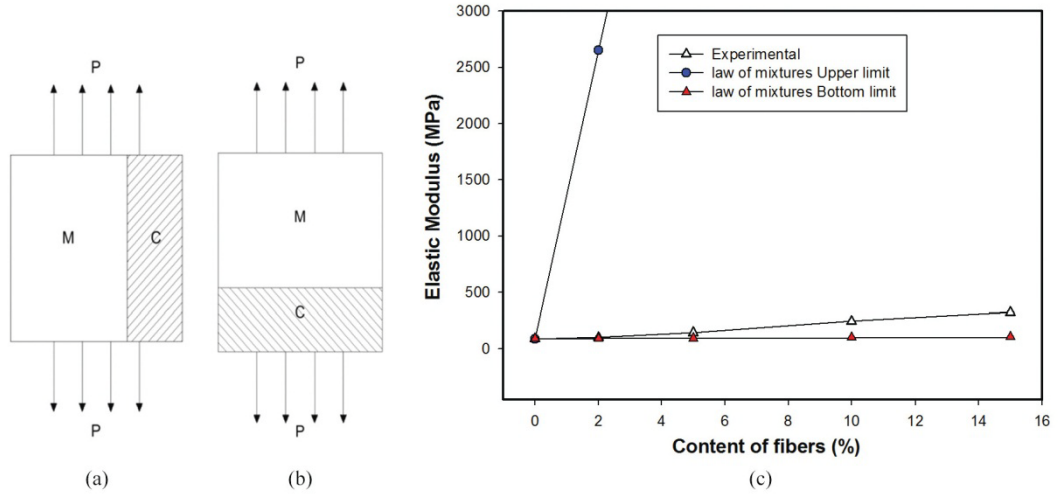

Figure 4. The law of mixtures. a) Plane-strain model b) Plane-stress model c) Experimental values versus the law of mixtures, upper and bottom limit, for the TPS-based composite reinforced with barley straw fibres.

$$E_c = E_m\left[\frac{1+ABV_p}{1-BV_p}\right] \quad (3)$$

$$A = \left[\frac{7-5V_m}{8-10V_m}\right] \quad (4)$$

$$B = \left[\frac{\frac{E_p}{E_m}-1}{\frac{E_p}{E_m}-A}\right] \quad (5)$$

The Poisson's coefficient (v_m) and the Young's Modulus (E_m) of the polymer matrix and the Young's modulus (E_p) and the volumetric fraction (V_p) of the particles are defined by the constants *A* and *B*.

When it comes to composites reinforced with short fibres, **Halpin & Tsai** developed a simplified model in order to predict the elastic modulus of unidirectional composites[18]. The Equations 6, 7 and 8 represent this model. The Equation 6 is suitable for composites with the fibres oriented parallel with respect to the stress applied whereas Equation 7 is suitable for the case of the fibres being oriented perpendicularly.

$$E_l = E_m\left(1-V_p\right)+E_pV_p \quad (6)$$

$$E_L = E_m\left[\frac{1+\xi BV_p}{1-BV_p}\right] \quad (7)$$

$$B = \left[\frac{\frac{E_p}{E_m}-1}{\frac{E_p}{E_m}-\xi}\right] \quad (8)$$

The aspect ratio of the fibres is represented by the parameter ξ. As was shown previously in the microscopic characterization of the natural fibres, the average aspect ratio of the barley straw fibres is 25. Equation 6 is exactly the same as Equation 1 of the **law of mixtures** and for this reason only Equation 7 for fibres oriented perpendicularly to the stress applied will be represented.

Once all the parameters were introduced for both, **Kerner-Nielsen** and **Halpin-Tsay** models, the real and models responses were represented in Figure 5.

As can be seen in Figure 5, the **Kerner-Nielsen** model did not fit very well with the real behaviour of these biocomposites. On the contrary, the **Halpin-Tsai** model seems to behave similar to the experimental results. This can be explained taking into account that the **Halpin-Tsai** model considers the aspect ratio of fibres and the barley straw fibres present an average high aspect ratio of 25. Nevertheless, the Kerner-Nielsen model is more suitable for spherical particles.

Finally, the best results as far as rigidity (Young's modulus) and strength (Tensile strength) are concerned of the TPS-based materials developed will be compared with those of current polymers employed in the rigid-food packaging market. The oil-based polymers, which were chosen for this comparison, are: HDPE Rigidex HD6070EA (*Inneos*), PP HB300TF (*Borealis*) and a common PET found in literature, all of them recommended for rigid packaging applications. Moreover, PLA Ingeo 2003D (*NatureWorks*) will be also added in order to compare with a bioderived and biodegradable polymer. The mechanical results of all the commercial polymers were obtained from technical data sheets. Figure 6 shows the comparison where the Young's modulus (a) and the Tensile strength (b) are plotted versus the density of these materials.

As observed in Figure 6a the Young's modulus of the TPS-based material plasticized with 20% of glycerol (1691 MPa) is even higher than that of the commercial HDPE (1500 MPa) and slightly lower than that of the commercial PP (1700 MPa). However, the TPS-based materials are far from the commercial polymers regarding strength. The Tensile strength of the TPS plasticized with 20% of glycerol is 17.6 MPa and the tensile strength of

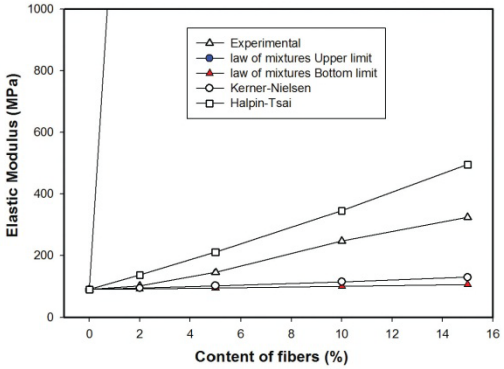

Figure 5. Experimental values versus the law of mixtures, Kerner-Nielsen and Halpin-Tsai models for the TPS-based composites reinforced with barley straw fibres.

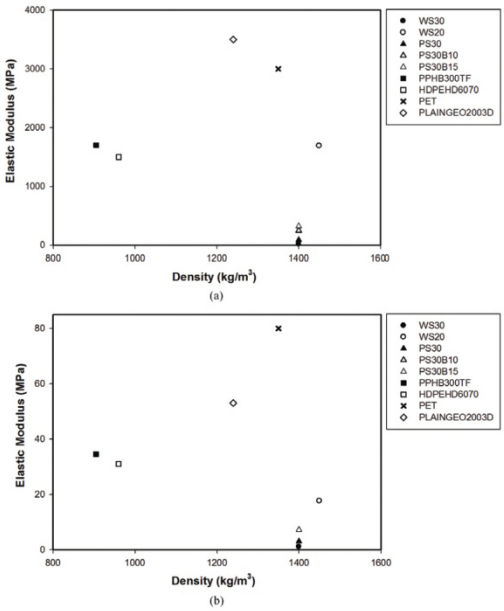

Figure 6. Young's modulus (a) and Tensile strength (b) versus density of the TPS-based materials with better results compared with oil-based polymers and PLA.

HDPE is almost double: 31 MPa. Moreover, the density of the TPS-based materials (≈1400Kg/m^3) is very high in comparison with the oil-based polymers such as PP (905 Kg/m^3), with the exception of PET (1350 Kg/m^3) and PLA (1240 Kg/m^3). When it comes to the botanical origin of starch (potato or wheat), no significant differences were observed.

Conclusions

This research work describes the production of TPS-based materials with the aim of replacing current oil-based polymers employed in the food-packaging market for the production of trays. The production method employed: extrusion and thermoforming, allowed firstly, plasticizing starch and secondly, the production of biocomposites with enhanced properties in comparison with the neat TPS matrix due to the employment of promising fibres such as barley straw and grape waste. SEM images showed a homogeneous distribution of both fibres along the TPS matrix although interphases between the grape fibres and the TPS matrix were observed, which resulted in poorer mechanical properties than for TPS-barley straw composites. The results of the **Halpin-Tsai** model were in good agreement with the experimental results of the TPS-based composites reinforced with barley straw fibres. This fact confirmed the importance that the aspect ratio of these fibres had in the final mechanical properties of the composites.

The best result regarding mechanical properties was obtained by reducing the amount of plasticizer up to 20%. This is because the TPS reinforced with natural fibres was plasticized with 30% of glycerol. Although the properties of the TPS-based materials regarding rigidity and strength are in most cases below the properties of the current oil-based polymers, it is fair to point out that the materials developed are completely bioderived, biodegradable and economically competitive, which add an extra value to them. Last but not least, it should be taken into consideration that current policies and laws are promoting the entrance of these biodegradable polymers in the food-packaging market.

References

1. Davis, G. & Song, J. H. - Ind. Crops Prod., **23**, p.147 (2006). http://dx.doi.org/10.1016/j.indcrop.2005.05.004
2. Kale, G.; Kijchavengkul, T.; Auras, R.; Rubino, M.; Selke, S. E. & Singh, S. P. - Macromol. Biosci., **7**, p.255 (2007). PMid:17370278. http://dx.doi.org/10.1002/mabi.200600168
3. Ludueña, L.; Vázquez, A. & Alvarez, V. - Carbohydr. Polym., **87**, p.411 (2012).
4. Auras, R.; Harte, B. & Selke, S. - Macromol. Biosci., **4**, p.835 (2004) PMid:15468294. http://dx.doi.org/10.1002/mabi.200400043
5. Corre, Y.-M.; Bruzaud, S.; Audic, J.-L. & Grohens, Y. - Polym. Test., **31**, p.226 (2012). http://dx.doi.org/10.1016/j.polymertesting.2011.11.002
6. Chanprateep, S. - J. Biosci. Bioeng., **110**, p.621 (2010). PMid:20719562. http://dx.doi.org/10.1016/j.jbiosc.2010.07.014
7. Mensitieri, G.; Di Maio, E.; Bunocore, G. G.; Nedi, I.; Oiveiro, M.; Sansone, L. & Iannace, S. - Trends Food Sci. Technol., **22**, p.72 (2011). http://dx.doi.org/10.1016/j.tifs.2010.10.001
8. Jansen, L. & Moscicki, L. - "Thermoplastic Starch. A green material for various industries", Wiley VCH, (2009). http://dx.doi.org/10.1002/9783527628216
9. Satyanarayana, K. G.; Arizaga, G. G. C. & Wypych, F. - Progr. Polym. Sci., **34**, p.982 (2009). http://dx.doi.org/10.1016/j.progpolymsci.2008.12.002
10. Yu,L.;Dean,K.&Li,L.-Progr.Polym.Sci.,**31**,p.576(2006). http://dx.doi.org/10.1016/j.progpolymsci.2006.03.002
11. Wollerdorfer, M. & Bader, H. - Ind. Crops Prod., **8**, p.105 (1998). http://dx.doi.org/10.1016/S0926-6690(97)10015-2
12. Sobczak, L.; Brüggemann, O. & Putz, R. F. - J. Appl. Polym. Sci., **127**, p.1 (2013). http://dx.doi.org/10.1002/app.36935
13. BeMiller, J. & Whistler, R. - "Starch: Chemistry and Technology", Elsevier (2009).
14. Li, H.; Michel, A. & Huneault, A. - J. Appl. Polym. Sci., **119**, p.2439 (2011). http://dx.doi.org/10.1002/app.32956
15. Kalia, S.; Kaith, B. S. & Kaur, I. - "Cellulose fibers: Bio- and Nano-Polymer composites", Springer (2011). http://dx.doi.org/10.1007/978-3-642-17370-7
16. Cheng, Q.; Wang, S. & Harper, D. P. - Compos. Part A, Appl. Sci. Manuf., **40**, p.583 (2009). http://dx.doi.org/10.1016/j.compositesa.2009.02.011
17. Nielsen, L. E. – J. Appl. Phys., **41**, p.(1970).
18. Affdl, J. C. H. & Kardos, J. L. – Polym. Eng. Sci., **16**, p.344 (1976). http://dx.doi.org/10.1002/pen.760160512

Received: 02/06/13
Revised: 10/08/13
Accepted: 01/30/14

4.3- Foamed starch-based biocomposites.

In principle, the microwave foaming process seemed to be an interesting strategy to produce biodegradable foamed food-packaging trays based on starch with the aim of replacing common XPS (extruded expanded polystyrene) trays found in the market (*Figure 4.2a*). However, there are some limitations, mentioned in *section 4.1*, which make this process more suitable for other applications such as the production of foams for *protective-packaging* applications (*Figure 4.2b*). In this particular case, the aim is the replacement of synthetic foams employed in this market, such as EPS (expanded polystyrene).

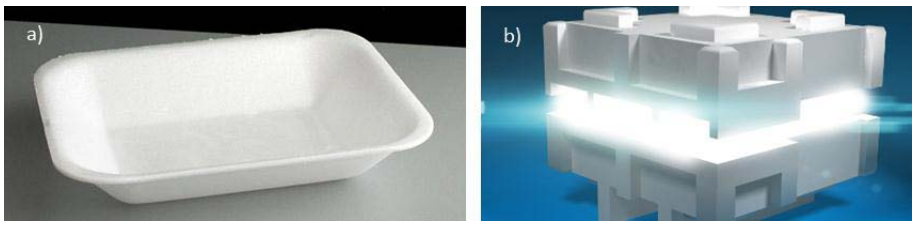

Figure 4.2. XPS *food-packaging* tray and EPS box for *protective-packaging*.

The article included in this section described an approach to produce starch foamed blocks reinforced with natural fibres for *protective-packaging* applications based on microwave foaming. This article was published in an international journal: *Industrial Crops and Products*, and its title is: *Cellular Structure and mechanical properties of starch-based foamed blocks reinforced with natural fibres and produced by microwave heating.* Previous works found in literature (*section 2.5.1.3*) produced starch foams in a similar way to those obtained in this article but from pellets, which resulted in foams with poor mechanical performances due to the lack of adhesion between the expanded pellets. Moreover, they did not use natural fibres to improve the properties of the foams. In this work an interesting strategy is followed based on using thermoformed sheets for the production of continuous starch foamed blocks of a defined shape.

After revising the existing literature related to the production of starch-based foams (*section 2.5*), it is evident that there are few studies establishing consistent relationships between their cellular structures and their mechanical properties . This article aims to provide more insight into these relationships by characterizing the cellular structure in more detail. Morphological parameters of the cellular structure, such as *cell size* and *anisotropy ratio* were obtained by image analyses of SEM micrographs and related to the mechanical properties obtained under compression tests, such as the *compressive modulus*, *compressive strength* and the *energy absorbed.* The aim of establishing these relationships was especially challenging, taking into account the role that natural fibres play in modifying not only the cellular structure but also the properties of the solid matrix within the cell walls and struts.

One of the most interesting and innovative aspects of this article is the comparison performed between the mechanical properties of the solid precursors and those of the foams produced. It is generally assumed that foam properties exponentially decrease with density as described in most of the analytical models found in literature, such as the cubic cell model of *Gibson* and

Ashby (equation2.1). This general behaviour is graphically illustrated in Figure 2.14. . However, the production of starch foams in which water acts as the plasticizer and the blowing agent breaks this common assumption. This article aims to explain what happens during the cellular structure stabilization in these foamed systems (s*ection 2.4*) and the mechanical properties of the material before and after foaming by using the *Gibson & Ashby* model.

Industrial Crops and Products 66 (2015) 194–205

Contents lists available at ScienceDirect

Industrial Crops and Products

journal homepage: www.elsevier.com/locate/indcrop

Cellular structure and mechanical properties of starch-based foamed blocks reinforced with natural fibers and produced by microwave heating

A. Lopez-Gil[a,*], F. Silva-Bellucci[b], D. Velasco[a], M. Ardanuy[c], M.A. Rodriguez-Perez[a]

[a] Cellular Materials Laboratory, (CellMat), Condensed Matter Physics Department, University of Valladolid, Paseo de Belén 7, 47011, Valladolid, Spain
[b] Ministério da Ciência, Tecnologia e Inovação–MCTI, Rua: Esplanada dos Ministérios, Bloco E, 01, CEP 70067-900 Brasília, DF, Brazil
[c] Departament d'EnginyeriaTèxtil i Paperera.UniversitatPolitècnica de Catalunya–Barcelona TECH, C/Colom, 11, E-08222 Terrassa, Spain

ARTICLE INFO

Article history:
Received 3 September 2014
Received in revised form
17 November 2014
Accepted 13 December 2014

Keywords:
Starch
Foam
Bicomposites
Biodegradable
Microwave heating
Natural fibers

ABSTRACT

The cellular structure and mechanical properties in compression of starch-based foams filled with natural reinforcements, such as grape wastes, cardoon wastes and barley straw fibers, have been studied in this work. The foams were produced by a microwave foaming process in which water is the plasticizer and at the same time the blowing agent. The use of thermoformed sheets as solid precursors for foaming allowed the production of foamed blocks with cells elongated in the expansion direction and with better properties in terms of rigidity and strength than foams produced in previous works by microwave heating of pellets. Moreover, the natural reinforcements increased not only the rigidity and strength, but also the toughness of these foams. Finally, the modeling of the compressive modulus using scaling laws shows how the stabilization of the cellular structure by the drying of the polymer matrix increases the rigidity of the solid cell walls. The flexible solid thermoplastic starch based precursor turns while foaming into a rigid starch-based foam, which could be suitable either for structural applications, due to its high stiffness and strength, or for packaging due to its complete biodegradability under controlled conditions.

1. Introduction

The plastic industry have made great efforts during the last decades to replace common petroleum-based polymers by biobased and biodegradable polymers as an alternative approach to recycling, incineration and energy recovery of plastic waste (Davis and Song, 2006; Taurino et al., 2010; Zare, 2013). Biodegradable polymers (Chandra and Rustgi, 1998; Yu et al., 2006; Gisha et al., 2011) are completely degraded by microorganisms in a few weeks under controlled conditions and the resulting compost is generally employed in agriculture fields (Lörcks, 1998; Kale et al., 2007). Among them starch is one of the most promising because of its low price and abundant world production. It is extracted from cereals and tubers in the form of semicrystalline granules composed of amylose and amylopectin (James and Roy, 2009; Andréa and Bertolini, 2010). Starch was originally used as filler in blends with synthetic polymers with the aim of increasing the biodegradability and at the same time the stiffness of the blend (Thakore et al., 2001; Park et al., 2002; Pedroso and Rosa, 2005). Later, the production of thermoplastic starch (TPS) extended the range of applications of this polymer. TPS is a mostly amorphous polymer that possesses properties similar to those of conventional thermoplastics. However, it is highly hydrophilic and therefore, its use in applications such as food packaging is not possible without being chemically modified or blended with other polymers. Currently, TPS can be found in packaging applications such as plastic bags (DaRóz et al., 2006; Leon and Leszek, 2009; Prachayawarakorn et al., 2010; Canché-Escamilla et al., 2011; Da Róz et al., 2011; Olivato et al., 2013; Lopez-Gil et al., 2014).

Starch based foams have been produced by several techniques but one of the most employed has been extrusion foaming to produce snacks in the food industry (Moraru and Kokini, 2003; Chanvrier et al., 2007; Elisa et al., 2012a; Elisa et al., 2012b) and loose fill chips for protective packaging (Lee et al., 2007; Pushpadass et al., 2008; Pushpadass et al., 2010). Baking is another technology that has been studied in detail (Shogren et al., 1998a; Shogren et al., 1998b; Shogren et al., 2002). It is a very simple process, which takes place in only one step. Nevertheless, cycle times are high and the cellular structures obtained are in general non-homogeneous. Microwave foaming is one of the most

* Corresponding author. Tel.: +34 983184035; fax: +34 983423192.
E-mail address: alopgi@fmc.uva.es (A. Lopez-Gil).

http://dx.doi.org/10.1016/j.indcrop.2014.12.025
0926-6690/

promising technologies for the production of foamed starch products. The origin of this technology dates back to the microwave expansion of popcorn (Hoseney et al., 1983) and to the production of a third-generation of snacks expanded by microwave radiation (Boischot et al., 2002). The main advantage of this method is that the increase in temperature comes from the interaction of water with the microwave radiation. The volumetric heating of the polymer and subsequent generation of steam is more homogeneous than in conventional techniques such as baking because water is homogeneously distributed throughout the polymer matrix after plasticization. Moreover, cycle times and energy consumption can be reduced with respect to conventional heating methods. There are a few previous works in literature in which thermoplastic starch pellets produced by extrusion are foamed inside microwave ovens either by free expansion (Boischot et al., 2002; Zhou et al., 2006) or by using molds to obtain specific shapes (Zhou et al., 2007). Boischot et al. (2002) reported the basics of starch foams nucleation and expansion under microwave radiation and the stabilization of the cellular structure by drying of the polymer matrix. This paper used starch based pellets as raw materials for the microwave foaming process. In the work of Zhou et al. (2007) a method to produce starch-based foamed blocks is described in which plasticized starch pellets are placed inside the cavity of a PTFE mold and later foamed by microwave radiation. However, the adhesion between the foamed pellets was poor resulting in foamed blocks with low mechanical properties in terms of stiffness and strength. In the work of Peng et al. (2013)a a microwave heated thermo-mechanical analyses was carried out to study the influence of additives such as glycerol and PVOH in the foamability of starch-based materials under microwave radiation. Moreover, the effect of microwave expansion in the dielectric properties of thermoplastic starch was studied by using a microwave calorimeter (Peng et al., 2013a; Peng et al., 2013b). Finally, the work of Sjöqvist and Gatenholm (2005) focused on foaming batters of starch containing water by microwave radiation instead of thermoplastic starch pellets produced by extrusion. In this way a production step is taken off from the production process because extrusion is not needed (Sjöqvist and Gatenholm, 2005).

Natural fillers based on cellulose have been widely used in blends with biopolymers to enhance their mechanical properties. In the particular case of starch-based foams several works were found in literature. In the works of Shogren et al. (2002) and Lawton et al. (2004) baked starch foamed trays for food packaging reinforced with aspen fibers were produced and characterized (Shogren et al., 2002; Lawton et al., 2004). Aspen fiber addition up to 15% resulted not only in increasing the strength of the foamed trays but also their flexibility. Jute and flax fibers with different aspect ratios were mixed with starch and later foamed by baking in the work of Soykeabkaew et al. (2004). When the amount of both jute and flax fibers increased up to 10%, the flexural modulus and the flexural strength of these foams also increased (Soykeabkaew et al., 2004). Kaisangsri et al. (2012) developed by using the baking process cassava starch-based trays in which kraft fibers were added in several concentrations resulting in an increase of both tensile strength and elongation at break (Kaisangsri et al., 2012). Glenn et al. (2001) produced several foams of starch with softwood fiber by baking resulting in an improvement of their flexibility (Glenn et al., 2001). Moreover, these properties were compared with those of commercial extruded polystyrene and paper board trays. Bénézet et al. (2012) also reported an increment of the mechanical properties when using different kinds of natural fibers such as wheat straw, hemp, cotton linter and cellulose in the production of starch-based foams by extrusion foaming (Bénézet et al., 2012). Nevertheless, as far as we know there are not papers dealing with the foaming by microwave radiation of starch-based composites reinforced with natural fillers.

In this work, starch based foamed blocks were obtained by a production method which consists of three steps: plasticization of starch with water by extrusion, thermoforming of cylindrical solid precursors and foaming by means of microwave radiation. The main difference with respect to previous works is that foams were obtained from thermoformed sheets instead from individual pellets with the aim of obtaining continuous foamed blocks with higher mechanical properties. Moreover, natural reinforcements such as barley straw fibers, grape waste and cardoon waste were blended with thermoplastic starch in order to improve the mechanical properties of the starch-based foamed blocks produced. These foams were characterized in detail by image analysis of the cellular structure and by mechanical tests in compression from where mechanical parameters such as the compressive modulus, the compressive strength and the energy absorbed were analyzed and discussed in terms of the materials structure.

2. Materials and production process

2.1. Raw materials

Native wheat starch (Meritena 200) provided by Tereos Syral was selected as the polymer matrix. Water was employed not only as the plasticizer of the polymer matrix but also as the blowing agent. Three natural reinforcements were selected with the aim of improving the mechanical properties of the polymer matrix: barley straw fibers, cardoon waste and grape waste. Barley straw fibers, which were kindly provided by the Department of Textile Engineering of the Unversitat Politècnica de Catalunya, were previously treated with hot water and with an alkaline solution with the aim of isolating the cellulosic fibers (Ardanuy-Raso et al., 2011). Matarromera Group (Spain) and Riberebro Group (Spain) provided grape and cardoon wastes, respectively, in the form of particles. These two last wastes were not chemically treated and they were used as received. These reinforcements from different natural origins were selected on the one hand, because of their chemical affinity with starch. They are mainly composed of cellulose which is a polysaccharide as well as starch. On the other hand, they were selected because each one have a different morphology in terms of shape, size and aspect ratio as will be described in the following sections. The inherent humidity of starch powders is 13 wt% (weight percentage) while that of barley straw, grape and cardoon fillers are 4.2, 3.5 and 5.1 wt% as specified by the suppliers. Finally, conventional salt was also employed because increases the absorption of microwave radiation and as a consequence allows reducing foaming times (Zhou et al., 2006).

2.2. Production of the solid precursors

Four formulations based on thermoplastic starch were produced: one of them without reinforcement and the other three with the addition of the natural reinforcements. These four formulations and their compositions expressed in weight percentage (wt%) are shown in Table 1.

First of all, a 3 mol/l solution of salt in water was prepared which in turn was employed to obtain a starch-based batter (70% in weight

Table 1
Starch based formulations.

Formulation	Thermoplastic starch[a]	Barley	Grape	Cardoon
WS	100	–	–	–
WSB	95	5	–	–
WSG	95	–	5	–
WSC	95	–	–	5

[a] 70% Starch/30% water solution of salt.

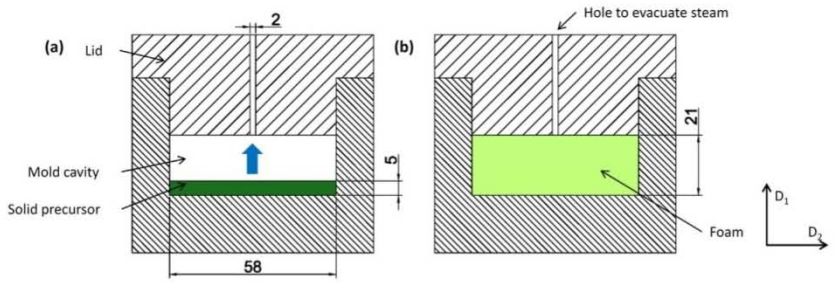

Fig. 1. (a) PTFE mold with the solid precursor before foaming. (b) PTFE mold with the foam inside after foaming.

of starch). The natural reinforcements were manually mixed with the starch batter before the extrusion process, all of them in the same weight percentage: 5%. This percentage was chosen taking into account previous works from literature in which high amounts of fibers, more than 10%, resulted in the agglomeration of fibers and therefore a decrease of the foam strength (Lawton et al., 2004). Moreover, the expansion of the polymer can be affected by the incorporation of high amounts of natural fillers because they can influence the melt viscosity during foaming.

Secondly, the plasticization of the formulations was carried out in a bench-top co-rotating twin-screw extruder model ZK 25 T, Dr Collin. The temperature profile was set to 60–80-120–80-70 °C and the screw speed to 100 rpm. The batters of starch with the natural reinforcements were manually feed into the extruder and the strands obtained at the exit of the die were air-cooled and pelletized. The temperature of the extruder in the last two zones was set below the vaporization temperature of water (100 °C) with the aim not only of avoiding a premature expansion of thermoplastic starch but also of reducing as much as possible the loose of water during this production step.

Circular-shaped sheets of the thermoplastic starch based composites were produced by thermoforming in a hot plates press. Temperature and time were set, respectively, to 70 °C and 15 min and the pressure applied was 22 bars. The dimensions of these thermoformed sheets were 150 mm in diameter and between 5 and 6 mm in height.

Finally, solid precursors were cut from these thermoformed sheets. Their diameter is practically the same as that of the mold cavity (58 mm) in which the microwave foaming process was later carried out. In this way, the expansion took place mainly in one direction (the thickness direction).

2.3. Microwave foaming

The microwave foaming process was performed in a conventional microwave oven model SHARP R-939. Moreover, a cylindrical PTFE mold was employed mainly for two reasons: on the one hand, PTFE is a material with a low effective loss factor in the microwave region and therefore, most of the microwave radiation was absorbed exclusively by the thermoplastic-starch based solid precursors. On the other hand, the foams could be easily demolded because starch does not stick to this material (Zhou et al., 2007). A scheme of the PTFE mold employed with its most important dimensions (mold cavity diameter and height in mm) as well as the height of the solid precursor is shown in Fig. 1. The scheme corresponds to one of the expansion planes which is represented by D_1 and D_2 axis. D_1 represents the expansion direction which is also indicated by the arrow in the scheme on the left. The expansion of the polymer was exclusively restricted to this direction because the diameter of the solid precursor is the same as that of the mold cavity. It is important to note that several holes of 2 mm in diameter that connect the cavity of the mold with the external area were made in order to avoid excessive steam pressures inside the mold.

The PTFE mold was preheated in a convection oven at 160 °C for 30 min prior to foaming in order to obtain a homogeneous distribution of temperatures during the microwave heating (Zhou et al., 2007). Immediately after preheating the mold, the foaming process was carried out in three steps. Firstly, the solid precursor was placed in the mold cavity, and then the mold was closed and put into the microwave oven. Secondly, and after setting microwave power and foaming time to 900 W and 50 s, respectively, the microwave heating started. After this time, the mold was taken out from the oven and the starch-based foam obtained was demolded. Fig. 2 shows pictures of one of the foams produced. This specific material is the one reinforced with grape waste. The arrow in the photograph on the left represents the foam height and that of photograph on the right represents its diameter.

Five foams of each formulation were produced with very homogeneous shapes and dimensions (approximately 58 mm in diameter and 21 mm in height) except for those reinforced with barley straw fibers, whose expansions were lower and hence, their heights (17.6 mm). A thin solid skin layer was observed in all the foams produced.

3. Characterization

3.1. Density

The density of solid precursors and foams was geometrically calculated by the ratio between their weight and volume as explained in the ASTM standard D1622-08. The samples dimensions (diameter and height) and weight were measured before and after foaming by a digital caliper and a precision balance, respectively.

3.2. Evolution of the water content

The weight loss percentage during foaming was calculated by weighing the samples before and after foaming and using the Eq. (1).

$$\text{weight loss}(\%) = \frac{\text{precursor weight} - \text{foam weight}}{\text{precursor weight}} \times 100 \qquad (1)$$

The evolution of the water content during the whole production process, including extrusion and thermoforming, was measured by means of drying samples obtained from each step in a convection oven until a constant weight was achieved (three decimal precison). The amount of water of each sample (WC) was calculated by Eq.

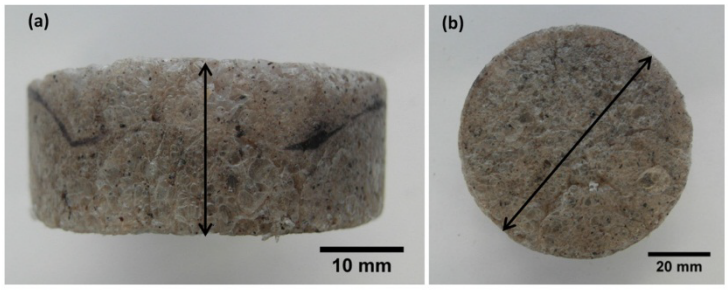

Fig. 2. (a) WSG foam in the expansion plane(D_1/D_2). (b) WSG foam in the plane perpendicular to the expansion direction (D_1).

(2) where W_i represents the initial weight of the sample and W_f represents the final weight.

$$\mathrm{WC}(\%) = \frac{W_t - W_f}{W_i} \times 100 \quad (2)$$

3.3. Natural fibers and cellular structure morphology

The morphological characterization of natural fibers and foams cellular structure was carried out by image analysis. In the case of natural fibers a public domain of JAVA image processing software called *FIJI/Image J* was employed. First of all, micrographs of the three natural fibers were taken by a Leica optical microscope model DM2500M. Secondly, micrographs were refined to improve the contrast between particles and background. Finally, they were binarized and particles substituted by ellipses. The particles area was taken as the area of their correspondent ellipses and the aspect ratio was calculated as the ratio between their longest and shortest dimensions. Three micrographs of each kind of fiber were analyzed with the aim of obtaining more accurate results.

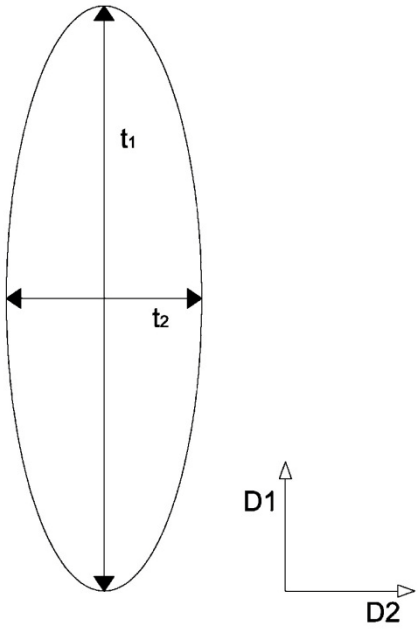

Fig. 3. Dimensions of the cell in the expansion direction (t_1) and in the direction perpendicular to it (t_2).

On the other hand, the cellular structure was characterized by using a method which combines the employment of the aforementioned *FIJI/Image J*software**,** together with image processing routes, a small userís assistance and theoretical expressions. This method allowed estimating common cellular structure features such as cell size in 2D (Φ), cell size distribution and anisotropy ratio (Pinto et al., 2013). The application finds the center of each cell in the image and measures the cell diameter (t) in eight different directions (angles). The size of each cell in 2D (Φ_i) is calculated as the average between these eight measurements. The average foam cell size in 2D (Φ) is calculated as the average for all the cells measured in the image as expressed in Eq. (3) where n is the total number of cells. The anisotropy ratio (R) is calculated as the ratio between the length of the cell in one specific direction (t_1) and the length in the direction perpendicular to it (t_2) as shown in Eq. (4). A cell in 2D represented as an ellipse is shown in Fig. 3 in which the previous dimensions can be seen. In this particular case the characterization of the cellular structure was carried out in the expansion plane (D_1/D_2) and therefore t_1 corresponds to the length of the cell in the expansion direction (D_1) and t_2 to the length of the cell in the direction perpendicular to it (D_2).

$$\Phi = \frac{\sum_{i=1}^{n} \Phi_i}{n} \quad (3)$$

$$R = \frac{t_1}{t_2} \quad (4)$$

The homogeneity of the cellular structure in terms of the cell size in 2D is expressed by the normalized standard deviation (NSD). This parameter is calculated as the ratio between the standard deviation (SD) and the average cell size in 2D (Φ) as shown in Eq. (5). The standard deviation is calculated by Eq. (6).

$$\mathrm{NSD} = \frac{\mathrm{SD}}{\Phi} \quad (5)$$

$$\mathrm{SD} = \frac{\sqrt{\sum_{i}^{n} (\Phi_i - \Phi)^2}}{n-1} \quad (6)$$

The SEM micrographs were taken by a scanning electron microscope model JSM-820 from JEOL, Japan. The samples were prepared in this way: firstly, a small portion of the foam was extracted by cutting. Secondly, the cut sample was immersed in liquid nitrogen and once completely frozen it was fractured in a plane parallel to the expansion direction (D_1/D_2). Then, a thin layer of Au (20 nm) was

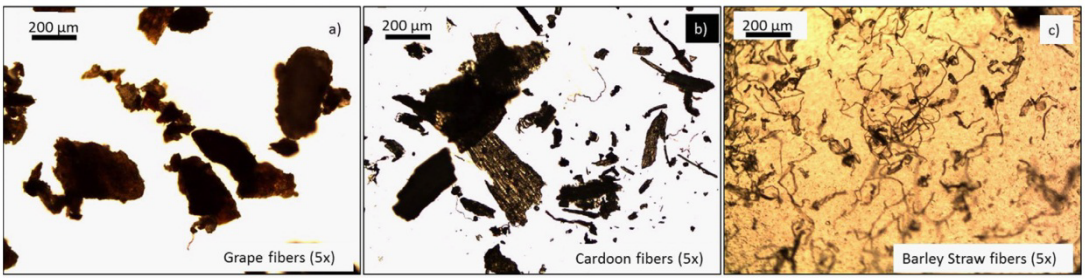

Fig. 4. Microscopy images of the natural fibers. (a) Barley straw fibers (b) grape waste, (c) cardoon waste.

evaporated over the fractured surface in order to make it electrically conductive and finally the micrographs were taken.

3.4. Open cell content measurements

The percentage of open cells (OC) was measured with a gas pycnometer model AccuPyc II 1340 Micromeritics following the standard ASTM D2856-94. Five measurements were carried out in cubic samples of each kind of foam. Eq. (7) was employed to calculate the open cell content.

$$\mathrm{OC} = \frac{V - (2V_1 - V_2)}{V(V_f)} \times 100 \tag{7}$$

where V represents the geometric volume of the sample, V_1 is the volume of the cubic samples measured by the gas pycnometer and V_2 is the volume of the same cubic samples after being cut in three planes. In this way it is possible to obtain a more accurate volume of the sample without considering the cells located at the surface, which were open because the sample had to be cut in order to be extracted from the foamed block. Finally, V_f is the porosity of the foamed sample which was calculated by Eq. (8) in which ρ_s and ρ_f are the density of the solid and that of the foam, respectively.

$$V_f = 1 - \frac{\rho_f}{\rho_s} \tag{8}$$

3.5. Compressive mechanical tests

Compressive mechanical tests of the cylindrical foamed samples and the solid precursors were carried out in a Universal testing machine Mod. 5.500R6025 (INSTRON) and following the standard ASTM D 1621. The strain rate, which was defined as the ratio h/10 (mm/min) being h the height of the sample, was kept constant during the test and strain–stress curves were recorded. The measured solid samples were prims with these dimensions: 20 × 20 × 6 mm. The last dimension corresponds to the thickness of the solid precursor. The skins on the top and bottom surfaces of the foamed cylinders were removed by polishing before mechanical testing. All the foams were conditioned in a laboratory with a controlled atmosphere (50% of relative humidity and 23 °C) during one-week prior to be tested. Under these conditions the foamed samples absorbed a 9% of humidity on average and no significant differences between the pure foams and those reinforced with natural fillers were found.

Mechanical parameters such as compressive modulus (E_c), compressive strength (σ_c), and the absorbed energy per unit volume (W) were obtained from the strain–stress curves. The compressive modulus of both the solids and the foams was calculated as the slope of the linear elastic region. The calculus of the compressive strength will be explained later in the results section due to the different shape of the stress–strain curves found for each material. The energy absorbed per unit volume (W) up to a given deformation ϵ_f (75%) is the area below the stress–strain curve and it was calculated using Eq. (9) in which ϵ is the strain and σ is the stress.

$$W = \int_0^{\epsilon f} \sigma(\epsilon)\mathrm{d}\epsilon \tag{9}$$

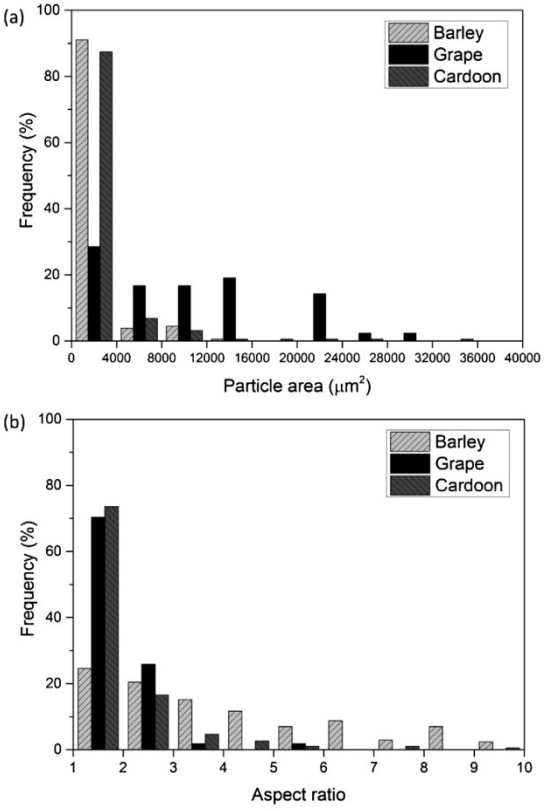

Fig. 5. Particle size distribution (a) and aspect ratio distribution (b) of barley straw, grape and cardoon reinforcements.

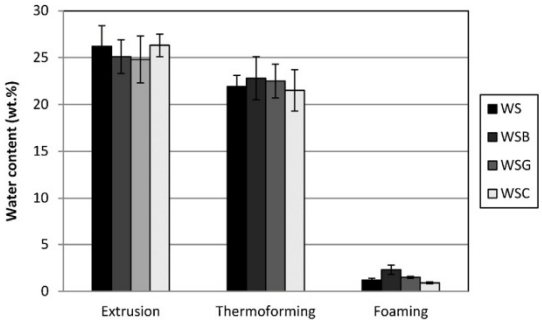

Fig. 6. Water content evolution during the production process.

4. Results and discussion

4.1. Natural reinforcement morphology

The natural reinforcements employed in this work were morphologically characterized with the aim of knowing in more detail common morphological parameters such as particle size and aspect ratio which could both influence the cellular structure and the mechanical properties of the foams obtained. Some examples of the micrographs obtained are shown in Fig. 4.

Grape and cardoon fillers present a particle-shaped morphology while barley straw presents a fiber-shaped morphology. Grape and cardoon waste are composed of particles whose sizes, measured as the area in 2D, are even larger than 300,000 μm^2. Nevertheless, the particle size distribution is non-homogeneous especially in the case of cardoon where particles even smaller than 100 μm^2 can also be observed. The size of barley straw fibers is in general lower than that of grape and cardoon and their aspect ratios reach values even higher than 10. Taking into account the non-homogeneity of both, particle size and aspect ratio, the numerical distributions of both characteristics were measured and the results are summarized in Fig. 5.

First of all, it is fair to point out that those particles whose areas were higher than 40,000 μm^2 and whose aspect ratios were higher than 10 were removed of the analyses so as to improve the perception of these distributions considering that the quantity of particles above these values was small. With regards to the particle area, barley and cardoon fillers present a more homogeneous distribution with most of the particles located at the range between 0 and 4000 μm^2. On the contrary, grape fillers present a much wider distribution in which most of the particles are larger than 4000 μm^2. On the other hand, barley straw fibers present a wide distribution of aspect ratios in which fibers with values up to 10 were found. On the contrary, the aspect ratio of grape and cardoon is located mainly in the range between 1 and 2. Therefore, the results of this characterization show that the morphology of the three selected fibers is very different, and in fact this was one the key reasons to select these tree materials.

4.2. Density and weight loss during production.

The density of the solid precursors and foams are shown in Table 2. Five samples of each formulation were measured in order to obtain more accurate results. The density of the solid material did not change significantly when the fillers were added. This result is expected taking into account the similar density of the fillers with respect to thermoplastic starch and the low weight fraction added (5%). The density of the pure foam and those of the foams reinforced with grape and cardoon fillers were very similar although the lowest density was obtained for the pure foam. On the contrary, the density of the foam reinforced with barley straw fibers is higher.

Table 2 also shows the expansion ratio of these foams calculated by two methods: the first value is obtained as the ratio between the density of the solid and the density of the foam (ER_1) and the second one is the ratio between the height of the foams and the height of the solid precursors (ER_2). This last calculation was possible considering that the expansion of the polymer inside the mold cavity took place in only one direction. There is a clear disagreement between both values. For instance, ER_1 of the pure foam (WS) is 4.79 while ER_2 is only 3.87. The reason for such a difference is that water, which is the blowing agent of the process, was lost during foaming so there was not only an increase of the volume of the polymer matrix but also a loss of mass. In other words, not all the steam generated was retained inside the cells of the foam. Most of it diffused throughout the polymer matrix and escaped outside of the foamed structure. The loss of weight during the foaming process was calculated for each kind of foam and it is shown in the last column of Table 2. Approximately a 20% on average of the original weight of the solid precursor is lost. This loss of weight is mainly attributable to the loss of water. Apparently there is no influence of the natural fillers because all the values are very similar.

The water content was measured during the whole process because it was a key parameter not only during foaming, water was used as blowing agent, but also during the rest of the production steps because water was also used as the plasticizer of the polymer matrix. Fig. 6 shows the water content (in weight percentage) of samples obtained after each production step.

Extrusion and foaming were the processes with higher amount of water lose. As far as the extrusion process is concerned, not only the initial amount of water added to starch (30 wt%) should be considered but also the inherent humidity of the starch powders and that of the fibers. These values were given in Section 2.1. In the middle zone of the extruder the temperature was set to a temperature higher than the boiling temperature of water (120 °C). In addition, high shear forces are applied to the molten polymer due to the co-rotating movement of the screws. These two facts could result in polymer melt temperatures along the extruder length high enough to vaporize part of the water as it is confirmed in Fig. 6. The thermorforming process also induced some water loss similar for the analyzed materials. During foaming, it is clear (Table 2), that the amount of water lost is also very high because it is the blowing agent of the process. The amount of water remaining in the foamed blocks produced is very small in accordance with related works found in literature (Shogren et al., 1998a; Soykeabkaew et al.,

Table 2
Solids and foams density.

Sample	Solid density (kg/m^3)	Foam density (kg/m^3)	ER_1	ER_2	Weight loss (%)
WS	1398 (±25)[a]	292 (±13.4)	4.79	3.87	19.0 (±4.1)
WSB	1401 (±32)	347 (±22.8)	4.04	3.21	20.8 (±1.7)
WSG	1362 (±63)	301 (±23.8)	4.52	3.60	20.7 (±1.0)
WSC	1443 (±48)	303 (±25.2)	4.76	3.80	20.0 (±1.1)

[a] The values in brackets represent the standard deviation.

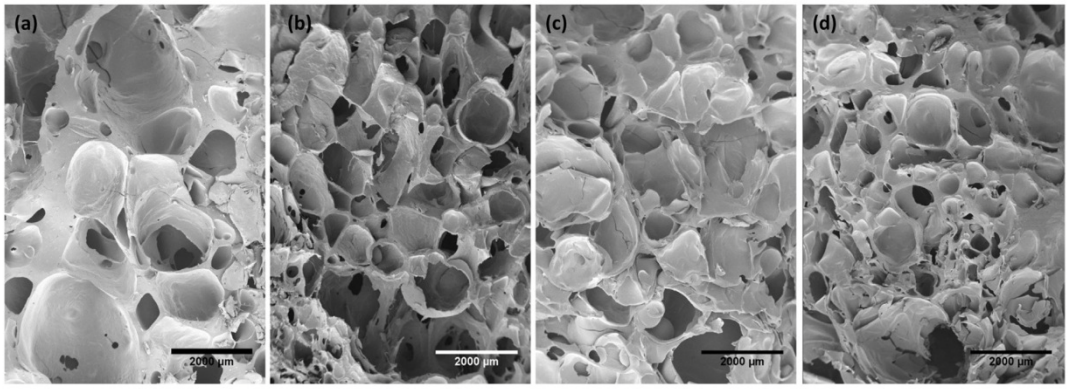

Fig. 7. SEM micrographs of the cellular structure morphology in the expansion plane (D_1/D_2). (a) WS_f (12x). (b) WSB_f (12x). (c) WSG_f (12x). (d) WSC_f (12x).

2004). The influence of the fibers in the water loss was scarce and no clear tendencies were obtained in this case.

4.3. Cellular structure

Representative SEM micrographs of the foams cellular structure in a plane parallel to the expansion direction (D_1/D_2) are shown in Fig. 7.

In general all the foams present a non-homogeneous cellular structure and the addition of fillers involved a reduction of the cell size. Moreover, several cracks and holes can be observed in the cell walls for all the analyzed materials suggesting that these foams present a highly interconnected cellular structure. This is confirmed by the gas picnometry measurements in which the open cell content was near 100% for all the foams produced (Table 3). Fig. 8 shows SEM micrographs with higher magnifications in which it is possible to detect these interconnections.

SEM micrographs with higher magnifications than the previous ones are also shown in Fig. 9 with the aim of evaluating the degree of adhesion between the fillers and the polymer matrix.

The adhesion degree between the fillers and the starch based polymer matrix seem to be very good because there are not interphases between them. In addition, in some cases the fillers are completely embedded within the polymer matrix. This is due to the chemical affinity between the fillers and the matrix (polysaccharide based materials) and it was an additional reason to select the fibers under study.

Cell size distributions are presented in Fig. 10.

In general all the cell size distributions are very wide with sizes between 100 μm and 1600 μm. Nevertheless, most of the cells sizes are located in the range between 200 and 600 μm. The only differences found are on the one hand, in the range between 1200 and 1600 μm, where the pure foam (WS) presents a higher percentage of cells (more than 10%) than the other foams. On the other hand, in the range of 0–200 μm the highest frequency of cells is found for the foam reinforced with cardoon waste in which almost 23% of the cells measured presented cell sizes below 200 μm.

Other morphological parameters of the cellular structure such as the average cell size in 2D (Φ), the normalized standard deviation of the cell size (NSD), the relative cell size in 2D (relative Φ) and the average anisotropy ratio (R) were measured by image analyses. The average values of these parameters together with the open cell content (OC) are shown in Table 3.

On the one hand, the average cell size was reduced when natural fillers were added in the formulations. Nevertheless, it should be taken into account that the expansion ratio was also influenced by the addition of natural fillers; especially in the case of the barley straw fibers based foam (WSB_f). For this reason, the average cell size in 2D relative to the density (relative Φ) was also calculated. It can be seen how grape fillers scarcely affect the cell size while the addition of barley straw fibers and cardoon fillers involved a clear reduction. This could be due to a heterogeneous nucleation of cells in the initial stages of foaming. As it was shown in the characterization of the natural fillers morphology, the particle size of cardoon and barley straw fibers was clearly lower than that of grape waste. In the first two cases most of the particles had sizes below 4000 μm^2 while most of the grape particle sizes are above 4000 μm^2. The presence of small particles in the samples in which the polymer is reinforced with barley and cardoon fillers could induce when water starts to vaporize, a higher nucleation rate and the growing of smaller cells than in the case of the pure sample and the sample reinforced with grape waste. This effect of heterogeneous nucleation in starch-based foams has been reported before with fillers such as bran and talc powder (Zhou et al., 2006). The NSD values are very similar for all the foams produced (between 0.53 and 0.62) indicating that the cell size dispersion is high independently of the formulation produced as it was shown in Fig. 10.

The results for the anisotropy ratio showed that all the foams presented elongated cells in the expansion direction. The anisotropy ratios calculated are in a range between 1.2 and 1.4. This is an expected result that can be explained taking into considera-

Table 3
Cellular structure parameters.

Samples	Φ (μm)	NSD	Relative Φ (μmm³/kg)	R	OC (%)
WS_f	583.4 (±337.2)[a]	0.58	2.00	1.21 (±0.58)	98.7(±0.2)
WSB_f	504.4 (±265.1)	0.53	1.45	1.39 (±0.55)	99.2(±0.3)
WSG_f	545.4 (±300.6)	0.55	1.96	1.32 (±0.96)	97.2(±0.5)
WSC_f	396.6 (±246.7)	0.62	1.31	1.28 (±0.78)	98.2(±0.1)

[a] The values in brackets represent the standard deviation.

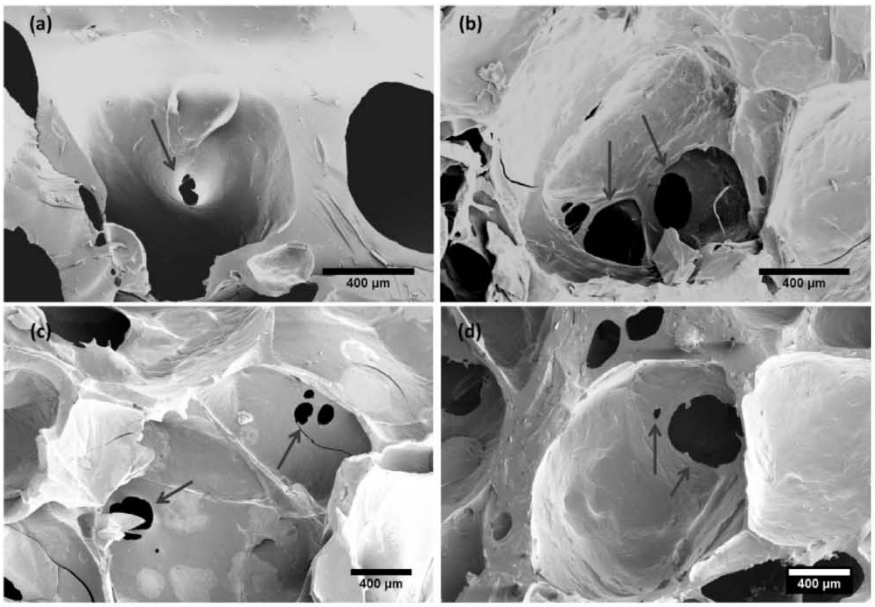

Fig. 8. SEM micrographs of cells interconnected. (a) WS_f (60x). (b) WSB_f (60x). (c) WSG_f (40x). (d) WSC_f (40x).

tion that the expansion is restricted to only one direction because the diameter of the solid precursor is exactly the same as that of the mold cavity. The reinforced foams present in general a higher anisotropy ratio than the pure foam indicating that the inclusion of the fillers within the cell walls and struts could induce some additional orientation of the cells during the expansion process.

4.4. Mechanical properties

Compressive stress–strain curves, not only of the foams but also of the solids, are represented in Fig. 11(a).The linear elastic zone (low strains < 10%) is represented in Fig. 11(b). Solids are denominated with the letter *s* and foams with the letter *f* at the end of the denomination previously established. Three samples of each material were tested for both the solid precursors and the foams and the average curve is presented in Fig. 11.

The stress–strain curves of the pure foam (WS_f) and the foams reinforced with cardoon (WSC_f) and grape fillers (WSG_f) are in general very similar because a peak, which is located just after the linear elastic zone, represents the collapse of the cells and after this peak the stress remains practically constant when increasing strain (plateau). The compressive strength is then the stress in which this peak takes place. On the contrary, in the case of the foams reinforced with barley straw fibers (WSB_f) this peak do not appear and the stress increases with strain after the collapse of the cells. In this case, the compressive strength had to be calculated as the crossing point between tangents to the elastic zone and to the plateau. The fact of obtaining foams with different expansion ratios depending on the natural filler employed affected also the shape of the stress–strain curves. Higher densities imply higher compressive strengths and therefore the plateau region is located at higher stresses. The plot in Fig. 11(a) shows how the plateau for the foam reinforced with barley straw fibers (WSB_f), whose expansion ratio was lower, takes place at higher stresses than that of the pure foam (WS_f) (Gibson and Ashby, 1997).

The curves of the solids are very different in comparison with those of the foams because the stress increases with strain without any peak and plateau region. This is due to the fact that the solids are flexible polymers due to the plasticizer (water) as it will be explained later. In this case the compressive strength was calculated as the stress at 5% strain.

The compressive modulus (E_c), the compressive strength (σ_c) and the absorbed energy per unit volume (W) of both, solids and foams are shown in Table 4 together with their density values.

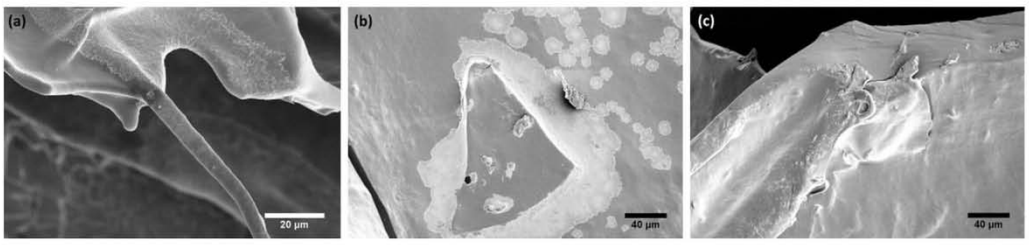

Fig. 9. SEM micrographs of the fillers in the polymer matrix. (a) WSB_f (1000x). (b) WSG_f (350x). (c) WSC_f (350x).

Table 4
Solid and foams mechanical properties.

Sample	ρ(kg/m^3)	E_c (MPa)	σ_c (MPa)[b]	W(MJ/m^3)[c]
WS_s	1398 (±25)[a]	16.6 (±1.3)	0.87 (±0.02)	10.13(±1.5)
WSB_s	1401 (±32)	18.4(±2.1)	1.02 (±0.03)	17.74(±2.3)
WSG_s	1362 (±63)	21.4 (±1.5)	1.07(±0.10)	10.80(±2.2)
WSC_s	1443 (±48)	13.4 (±2.8)	0.67 (±0.05)	6.86(±0.8)
WS_f	292 (±13.4)	46.8 (±8.3)	1.24 (±0.11)	1.91 (±0.3)
WSB_f	347 (±22.8)	52.8 (±11.1)	2.18 (±0.26)	4.54 (±0.6)
WSG_f	301 (±23.8)	51.3 (±6.9)	2.03 (±0.16)	2.65 (±0.6)
WSC_f	303 (±25.2)	43.7 (±10.2)	1.92 (±0.32)	2.72(±0.3)

[a] The values in brackets represent the standard deviation.
[b] The σ_c of the solids was calculated as the stress at 5% strain.
[c] This value was calculated up to strains of 75%.

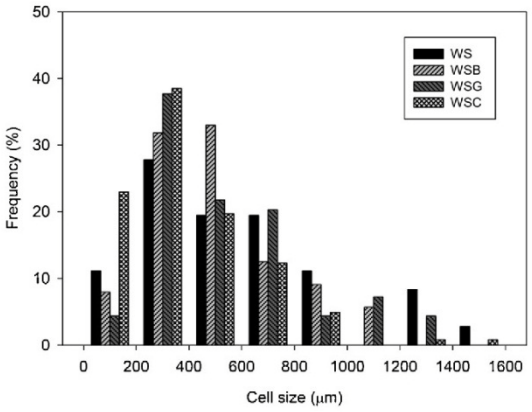

Fig. 10. Cell size distributions of the foams produced.

As it was mentioned in the introduction, previous works found in literature in the field of foaming TPS by microwave radiation produced TPS foamed blocks by expanding pellets inside the cavity of a PTFE mold (Zhou et al., 2007). However, the stiffness and strength of these foamed blocks were very low in comparison with those of the foams produced in this work mainly due to the poor interfacial adhesion between pellets just after the expansion of the polymer. For instance, in the work of Zhou et al. (2007) the starch block foams developed presented compressive modulus of 0.057 MPaand a stress at 10% strain of 0.48 MPa, values which are clearly lower than those obtained in this work (approximately 800 times for the modulus and 2.5 times for the compressive strength) where foamed blocks with similar densities were produced but starting from thermoformed sheets instead of individual pellets.

Moreover, it should be taken into account that the cells of the foams obtained in this work are oriented in the expansion direction. The average anisotropy ratios of all the foams are higher than 1.2 as observed in Table 3. On the contrary, when expanding pellets inside the cavity of the mold, the expansion is isotropic at least until the pellets contact each other. In this way, almost isotropic cellular structures are obtained. It is known from literature that foams with anisotropic cellular structures resulted in better mechanical properties than isotropic foams when measuring the properties in the expansion direction (Gibson and Ashby, 1997). Even though anisotropy should not be disregarded, the main reason for the better mechanical properties of the foams produced in this work is connected with the fact of obtaining continuous foamed blocks in which the adhesion between pellets is not playing any role.

With the aim of eliminating the influence of the density in the results the relative compressive modulus and relative compressive strength with respect to the density were calculated and plotted in Fig. 12.

There are clear differences between the compressive modulus and the compressive strength results. Firstly, the relative compressive modulus only increased when grape fillers were added to the starch polymer matrix. On the contrary, the relative compressive modulus of the foams WSB_f and WSC_f slightly decreased with respect to the pure foams (WS_f). Secondly, the relative compressive strength improved not only with the addition of grape fillers but also with the addition of cardoon and barley straw fibers. In any case, the relative compressive strength of the foam reinforced with grape fillers presented the highest value, as in the case of the relative compressive modulus.

The reason for such general improvement in the strength when adding fillers could be the reinforcing effect produced over the polymeric matrix. As the chemical groups in both materials are very similar, the adhesion between them was good resulting in an adequate load transfer from the polymer matrix to the filler during the mechanical test (Soykeabkaew et al., 2004). Fig. 9 shows how all the fillers are closely adhered to the polymeric matrix within the cell walls and struts. Nevertheless, the compressive modulus of foams is more dependent on the cellular structure and density than on the adhesion between polymer and filler (properties of the solid polymer). For this reason the compressive modulus values for the reinforced foams were not as good as those of the compressive strength (in comparison with those of the pure foams) (Gibson and Ashby, 1997).

The W values show an interesting result because the energy absorption of the foams reinforced with fillers is higher than that of the pure foams. This increment is especially notorious in the case of the foam WSB_f which is also reflected in the shape of the stress–strain curve. As it was previously mentioned, the stress for this foam grows with strain after the collapse of the cells and the characteristic plateau region of foams, in which the stress remains

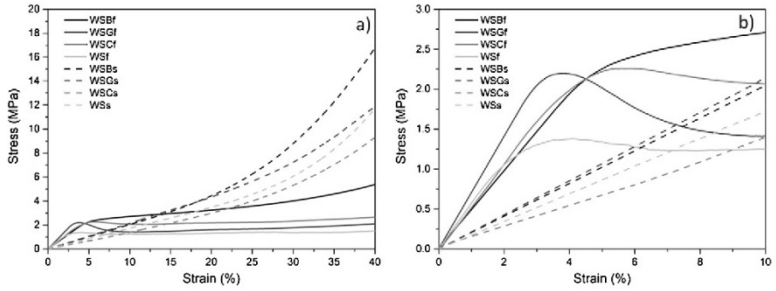

Fig. 11. Stress–strain curves of the solids and the foams produced.

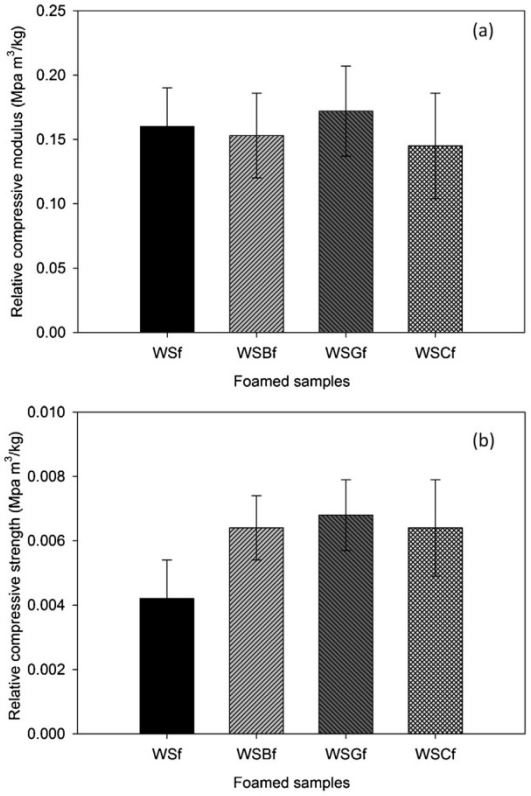

Fig. 12. Relative compressive modulus (a) and relative compressive strength (b) of the foams produced.

practically constant with strain, is not observed. This is probably due to a higher flexibility of this foam, which results in a more gradual collapse of the cells while buckling (Zhou et al., 2006). Changes in the properties of the thermoplastic starch based polymer matrix by the inclusion of these fibers should explain this behavior. This is proved in the total energy absorbed by this composite (WSB_s) which is clearly higher than those of the other solids (Table 4).

Fig. 13 shows energy absorption diagrams (Gibson and Ashby, 1997) of the four types of foams. In these diagrams the energy absorbed per unit volume is plotted versus stress. These plots are especially useful when trying to determine the foam which absorbs more energy for a given stress (depending on the application).

It is possible to see how the foams WS_f, WSG_f and WSC_f present a different behavior than that of the foam WSB_f. For this reason, all the results have been compared with respect to the WSB_f foam. In applications where a high stress has to be supported the best choice is the WSB_f foam while at low strains the best choices are the others because the energy absorbed is higher than that absorbed for the WSB_f foam. The crossing point between the curves of the three first foams and the WSB_f foam establish the border where a foam is more suitable depending on the stress applied. For instance, the crossing point of the foam WS_f and the foam WSB_f is 5.3 MPa. Below this stress the WS_f foam is more suitable whereas above it, the WSB_f foam is better.

A curious phenomenon can be seen from the comparison between the stress–strain curves of the solids and the foams. In

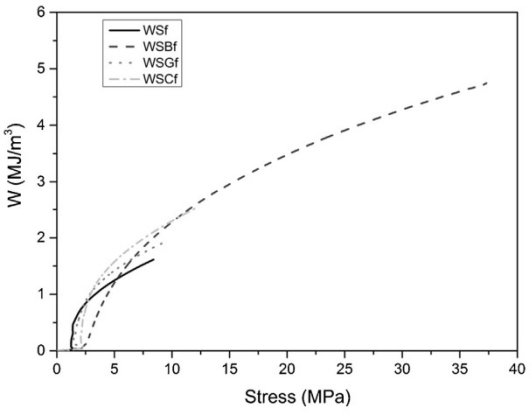

Fig. 13. Energy absorption diagrams.

general when foaming a solid polymer the mechanical properties, regarding stiffness and strength, decreases. The same happens with the W values. This fact is proved in the model of cubic cell proposed by Gibson and Ashby in which a correlation between the density and the compressive modulus of the solid and the foam were established (Gibson and Ashby, 1997). This is shown in Eq. (9).

$$\frac{E^*}{E_S} = \left(\frac{\rho^*}{\rho_S}\right)^n \tag{10}$$

In this equation, E^* is the compressive modulus of the foam and E_S is the compressive modulus of the solid. ρ^* y ρ_S are the density of the foam and the solid, respectively. The compressive modulus of the foam decreases with the density following a power-law relationship in which n is the exponent. This exponent is estimated as 2 for open cell polymeric foams. Only by increasing the compressive modulus of the solid or/and decreasing the exponent n by modifying the cellular structure it is possible to increase the properties of foams produced at the same density.

However, the results obtained in this research are clearly contrary to what is predicted by the model because the compressive modulus of the thermoplastic starch foams produced are clearly higher than those of the correspondent solids (Table 4).

In fact, the starting point of this foaming process is a flexible polymer based on thermoplastic starch and the ending point is a rigid foam. Fig. 14(a) shows how on average the compressive modulus of the foams (represented by white marks) is more than 20 MPa higher than the compressive modulus of the solids (represented by black marks).

In Fig. 14(b) the marks filled with gray color represents the theoretical properties of the cell walls and struts of the foams which were calculated from the compressive modulus of the foams taking the exponent n of the Eq. (10) as 2. The estimated compressive moduli are clearly higher than those of the solid precursors (marks filled with black color). The reason for such a strange behavior lies in the fact that the polymer matrix is changing its properties during the foaming process due to the loss of water. The water is vaporized and turns into steam, which is the driving force for the expansion of the thermoplastic starch matrix. Nevertheless, water is acting at the same time as the plasticizer of starch and due to the fact that it is progressively being released from the polymer matrix during the microwave radiation, the stiffness of the matrix simultaneously increases.

This is also the reason why the cellular structure is stabilized. In common foaming processes for polymers the cellular structure is

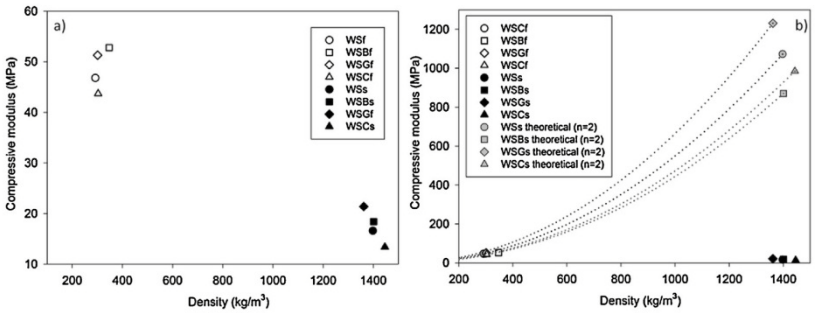

Fig. 14. (a). Compressive modulus versus density of solids and foams. (b) Theoretical compressive modulus versus density of the solid materials compared with the compressive modulus of the foams.

generally stabilized either by fast cooling, decreasing the temperature below the melting point of the polymer, or by crosslinking of the polymer matrix. In this case, during the foaming process the polymer matrix is constantly increasing its glass transition temperature because of the water loss. When the glass transition temperature becomes higher than the foam temperature the expansions reaches its maximum level and the cellular structure is stabilized (Boischot et al., 2002). Then, the mechanical properties of cell walls and struts in the foams produced are different from those of the solid precursor. These foams are composed of rigid and at the same time brittle cell walls and struts while the solid precursor is a flexible polymer due to the high quantity of water that initially plasticize the polymer matrix.

5. Conclusions

Cylindrical foamed blocks based on thermoplastic starch were produced using a microwave foaming process and a PTFE mold. The foams were produced from thermoformed sheets, which allowed the production of a continuous block (without joining between pellets). The fact of obtaining continuous foamed blocks represent an interesting alternative to what is found in previous works where the foamed blocks were produced from expanding a group of pellets inside the cavity of the mold. This finally resulted in problems of adhesion between pellets and as a consequence, in a poor mechanical performance as far as stiffness and strength is concerned. For instance, the compressive modulus of starch foamed blocks produced from pellets was 0.057 MPa (Zhou et al., 2007) while that of the foams produced in this work was 46.8 MPa (800 times higher). Moreover, due to the fact that the expansion of the polymer was restricted inside a mold the cells were elongated in the expansion direction (D_1) and therefore, cellular structures with anisotropy ratios higher than 1.2 were obtained. This kind of cellular structure is expected to have higher compressive modulus and compressive strengths in the expansion direction than that of equivalent isotropic structures (Gibson and Ashby, 1997).

The analysis of the mechanical properties in compression of the starch based foams produced show how incorporating natural reinforcements to the starch-based polymer matrix it is possible to increase the strength of the pure foams, especially in the case of adding grape waste. From the evaluation of the cellular structure grape particles were the only natural reinforcement which did not considerably change the cellular structure at least in terms of cell size. On the contrary, barley straw fibers and cardoon waste produced a decrease of the cell size. Nevertheless, all the foams produced presented in general highly inhomogeneous cellular structures, with and without fibers, which results in in a wide distribution of cell sizes (NSD values higher than 0.5).

The energy absorbed per unit volume of the foam reinforced with barley straw fibers is higher than those of the other foams. This could be due to the fact that the toughness of the starch polymer matrix was increased by the addition of these fibers.

From the comparison of the mechanical properties of the solid and those of the correspondent foams it is appreciated how the compressive modulus of the foams produced is higher than the compressive modulus of the solid. This is due to the loss of water during the foaming process. The initial solid precursor is a rubbery polymer because of the high amount of water that plasticize the polymer matrix while the final foam is composed of rigid glassy cell walls and struts. A modellization based on the cubic cell model proposed by Gibson and Ashby (1997) allowed estimating the compressive modulus of the cell walls and struts by assuming that the exponent n was equal to 2. The estimated compressive modulus of the cell walls and struts of the foams is approximately 50 times higher than those of the used-solid precursors.

Acknowledgments

Financial assistance from MCINN (MAT 2012-34901), the Junta of Castile and Leon (VA035U13), the FPI grant Ref: BES-2010-038746 (A. Lopez-Gil) and financial support from the Ministry of Economy and Competiveness of Spain (Actibiopack project: IPT-2011-1662-060000) is gratefully acknowledged.

References

Davis, G., Song, J.H., 2006. Biodegradable packaging based on raw materials from crops and their impact on waste management. Ind. Crop Prod. 23, 147–176.
Taurino, R., Pozzi, P., Zanasi, T., 2010. Facile characterization of polymer fractions from waste electrical and electronic equipment (WEEE) for mechanical recycling. Waste Manage. 30, 2601–2607.
Zare, Y., 2013. Recent progress on preparation and properties of nanocomposites from recycled polymers: a review. Waste Manage. 33, 598–604.
Chandra, R., Rustgi, R., 1998. Biodegradable polymers. Prog. Polym. Sci. 23, 1273–1335.
Yu, L., Dean, K., Lib, L., 2006. Polymer blends and composites from renewable resources. Prog. Polym. Sci. 31, 576–602.
Gisha, E., Luckachan, C., Pilla, K.S., 2011. Biodegradable polymers – a review on recent trends and emerging perspectives. J. Polym. Environ. 19, 637–676.
Lörcks, J., 1998. Properties and applications of compostable starch-based plastic material. Polym. Degrad. Stab. 59, 245–249.
Kale, G., Kijchavengkul, T., Auras, R., Rubino, M., Selke, S.E., Singh, S.P., 2007. Compostability of bioplastic packaging materials: an overview. Macromol. Biosci. 7, 255–277.
James, B., Roy, W., 2009. Starch: Chemistry and Technology, 3th ed. Elsevier.
Andréa, C., Starches, B., 2010. Characterization, Properties and Applications. Taylor and Francis Group.
Thakore, I.M., Sonal, D., Sarawade, B.D., et al., 2001. Studies on biodegradability morphology and thermomechanical properties of LDPE/modified starch blends. Eur. Polym. J. 37, 151–160.

Park, H.-M., Lee, S.-R., Chowdhury, S.R., Kang, T.-K., Kim, H.-K., Park, S.-H., Ha, C.-S., 2002. Tensile properties, morphology, and biodegradability of blends of starch with various thermoplastics. J. Appl. Polym. Sci. 86, 2907–2915.
Pedroso, A.G., Rosa, D.S., 2005. Mechanical, thermal and morphological characterization of recycled LDPE/corn starch blends. Carbohydr. Polym. 59, 1–9.
DaRóz, A.L., Carvalho, A.J.F., Gandini, A., Curvelo, A.A.S., 2006. The effect of plasticizers on thermoplastic starch compositions obtained by melt processing. Carbohydr. Polym. 63, 417–424.
Leon, J., Leszek, M., 2009. Thermoplastic Starch. A Green Material for Various Industries. Wiley-VCH.
Prachayawarakorn, J., Sangnitidej, P., Boonpasith, P., 2010. Properties of thermoplastic rice starch composites reinforced by cotton fiber or low-density polyethylene. Carbohydr. Polym. 81, 425–433.
Canché-Escamilla, G., Canché-Canché, M., Duarte-Aranda, S., Cáceres-Farfán, M., Borges-Argáez, R., 2011. Mechanical properties and biodegradation of thermoplastic starches obtained from grafted starches with acrylics. Carbohydr. Polym. 86, 1501–1508.
Da Róz, A.L., Zambon, M.D., Curvelo, A.A.S., Carvalho, A.J.F., 2011. Thermoplastic starch modified during melt processing with organic acids: the effect of molar mass on thermal and mechanical properties. Ind. Crop Prod. 33, 152–157.
Olivato, J.B., Grossman, M.V.E., Bilck, A.P., Yamashit, F., Oliveira, L.M., 2013. Starch/polyester films: simultaneous optimisation of the properties for the production of biodegradable plastic bags. Polymer 23, 32–36.
Lopez-Gil, A., Rodriguez-Perez, M.A., De Saja, J.A., Bellucci, F.S., Ardanuy, M., 2014. Strategies to improve the mechanical properties of starch-based materials: plasticization and natural fibres reinforcement. PolímerosCiência e Tecnologia. 24, 36–42.
Moraru, C.I., Kokini, J.L., 2003. Nucleation and expansion during extrusion and microwave heating of cereal foods. Compr. Rev. Food Sci. Food Saf. 2, 147–165.
Chanvrier, H., Appelqvist, I.A., Bird, A.R., Gilbert, E., Htoon, A., Li, Z., Lillford, P.J., Lopez-Rubio, A., Morell, M.K., Topping, D.L., 2007. Processing of novel elevated amylose wheats. Functional properties and starch digestibility of extruded products. J. Agric. Food Chem. 55, 10248–10257.
Elisa, L., Karkle, S.A., Dogan, H., 2012a. Cellular architecture and its relationship with mechanical properties in expanded extrudates containing apple pomace. Food. Res. Int. 46, 10–21.
Elisa, L., Karkle, L.K., Hulya Dogan, S.A., 2012b. Matrix transformation in fiber-added extruded products: impact of different hydration regimens on texture, microstructure and digestibility. J. Food Eng. 108, 171–182.
Lee, S.T., Park, C.B., Ramesh, N.S., 2007. Polymeric Foams. Science and Technology. Taylor and Francis Group.
Pushpadass, H.A., Babu, G.S., Weber, R.W., Hanna, M.A., 2008. Extrusion of starch-based loose-fill packaging foams. Effects of temperature, moisture and talc on physical properties. Packag. Technol. Sci. 21, 171–183.
Pushpadass, H.A., Weber, R.W., Dumais, J.J., Hanna, M.A., 2010. Biodegradation characteristics of starch–polystyrene loose-fill foams in a composting medium. Bioresour. Technol. 101, 7258–7264.
Shogren, R.L., Lawton, J.W., Doane, W.M., et al., 1998a. Structure and morphology of baked starch foams. Polymer 39, 6649–6655.
Shogren, R.L., Lawton, J.W., Tiefenbacher, K.F., 1998b. Starch–poly(vinyl alcohol) foamed articles prepared by a baking process. J. Appl. Polym. Sci. 68, 2129–2140.
Shogren, R.L., Lawton, J.W., Tiefenbacher, K.F., 2002. Baked starch foams: starch modifications and additives improve process parameters structure and properties. Ind. Crop Prod. 16, 69–79.
Hoseney, R.C., Zeleznak, K., Abdelrahman, A., 1983. Mechanism of popcorn popping. J. Cereal Sci. 1, 43–52.
Boischot, C., Moraru, C.I., Kokini, J.L., 2002. Factors that influence the microwave expansion of glassy amylopectin extrudates. Cereal Chem. 80, 56–61.
Zhou, J., Song, J., Parker, R., 2006. Structure and properties of starch-based foams prepared by microwave heating from extruded pellets. Carbohydr. Polym. 63, 466–475.
Zhou, J., Song, J., Parker, R., 2007. Microwave-assisted moulding using expandable extruded pellets from wheat flours and starch. Carbohydr. Polym 69, 445–454.
Peng, X., Song, J., Nesbitt, A., et al., 2013a. Microwave foaming of starch-based materials: dielectric performance (I). J. Cell. Plast. 49, 245–258.
Peng, X., Song, J., Nesbitt, A., et al., 2013b. Microwave foaming of starch-based materials thermo-mechanical performance (II). J. Cell. Plast. 49, 147–160.
Sjöqvist, M., Gatenholm, P., 2005. The effect of starch composition on structure of foams prepared by microwave treatment. J. Polym. Environ. 13, 29–37.
Lawton, J.W., Shogren, R.L., Tiefenbacher, K.F., 2004. Aspen fiber addition improves the mechanical properties of baked corn starch foams. Ind. Crop Prod. 19, 41–48.
Soykeabkaew, N., Supaphol, P., Rujiravanit, R., 2004. Preparation and characterization of jute- and flax- reinforced starch-based composite foams. Carbohydr. Polym 58, 53–63.
Kaisangsri, N., Kerdchoechuen, O., Laohakunjit, N., 2012. Biodegradable foam tray from cassava starch blended with natural fiber and chitosan. Ind. Crop Prod. 37, 542–546.
Glenn, G.M., Orts, W.J., Nobes, G.A., 2001. Starch: fiber and $CaCO_3$ effects on the physical properties of foams made by a baking process. Ind. Crop Prod. 14, 201–212.
Bénézet, J.C., Stanojlovic-Davidovic, A., Bergeret, A., et al., 2012. Mechanical and physical properties of expanded starch reinforced by natural fibres. Ind. Crop Prod. 37, 435–440.
Ardanuy-Raso, M., Algaba-Joaquín, M.I., Garcia-Hortal, J.A., López-Gil, A., Rodríguez-Pérez, M.A., 2011. Morphology and mechanical properties of biocomposites based on thermoplastic starch and cellulosic fibres from agricultural residues. 4th International Technical Textiles Congress.
Pinto, J., Solórzano, E., Rodriguez-Perez, M.A., et al., 2013. Characterization of the cellular structure based on user-interactive image analyses procedures. J. Cell. Plast. 49, 555–575.
Gibson, L.J., Ashby, M.F., 1997. Cellular Solids: Structure and Properties, 2nd ed. Cambridge University Press, Cambridge, UK.

4.4- Summary and Conclusions.

First of all, several biobased and biodegradable formulations were produced based on thermoplastic starch, which could be applied for the production of solid flexible materials for *food-packaging* applications and for the production of rigid foamed materials for *protective-packaging* applications. Their production required the optimization of lab-scale production processes such as *extrusion*, *thermoforming* and *microwave foaming*.

The processing parameters were carefully selected and varied depending on the formulation and the final application. In this sense, the most important modifications of parameters derived from the kind of plasticizer used: glycerol or water. The use of water required softer conditions (temperatures and pressures) than those employed with glycerol in order to avoid losing it prior to foaming (water acts as the blowing agent).

From a structural point of view, the most important variations were found after adding natural fillers. The solid composites obtained showed, in general, a good dispersion of fibres along the polymer matrix, suggesting that processing conditions were chosen properly. The adhesion degree varied depending on the fibre employed which could be due to their different chemical composition. Interphases between grape fillers and the polymer matrix were detected whereas barley straw fibres presented very good adhesions. On the contrary, a proper adhesion degree between all the fibres and the polymer matrix was achieved in the foamed materials.

These morphological differences are also reflected on the mechanical properties obtained. Only the addition of barley straw fibres produced a clear improvement in the stiffness and strength of solid TPS while the foamed materials did not show this behaviour. In this case, grape fillers produced the better results not only in the compressive modulus but also in the compressive strength. These differences found for both kinds of materials (solids and foams) could be attributed to different factors:

- The mechanical tests performed were different: tensile tests for solids and compressive tests for foams.
- The plasticizer used was different: glycerol for solids and water for foams, which varied the chemistry of the polymer matrix and the processing parameters employed.
- The foaming process induced changes in the polymer matrix properties (loss of plasticizer) that could promote variations in the adhesion degree between the polymer and the fibres during expansion.
- The cellular structure of the foams was clearly influenced by the presence of fibres. The addition of barley straw fibres and cardoon fibres, which present smaller sizes than those of grape fibres, reduced the cell size of the foams produced likely due to a heterogeneous nucleation of cells during the first stages of foaming.

In any case, it is clear that the addition of fibres represented an interesting and successful strategy to improve the mechanical properties of both systems, the solid and foamed materials

based on TPS. In the particular case of the foamed systems, the compressive properties of the developed foams were clearly higher than those previously published by other authors.

The employment of analytical models frequently used in literature to describe the mechanical properties of solid composites and foamed materials proved to be an interesting tool to evaluate certain aspects of both kinds of materials. In the case of the solid biocomposites, the *Halpin & Tsai* model fitted very well with the experimental results obtained with the composite reinforced with barley straw fibres. On the other hand, the *Gibson & Ashby* model allowed the prediction of the properties of the solid cell walls and struts of the starch-based foams produced by microwave radiation. This is important because the properties of the polymer matrix changes gradually during foaming. Water goes from the polymer matrix to the cells making the polymer matrix less plasticized at the end of the process.

Finally, the formulations and materials produced permitted the development of lab-scale production routes for *food-packaging* trays and *protective-packaging foams*. In the first case, the production route is very similar to that employed in industry for the production of solid flexible trays based on PET and PP because it consists of two stages: extrusion and thermoforming. This means that the solid formulations employed could be scaled-up for the production of food-packaging trays. In the second case, the production route was adapted for the production of foamed food-packaging trays. However, it is also suitable for the production of protective packaging foams of a defined shape such as those employed for packing household appliances. These production routes will be explained in more detail in *chapter 6*.

CHAPTER 5:

DEVELOPMENT OF POLYPROPYLENE FOAMS

Contents

5.1- Introduction.

Polypropylene (PP) represented, within the framework of the European project *NANCORE,* the main alternative to replace common polymers employed in the market of structural foams, such as PVC, PET, PU, SAN, etc. fundamentally because it is a low-cost polyolefin (abundant production) and moreover because of all the polyolefins, it is the one which offers the greatest stiffness and strength. Nevertheless, this polymer presented some drawbacks when used for foaming applications that had to be overcome. These drawbacks are highlighted in the red boxes of the scheme shown in Figure 5.1.

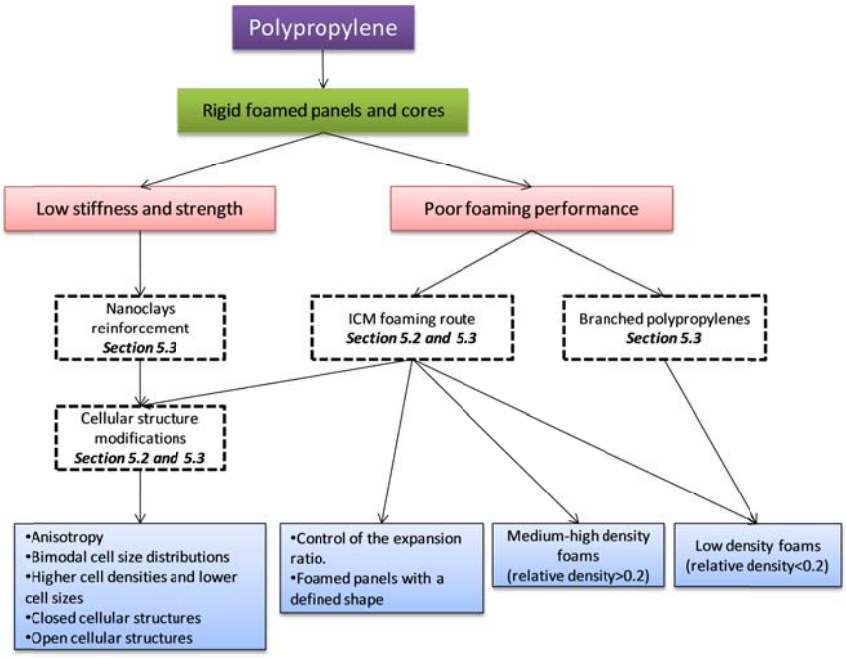

Figure 5.1.Drawbacks of polypropylene for foaming applications and strategies used in this work to overcome them.

First of all, the stiffness and strength of PP are still far from those of the polymers commonly employed in structural applications (PVC, PET, PU etc.) and secondly, the foaming performance of conventional linear polypropylenes is poor making the production of low-density foams with fine cellular structures very difficult. The path to solve these drawbacks set the evolution of the project during the four years it lasted and the two works included in this thesis represent a clear example of this evolution.

At the beginning of the project the only clear thing was the type of PP to be employed to obtain high expansion ratios (*branched polypropylene*) but there were a lot of doubts about a suitable production process. In principle, three existing technologies could have been applied: free foaming, gas dissolution foaming and compression moulding. In the first place, the *free foaming* process was considered because it is carried out under the action of temperature exclusively. Hence, the scaling-up of the process would have been affordable. Nevertheless, the cellular structures obtained are poor: large cell sizes and wide cell size distributions. In the second place, the *gas dissolution* process represented one of the most interesting approaches because it allows microcellular structures to be obtained due to the high pressures applied (high nucleation

rates ≈10^9 cells/cm^3). However, obtaining foams with a defined shape is difficult and the scaling-up of the technology would have been very expensive because stainless-steel autoclaves with thick walls are required. Finally, *compression moulding* seemed to be the most adequate foaming route because it combines the advantages of the previous ones: high pressures and easy scaling-up (the main equipment needed is hydraulic presses to transmit the pressure and temperature). There was a major drawback. This technology requires cross-linking the polymer matrix because otherwise, the polymer would leak out from the mould after releasing the pressure.

For these reasons, the *ICM route* emerged as the most promising strategy to produce this kind of foams. A more detailed description of the process was performed in *section 3.2.3*. Its main peculiarity with respect to the conventional *compression-moulding* route is that due to the mould design PP foams can be produced with a defined shape without cross-linking the polymer matrix. Moreover, this process had already been successfully applied for the production of other thermoplastic foams. However, there was a lack of knowledge about how processing parameters of this process such as pressure, temperature, blowing agent content and expansion ratio to name a few, influenced the structures and hence, the mechanical properties of PP foams. This is the reason why the work included in *section 5.2* was performed.

Not only is the production process important for obtaining the suitable foam for a determined structural application, but also the polymer employed. For this application, in which low-density rigid foams are required, a polymer combining both, good foaming performance and great stiffness and strength, is required. These are properties, possessed by the high melt strength branched polypropylene employed in the work included in *section 5.3*. In this work, nanoclays are used with the principal aim of increasing the mechanical properties of the solid cell walls and struts in the final foam which is produced. Indeed, this work tries to broaden the comprehension about the particular foamed systems in which a polymer is combined with a nanoparticle.

One of the most interesting aspects of the works developed during this chapter is the great variety of cellular structures obtained. On the one hand, in the work included in *section 5.2*, different cellular structure were obtained in terms of *cell size*, *cell density* and *open cell content* by modifying the blowing agent content and the expansion ratio (medium-high-density PP foams). On the other hand, in the work included in *section 5.3, anisotropic cellular structures* were obtained by restricting the expansion of the polymer in one single direction (low-density PP foams). Moreover, the addition of nanoclays represented another source of cellular structure variation because their addition involved the production of foams with higher cell densities and with *bimodal cell size distributions*.

The next two sections present the results obtained in the form of articles which have already been already published (in the case of the work included in *section5.2*) or sent to international scientific journals (in the case of the work included in *section 5.3*). The section has been classified according to the density of the foamed PP panels obtained: medium-high density foams with a relative density > 0.2 (section 5.2) and low density foams with a relative density <0.2 (*section 5.3*).

5.2- Production of medium-high density PP-based foams.

For the development of PP foams to be employed for structural applications the first step was to perform a detailed analysis of the relation *production-structure-properties* and thus, optimizing formulations and production parameters for this particular polymer matrix. An example of this relation is given in the work included in this section: *Production of non-cross-linked thermoplastic foams with a controlled density and a wide range of cellular structures*, which was published in an international scientific journal ("*Journal of Applied Polymer Science*").

The objectives of this work are firstly, optimizing formulations and production parameters in the ICM route and secondly, gaining knowledge about how different cellular structures and expansion ratios affect the mechanical properties of PP foams. In this sense, a linear PP was employed because its low stability in the molten state makes it very sensitive to different blowing agent contents (from 1 to 15 wt%) and to the different expansion ratios (1.6, 2 and 3) to which the molten polymer was subjected. The cellular structures obtained were characterized in detail with the aim of defining important morphological parameters of these foams such as cell size, cell density and open cell content and correlating them with the foams mechanical properties in the compression, tension and bending modes

Applied Polymer SCIENCE

Production of non-crosslinked thermoplastic foams with a controlled density and a wide range of cellular structures

Alberto Lopez-Gil,[1] Cristina Saiz-Arroyo,[2] Josias Tirado,[1] Miguel Angel Rodriguez-Perez[1]

[1]Cellular Materials Laboratory, (CellMat), Condensed Matter Physics Department, University of Valladolid, Science School, Paseo de Belén, 7, 47011, Valladolid, Spain

[2]CellMat Technologies S.L. Centro de Tecnologías y Transferencia Aplicadas (CTTA), Paseo de Belén, 9 A, 47011, Valladolid, Spain

Correspondence to: A. Lopez-Gil (E-mail: alopgi@fmc.uva.es)

ABSTRACT: A novel foaming route, with respect to existing industrial foaming processes, called "Improved Compression Molding" (ICM), which allows producing non-crosslinked thermoplastic foams in a wide density range, is described in this work. This process is different from others because it is possible to control independently density and cellular structure and therefore, tailored cellular polymers can be produced. To understand the process, a collection of polypropylene foams, with relative densities ranging from 0.3 to 0.6 were produced. The influence of foaming parameters, on foams microstructure and mechanical response was analyzed. Results revealed that for similar densities, foams with different open cell content and cell size can be achieved. In addition, it was proved that mechanical behavior strongly depends on the degree of interconnectivity of the cells. The analysis of the relative mechanical properties allowed determining the influence of microstructure on mechanical behavior as well as quantifying the efficiency of the foaming process to produce light-weight stiff materials. © 2015 Wiley Periodicals, Inc. J. Appl. Polym. Sci. **2015**, *132*, 42324.

KEYWORDS: foams; polyolefins; structure-property relations; synthesis and processing; thermoplastics

Received 24 November 2014; accepted 5 April 2015

DOI: 10.1002/app.42324

INTRODUCTION

Polymeric foams can be defined as two-phase materials in which a gas is dispersed in a continuous macromolecular phase.[1] Due to their outstanding properties, thermoplastic foams have become essential items and although they are mainly used as thermal insulators or impact absorbing elements, they have found applications in almost every field.[2–4]

Since their development in 1940s, both scientific and industrial communities have focused their attention on the development of foaming technologies able to satisfy the growing demand of thermoplastic foamed products.[3] Nowadays, no single foaming method dominates thermoplastic foam manufacture, and both continuous and batch processes are operated using either chemical or physical blowing agents. The most commonly used foaming processes to produce thermoplastic foams are extrusion, injection molding, compression molding or gas dissolution foaming in a batch process.[1–5]

The selection of the foaming process is conditioned mainly by the final application of the material which at the same time strongly depends on its relative density (i.e. the density of the foam divided by that of the corresponding solid). It is well known that the foaming process itself as well as the intrinsic characteristics of the polymeric matrix heavily determines the cellular structure of the foamed product.[4,5]

According to this, depending on the final application of the foam and the desired expansion ratio, the most suitable process is chosen. Thus, extrusion using a physical blowing agent is a good choice to produce low or ultra-low density foamed sheets or profiles for heat insulation or packaging applications.[3] Injection molding is the best election to produce net-shaped foamed parts. However, density reductions are limited to a 40%, and in addition this weight reduction strongly depends on size and shape of the part.[6] The gas dissolution foaming process produces low-density foamed products that have a very high quality, with fine cells and without residues coming from the blowing agent. However, the control of foam density is complicated in this type of process.[7] In addition, the investments are high due to the requirement of large high-pressure vessels and the cycle time to produce the foams is also very high.

Compression molding is a versatile process suitable for a wide variety of thermoplastic polymeric matrices. Two different variations are commonly used at industrial level.[4,5,8,9] The single stage process involves two steps, first compounding the polymer

with the blowing agent and all the required additives, (using an extruder or a Bambury type mixer) and second, the foamable compound is placed in a mold and subjected to a high mechanical pressure and to a temperature higher than the decomposition temperature of the blowing agent. Once the entire blowing agent has been decomposed, pressure is released and expansion takes place. The main advantage of the single-stage variation is its simplicity; however it presents several disadvantages being the most important the difficulty of controlling the final foam density. In addition when using low-melt strength thermoplastics, or when high expansion ratios are required, it is necessary to crosslink (either chemically or by irradiation) the polymer to bear the extensional forces occurring during expansion, thus avoiding premature collapse of the foam or the presence of a high number of broken cell walls.[4]

Using the single stage process, densities lower than 70 kg/m^3 are difficult to achieve. To obtain lower densities, a second variation known as two-stage compression molding is used.[5] In this process, expansion takes place in two steps and this, together with the crosslinking of the polymeric matrix, allows lowering the density of the foamed products to values as low as 20 kg/m^3. Second expansion takes place at atmospheric pressure in a mold having the desired size and shape.

Compression molding, either the single or the two-stage variation, present several drawbacks. In the single-stage process, the control of density is made by means of the blowing agent concentration, crosslinking agent concentration, pressure and temperature, and in general is not very accurate.[4] In the two-stage process, the control of density is much accurate however, the foam blocks produced by this method are non-homogenous, with density and cellular structure varying along the block thickness, (cells are smaller close to the surface of the blocks and density is higher in this zone).[10–14] In addition, in both processes the crosslinking of the polymer matrix is necessary which harms its recyclability by conventional re-melting techniques.[15]

The Improved Compression Molding Route, (ICM) can be considered as an alternative foaming route to provide a solution to the aforementioned drawbacks. Its main feature is the use of self-expandable molds that allow controlling the final expansion ratio by mechanical means and obtaining non-crosslinked net-shaped foamed parts in a relative density range between 0.1 and 0.9. These molds have the ability of applying pressure to the polymer while the blowing agent is being decomposed, which allows dissolving the gases generated into the polymer prior to the pressure release and final expansion. In addition, as the molds are capable of controlling the expansion degree it is possible to regulate in a very accurate way both the size and the shape of the foamed part. Moreover, the mold can be designed and produced with different geometries depending on the final application of the foamed part.

The ICM foaming route permits an excellent control of the cellular structure by properly handling temperature and pressure during the process and the chemical composition of the sample in terms of blowing agent content. The cellular structure, with regards to cell size, type, and shape, can be tailored to the final application and hence, it is possible to produce customized foams with similar densities but with significantly different cellular structures. For example, for structural purposes samples with a good mechanical response (i.e. with an almost zero open cell content) are desirable, while for sound absorption applications a high degree of interconnection between the cells is preferred. The ability of this technique to produce foams with different cellular morphologies will be proved in the experimental part of this article.

Even though the independent control of density and microstructure is probably the main characteristic of the ICM there are others that should also be taken into consideration. Any thermoplastic polymer or thermoplastic based composite or nanocomposite can be foamed by this process without the necessity of crosslinking the polymeric matrix. Up to now, pure polymers such as LDPE or EVA, composites such as LDPE/ATH, EVA/ATH, blends of EVA and starch, and nanocomposites based on LDPE and silica nanoparticles have been successfully foamed using the ICM process.[16–23]

Therefore, this article is focused on the analysis of the relationship between the ICM route and the structure and properties of polymeric foams produced by this process. For this purpose, a collection of polypropylene foams with relative densities in the range between 0.3 and 0.6 and with different chemical compositions have been prepared using such process. Foamed discs and cylinders were prepared using a polypropylene matrix.

MATERIALS

A linear random polypropylene copolymer, (200CA10 from Inneos) with a melt flow index of 10 g/min, (measured at 230°C and 2.16 kg) was used to produce all the analyzed samples. Its melting point is 150.4°C and its crystallinity degree is 44.4%, (both were measured by DSC). Azodicarbonamide (Porofor ADC/M-C1 from Lanxess) with an average particle size of (3.9 ± 0.6) μm was used as blowing agent. In order to prevent thermal oxidation of the polymer a small amount of a commercial antioxidant, (Irganox B561 from Ciba) was used in all formulations. Stearic acid (Stearic acid 301 from Renichem) was used as processing aid.

FOAMING PROCESS

As it was mentioned in the introduction, polypropylene foams have been produced using the improved compression molding process (ICM). It comprises the following three steps:

1. Melt-Compounding of Raw Materials: Polymer, blowing agent, the antioxidant, and the processing aid were melt-mixed in a twin screw extruder (Collin mod ZK25T). The temperature profile was varied from 135°C in the hopper to 155°C in the die. Such profile was chosen in order to avoid premature decomposition of the blowing agent during the compounding steps. The material was water cooled and pelletized.Pellets with four different blowing agent concentrations namely 1, 5, 10, and 15 wt % were prepared. Varying blowing agent concentration will permit gaining knowledge

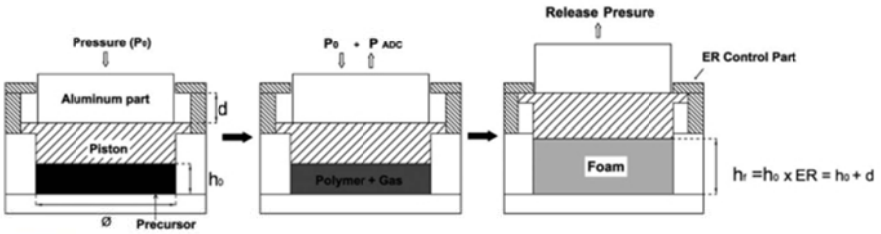

Figure 1. Schematic draw of one self-expandable mold used to produce polypropylene foams via the improved compression molding route.

on the relationship between chemical composition, processing parameters, and cellular structure.

2. Production of Solid Precursors: The second step comprises the fabrication of solid foamable precursors using the previously obtained pellets. Solid cylinders with 20 mm in diameter and 15 mm in height, and discs with 150 mm in diameter and 2 mm in thickness were produced using stainless steel molds and a hot plates press. In both cases the temperature of the press was fixed at 175°C (lower than the decomposition temperature of the azodicarbonamide (ADC) which is in the range between 200 and 220°C).[24] The applied pressure (P_0) was 95 MPa for cylinders and 5 MPa for discs. Pressure and temperature were applied simultaneously for 15 min. Those values were chosen in order to assure a proper densification of the pellets.
3. Foaming Step: The aforementioned thermoformed precursors were introduced in a self-expandable mold with the ability of controlling the expansion ratio of the material. The ICM route can be carried out by using directly as solid precursors the pellets obtained after the melt-compounding process. Nevertheless, in this work thermoformed solid precursors were preferred because they allowed measuring the mechanical properties of the solid materials prior to the foaming step.

Figure 1 shows a schematic draw where it is represented the evolution of both sample and mold during a typical foaming experiment.

In the first stage, the solid thermoformed precursor (or equivalent mass of pellets) is introduced in the mold and an initial pressure (P_0) and foaming temperature (T_F) are applied. The cavity where the precursor is introduced has a defined initial height (h_0). The gas generated starts to be dissolved in the polymer as the blowing agent decomposes (second step) and the pressure increases above P_0. After a certain time (t_F), the pressure is stabilized at a certain value (P_F). This pressure denotes the moment in which the entire blowing agent has been decomposed and then, pressure is released (third step) allowing the piston to displace vertically by the expansion of the polymer inside the mold. The distance covered by the piston is defined taking into account the desired expansion ratio ($ER = h_f/h_0$). Therefore, the final height of the sample is defined as follows:

$$h_f = h_0 + d \quad (1)$$

The movement of the piston is restricted to such distance (d) by the part named "*ER Control Part*". Such parts are interchangeable depending on the desired expansion ratio. Finally, the mold is rapidly introduced in a tank containing cool water to stabilize the cellular structure.

One of the main differences between the ICM route and the conventional one-step compression molding lies in the pressure applied to the foam during foam growing. This difference promotes significant advantages of the ICM process over the conventional compression molding process. On the one hand, the possibility of achieving an accurate control of foam density and on the other hand, the possibility of modifying the microstructure of the foamed part, (in terms of cell size, cell type and cell shape) by acting on both foaming parameters and chemical composition.

The different foaming parameters mentioned, this is t_F, P_0, and T_F are chosen depending on the polymeric matrix type, chemical composition (blowing agent concentration), and sample geometry. In this work, an initial pressure (P_0) of 100 MPa for cylinders and of 4 MPa for discs was applied to the mold. Foaming temperature (T_F) in both cases was 205°C and P_F varied depending on both geometry and azodicarbonamide concentration. Foamed discs and cylinders with the four aforementioned ADC concentrations have been prepared. Samples were expanded to three different expansion ratios (ER) 1.6, 2, and 3 which correspond to nominal densities of 562.5, 450, and 300 kg/m^3, (i.e. relative densities of around 0.6, 0.4, and 0.3 respectively). Samples denomination is as follows, a capital C (for cylinders) or a capital D (for discs) followed by two numbers, the first one indicates the ADC concentration (1, 5, 10 or 15) and the second one, the expansion ratio (1 for 1.6, 2 or 3).

CHARACTERIZATION

Density

Density measurement of both solid precursors and foams was performed by the geometric method; this is by dividing the weight of each specimen between its corresponding volume (ASTM Standard D1622-08). The relative density was calculated as the density of the foams divided by the density of the solid precursor from which the foam was produced

Microstructural Characterization

Cellular structure of both foamed discs and cylinders was analyzed by using scanning electron microscopy (SEM). In order to keep the microstructure, samples were frozen in liquid nitrogen and afterwards fractured. Surface fracture was made conductive

by sputtering deposition of a thin layer of gold and observed using a Jeol JSM-820 SEM. Cell diameter as well as cell density were measured using an image processing tool based on the software Image J.[25] The samples were always taken from the central part of the cylindrical samples.

Open Cell Content

The analysis of the open cell content of foamed samples is essential to understand their mechanical response. In addition, is very useful to be able to determine if they could be potentially used as sound absorbers. In this study, the percentage of open cells (C) was measured with an Eijkelkamp 08.06 Lange air pycnometer according to ASTM D6226-10. The eq. (2) was used according to the ASTM standard:

$$C = \frac{V_{Sample} - V_{Pycnometer}}{V_{Sample} \cdot p} \quad (2)$$

where the geometrical volume, V_{Sample} (calculated from the specimen dimensions), is subtracted from the total volume measured with the pycnometer, $V_{Pycnometen}$ and divided by the volume of air contained in the sample, ($V_{Sample} \cdot p$), where p is the sample porosity calculated by: 1-(ρ_f/ρ_s); ρ_f is the foam density and ρ_S is the density of the polymeric matrix, in this case polypropylene (900 kg/m^3).

Mechanical Response

Mechanical response of foamed polypropylene was measured under different conditions, thus, compression, tensile and bending, tests were carried out. In addition, the solid precursor materials (polypropylene with different ADC contents) were also characterized.

Compression tests were performed in the solid and foamed cylinders using a universal testing machine (Instron model 5500R6025). Experiments were performed at room temperature and at a crosshead rate of 10s^{-1}. The maximum static strain was 75% for all the experiments. Elastic modulus and collapse stress were determined from the stress–strain curves.

Tensile tests were also performed using an Instron 5500R6025, in accordance with ISO 527, at a strain rate of 20 mm/min. Type 1A specimens were machined from foamed and un-foamed discs and five replicates for each material were performed in order to ensure the reproducibility of the results. Elastic modulus and yield strength were determined from tensile tests.

Flexural tests were performed using the same universal testing machine and in accordance with ISO 178 at a strain rate of 5 mm/min. Flexural modulus as well as flexural strength was calculated from the resulting curves.

In all cases, samples were tested under controlled conditions of 23°C and a 50% of relative humidity.

Further information about testing procedure can be found elsewhere.[26–30]

RESULTS AND DISCUSSION

Foaming Process

The hot-plates press in which the foaming experiments were conducted is equipped with a sensor able to measure the pressure during the experiments. Figure 2 shows an example of how pressure evolves with time (a) for a foamed disc and (b) for a foamed cylinder.

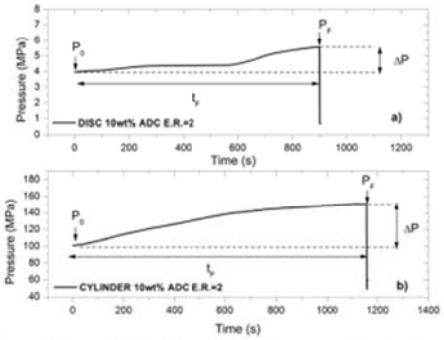

Figure 2. Curves showing the evolution of pressure with time during foaming experiments corresponding (a) to discs and (b) cylinders.

In both cases, the pressure (b) increases as the experiment progresses. However, there are some differences between both types of samples. While for cylinders the increase is produced from the very beginning of the experiment, for discs this increase takes a longer time. This difference is related with the different size of both molds. The mold used for disc is much bigger and then requires longer time to warm and to reach the melting temperature and the decomposition point of the ADC and then to increase the pressure.

There are other differences related with the total increment of pressure ($\Delta P = P_F - P_0$) and foaming time (T_F). Figure 3(a,b) summarize the average values of T_F for discs and cylinders respectively. Foaming time is slightly shorter for discs than for cylinders. Although the mold is bigger for discs, cylinders are thicker than discs (20 and 2 mm respectively) and hence they need a slight longer time for the ADC to be fully decomposed. Moreover, T_F remains approximately constant for each type of samples (discs or cylinders) being not possible to observe any trend with density or with ADC concentration.

Pressure increment (ΔP) has been calculated for the whole collection of samples and values are plotted as a function of ADC content in Figure 3(c) (discs) and Figure 3(d) (cylinders). For discs, ΔP increases linearly as ADC concentration does however, for cylinders this trend is not maintained. In addition, the values of ΔP reached by either discs or cylinders are significantly different, a maximum of 2 MPa for discs and a maximum of around 120 MPa for cylinders.

As very different initial pressures were applied to these geometries, (4 MPa for discs and 100 MPa for cylinders), the evolution of the pressure during foaming could be also different. It seems that the much higher applied pressure in cylinders hinders the real effect of ADC decomposition, leading to not linear trends between pressures and blowing agent concentration.

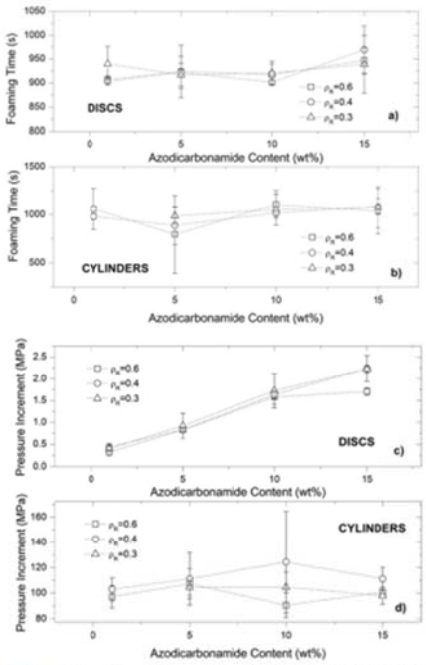

Figure 3. Average values of foaming time for PP foams ((a) discs, (b) cylinders) and average values of pressure increment ((c) discs, (d) cylinders).

It was said in the introduction that one of the main advantages of the ICM route with respect to the conventional one is the accurate control of foam density that can be achieved. Table I summarizes average density values of both foamed discs and cylinders and their respective relative densities. In addition, the coefficient of variation (CV) calculated as the ratio between the density and the standard deviation is also presented in this table. These values were calculated using the density and standard deviation values of five different samples of each type. These values provide information about the accuracy and repeatability of the process.

The results indicate that a higher degree of repeatability is reached for discs than for cylinders because the average CV for the disc samples is lower (0.028) than that of the cylinder samples (0.045); the high pressures applied to the latter type of samples during the foaming step can produce small leakages of polymers out of the mold leading to samples with densities different than the nominal one.

Table I is also includes other parameter that has been called % Deviation (%D) which measures the deviation of the foam density from the expected nominal density. It has been calculated using eq. (3).

$$\%D = \frac{\rho_{Real} - \rho_{Nominal}}{\rho_{Nominal}} \times 100 \quad (3)$$

where ρ_{Real} is the measured density of the samples and $\rho_{Nominal}$ corresponds to expected nominal densities for the three considered expansion ratio (i.e. 562.5 kg/m^3 for ER=1.6, 450 kg/m^3 for ER=2, and 300 kg/m^3 for ER=3). When %D is negative it means that the experimental value is lower than the expected one and when it reaches positive values, it means that experimental value is higher than nominal one.

Table I. Average Density Values (ρ), Coefficient of Variation (CV), Relative Density (ρ_R), and Percentage of Deviation (% D) with respect to the Nominal Density Values (i.e. 562.5, 450, and 300 kg/m^3 for 1, 2, and 3 samples)

	CYLINDERS						DISCS				
	Sample	ρ (kg/m^3)	CV	ρ_R	%D		Sample	ρ (kg/m^3)	CV	ρ_R	%D
1 wt % ADC	C1-1	525.2	0.046	0.59	−6.61	1 wt % ADC	D1-1	606.2	0.024	0.72	7.78
	C1-2	423.8	0.012	0.48	−3.81		D1-2	459.9	0.043	0.54	2.20
	C1-3	294.0	0.025	0.33	−1.97		D1-3	308.2	0.009	0.35	2.67
5 wt % ADC	C5-1	530.0	0.039	0.58	−5.77	5 wt % ADC	D5-1	541.7	0.022	0.61	−3.68
	C5-2	461.3	0.084	0.49	2.52		D5-2	426.6	0.026	0.48	−5.17
	C5-3	284.0	0.026	0.31	−5.31		D5-3	317.3	0.008	0.38	5.79
10 wt % ADC	C10-1	502.2	0.067	0.57	10.70	10 wt % ADC	D10-1	539.8	0.022	0.62	−4.01
	C10-2	424.5	0.056	0.46	−5.66		D10-2	416.1	0.022	0.45	−7.51
	C10-3	288.3	0.014	0.31	−5.55		D10-3	303.8	0.041	0.34	1.29
15 wt % ADC	C15-1	450.8	0.067	0.48	19.84	15 wt % ADC	D15-1	482.8	0.066	0.55	14.15
	C15-2	387.9	0.094	0.42	13.78		D15-2	382.4	0.005	0.43	15.00
	C15-3	287.9	0.012	0.30	−7.00		D15-3	299.5	0.051	0.33	−0.15

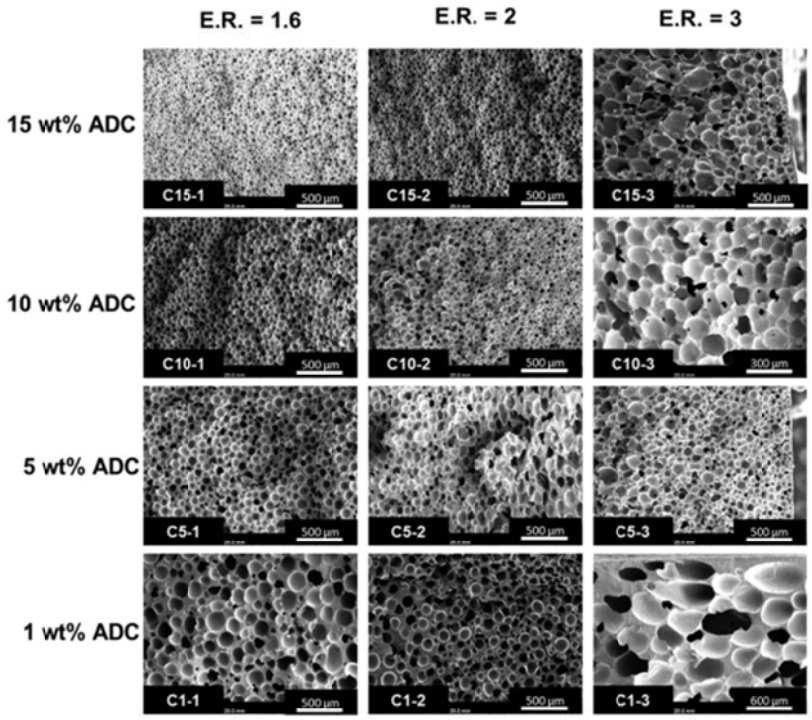

Figure 4. Micrographs corresponding to cylindrical shaped PP foams produced using the ICM route. Note: Images for samples C-10-3 and C-1–3 were taken with a different magnification.

The values in the table indicate that %*D* increases as ADC concentration does and it is higher for cylinders than for discs. As ADC content increases the pressure inside the mold also does and the polymer can easily escape from the mold. Negative values, this is experimental values of density lower than nominal one are in general due to leakages of material out of the mold, either because of high applied pressures, as in the case of cylinders or because the high pressure generated by the decomposition of high amounts of ADC, (samples with 15 wt % of ADC). Positive values of %*D*, this is densities higher than expected ones, can be due to the shrinkage of the foamed product during solidification.

Microstructure

The analysis of the cellular structure of polypropylene foams produced by the improved compression molding route has been focused on cylindrical shaped samples. SEM micrographs showing the cellular structure of foams with different densities and blown using different ADC concentrations are shown in Figure 4.

As it can be observed, as both density or blowing agent concentration are varied a wide collection of different cellular structures can be achieved. Although all the samples exhibit an isotropic cellular structure some differences related with the effect of density and ADC concentration can be inferred from the micrographs. On the one hand, as blowing agent amount increases, cell size decreases and cell density increases and on the other hand, as density decreases cell size increases and cell density decreases. To both quantify and easily understand those effects, cell density and cell size have been measured and the average values of both of them are plotted as a function of ADC content in Figure 5.

As density decreases, cell size increases, being the cell size of samples with the higher relative density around three times lower than that of the samples with the lower relative density. With regard to cell density, it can be observed in Figure 5 that it decreases as density does. As density decreases, the polymer has to expand to higher values and hence, cell walls are thinner and coalescence and/or coarsening phenomena can easily take place.[4]

The variation in ADC concentration also has an important effect on both cell size and cell density. The increment in blowing agent concentration leads to significant cell size reductions,

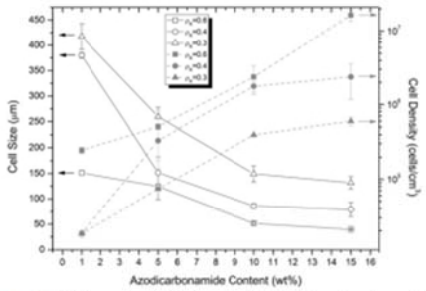

Figure 5. Cell size and cell density of cylindrical shaped polypropylene foams produced using the ICM route.

even reaching values of cell sizes below 100 μm for samples with high ADC concentrations (10 and 15 wt %). Chemical blowing agents such as azodicarbonamide are self-nucleating,[5] so as blowing agent concentration increases the number of available nucleating sites also does, leading to smaller cell sizes and higher cell densities.

Among cell density and cell size other parameters such as the cell size distribution influences the macroscopic response of foamed materials.[2] Typically, histograms of cell size distributions are plotted and afterwards compared, however, due to the high number of samples included in the study the standard deviation of the cell size distribution (*SD*), (accounting for the width of the cell size distribution) has been calculated using eq. (4):

$$SD = \sqrt{\sum_{i=1}^{n} \frac{(\phi_i - \phi)^2}{n}} \quad (4)$$

where n is the number of counted cells, ϕ_i is the cell diameter of cell i and ϕ is the average diameter of the cells. This parameter is a measure of the homogeneity of the cell size distribution.

Results, [Figure 6(a)] clearly indicate that as blowing agent concentration increases, more homogeneous cellular structures are achieved. In addition, it can be observed that samples with relative densities between 0.4 and 0.6 exhibit very similar values of *SD*. For lower densities ($\rho_R = 0.3$) values of *SD* significantly increase. For these samples the polymer is subjected to higher stretching forces that can lead to a higher proliferation of coarsening and/or coalescence phenomena as it was previously mentioned.

Other important parameter to take into account is the open cell content (*C*). It is known that this parameter can have a high influence on the mechanical response of polymeric foams.[2] In addition, for this study a conventional linear PP grade has been used, and hence it is worthy to know how the process itself and the chemical composition of the samples affect the open cell content. Experimental measurements were performed using an air pycnometer and results are plotted as a function of blowing agent concentration in Figure 6(b).

As it can be observed there is a significant difference between samples with relative densities around 0.3 and the rest of samples. For those samples, open cell content remains constant (around a 60%) regardless of the azodicarbonamide concentration used to blown them. Those results indicate that at low densities, open cell content is conditioned mainly by expansion ratio. When the polymer needs to expand to higher ratios, cell walls become thinner and hence cell walls are easily breakable leading to a higher number of interconnections between cells. On the other hand, for samples with relative densities between 0.4 and 0.6 it can be observed how open cell content increases as blowing agent concentration does. In this case, an excess of pressure in the system (due to higher contents of the blowing agent) can break cell walls leading to a higher degree of interconnection between the cells.

Analysis of the Mechanical Response

The analysis of mechanical response has been performed using relative values; this is considering the property of the foam divided by that of the solid. This type of analysis allows analyzing the influence of density and blowing agent amount, and in addition permits accounting for the influence of cellular structure on the mechanical properties. It has been reported by several authors[2,7,10,31–35] that the properties of a cellular polymer can be predicted using the following equation:

$$\frac{P_f}{P_s} = C\left(\frac{\rho_f}{\rho_s}\right)^n \quad (5)$$

where P_f is the property of the foam and P_s is the same property but for the solid polymer, and (ρ_f/ρ_s) is the relative density of the foam. C and n are parameters that can be determined experimentally.

Most foamed products exhibit values of C close to 1 and values of n in a range between 1 and 2. n is closely related with the cellular structure of the foamed product, being closer to 1 for materials with closed cell cellular structures, homogeneous cell size distributions and small cell sizes and it is closer to 2 as open cell content and cellular structure inhomogeneity increase.[2] Hence, eq. (5) allows analyzing in a quite simple way the efficiency of the foaming process in terms of producing low density foams with good mechanical performance.

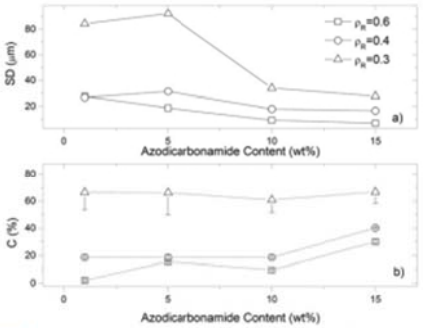

Figure 6. (a) SD coefficient for the analyzed cylinders. (b) Open cell content of cylindrical samples.

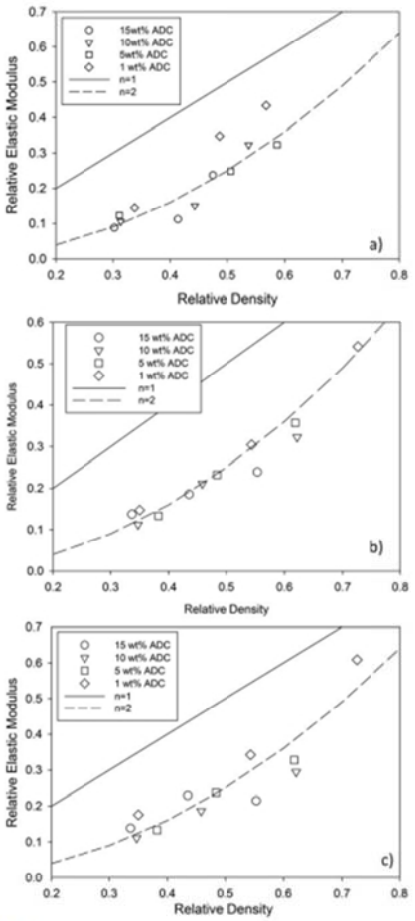

Figure 7. Relative elastic modulus measured in different configurations. (a) Compression. (b) Tensile. (c) Three point bending.

For instance when the aforementioned property is the elastic modulus (E) it can be concluded that for similar values of relative density (ρ_f/ρ_s) the foamed material reaching a value of n closer to 1 will exhibit better specific mechanical properties (higher value of E_f/E_s). As most foams exhibit values of n between 1 and 2, the reduction in mechanical properties is always greater than the corresponding density reduction. This means that the value of n can be considered as an index of under what conditions which of the analyzed foams will have a better mechanical performance.

Figure 7(a–c) shows the relative elastic modulus measured in compression, tensile and bending tests as a function of relative density. n has been calculated considering the relative elastic modulus values measured in different configurations and results are presented in Table II. As it was expected n reaches values between 1 and 2 which is in agreement with the theoretical estimations.

It can be inferred from Figure 7(a) that the cellular structure that maximizes stiffness is the one exhibited by samples blown using 1 wt % of ADC; the value of n obtained for this samples is the closest to 1. So, although those samples presented the highest value of the average cell size, its very low open cell content [close to 0, see Figure 6(b)] lead to better mechanical performance than the ones obtained for samples with lower cell sizes. This means that for the same relative density the role played by open cell content is more significant than the one played by cell size or cell size distribution homogeneity. This result is in concordance with previous studies of our group[7,10] and from other researchers.[33]

When the same type of analysis is performed with the results obtained from tensile tests, [Figure 7(b)] it can be concluded that in this case there is no significant differences between the samples made using different ADC concentrations. In fact, values of n are very similar although for 1 wt % of azodicarbonamide is slightly smaller. It seems that the different types of cellular structures achieved do not have a significant effect on the mechanical response of the samples when they are subjected to uniaxial tensile forces.

Finally, when the results obtained from flexural tests are analyzed [Figure 7(c)] it can be concluded that once more the cellular structure showing the best mechanical performance is obtained using a 1 wt % of azodicarbonamide. In fact the value of n showed by those samples is considerably smaller than that for the other materials. As it was detected for compression tests, open cell content plays a more important role than cell size or cell size distribution in the mechanical response.

If values of n are compared now for the different measurement configurations, analyzed polypropylene foams have a better response in compression or bending than in tension due to the lower value of n.

Besides the analysis of elastic modulus in relative terms, the same type of study can be performed for parameters accounting for the post-elastic behavior, this is, collapse stress, yield stress or flexural strength. Figure 8(a–c) show those three parameters

Table II. Values of n Obtained from the Fitting of Relative Elastic Modulus [Eq. (5)] Calculated for Different Types of Mechanical Tests

n-Elastic modulus	Compression	Tensile	Three-point bending
1 wt % ADC	1.55	1.90	1.67
5 wt % ADC	2.02	2.08	2.14
10 wt % ADC	2.00	2.17	2.32
15 wt % ADC	2.12	2.14	2.10

represented as a function of relative density. In addition, experimental data have been fitted to a power law according to eq. (5). The results obtained for n are shown in these figures and in Table III. As it can be observed, the highest value of n are obtained for collapse stress and yield strength, this is when samples are subjected to uniaxial tensile forces. On the other hand, the closer values to $n = 1$ regardless ADC-concentration are reached by flexural strength. Therefore, results in Table III are indicating that the samples under study have a superior performance in terms of strength when they are subjected to flexural forces.

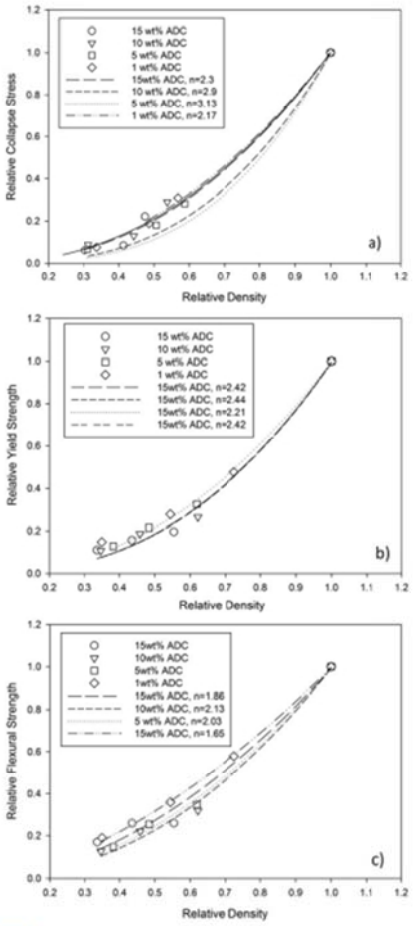

Figure 8. (a) Relative collapse stress. (b) Relative yield strength. (c) Relative flexural strength.

Table III. Values of n Obtained from the Fitting of Collapse Stress, Yield Strength, and Flexural Strength to Eq. (5)

n-Plastic collapse	Collapse stress *compression*	Yield strength *tensile*	Flexural strength *three-point bending*
1 wt % ADC	2.17	2.42	1.65
5 wt % ADC	3.13	2.21	2.13
10 wt % ADC	2.9	2.44	2.03
15 wt % ADC	2.3	2.42	1.86

As it happened for the elastic modulus (Table II), the values of n closer to 1 are always obtained when the smallest amount of azodicarbonamide is used.

CONCLUSIONS

A detailed description of the improved compression molding foaming route has been undertaken along the article. In addition to easily understand all the concepts and parameters involved in the process, a collection of polypropylene foams with relative densities ranging from 0.3 to 0.6 have been produced using such foaming route.

It has been proved that the ICM route is suitable to produce foams from a conventional linear polypropylene without the necessity of crosslinking it, achieving an accurate control of foam density due to the use of special molds and a closed control of both pressure and temperature. In addition, it has been detected that a good accuracy in the foam density can be achieved using lower initial pressures and/or lower blowing agent concentrations.

A proper set of foaming parameters together with the variation of chemical compositions (by means of using different blowing agent concentrations) can lead to a wide variety of cellular structures in terms of cell sizes, cell size homogeneity or open cell content. It was found that using high initial pressures and high ADC concentrations, cellular structures with cell sizes below 100 μm and with a very narrow cell size distribution can be achieved. As density is lowered, the polymer is expanded to higher ratios and as a consequence the open cell content reached values of 60%. Mechanical response of the foams has been determined using different measuring configurations. The analysis of mechanical properties in terms of relative values has been used to understand the influence of microstructure on mechanical behavior. The results, (regardless of measurement configuration) show that the cellular structure maximizing mechanical response is the one with the almost-zero open cell content which is presented by samples produced using the smallest amount of azodicarbonamide. So, for the same density values, these results indicate that cell size plays a secondary role when it is compared to open cell content, because samples with more homogeneous cell size distributions and very fine cell sizes but with higher open cell contents have a poorer mechanical performance. Regarding the general behavior of the analyzed materials and taking into account the values of n parameter, it

can be said that they behave better in compression and bending and slightly worse in tension.

As a general conclusion it can be said that the ICM route is a suitable foaming process to produce non-crosslinked net-shaped foams that can be applied to a wide variety of thermoplastic polymeric matrices. The accurate control of density, together with the possibility of achieving different types of cellular structures is the main characteristics of this process.

Financial assistance from MINECO (MAT 2012–34901) and the Junta of Castile and Leon (VA035U13), the FPI grant Ref: BES-2010–038746 (A. Lopez-Gil), the Torres Quevedo Program Ref. PTQ-12–05504 (C. Saiz-Arroyo) and the program "Formación e Incorporación de Investigadores" of MINECO Ref: PTA 2011–5282-E (Josías Tirado Mediavilla) are gratefully acknowledged.

REFERENCES

1. Rodríguez-Pérez, M. A. *Adv. Polym. Sci.* **2005**, *184*, 97.
2. Gibson, L.; Ashby, F. In Cellular Solids. Structure and Properties; Cambridge University Press: United Kingdom, **1997**.
3. Gendron, R. In Thermoplastic Foam Processing. Principles and Development; CRC Press: Boca Raton, Florida, **2004**.
4. Klempner, D.; Sendijarevic, V. In Handbook of Polymeric Foams and Foam Technology; Hanser Publishers: Munich, **2004**.
5. Eaves, D. In Handbook of Polymeric Foams. Rapra Technology: United Kingdom, **2004**.
6. Okamoto, K. T. In Microcellular Processing; Hanser Publishers: Munich, **2004**.
7. Saiz-Arroyo, C.; de Saja, J. A.; Velasco, J. I.; Rodríguez-Pérez, M. A. *J. Mater. Sci.* **2012**, *47*, 5680.
8. Puri, R. R.; Collington, K. T. *Cell. Polym.* **1988**, *7*, 56.
9. Puri, R. R.; Collington, K. T. *Cell. Polym.* **1988**, *7*, 219.
10. Martínez-Díez, J. A.; Rodríguez-Pérez, M. A.; de Saja, J. A.; Arcos y Rabago, L. O.; Almanza, O. *J. Cell. Plast.* **2001**, *37*, 21.
11. Ruiz-Herrero, J. L.; Rodríguez-Pérez, M. A.; de Saja, J. A. *Polymer* **2005**, *46*, 3105.
12. Rodríguez-Pérez, M. A.; Almanza, O.; Ruiz-Herrero, J. L.; de Saja, J. A. *Cell. Polym.* **2008**, *27*, 179.
13. Rodríguez-Pérez, M. A.; González-Peña, J. I.; de Saja, J. A. *Eur. Polym. J.* **2007**, *43*, 4474.
14. Rodríguez-Pérez, M. A.; González-Peña, J. I.; de Saja, J. A. *Polym. Int.* **2009**, *58*, 620.
15. Saiz-Arroyo, C.; Rodríguez-Pérez, M. A.; de Saja, J. A. *J. Appl. Polym. Sci.* **2012**, *52*, 751.
16. Rodríguez-Pérez, M. A.; Lobos, J.; Pérez-Muñoz, C. A.; de Saja, J. A.; González, L.; Del Carpio, B. M. A. *Cell. Polym.* **2008**, *27*, 347.
17. Rodríguez-Pérez, M. A.; Lobos, J.; Pérez-Muñoz, C. A.; de Saja, J. A. *J. Cell. Plast.* **2009**, *45*, 389.
18. Román-Lorza, S.; Rodríguez-Pérez, M. A.; de Saja, J. A. *Cell. Polym.* **2009**, *28*, 249.
19. Román-Lorza, S.; Rodríguez-Pérez, M. A.; De Saja, J. A.; Zurro, J. *J. Cell. Plast.* **2010**, *10*, 1.
20. Román-Lorza, S.; Sabadell, J.; García-Ruiz, I. J.; Rodríguez-Pérez, M. A.; De Saja, J. A. *Materials Science Forum* **2010**, *636/637*, 98.
21. Rodríguez-Pérez, M. A.; Simoes, R. D.; Constantino, C. J. L.; de Saja, J. A. *J. App. Polym. Sci.* **2011**, *212*, 2324.
22. Rodríguez-Pérez, M. A.; Simoes, R. D.; Román-Lorza, S.; Alvarez-Lainez, M.; Montoya-Mesa, C.; Constantino, C. J. L.; De Saja, J. A. *Polym. Eng. Sci.* **2011**, *52*, 62.
23. Saiz-Arroyo, C.; Rodríguez-Pérez, M. A.; Velasco, J. I.; De Saja, J. A. *Compos. B. Eng.* **2013**, *48*, 40.
24. Batthi, A. S.; Dellimore, D. *Thermochim. Acta.* **1984**, *76*, 63.
25. Pinto, J.; Solórzano, E.; Rodriguez-Perez, M. A.; De Saja, J. A. *J. Cell. Plast.* **2013**, *49*, 555.
26. Rodríguez-Pérez, M. A.; Velasco, J. I.; Arencón, D.; Almanza, O.; De Saja, J. A. *J. App. Polym. Sci.* **2000**, *75*, 156.
27. Landete-Ruiz, M. D.; Martínez-Díez, J. A.; Rodríguez-Pérez, M. A.; de Saja, J. A.; Martín-Martínez, J. M. *J. Adhes. Sci. Technol.* **2002**, *16*, 1073.
28. Mills, N. J.; Rodríguez-Pérez, M. A. *Cell. Polym.* **2001**, *20*, 79.
29. Almanza, O.; Rodríguez-Pérez, M. A.; De Saja, J. A. *Polym. Int.* **2004**, *53*, 2038.
30. Velasco, J. I.; Antunes, M.; Ayyad, O.; López-Cuesta, J. M.; Gaudón, P.; Saiz-Arroyo, C.; Rodríguez-Pérez, M. A.; De Saja, J. A. *Polymer* **2007**, *48*, 2098.
31. Sun, H.; Sur, G. S.; Mark, J. E. *Eur. Polym. J.* **2002**, *38*, 2373.
32. Velasco, J. I.; Antunes, M.; Realinho, V.; Ardanuy, M. *Polym. Eng. Sci.* **2011**, *51*, 2120.
33. Herrera-Tejeda, E.; Zepeda-Sahagún, C.; González-Núñez, R.; Rodrigue, D. *J. Cell. Plast.* **2005**, *41*, 417.
34. Matuana, L. M.; Park, C. B.; Balatinecz, J. J. *Polym. Eng. Sci.* **1998**, *38*, 1862.
35. Weller, J. E.; Kumar, V. *Polym. Eng. Sci.* **2010**, *50*, 2170.

5.3- Production of low-density PP-based foams.

The knowledge obtained throughout the work performed in *section 5.2* was fundamental to design the work included in this section*(Anisotropic polypropylene foams filled with nanoclays: microstructure and elastic properties)*. In this case, PP based foams were produced by the same route (ICM foaming process) but employing a polymer (branched polypropylene) able to be expanded to higher expansion ratios than the linear one employed in *section 5.3*. This is because of the strain-hardening phenomenon experienced by this specific polymer. For this reason, lower densities than the ones obtained in *section 5.2* were achieved (relative density < 0.2). Some additional foaming parameters not considered in *section 5.2* were analysed in this section. This is the case of the foaming pressure, which is studied in this work by producing foams at four different pressures (from 0.5 MPa to 81MPa). Moreover, the addition of nanoclays represented an interesting strategy to improve the mechanical properties of the virgin polymer and to modify the cellular structure (heterogeneous nucleation of cells) in such a way that foams with better mechanical performances could be obtained. This is another important goal of this work: studying the effect that nanoclays have in these PP-based foams produced at different pressures.

One interesting feature of the low-density foams produced is the formation of anisotropic cellular structures due to the fact that the expansion is restricted to only one direction. A detailed characterization of the cellular structures obtained has been performed, focusing especially on anisotropy, due to the importance of this morphological parameter on the final mechanical properties obtained. The linear-elastic mechanical properties in compression (compressive modulus) were correlated with the anisotropic cellular structure. Moreover, the predictions of two analytical models found in literature to describe the mechanical behaviour of anisotropic foams, which are based on idealized cells such as rectangular prisms and elongated tetrakaidecahedrons (*section 2.3.2*), were compared with the experimental results.

Anisotropic polypropylene foams filled with nanoclays: microstructure and properties.

A. Lopez-Gil[1,2],M. Benanti[2,3], E. Lopez-Gonzalez[2], J.L. Ruiz-Herrero[2], F. Briatico[3], M.A. Rodriguez-Perez[2]

[1] CellMat Technologies S.L. CTTA. Paseo de Belén 9A, 47011, Valladolid, Spain.

[2]Cellular Materials Laboratory, (CellMat). Condensed Matter Physics Department, University of Valladolid, Paseo de Belén 7, 47011, Valladolid, Spain.

[3]Dipartimento di Chimica, Materiali e Ingegneria Chimica "Giulio Natta", Politecnico di Milano, piazza Leonardo da Vinci 32, 20133 Milano, Italy.

Abstract

This work deals with the production and characterization of low density rigid foams (relative density < 0.2) based on a high melt strength branched polypropylene and able to be employed for structural applications such as in the core of sandwich panels. The improved compression-moulding route (ICM) was selected as the foaming process because it allows the production of foams with the same density and varied cellular structures. In this case, anisotropic cellular structures were obtained because the expansion of the polymer was restricted in one single direction. The anisotropy ratio and other cellular structure parameters, such as cell size and open cell content were modified by means of reinforcing the polymer matrix with nanoclays and by applying different pressures during the foaming process. The mechanical anisotropy of these foams was characterized by measuring the compressive modulus in three different directions. The experimental results were compared with theoretical models found in literature that describe the mechanical response of low-density open-cell polymer foams such as the rectangular (Huber &Gibson) and elongated tetrakaidecahedron (Kelvin) cell models. The purpose was to evaluate if these models are also suitable to describe the mechanical behaviour of anisotropic low-density rigid foams with a partially open cellular structure such as the PP foams produced in this work.

1- Introduction

Polypropylene (PP) is an ideal candidate to replace more common thermoplastics used for foaming applications such as polystyrene (PS) and polyethylene (PE) because of its high thermal stability, stiffness, strength and impact strength [1]. Several foamed products based on PP have been developed so far and they can be found in the market. The main example is **expanded polypropylene** (EPP), which is produced from a copolymer grade of PP by the *moulded bead process* and it is used as shock energy absorber in automotive applications [2,3]. However, the stiffness and strength of the final foamed parts produced from EPP are low in comparison with those of other foamed materials employed for structural applications such as polyvinyl chloride (PVC), polyethylene terephthalate (PET) and polyurethane (PU) foams. The production of PP foams from linear isotactic grades would increase their mechanical performance but this is a challenging task because of the low melt strength of this polymer. The development of branched grades allowed to broaden the foaming applications of this polymer [1] because when it is subjected to high expansions rates, it experiences a sudden

increase of viscosity caused by the entanglements of polymer chains (*strain-hardening phenomenon*). This phenomenon allows PP foams with lower densities [4] to be obtained. DOW produced the first foamed sheet based on a branched PP in 1994 [5] and since then, the production of PP foams from branched PP or blends with linear PP has spread worldwide. However, the foamed sheets conventionally produced by extrusion foaming present poor cellular structures (large cell sizes) [6-8], which still prevents their use in structural applications replacing PVC, PET and PU foams.

In order to improve the cellular structure and consequently, the mechanical properties of these branched PP-based foams several strategies can be adopted. One of them is the reinforcement of the polymer matrix with nanoclays because they not only increase the properties of the solid material but are also able to promote significant alterations of the foaming mechanisms (nucleation, expansion and stabilization) [9]. These alterations could in turn result in positive modifications of the cellular structure from a structural point of view (cell size reduction, narrowing of the cell size distribution, etc.).

The literature dealing with PP foams reinforced with clays is abundant. Most of the works employed physical blowing agents such as CO_2 in an extrusion foaming process or in a batch-process carried out within an autoclave. The addition of clays in the extrusion foaming process even at very low contents (≤1wt%) allowed to increase the expansion ratio of the foams [18,19,20]. The main reason given for this behaviour is the increment of the cell nucleation rates and the suppression of the cell coalescence mechanism by the addition of nanoclays. In the work of *Chaudhary, A.K. et al*, in which a extrusion process was also used but with a chemical blowing agent, the reason given for the better foaming behaviour of the nanocomposites is the induction of the strain-hardening phenomenon in the linear PP matrix [21] The works in which the batch foaming process was employed gave rise to similar conclusions but the use of higher contents of clays produced some other interesting effects [22,23,24,25,26,27]. For instance, in the work of *Bhattacharya, S*. et al clay loadings in a branched PP above 4 wt% produced a decrease of the nucleation efficiency resulting in foams with larger cell sizes. In the work of Nam, P.H. et al the addition of 7.5 wt% of clays to a linear PP caused the formation of a bimodal distribution of cell sizes attributed to the presence of clay agglomerates. Other works employed different production routes. This is the case of the work of *Jiang, M et al*. in which the foams were produced by a two-stage injection foaming technique [28]. Moreover, *Antunes, M. et al* used a single-step compression moulding technique in which azodicarbonamide was the blowing agent employed. This last work stated that clays produced an enhancement of the polymer thermal stability increasing the foaming window and reducing the time in which the polymer starts to expand [29]. The work of *Ma, Y. et al* was the only one in which the *improved compression moulding route* (*ICM*) was employed to produce PP foams reinforced with nanoclays [30]. However, it was mostly focused on the X-ray microtomographic technique employed to analyse the cellular structure. The effect of nanoclays on the structure and in the mechanical properties obtained was not evaluated in detail.

In general, all the works mentioned lacked of an exhaustive study of the cellular structures obtained and they were highly influenced by the expansion ratio of the foams produced.

Moreover, the relationship cellular structure-mechanical property was not analysed in detail. Last but not least, most of the foams obtained present isotropic cellular structures because of the foaming method employed in which the expansion of the polymer is free.

The second strategy is to obtain foams with anisotropic cellular structures, whose mechanical properties are strongly dependent upon the direction in which they are measured. In general terms, the mechanical properties measured in the plane perpendicular to the direction where the cells are elongated are higher than in the equivalent isotropic structure. The *improved compression moulding route* (*ICM*) is a foaming process based on using *self-expandable moulds*, which allows the aforementioned cellular structures to be obtained by simply modifying processing parameters and formulations [10-17]. The degree of elongation of the cells can be quantified by the shape anisotropy (R), defined as the ratio between the maximum length of the cell and the minimum length in the perpendicular direction. In literature there are several models that attempt to describe the elastic response of polymeric foams under a compressive load. Some of these models consider that the only mode of deformation of the struts is *uniaxial compression* and in these cases the compressive modulus only depends linearly on the density. In other cases the main mode of deformation is *bending* and the dependence of the compressive modulus with density is quadratic [18-21]. This is the case of the cubic cell model of Gibson &Ashby [18]. Huber and Gibson modified the cubic cell model with the aim of describing the behaviour of anisotropic foams [31]. They assumed a rectangular open cell instead of a cubic open cell and introduced the anisotropy ratio in the model equation.

From solid mechanics considerations previously reported [19,23], the ratio between the modulus in expansion direction E_{exp} and that of the transversal direction E_{trans} for an open cell foam is related to R by equation 1. In the case of closed cell foams equation 2is valid, where f_s is the solid fraction contained in the cell edges and vertexes.

$$\frac{E_{exp}}{E_{transv}} = \frac{2R^2}{1+\left(\frac{1}{R^3}\right)} \tag{1}$$

$$\frac{E_{exp}}{E_{transv}} = f_s \frac{2R^2}{1+\left(\frac{1}{R^3}\right)} + (1-f_s)\frac{2R^2}{1+(1/R)} \tag{2}$$

The two models converge for open cell foams (f_s=1). The developed relations do not depend on the properties of the material (modulus of the solid polymer, E_s, and relative density, ρ_f/ρ_s) but only on the geometry of the equivalent rectangular cell (R).

These models simulate the mechanical behaviour of foams with very simple cell geometries such as cubes and rectangular prisms, which do not represent the real morphology of the cells. A more complicated cell geometry is the tetrakaidecahedron, which is known as the Kelvin cell model [32].Several authors employed elongated tetrakaidecahedron with the aim of analysing non-isotropic foams [33,34]. *Sullivan et al* [35,36] defined a model for open cell foams (f_s=1) based on an elongated tetrakaidecahedron by specifying three independent dimensions and introducing an additional shape parameter called Q. The ratio of elastic modulus in the

expansion direction (E_{exp}) to the modulus in the in-plane direction (E_{transv}) can be expressed as a function of *R, Q* and ρ_f/ρ_s by equation 3.

$$\frac{E_{exp}}{E_{transv}} = \frac{R^2}{4}\left[\frac{\left(2\widetilde{Q}^{\,2}R^2 + \frac{64Q^3}{\sqrt{16+\widetilde{Q}^{\,2}R^2}}\right)C_1 + \frac{8RC_2\widetilde{Q}^{\,3}\left(32+4Q\sqrt{16+\widetilde{Q}^{\,2}R^2}\right)}{\left(4Q+2\sqrt{16+\widetilde{Q}^{\,2}R^2}\right)(16+\widetilde{Q}^{\,2}R^2)}\left(\frac{\rho_f}{\rho_s}\right)}{16\,C_1 + \frac{8R^3C_2\widetilde{Q}^{\,5}}{\left(4Q+2\sqrt{16+\widetilde{Q}^{\,2}R^2}\right)(16+\widetilde{Q}^{\,2}R^2)}\left(\frac{\rho_f}{\rho_s}\right)}\right] \quad (3)$$

A more detailed explanation of the different parameters involved in the equation can be found in the works of *Sullivan et al*, in which the stiffness and strength ratios of several flexible and rigid foams with anisotropy ratios between 1 and 1.8 were compared with the modified Kelvin model for three values of *Q* (1, $\sqrt{2}$ and 2) and for different relative densities. Moreover, in the work of *Hamilton et al* [37] low-density reinforced polyurethane foams with anisotropy ratios between 1 and 2 were evaluated by the *rectangular cell model* and the *modified Kelvin model*.

Taking into account the previous information the objectives of this work are firstly, the development of low relative density (ρ_f/ρ_s<0.2) pure and nanoreinforced PP foams with fine cellular structures and good stiffness by the ICM route. Secondly, the study of the relationship between process (foaming pressure), structure (cell size, cell density, open cell content and anisotropy) and properties (compressive modulus) of the foams produced and how the presence of anisotropy and the incorporation of nanoclays affect this relationship. Finally, to evaluate if the models generally used for low density foams with elongated cells such as the *rectangular* and *Kelvin cell models* are suitable for anisotropic rigid foams of higher density such as the materials developed in this work.

2- Materials

A branched high melt strength polypropylene (*PP Daploy WB135HMS*) provided by *Borealis* was employed as the polymer matrix. The nanoreinforcement employed was a montmorillonite-type nanoclay organomodified with a quaternary ammonium salt (95 meq/100 g clay)provided by *Southern Clay Products* (*Cloisitie 20A*). A PP homopolymer modified with maleic anhydride (*Polybond 3200*) provided by *Chemtura* was used as the coupling agent. The chemical blowing agent employed was azodicarbonamide (ADC) *Porofor MC-1* provided by *Lanxess* with a decomposition temperature of 210ºC and an average particle size of 3.9 µm. A mixture of commercial antioxidants (*Irganox B561* and *Irgafos 168*), both supplied by *CIBA*, was added in all the formulations produced to prevent the thermal oxidation of the polymer.

3- Production route

The production route is composed of two main processes: the compounding of the raw materials and the production of the foams by the improved compression moulding route (*ICM*). They have been described separately in the following sections for the sake of clarity.

3.1- Compounding process.

Polypropylene foams were produced based on two different formulations: one pure (*PP*) and the other one based on polypropylene reinforced with nanoclays (*NP*), both blended with 2.5% of ADC. All the formulations were produced by melt-blending in a bench-top co-rotating twin-screw extruder *model ZK 25 T, Dr.Collin* that has five heating zones and a L/D of 24.

The nanocomposite (*NP*) production was carried out prior to the incorporation of the blowing agent. Firstly, a masterbatch of nanoclays (50 wt.%) and coupling agent (50 wt%) was produced. Both materials were manually mixed prior to being fed into the extruder. The temperature profile was set to 180-185-190-195-200 ºC and the screw speed to 50 rpm. The blend produced came out of the extruder die in the form of a molten strand which was immediately cooled by water, pelletized and finally dried in a vacuum oven at 60 ºC for at least 24 hours. The reason for drying the blend is the high susceptibility of both, nanoclays and the coupling agent to absorb water because of its hydrophilic chemical nature. Secondly, the *nanoclay-coupling agent* masterbatch was diluted with the branched polypropylene in order to produce the final nanocomposite (5 wt.% of nanoclays) in the same extruder and under the same production parameters.

Both, the pure polypropylene (*PP*) and the nanocomposite (*NP*), were melt blended with azodicarbonamide (2.5 wt%) and with a mixture of antioxidants (0.1 wt%) in the same extruder used for the production of the nanocomposite. The mixture of antioxidants is composed of *Irgafos168* (80 wt%) and *Irganox1010* (20 wt%). In this case, the temperature profile was set to 135-140-145-150-155 ºC and the screw speed to 120 rpm. The temperature is low enough in order to avoid a premature decomposition of the blowing agent. The molten compound obtained at the exit of the die was water cooled, pelletized and dried in a vacuum oven at 60 ºC for at least 24 hours. The compounds were extruded again under the same production parameters with the aim of obtaining a more homogeneous dispersion of ADC particles along the polymer. The materials obtained after the homogenization step were also dried under the same conditions previously described with the aim of avoiding the influence of water on the production of the foams.

3.2- Foaming process.

Disc-shaped foams were produced by the *ICM* foaming route whose main feature is the use of a *self-expandable mould* (150 mm diameter). The mould and the main steps involved in this foaming route are shown in Figure 2. The axis on the right was included to specify the expansion direction (D_1) and the direction perpendicular to it (D_2). The moulds are *self-expandable* because the piston (1) moves up pushed by the expanding polymer immediately after releasing the pressure. The total distance covered by the polymer during its expansion is established by a built-in blocking system (2) in which a metallic ring (3) of a determined height is used to set the foam expansion ratio. The final foam density can be adjusted by simply replacing the metallic ring for another of a different height. Moreover, the molten polymer is retained inside the mould cavity not only during the application of the pressure but also during

the expansion process because the mould is hermetically sealed by rubber joints (4) allowing the production of non-crosslinked foams with defined shapes, discs in this particular case.

The process is split up into several steps. First of all, a certain amount of foamable compounded pellets (5), enough to reach the final foam density are placed into the mould cavity (Figure 1a). Then the mould is closed and placed between the hot plates of a hydraulic press, which is used to apply heat and pressure simultaneously. Secondly, pressure and temperature are applied for 15 minutes for all the foams produced (Figure 1b). After this time, during which the entire blowing agent decomposes (b), the applied pressure is reduced, producing the nucleation and growth of the cells (Figure 1c). Thirdly, the expansion of the polymer is limited by the built-in blocking system (2), which allows foamed discs of 10 mm in thickness and 150 mm in diameter to be obtained with the target foam density (6). The mould is finally immersed in water in order to cool and stabilize the foam.

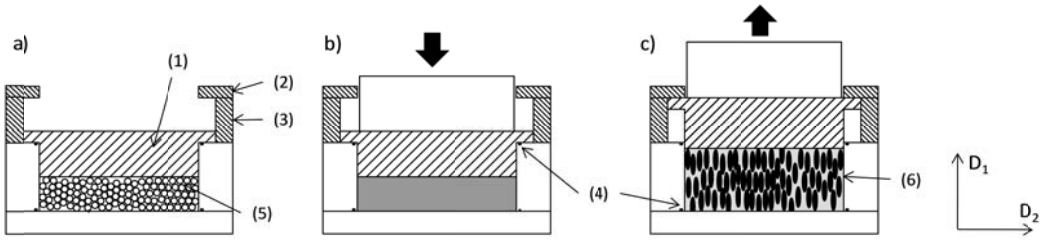

Figure 1.ICM foaming process. a) The mould with the pellets inside prior to the foaming process. b) The mould with the molten material inside during the time in which pressure and temperature are applied. c) The mould with the foam inside after releasing the pressure.

The temperature and pressure conditions employed to produce the foams are summarized in Table 1. The denomination of the materials in the first column indicates the formulation (*PP* or *NP*) and the pressure conditions. Different pressures from 0.5 to 8 MPa were used for both formulations. Moreover, the foaming temperatures used were different because the addition of nanoclays accelerated the blowing agent decomposition process involving the generation of a higher amount of gas (this will be explained later in the section 5.1).Therefore, the temperature used for the NP formulation was 10 C lower than that used with the PP formulation with the aim of equalling the amount of gas generated in both kinds of foams.

Foam sample	Temperature (ºC)	Pressure (MPa)
PP0.5	200	0.5
PP1.5	200	1.5
PP4	200	4
PP8	200	8
NP0.5	190	0.5
NP1.5	190	1.5
NP4	190	4
NP8	190	8

Table 1. Foams produced and production parameters.

4- Characterization.

4.1- Thermogravimetric analyses of the solid formulations.

A thermogravimetric analyser model TGA/SDTA 861 was used to perform two kinds of experiments over the solid formulations (PP and NP): a *dynamic analyses* and *isotherms*. On the one hand, in the *dynamic analyses* the samples were heated from 50ºC to 1000ºC at 20 ºC/min under N_2 atmosphere (60 cm^3/min). On the other hand, in the *isotherm program* the samples were heated from 50 to 190º C (NP) and from 50 to 200ºC (PP) at 20 ºC/min under N_2atmosphere(60 cm^3/min). The final temperatures (190 and 200ºC), which correspond to the foaming temperatures (Table 1), were maintained constant for about 30 minutes in an effort to simulate the foaming process. The loss of weight in percentage of the formulations was registered according to temperature in the case of the dynamic analyses, and according to time, in the case of the isotherms. Three samples of each formulation were measured in order to evaluate the reproducibility of the results obtained.

4.2- Density.

Density (ρ_f) was determined on each foamed specimen following the ASTM standard D1622-14. The density of the solid polymer (ρ_s) was measured using a gas pycnometer. The measured density of the pure formulation pellets (PP) was 0.90±0.01 g/cm^3 while that of the nanoreinforced formulation (NP) was slightly higher 0.92±0.02 g/cm^3.

4.3- Open cell content.

A gas pycnometer model *AccuPyc II 1340 Micromeritics* was used for the open cell content (OC) measurements following the standard *ASTM D6226-10*. Cubic samples (20x20x10 mm^3) extracted from each kind of foam were used for the experiments. Five measurements were carried out on each kind of foam. Equation 4 was employed to calculate the open cell content.

$$OC = \frac{V - (2V_1 - V_2)}{V(V_f)} x100 \quad (4)$$

Where V represents the geometric volume of the sample, V_1 is the volume of the cubic sample measured by the gas pycnometer and V_2 is the volume of the same cubic sample after being cut in two planes according to the standard. By using this method, it was possible to obtain a more accurate value of the open cell content without considering the cells located on the surface, which were open because the sample had to be cut in order to be extracted from the foamed disc. Finally, V_f is the porosity of the foamed sample, which was calculated by equation 5.

$$V_f = 1 - \frac{\rho_f}{\rho_s} \quad (5)$$

where ρ_s and ρ_f are the density of the solid and the foam, respectively.

4.4- Microstructure characterization.

SEM micrographs of the foams were taken in a plane parallel to expansion direction (D_1/D_2) and in the plane perpendicular to it using a scanning electron microscope model *Jeol JSM-820* (2–20kV and 10^{-9}-10^{-10}A). The samples (10x10x10 mm^3cubes) were previously prepared by cutting with a razor-sharp blade along the two planes previously specified and they were made conductive by a sputtering deposition of gold. Images were digitalized with a resolution of 1200 dpi. 3-5 images along the expansion plane (D_1/D_2) were taken at high magnification and later joined with *Photoshop CS7* in order to obtain high-resolution images of the entire thickness (≈10mm) of the foamed samples. Some examples of these images are shown in Figure 4 of *section 5.1*.

The cellular structure was characterized in two dimensions (in the images obtained from the expansion plane) by means of an image analysis tool based on the software Image J that allows the user to control the selection of cells to be measured [38]. Before the image analysis process the contour of each cell was marked in order to enhance the contrast and increase the accuracy of the analysis (Figure 3a).The cell size of each cell was defined as the average of the diameters measured in four different directions (0°, 90°, ±45°). The average foam cell size (Φ) is therefore, calculated as the average cell size of all the cells considered in the analysis as shown in equation 6 in which *n* represents the total number of cells.

$$\Phi = \frac{\sum_{i=1}^{n} \Phi_i}{n} \tag{6}$$

The cell size in the expansion direction (Φ_{i1}) and in the transversal direction (Φ_{i2}) for each cell was also measured as shown in Figure 2b in which the cell is theoretically represented as an ellipse. The average values for all the cells considered in the analysis was also calculated and expressed as Φ_1 and Φ_2 for the expansion and transversal directions, respectively. In addition, an image pixels count allows computing the area occupied by each cell (as indicated in Figure 2c as A_{cell}).

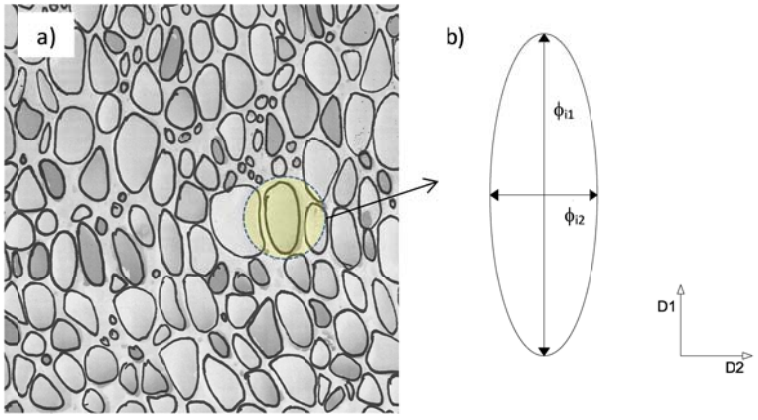

Figure 2. a) Part of an image before digital analysis with outlined border of cells. b) Cell size in the expansion (D_1) and transversal directions (D_2).

The Asymmetry Coefficient (*AC*) of the cell size distribution was calculated by employing equation 7 in which *SD* is the standard deviation of the cell size distribution calculated by equation 8.

$$AC = \frac{\sum_i^n (\Phi_i - \Phi)^3}{n(SD)^3} \tag{7}$$

$$SD = \frac{\sqrt{\sum_i^n (\Phi_i - \Phi)^2}}{n-1} \tag{8}$$

The homogeneity of the cell size distributions is described by the parameter *NSD* (normalized standard deviation), which is the ratio between *SD* and the average cell size, as expressed by equation 9.

$$NSD = \frac{SD}{\Phi} \tag{9}$$

The cell density (N_v) is defined by equation10 where *A* is the image area, *n* is the total number of cells contained in that area and *M* is the magnification factor of the micrograph [39,40].

$$N_v = \left[\frac{(nM^2)}{A}\right]^{3/2} \tag{10}$$

Anisotropy ratio R_i for each cell is calculated by equation 11.

$$R_i = \frac{\Phi_{i1}}{\Phi_{i2}} \tag{11}$$

Anisotropy ratio of the whole specimen is calculated in two ways. On the one hand, as the arithmetical average of R_i for all the cells considered in the analyses and on the other hand, as the weighted average (R_w) over the cells area, as shown in equations 12 and 13, respectively.

$$R = \frac{1}{n}\sum_i R_i \tag{12}$$

$$R_w = \frac{1}{A_{cell}}\sum_i R_i A_i \tag{13}$$

where *n* is the total number of cells, A_i is the area occupied by each cell and A_{cell} is the total area occupied by the cells in the analysed image. ($A_{cell} = \sum_i A_i$)

4.5- Mechanical characterization.

Compression tests were performed using a *mod. 5500R-6025 Instron universal machine* equipped with a 100 N load cell and compression plates. The displacement was measured by means of an extensometer. A constant apparent strain rate of 1.6×10^{-3} s^{-1} was used. Three cubic samples (10x10x10 mm^3) were extracted from each kind of foam and tested at small

strains (0-3%). As the overall strain proved to be completely recovered after each test, each sample was tested in the expansion direction (D_1) and in two transverse directions (D_2,D_3) as schematically represented in Figure 3.

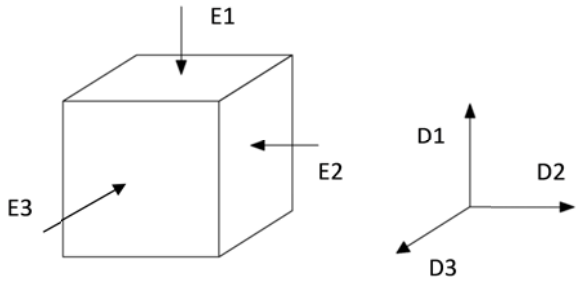

Figure 3. Scheme of the cubic PP foamed samples and the directions in which the compressive modulus (E) was measured.

All tests were conducted after materials had been conditioned at 23±1°C for at least 24h. Elastic modulus (E) was calculated as the slope of the linear part of the stress-strain curve. Friction between plates and sample surfaces was regarded as non-influent. Modulus in each direction was calculated as the average of all the measurements.

5- Results and discussion.

5.1- Thermal characterization of solid formulations.

The solid formulations produced (PP and NP) were thermally characterized by TGA in order to evaluate how the presence of nanoclays affects both, the thermal decomposition of the blowing agent and the thermal stability of the polymer matrix. This was accomplished by a dynamic analysis (temperature scan) and by isotherms performed at the same temperature of the foaming process. The dynamic analysis is shown in Figure 4.

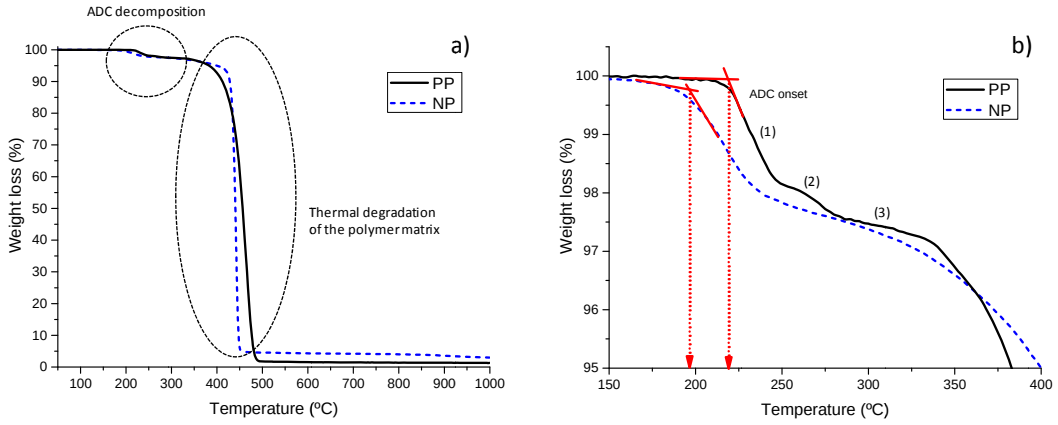

Figure 4.TGA dynamic analyses. a) All the range of temperatures (50-1000°C). b) A range of temperatures (150-400°C) focused on the ADC decomposition temperature.

Figure 4 includes two plots. The one on the left (a) shows the *dynamic analyses* in all the range of temperatures studied (50-1000ºC) in which two main weight losses are observed. The first

one is linked to the blowing agent decomposition. The second one is connected to the thermal degradation of the polymer matrix. Both weight losses were marked with circles on the plot. The one on the right is the same plot but focused on a narrower range of temperatures (150-400ºC) with the aim of observing in more detail the weight loss associated to the blowing agent decomposition reaction. The onset of the decomposition reaction corresponds to the temperature in which the tangents to the curve intersect (this intersection point is marked with red lines on the plot). This onset denotes the moment in which the decomposition reaction in gases starts to take place. The ADC onsets obtained for both formulations (NP and PP are observed in Table 2, together with the onset corresponding to the thermal degradation of the polymer (obtained in the same way), the total weight loss associated to the blowing agent decomposition reaction and the percentage of residues left after the test.

Formulation	ADC onset (ºC)	ADC weight loss (%)	Polymer onset (ºC)	Residue (%)
PP	217,5 ± 1,7	2,57 ± 0,01	397,7 ± 1,3	1,02 ± 0,31
NP	197,7 ± 1,3	2,60 ± 0,17	425,7 ± 4,0	3,80 ± 0,64

Table 2. Parameters obtained from the dynamic TGAs.

The ADC onset is clearly lower for the formulation NP (PP reinforced with nanoclays), which indicates that nanoclays are catalysing the decomposition reaction of the blowing agent. This is why the foaming temperature was lowered 10 ºC in the case of the NP formulation (Table 1). The total weight loss associated to the blowing agent decomposition reaction is very similar for both formulations, which is logical taking into account that they were produced by adding the same amount of blowing agent (2,5wt%). However, the curves are different. In the case of the PP formulation, the drop is not gradual and takes place in three stages. The first stage (1) corresponds to the exothermic thermal decomposition in gases and the following two (2 and 3) correspond to the endothermic decomposition of the solid products which were generated after the first reaction [41]. Another interesting effect was found in the thermal degradation of the polymer. The onset of the NP formulation (425,7 ºC) is higher than that of PP (397,7 ºC). Therefore, nanoclays are not only catalysing the ADC decomposition reaction but are also providing the polymer with higher stability in the molten state at high temperatures. A similar conclusion was obtained in the work of *Antunes, M. et al* in which the addition of clays broadened the foaming window of PP foams due to the higher thermal stability of the polymer matrix [29] . Finally, the total amount of residues found in the NP formulation (3,8 %) is higher than that found in the PP formulation (1,02 %). The difference is attributed to the presence of clays. However, the amount of residues is lower than the initial amount of nanoparticles added in the formulation (5 wt%) which could be partly due to the loss of the organomodification (quaternary ammonium salts) during the thermal process.

Figure 5 includes the isotherms performed at 190 and 200ºC over the NP and PP formulations, respectively. This analysis was carried out in order to evaluate in more detail the catalytic effect of nanoparticles.

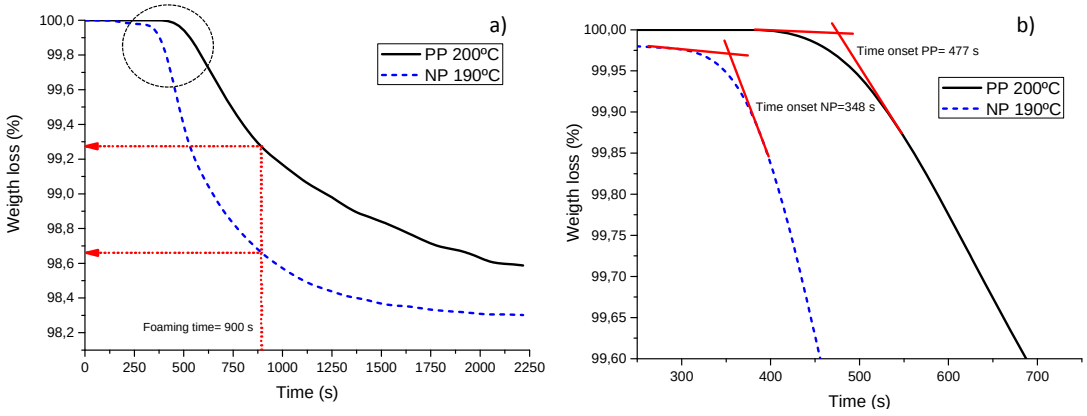

Figure 5.TGA isotherms. a) complete isotherms. b) isotherms focused on the moment in which the ADC starts to decompose in gases.

The plot on the left (a) shows the complete isotherms while the plot on the right (b) shows a zoom over the period of time in which both formulations start to lose weight. This moment was denominated as *time onset* and it was obtained in the same way as the ADC onset (Figure 4b), that is, as the crossing point between the tangents to the curve (as marked by red lines on the plot on the right). The *time onsets* for both formulations are observed in Table 3 along with the weight loss at 900 s, which corresponds to the foaming time, and with the weight loss at the end of the analysis (2250 s).

Formulation	Time onset (s)	Weight loss at 900 s (%)	Total weight loss (%)
PP	477 ± 11	0,76 ±0,02	1,44 ± 0,03
NP	354 ± 6	1,33 ±0,05	1,68 ± 0,01

Table 3. Parameters obtained from the isotherms.

The time onset of the NP formulation (348 s) is lower than that of the PP formulation (477s) even though the isotherm of the NP formulation was performed at a lower temperature (190ºC). This fact confirms the catalytic effect of the nanoclays over the blowing agent decomposition reaction. Not only ADC starts to react earlier but also the decomposition reaction is faster. This is observed in the slope of the NP curve, which is more pronounced than that of the PP curve. The previous facts involved a greater amount of ADC decomposed at 900 s (foaming time) in the NP formulation (weight loss at 900s). This is also reflected at the end of the isotherm where the amount of ADC decomposed in the NP formulation (1,68 %) is still higher than that decomposed in the PP formulation (1,44%). In spite of the fact that the total amount of ADC blended with the polymer matrix was 2,5wt%, the total weight loss registered at the end of the isotherms was lower. This is because at the temperatures at which the isotherms were performed not all the reactions involved in the ADC decomposition are completed, especially those linked to the decomposition of the solid products which are generated after the first reaction (generation of gases).

5.2- Microstructure.

The typical cellular structure of the studied foams in a plane parallel to the expansion direction (D_1/D_2) and in the plane perpendicular to it is shown in Figure 6.

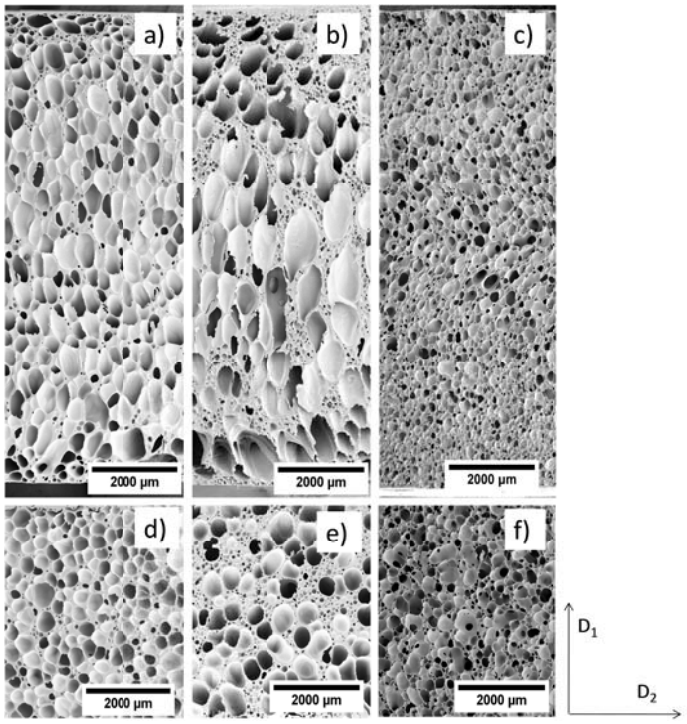

Figure 6. SEM images of some of the samples produced. Expansion plane (D_1/D_2): a) *PP0.5*. b) *NP0.5*. c) *NP8*. Perpendicular to the expansion plane: d) *PP0.5*. e) *NP0.5*. f) *NP8*.

All the pure PP foams present cellular structures, which are very similar to the one shown in Figure 6a. It is characterized by elongated cells in the expansion direction (D_1). Conversely, NP foams present cellular structures that differ with moulding pressure. On the one hand, the material prepared with the lowest pressure, *NP0.5*, (Figure 6b) presents a large number of small and almost spherical cells together with a small number of big cells, which are elongated in the expansion direction. The small cells are randomly distributed in the walls of the larger ones. On the other hand, the foam *NP8* (Figure6c) which was prepared with the highest pressure, presents a more homogenous cell size distribution. The images taken in a plane perpendicular to the expansion direction (Figure 6d-f) show that cells are essentially axial-symmetric in D_1 direction. This means that no significant differences are expected between the properties measured in directions D_2 andD_3. The reason why some of the foams produced present elongated cells is that the expansion was restricted inD_1, which coincides with the expansion direction as shown in Figure 1.

It is interesting to note that some cells, specifically those located in the upper and lower parts of the foamed disks, are elongated in another direction which is different fromD_1. The reason could be that the cells in the inner part continued growing even after the foam filled the mould (and up to the complete stabilization of the cellular structure) due to the occurrence of Tº gradients during cooling which are probably due to the high volume of the mould. As the cells

located near the upper and lower mould cavity surfaces did not have space to grow, they were deformed by the inner cells in such way that they were finally elongated in another direction different fromD_1.

The cell size distributions (bin size: 25 µm) for the 8 studied foams (*PP* and *NP*) is reported in Figures 7 and 8.

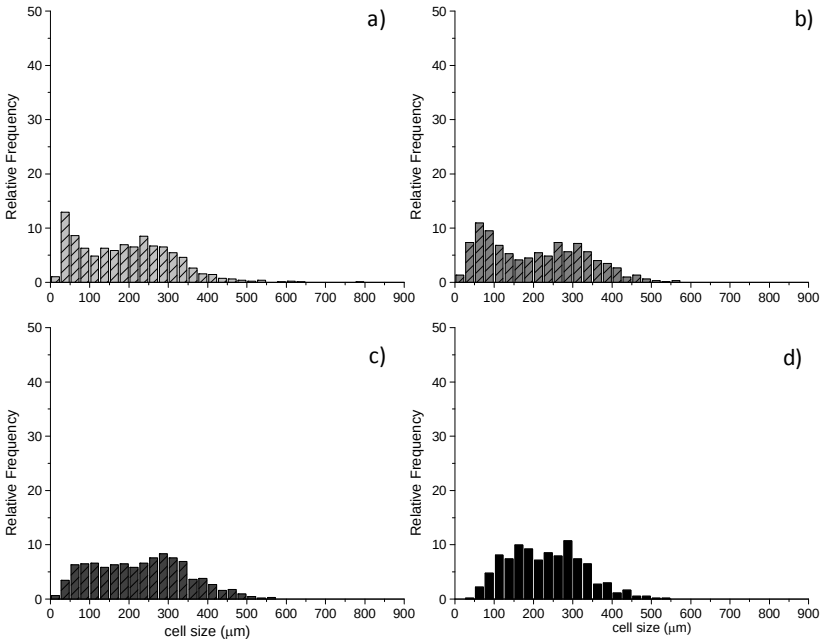

Figure 7.Cell size distributions of the pure PP foams. a*) PP0.5*. b) *PP1.5*. c) *PP4*. d) *PP8*.

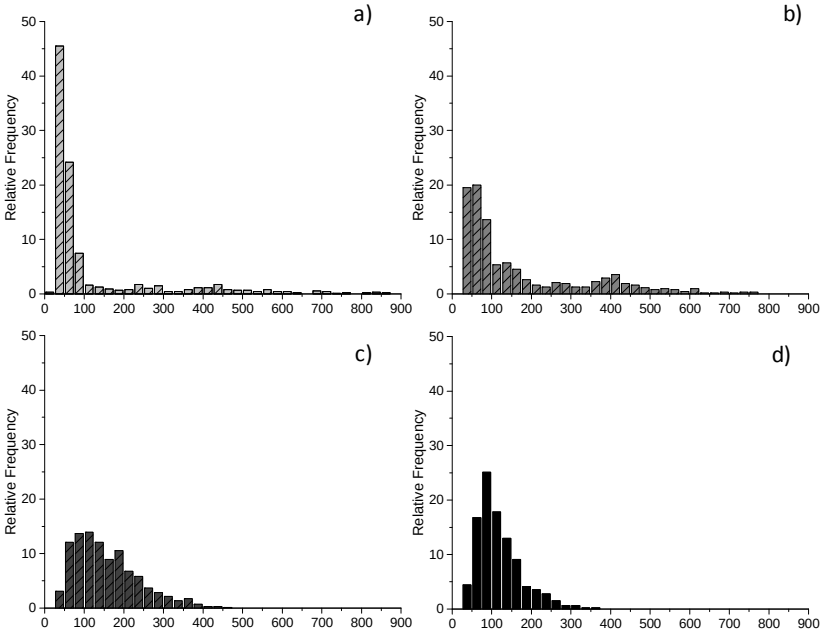

Figure 8.Cell size distributions of the nanoreinforced PP foams. a) *NP0.5*. b) *NP1.5*. c) *NP4*. d) *NP8*.

The cumulative curves of both, the area occupied by the cells and the number of cells are represented in Figure 9.

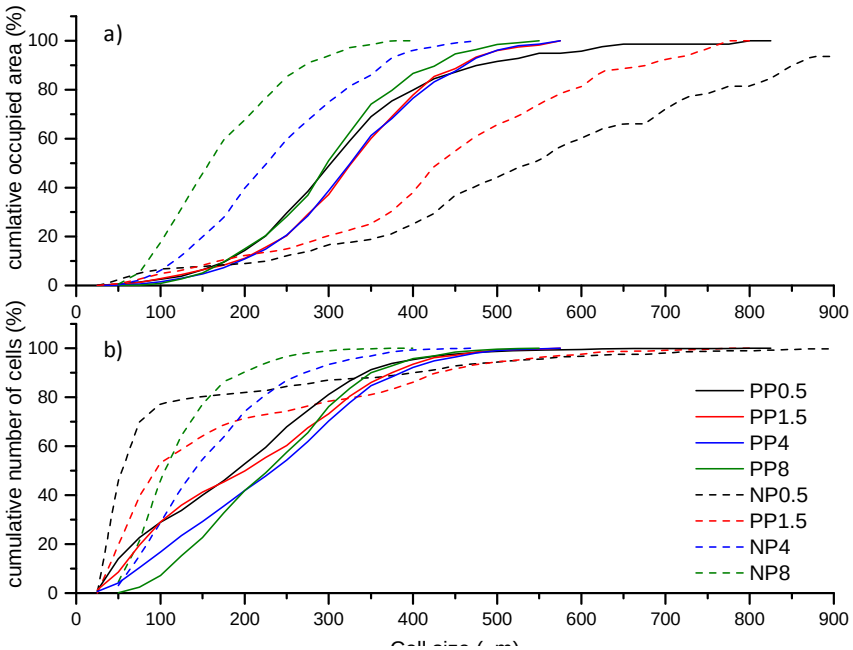

Figure 9.Cumulative curves of a) occupied area and b) number of cells.

All the *PP* foams appear to be very similar regarding the cell size distribution (Figure 7) This is confirmed in the cumulative distributions, both for cell number and cell area, which nearly superimpose each other (solid lines of Figure 9). On the contrary, the *NP* ones present very different trends in terms of the pressure applied, not only in the cell size distributions (Figure 8) but also in the cumulative curves (dashed lines of Figure 9) confirming what was shown qualitatively by SEM images in Figure 6.

One interesting feature of the foams developed, especially in the nanoreinforced foams, is the presence of mesoporosity (small cells within the cell walls of the larger ones), which can be quantitatively estimated from the previous plots. For instance, in the foam produced with the lowest pressure (*NP0.5*) about 80% of the cells have sizes below 100µm. However, the area that these cells occupy is below 10% constituting the reason why they can be considered as mesoporosity (i.e. the porosity of the solid frame). This mesoporosity tends to disappear when increasing the foaming pressure and the distribution tends to get narrower (Figure 8c and d).For instance, on the left side of the distribution the number of cells with sizes below 50 µm goes from more than 40% in *NP0.5* to less than 5% in *NP8*, while on the right side, cells with sizes larger than 300 µm represent more than 12% in *NP0.5* while only 1% in *NP8*.

The shape of the cell size distributions is measured by the *AC* values (asymmetry coefficient), which are shown in Table 2. The *AC* of the *NP0.5* foam, for instance, is very high (2.52) indicating a non-symmetric distribution with few large cells whose size are far from the average value. On the contrary, as pressure increases the *AC* values decrease and hence, the distributions tend to be more symmetric. In general, the cell size distribution symmetry of the *PP* foams is higher than those of the *NP* foams because their *AC* values are lower. NSD is also

sensitive to the presence of the clay particles. In fact, the presence of this phase increases this parameter, especially for the foams with a bimodal cell size distribution.

All the average parameters obtained from the image analyses of the cellular structures are shown in Table 2. These parameters can be influenced by two factors: on the one hand, the addition of nanoclays and on the other hand, the foaming pressure applied. Both aspects are discussed in more detail the following sections.

Materials	Density (kg/m^3)	Φ (µm)	AC_Φ	NSD_Φ	N_v(cells/cm^3)	*OC* (%)
PP0.5	173	193.2	0.63	0.62	$10.3 \cdot 10^4$	32.3
PP1.5	183	205.1	0.33	0.61	$8.15 \cdot 10^4$	35.0
PP4	182	219.5	0.42	0.57	$7.1 \cdot 10^4$	26.3
PP8	188	230.7	0.34	0.41	$6.1 \cdot 10^4$	13.5
NP0.5	182	125.1	2.52	1.37	$38.1 \cdot 10^4$	53.6
NP1.5	181	173.8	1.38	0.94	$14.1 \cdot 10^4$	84.2
NP4	189	156.0	0.90	0.52	$19.6 \cdot 10^4$	91.9
NP8	180	118.2	1.26	0.47	$45.09 \cdot 10^4$	91.8

Table 4. Average parameters of the cellular structure and open cell content.

Influence of nanoclays

The addition of nanoclays clearly influenced the cell size (Φ) and cell density values(N_v).The average cell size of all the NP foams is 143,3 µm while that of the pure foams is 212,1µm. The same result is observed for the N_v values but in an opposite way, as the average value of *NP* foams ($2.9 \cdot 10^5$) is higher than that of *PP* foams ($7.9 \cdot 10^4$). This is possibly due to a heterogeneous nucleation of cells caused by the presence of nanoclays in the molten polymer. The energy barrier that gas molecules have to overcome to form a single cell on the surface of a nanoclay particle is lower than that required in the molten polymer [10]. Nanoclays also influenced the level of interconnectivity between cells. In general the *OC* values of the *NP* foams are higher than that of the *PP* foams. This is confirmed by observing the cellular structure morphology of a pure foam (*PP1.5*) and the reinforced foam (*NP1.5*) produced with the same process. This comparison is shown in Figure 10.

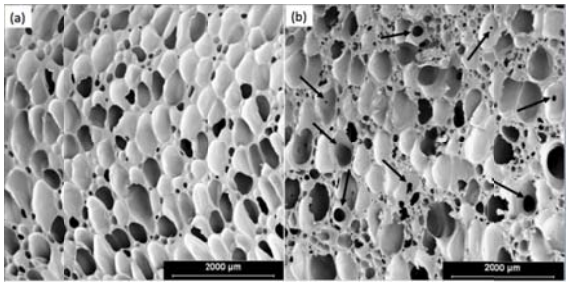

Figure 10.Cellular structure of (a) *PP1.5* foam and (b)*NP1.5* foam. Arrows indicate broken cell walls.

The cellular structure of the *NP1.5* foam shows a high number of interconnections between cells in the form of holes and ruptures within the cell walls which are indicated in the image by

black arrows, confirming what was measured by gas picnometry (*OC=84.2%*). On the contrary, the number of interconnections in the pure foam is considerably lower (*OC=35%)*as also observed in Figure 10. In spite of the high interconnectivity levels of the *NP* foams, the cells are still supported by walls. Nevertheless, these walls present small holes, which are responsible for the high open cell content values. The formation of this structure could be caused by a higher cell wall thinning during expansion. At some specific expansion ratio during the foaming process the cell wall membrane is so thin that it breaks, thus producing the holes and ruptures observed in Figure 9. It seems that the presence of clays could affect the rheological behaviour of the molten polymer. Branched PPs present the strain-hardening phenomenon by which the molten polymer experiences a sudden increase of extensional viscosity when stretched at high strains (as in a foaming process)[42]. However the presence of clays reduces this effect. This was observed in previous works in literature [43]. This fact would make the cell walls in NP foams less capable of supporting the pressure of the gas during expansion and as a consequence they break interconnecting the correspondent cells sharing the wall.

Influence of foaming pressure

The pressure applied over the *polymer/blowing agent* system also affected the cellular structures obtained. This processing parameter is very important in foaming processes because it determines the amount of blowing agent dissolved in the molten polymer prior to the expansion stage [44]. Nevertheless, PP foams do not seem to be influenced by pressure because both, Φ and N_v, are very similar (this was also observed in the cell size distributions of Figure 6). There is a slight tendency for the cell size to increase and the cell density to decrease on increasing pressure, but these variations are negligible when compared with those produced in *NP* foams. In this case, the cell density values drastically fall when the pressure is shifted from 0.5 MPa to 1.5 MPa. In fact, the general trend obtained with *NP* foams is rather contradictory because the highest cell density values were obtained with the foams produced at the lowest (0.5 MPa) and the highest (8 MPa) pressures. However, the cellular structure morphology of these foams is very different. *NP0.5* is characterized for presenting a bimodal distribution of cell sizes while *NP8* is characterized for presenting a more homogeneous structure with a narrower cell size distribution. This is confirmed by the *NSD* values, which progressively decrease as the pressure increases.

An explanation for this behaviour was found in the TGA measurements previously performed over the two solid formulations (PP and NP). Figure 4 showed a clear reduction of the temperature (ADC onset) at which the blowing agent starts to decompose when adding nanoclays. The foaming temperature was decreased when using the NP formulation (190ºC) in order to compensate for this effect and to generate the same amount of gas in the two formulations. Nevertheless, the results obtained with the isotherms (Figure 5) indicated that the blowing agent in the presence of nanoclays, even after decreasing the foaming temperature 10ºC, was able to generate a higher amount of gas than in the pure formulation (weight loss at 900 s).

This fact is consistent with the cellular structures obtained. In the case of the pure formulations, all the gas generated was able to be dissolved within the molten polymer in all the range of external pressures studied (from 0.5 to 8 MPa). For this reason, the cellular structures obtained are very similar. However, the amount of gas generated in the nanoreinforced formulations (NP) was higher, which made the *polymer/blowing agent* system more sensitive to pressure variations. This means that the amount of gas dissolved at high pressures (8 MPa) could be higher than that dissolved at low pressures (0.5 MPa). The cell size and cell density are parameters of the cellular structure, which depend on the amount of gas dissolved within the polymer. The higher the amount of gas dissolved the higher the nucleation rate and as a consequence, the number of cells in the final foam. This is why the cell density and cell size values obtained with the NP varied according to the pressure exerted.

An additional effect, in combination with the previous one, could explain the formation of the bimodal cell size distributions in the NP foams. The gas molecules, which could not be dissolved into the polymer matrix when employing low external pressures, formed cells even before releasing the external pressure applied. This involved a foaming process with two nucleating stages. A few cells nucleated in a first step (during the application of the external pressure) and hence, they had more time to grow, resulting in the formation of large cells, while most of the cells nucleated in a second stage (after releasing the external pressure) with less space and time to grow and therefore, of smaller sizes. A similar effect was observed in a previous work in which a two-step depressurization batch process was used for the formation of a bimodal cellular structure but in this case using polystyrene foams and CO_2 as the physical blowing agent [45].

The open cell content is another parameter, which is also connected with the amount of gas dissolved. In the NP foams produced at high pressures, the amount of gas dissolved into the molten polymer grows and therefore, the pressure inside the cells in the expansion process is higher, making the cell walls more prone to break. The results in Table 4 confirm the previous hypothesis because the foams NP4 and NP8 present higher OC values.

Anisotropy evaluation

Table 3 reports the average values of cell size in the expansion direction (Φ_1) and in the transversal direction (Φ_2) for all the studied foams. The average anisotropy ratio R (calculated using equation 12) and the average anisotropy ratio weighted over the area of each cell R_w (calculated using equation 13), are also shown.

Materials	Φ_1 (µm)	Φ_2(µm)	R	R_w
PP0.5	159.0±126	111.2±81	1.43±0.66	1.49±1.61
PP1.5	165.4±113	111.8±75	1.48±1	1.54±0.87
PP4	179.9±108	124.9±73	1.41±0.58	1.49±0.41
PP8	202.4±88	158.1±67	1.28±0.61	1.35 ±0.63
NP0.5	106.5±131	78.9±123	1.35±0.55	1.75±0.49
NP1.5	144.2±151	102.3±104	1.41±0.57	1.64±0.32
NP4	145.1±94	126.2±72	1.15±0.42	1.09±0.56
NP8	101.5±82	76.3±76	1.33±0.45	1.26 ±0.43

Table 5.Average cell size in the expansion (Φ1) and transversal (Φ2) directions. Average anisotropy ratio in the expansion direction R(equation 12)and Rw. (equation 13).

The results show that in all the cases, $\Phi_1 > \Phi_2$ and hence, $R > 1$. This indicates that all the foams produced present anisotropic structures, which is consistent with the fact that the expansion of the polymer was restricted to only one direction (D_1). However, the degree of anisotropy and the tendencies with respect to the pressure applied seem to change when the anisotropy ratio of each cell is weighted with their correspondent occupied area. The plots of Figure 10 show the values of R and R_w for all the *PP* and *NP* foams.

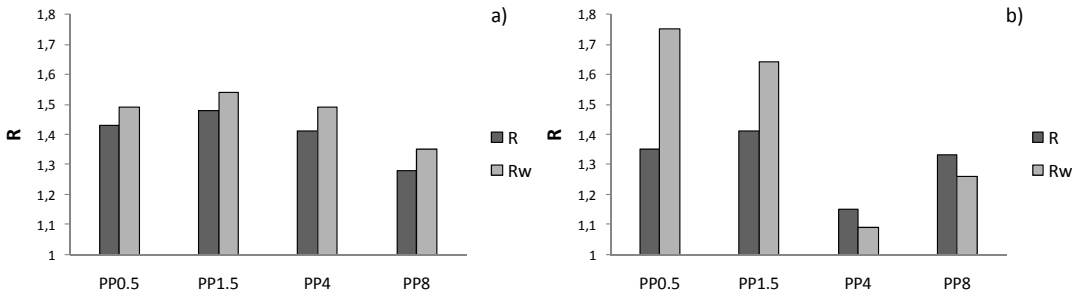

Figure 11. a) R and R_w values of PP foams. b) R and R_w values of NP foams.

There is no apparent trend regarding foaming pressure when only the R values are considered and in general the *NP* foams present lower anisotropy ratios that the *PP* foams. This is caused by the great number of small cells present in the NP foams produced with the lower pressures, which are isotropic. On the contrary, when considering R_w a clear trend appears only in the case of the *NP* foams. The R_w values of the foams produced with the lower pressures (*NP0.5* and *NP1.5*) are clearly higher than those of the correspondent pure foams (*PP0.5* and *PP1.5*) and they seem to decrease with the applied pressure. The results of R_w seem to be consistent with the cellular structures shown in Figure 6 and with the explanation given before for the formation of the bimodal cell size distributions. The foaming process of the NP foams produced at low pressures is controlled by two nucleation stages. The cells formed during the first nucleation stage not only had more time to grow but also more space and therefore, they grew with a greater elongation (the expansion of the polymer is restricted to only one direction). However, the cells formed during the second stage, had less space and less time. As a consequence they became practically isotropic.

Although no unique correlation is observable, it can be supposed that different combinations of *R*and cell size will have a different influence on the mechanical behaviour of foams. In fact, according to the classic beam theory, with which cellular materials mechanics are commonly analysed [18,22,26] the elastic deformation of cells depends on the third power of their size. This means that bigger cells contribute much more than smaller ones to specimen deformation [46] and their anisotropy has a greater influence on the elastic modulus of the material. For this reason R_w is then considered to better represent the anisotropic structure of the materials. The results of the next section will show this fact

5.3- Mechanical behaviour.

Foamed structures subjected to small deformations react elastically with a modulus dependant on its microstructure and, in the case of anisotropic foams, on the direction of the load. The results of the mechanical tests are summarized in Table 6. The E_{exp} values represent the average over the moduli measurements in the expansion direction (D_1).E_2andE_3 are the averages of the moduli in the transversal directions measured on the samples along directions D_2 andD_3. In the majority of the analysed materials, $E_2 \approx E_3$, hence, their average(E_{transv}) is taken as the modulus of the materials in the transversal direction. The ratio of modulus (E_{exp}/E_{transv}) is reported too and indicates the mechanical anisotropy of the material

Material	E_{exp}[MPa]	E_2 [MPa]	E_3[MPa]	E_{transv}[MPa]	E_{exp}/E_{transv}
PP0.5	81.4±1.2	32.7±4.1	33.8±1.4	33.2±4.3	2.4±0.3
PP1.5	96.2±1.3	33.8±3.2	39.4±4.1	36.6±5.2	2.6±0.4
PP4	96±5.7	39±2.8	44±1.6	41.5±3.2	2.3±0.2
PP8	66.3±2.6	30.6±0.8	44±1.3	37.3±1.6	1.8±0.1
NP0.5	134.4±7.7	33±4.4	55±2.7	44.0±5.2	3.0±0.4
NP1.5	118.3±4.9	50.1±6.5	44.4±2.5	47.2±6.9	2.5±0.4
NP4	73.2±8.4	47.6±2.5	48.5±4.5	48.0±5.2	1.5±0.2
NP8	78±5.4	33.4±3.2	30±3.8	31.7±10.4	2.5±0.8

Table 6.Compressive moduli values.

Figure 12 represents both, the E_{exp} and the E_{transv} values, as a function of R_w for all the foams produced.

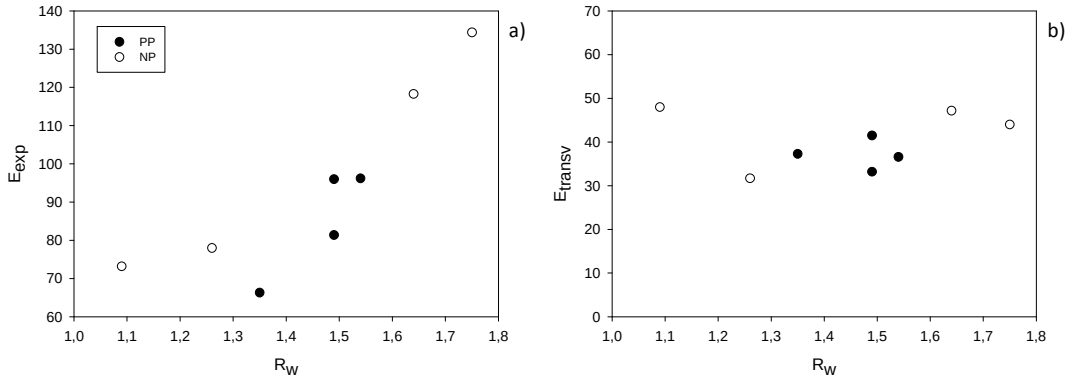

Figure 12.a) E_{exp} versus R_w. b)E_{transv} versus R_w.

These plots prove that R_w has a clear influence on the elastic modulus when the foams are measured in the expansion direction (E_{exp}). The trend obtained indicates that the elastic modulus increases with the R_w values. Therefore, the large anisotropic cells characteristic of the NP foams produced at low pressures have more influence on the measured mechanical properties. In the case of the measurements performed in the transversal direction (E_{transv}) there is not any apparent trend with R_w. However, in both cases (E_{exp} and E_{transv}) the NP foams present higher modulus than the PP foams. The only exception was found in the E_{exp} measurements of the foams produced at high pressures (low R_w) due to their highly isotropic structure. However, the measurements performed in the transversal direction (E_{transv}) showed how practically all the NP foams present higher values of the modulus than the PP foams. This fact proves the reinforcing effect of nanoclays on the polymer matrix within the cell walls and struts because even though they promote high levels of interconnectivity in these foams (Table 4), the modulus obtained are higher.

Mechanical properties can be correlated with structural characteristics of the materials by means of the models presented in the introductory section. Those models demonstrated to be predictive of the behaviour of cellular materials while they follow these conditions: periodicity of the cellular structure, narrow cell size distributions, low relative density and open cell structures [18,22,26]. The materials which are the object of this investigation only partly satisfy these conditions. It is nonetheless also worth attempting to apply the models also to polymer foams with higher densities and partially open cell structures, like the PP-based ones produced in this work. In Figure 12.a the experimental data [22,26] for stiffness ratio (E_{exp}/E_{transv}) are compared with the *Huber & Gibson* relation for open cell foams (f_s=1) obtained using equation 1 [22] and with the *Huber &Gibson* relation for closed cell foams (equation 2) and different values of f_s. In Figure 13b the comparison is carried out with the prediction given by the *elongated Kelvin cell model* with different values of *Q* obtained using equation 3 (dashed lines) [26]. The elongated *Kelvin* cell model curves are calculated for different values of *Q* (2, $\sqrt{2}$, 1) and for a relative density similar to that of the studied foams (ρ_f/ρ_s= 0.19) [26].

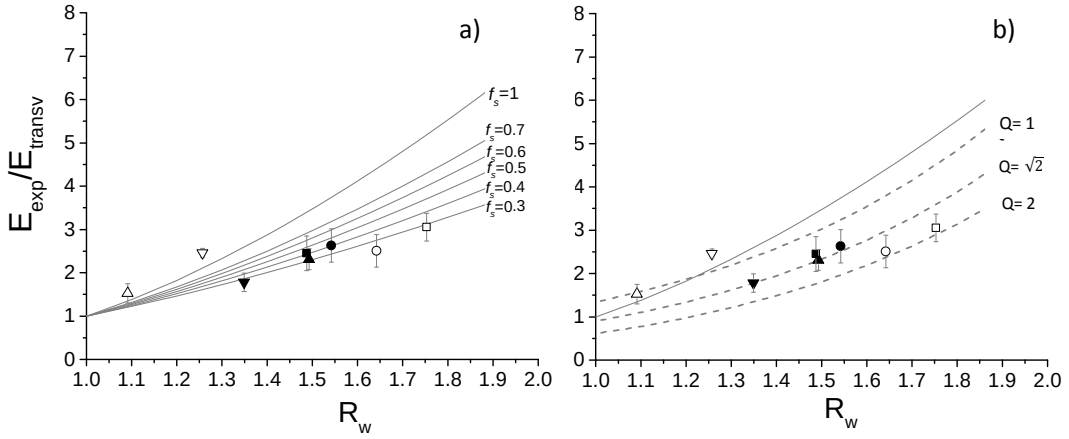

Figure 13.Moduli ratio of studied materials (*PP* and *NP* foams) reported as a function of *R* (full dots) and as a function of R_w (hollow dots) and comparison with literature models. a,b) *Huber-Gibson* for open cell foams (f_s=1) and elongated Kelvin cell model (f_s=1). c,d) *Huber-Gibson* for closed cell foams and different values of f_s.

These analytical models fit well with the experimental results when considering low R_w values but they failed to describe the mechanical behaviour of foams with R_w>1.6. On the one hand, the NP foams produced at low pressures (R_w=1,09 and 1,26) fit well with the Huber-Gibson model for open cell foams. These foams satisfy two conditions of the model because they present highly homogeneous cell size distributions and high open cell contents. On the other hand, the PP foams seem to follow the trend marked by the Huber-Gibson model for closed cell foams when f_s is in between 0.3 and 0.4. This is in good agreement with the fact that the pure foams present low open cell contents. However, they also fit well with the Kelvin model when $Q = \sqrt{2}$, which describes the mechanical behaviour of open cell foams. This may be caused by the possibility of adjusting the model with the morphological parameter Q. On the contrary, when considering high R_w values (R_w>1.6) the models do not follow the trend marked by the experimental values. This could be due to the presence of bimodal cell size distributions, which make the cellular structure of these foams non periodic and non-homogeneous. Therefore, it seems to be necessary to adjust the previous models or to develop new ones in order to be able to describe the mechanical properties of these medium-low density foams with non-homogeneous cell size distributions properly.

6- Conclusions.

The use of the ICM technology allowed the production of PP foams with densities lower than 0.2 g/cm^3 and with very different cellular structures depending on the pressure applied and on the presence of nanoclays in the formulations. Cellular structural parameters such as cell size, cell density anisotropy ratio, etc. were accurately measured by means of a user-interactive digital image correlation software that allowed a proper correlation of these parameters with the mechanical properties obtained.

The presence of nanoclays not only promoted heterogeneous nucleation of cells (cell size was reduced) but also induced a catalytic effect in the blowing agent decomposition reaction, which involved the generation of higher amounts of gas and the formation of a bimodal cell size distribution (mesoporosity)in the specimens produced at the lowest pressures. A two-stage nucleation process could be the reason underlying the presence of two populations of cells, in which the large cells nucleated in the first stage and the small cells, but more numerous, in the second stage. Moreover, nanoclays induced ruptures of the cell walls producing partially open cellular structures.

The unidirectional expansion of the polymer in the ICM process promoted the formation of anisotropic cellular structures. Cells anisotropy was analysed and different trends for each material were observed. In particular, it was noted that the smaller cells of the NP foams (mesporosity) tend to have rounded shape. Taking into consideration this fact, anisotropy ratio weighted over the cell area(R_w) was taken as being a more representative parameter of the foam structure.

These morphological changes had a measurable effect on the elastic moduli of the foams measured in compression, which reflected the structural anisotropy morphologically observed. The modulus in the expansion direction is, in fact, higher than that in the transversal direction in all the studied foams and there is a clear relation between the modulus measured in the expansion direction and the cellular anisotropy. Moreover, the incorporation of clays, apart from the previously mentioned modification of the cellular structure allowed the improvement of the elastic mechanical properties in all the analysed directions.

Lastly, the application of two different micromechanical relations, based on two different cells (rectangular and tetrakaidecahedron cell), was attempted. Acceptable correspondence between experimental data and the *Huber-Gibson* model, both for open cell and closed cell foams, was obtained when considering low R_w because in this case, the cellular structures are more homogeneous in terms of cell size distribution satisfying one of the main conditions of this model. However, in the case of the foams with the bimodal cell size distribution there was not a good correlation, which could be due to the non-periodicity and lack of homogeneity in these structures.

References.

[1] Klempner, D. and Frisch, K.C. Handbook of polymeric foams and foam technology. *Hanser Publishers*.1991.

[2] Bouix, R.; Viot, P. and Lataillade, J.L. Polypropylene foam behavior under dynamic loadings: strain rate, density and microstructure effects. *International journal of impact engineering*. 39, 329-342.2009.

[3] Zhai, W.; Kim, Y.W. and Park, C.B. Steam-chest molding of expanded polypropylene foams. 1. dsc simulation of bead foam processing. *Industrial and engineering chemistry research*. 49, 9822-9829. 2010.

[4] Naguib, H.E. and Park, C.B. Strategies for achieving ultra-low density polypropylene foams. *Polymer engineering and science*. 42, 1481-1492. 2002.

[5] Suh, K.W.; Park, C.P.; Maurer, M.J.; Tusim, M.H.; Genova, R.; Broos, R. and Sophiea, D.P. Lightweight Cellular Plastics. *Advanced materials*. 12, 1779-1789.2000.

[6] Stange, J. and Münstedt, H. Effect of long-chain branching on the foaming of polypropylene with azodicarbonamide. *Journal of cellular plastics*. 42, 445-467. 2006.

[7] Naguib, H.E. and Park, C.B. Strategies for achieving ultra low-density polypropylene foams. *Polymer engineering and science*. 42, 1481-1492. 2002.

[8] Nam, G.J.; Yoo, J.H. and Lee, J.W. Effect of long-chain branches of polypropylene on rheological properties and foam-extrusion performances. *Journal of applied polymer science*.96, 1793-1800.2005.

[9] Lee, L.J.; Zeng, C.; Cao, X.; Han, X.; Shen, J. and Xu, G. Polymer nanocomposite foams. *Composites Science and Technology*. 65, 2344-2363.2005.

[10] Rodríguez-Pérez, M.A.; Lobos, J.; Pérez-Muñoz, C.A.; de Saja, J.A.; González, L. and del Carpio B.M.A. Mechanical behaviour at low strains of LDPE foams with cell sizes in the microcellular range: advantages of using these materials in structural elements. *Cellular polymers.* 27, 347-362.2008.

[11] Rodríguez-Pérez, M.A.; Lobos, J.; Pérez-Muñoz, C.A. and de Saja, J.A. Mechanical Response of polyolefin foams with high densities and cell sizes in the microcellular range. *Journal of cellular plastics*. 45, 389-403. 2009.

[12] Román-Lorza, S. Formulación y caracterización de materiales celulares retardantes de llama libres de halógenos basados en poliolefinas. *Tesis Doctoral*. Universidad de Valladolid. 2010**.**

[13] Román-Lorza, S.; Rodríguez-Pérez, M.A. and de Saja. J.A. Cellular structure of halogen-free flame retardant foams based on LDPE. *Cellular polymers*. 28, 249-268. 2009.

[14] Román-Lorza, S.; Rodríguez-Pérez, M.A.; de Saja, J.A. and Zurro, J. Cellular structure of EVA/ATH halogen-free flame retardant foams. *Journal of cellular plastics*. 10, 1-21. 2010.

[15] Román-Lorza, S.; Sabadell, J.; García-Ruiz, J.J.; Rodríguez-Pérez, M.A. and de Saja, J.A. Fabrication and characterization of Halogen Free Flame Retardant Polyolefin Foams. *Materials science forum* 636/637, 98-205. 2010.

[16] Rodríguez-Pérez, M.A.; Simões, R.D.; Constantino, C.J.L. and de Saja, J.A. Structure and physical properties of EVA/Starch precursor materials for foaming applications. *Journal of applied polymer science*. 212, 2324-2330. 2011.

[17] Rodríguez-Pérez, M.A.; Simões, R.D.S.; Román-Lorza, M.; Álvarez-Laínez, C.; Montoya-Mesa, C.; Constantino, C.J.L. and J.A. de Saja. Foaming of eva/starch blends: characterization of the structure, physical properties and biodegradability. *Polymer engineering and science*. 52, 62-70. 2012.

[18] Zhai, W.; Kuboki, T.; Wang, L. and Park, C.B. Cell structure evolution and the crystallization behavior of polypropylene/clay nanocomposites foams blown in continuous extrusion. *Industrial Engineering Chemistry*. 49, 9834-9845. 2010.

[19] Zhai, W. and Park, C.B. Effect of nanoclay addition on the foaming behavior of linear polypropylene-based soft thermoplastic polyolefin foam blown in continuous extrusion. *Polymer Engineering and Science*. 51, 2387-2399. 2011

[20] Zheng, W.G.; Lee, Y. H. and Park. C.B. Use of Nanoparticles for improving the foaming behaviors of Linear PP. *Journal of Applied Polymer Science*. 117, 2972-2979. 2010.

[21] Chaudhary, A.K. and Jayaraman K. Extrusion of linear polypropylene–clay nanocomposite foams. *Polymer Engineering & Science*. 51, 1749-1756, 2011.

[22] Bhattacharya, S.; Gupta, R.K.; Jollands, M. and Bhattacharya, S.N. Foaming behavior of high-melt strength polypropylene/clay nanocomposites. *Polymer Engineering & Science*. 49, 2070-2084. 2009.

[23] Nam, P.H.; Maiti, P.; Okamoto, M. and Kotaka, T. Foam processing and cellular structure of polypropylene/clay nanocomposites. *Polymer engineering & science*. 42, 1907-1918.2002

[24] Taki, K.; Yanagimoto, T.; Funami, E.; Okamoto, M. and Ohshima, M.Visual observation of CO_2foaming of polypropylene-clay nanocomposites. *Polymer Engineering & Science*. 44, 1004-1011, 2004.

[25] Oh, K.; Seo, Y.P.; Hong, S.M.; Takahara, A.; Lee, K.H. and Seo, Y. Dispersion and reaggregation of nanoparticles in the polypropylene copolymer foamed by supercritical carbon dioxide. *Physical Chemistry Chemical Physics*. 15, 11061-11069. 2013

[26] Dolomanova, V; Kumar, V.; Pyrz, R.; Madaleno, L.A.O.; Jensen, L.R. and Rauhe, J.C.M. Fabrication of microcellular pp-mmt nanocomposite foams in a sub-critical CO_2 process. *Cellular Polymers*. 31, 125-144. 2012.

[27] Jiang, X.L.; Bao, J.B.; Liu, T.; Zhao, L.; Xu, Z.M. and Yuan, W.K. Microcellular Foaming of Polypropylene/Clay Nanocomposites with Supercritical Carbon Dioxide. *Journal of Cellular Plastics*. 45, 515-538. 2009

[28] Jiang, M.; Li, H.R.; Fang, D.; Liu, L.; Tai, Q.L. and Li, L.C. Structure-Property Relationship in Injection Molded Polypropylene/Clay Composite Foams. *Materials and Manufacturing Processes*. 29, 160-165, 2014.

[29] Antunes, M.; Velasco, J.I.; Realinho, V. and Solorzano E. Study of the Cellular Structure Heterogeneity and Anisotropy of Polypropylene and Polypropylene Nanocomposite Foams. *Polymer Engineering &Science*. 49, 2000-2413. 2009.

[30] Ma, Y.; Pyrz, R.; Rodriguez-Perez, M.A.; Escudero, J.; Rauhe, J.C. and Su. X. X-ray microtomographic study of nanoclay-polypropylene foams. *Cellular Polymers*.30, 90-110, 2011.

[31] Huber, A.T and Gibson, L.J. Anistropy of polymer foams. *Journal of materials science*. 23, 3031-3040. 1998.

[32] Thomson, W. (Lord Kelvin). On the division of space with minimum partitional area. Philosphical magazine. 24, 503-514. 1887.

[33] Gong, L.; Kyriakides, S and Jang, W.Y. Compressive response of open cell foams. Part I: morphology and elastic properties. *International journal of solids and structures*. 42,1355-1379. 2005.

[34] Gong, L.; Kyriakides, S. and Triantafyllidis, N. On the stability of kelvin cell foams under compressive loads. *Journal of the mechanics and physics of solids.* 53, 771-794. 2005.

[35] Sullivan, R.M.; Ghosn, L.J. and Lerch, B.A.A general tetrakaidecahedron model for open-celled foams. *International journal of solids and structures.* 45, 1754-1765. 2008.

[36] Sullivan, R.M and Ghosn, L.J. Shear moduli for non-isotropic, open cell foams using a general elongated Kelvin foam model. *International journal of engineering science*. 47, 990-1001.2009.

[37] Hamilton, A.R.; Thomsen, O.T.; Madaleno, L.A.O.; Jensen, L.R.; Rauhe, J.C.M. and Pyrz, R. Evaluation of the anisotropic mechanical properties of reinforced polyurethane foams. *Composites science and technology*. 87, 210-217. 2013.

[38] Pinto, J.; Solórzano, E.; Rodriguez-Perez, M.A. and de Saja, J.A. Characterization of the cellular structure based on user-interactive image analyses procedures. *Journal of cellular plastics*. 49, 555-575. 2013.

[39] Kumar, V. Process synthesis for manufacturing microcellular thermoplastic parts. *PhD. Thesis*. Massachusetts Institute of Technology. Cambridge, MA. 1988.

[40] Weller, J.E. and Kumar V. Solid-state microcellular polycarbonate foams. I. The steady-state process space using subcritical carbon dioxide. *Polymer engineering & Science*. 50, 2160-2169.2010.

[41] Bhatti, A.S. and Dollimore, D. The thermal decomposition of azodicarbonamide. *Thermochimica Act*a. 76, 63-67. 1984.

[42] Spitael, P. and Macosko, C.W. Strain hardening in polypropylenes and its role in extrusion foaming. Polymer Engineering and Science. 44, 2090-2100.2004.

[43] Laguna-Gutierrez, E.; Lopez-Gil, A.; Saiz-Arroyo, C.; Van Hooghten, R.; Moldenaers, P.; Rodriguez-Perez, M.A. Extensional rheology/cellular structure/mechanical behaviour relationships in HMS PP/montmorillonite foams. Laguna-Gutierrez, E.; Lopez-Gil, A.; Saiz-Arroyo, C.; Van Hooghten, R.; Moldenaers, P.; Rodriguez-Perez, M.A. 2015. *Submitted*

[44] Lee, S.T.; Park, C.B. and Ramesh, N.S. Polymeric Foams. Science and Technology. *Taylor and Francis Group*. 2007.

[45] Bao, J.B.; Liu, T.; Zhao, L. and Hub, G.H. A two-step depressurization batch process for the formation of bi-modal cell structure polystyrene foams using scCO_2. *Journal of Supercritical Fluids*. 55, 1104-1114. 2011.

[46] Fazekas, A.; Dendievel, R.; Salvo, L. and Bréchet Y. Effect of microstructural topology upon the stiffness and strength of 2D cellular structures. *International Journal of Mechanical Sciences*. 44, 2047-2066. 2002.

5.4- Conclusions.

The main objectives of this thesis regarding the production of PP foams have been fulfilled. First of all, the production parameters of the ICM foaming route and the formulations employed were successfully optimized for this polymer during the first work (*Section 5.2*) leading to the production of PP foams with varied expansion ratios and cellular structures. On the one hand, cellular structures with cell sizes below 100 μm and with a very narrow cell size distributions were achieved by applying high initial pressures and high blowing agent contents (15 wt%). The open cell content of these foams was influenced by the expansion ratio in the sense that the increments of the expansion ratio involved an increment of the open cell content. On the other hand, when the blowing agent was drastically reduced from 15 wt% to 1 wt% the cell size increased and the open cell content decreased resulting in the production of closed cell foams with greater mechanical performance. The role played by the open cell content prevails over that of cell size when determining the stiffness (elastic modulus) of these foams. This was evaluated by mechanical tests performed under different configuration loads (compression, tensile and bending). The collapse, yield and bending strengths were not as sensitive to cellular structure variations as the elastic modulus. Figure 5.2 shows an example of how the cellular structure varied (cell size increment) when decreasing the blowing agent content for foams produced with the same expansion ratio (1.6).

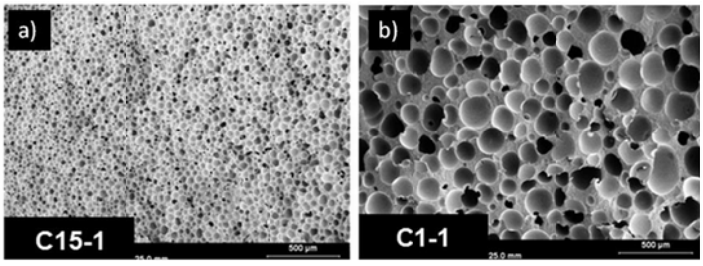

Figure 5.2. PP foams produced with different contents of ADC and the same expansion ratio (1.6) a) 15 %.wt b) 1%.wt.

The ICM route proved to be a suitable production route to obtain non-crosslinked and shaped rigid foams, which could be applied for foaming any thermoplastic polymer. However, the production of foams based on PP able to replace more common materials applied to structural applications such as PET and PVC foams require the use of a polymer matrix with a higher foaming performance. In the work performed in *section 5.3*, a branched PP was used which allowed the production of low density PP foams ($\rho < 200 kg/m^3$). This reduction of density also involved a reduction of mechanical properties as predicted in the *Gibson* and *Ashby* model (cubic cell) in which the relative density is the fundamental parameter determining foam properties. With the aim of decreasing the role played by density, the polymer matrix was reinforced with nanoclays. The presence of nanoclays within the polymer matrix and the employment of low foaming pressures (below 4 MPa) promoted interesting cellular structure variations such as the appearance of bimodal distributions of cell sizes (Figure 5.3) in which a large number of small and isotropic cells are surrounded by a lesser number of bigger and anisotropic cells. The appearance of the double population of cells is explained by the catalytic effect induced by nanoclays in the blowing agent decomposition reaction, which involved the

generation of a higher amount of gas. Therefore, the polymer/blowing agent system is more sensitive to pressure variations (at least in the range of pressures studied in this work). This fact together with the employment of low foaming pressures caused a two-stage nucleation process, which was responsible for the formation of two populations of cells as shown in Figure 5.3a.

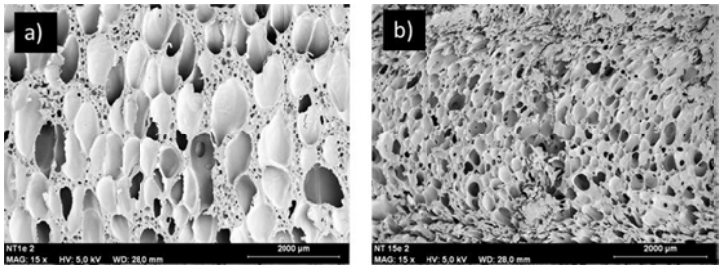

Figure 5.3.Nanoclay reinforced PP foams: a) produced at low pressures (0.5 MPa) b) produced at high pressures (80MPa).

The characteristic bimodal cell size distribution of the nanoreinforced foams produced with low pressures evolved to very homogeneous cell size distributions of lower than average cell sizes (Figure 5.3b). In this case, the heterogeneous nucleation phenomenon, which is typically found in polymers reinforced with particles prevails, making these foams more homogeneous and with lower cell sizes than those obtained with pure foams. Moreover, these nanoreinforced foams, in spite of their higher open cell contents, present better mechanical properties when measured not only in the expansion direction but also in the transversal direction. This fact is a clear indicator of the reinforcement induced by nanoparticles in the polymer matrix within the cell walls and struts.

The anisotropic character of these foams was studied in detail because this morphological feature was determinant in order to produce PP based foams with mechanical properties similar to those of the foams employed in the market, which present more isotropic structures. These anisotropic structures were the result of restricting the expansion of the polymer to only one direction (ICM process). The study of the morphological and mechanical anisotropy of these foams was tackled by characterizing the cellular structure (image analyses) and the mechanical properties in compression in the linear-elastic region (compressive modulus). The mechanical anisotropy behaviour (E_{exp}/E_{transv}) perfectly resembled that of the morphological anisotropy (R), highlighting the importance of this structural parameter in the mechanical properties of these PP-based foams. A different methodology to characterize the morphological anisotropy (R) was established based on the correlation found between anisotropy ratio and cell size. The bigger cells presented higher elongations (anisotropies) than the smaller cells, which were practically isotropic. For this reason, the shape anisotropy of the cells (measured in two dimensions) was weighted by their area (R_w).

Finally, common models employed to describe the mechanical behaviour of anisotropic cellular structures, such as the Huber-Gibson model (rectangular prismatic cells) and the Kelvin model (tetrakaidecahedron cells) provided a good correlation with the experimental results when foams with $R_w < 1.6$ were considered. However, in the case of foams with high R_w values

and with a bimodal distribution of cell sizes there was not a good correlation. These models are suitable to predict the mechanical properties of low-density and open-cell foams with highly periodic cellular structures and these kinds of PP foams do not fulfil these conditions entirely, which could be the reason for the lack of correlation.

All the work developed in this chapter resulted in the production of PP foams with very high mechanical performances and with varied cellular structures that make them a very promising alternative to the current foams employed in the market of structural lightweight components, such as the core of sandwich panels. For this reason, this development was used to elaborate a patent, which is included in an ANEX of this thesis. Moreover, a comparative study of the mechanical properties of these PP foams with respect to those of PVC and PET foams is also included in *Chapter 6*.

CHAPTER 6:

PRODUCTION OF PROTOTYPES. APPLICABILITY OF THE DEVELOPED MATERIALS

Contents

6.1- Introduction.

The formulations developed and the production processes optimized at lab-scale during this thesis within the framework of two public-private cooperation projects (*ACTIBIOPACK* and *NANCORE*) allowed the production of more sustainable and environmentally-friendly materials than those usually found in the market of food-packaging trays and structural foamed panels. However, the existing gap between the production of these materials at lab-scale and the real production conditions at industrial scale is huge. Filling this gap is a hard task that requires detailed knowledge of the industrial processes and the products developed. In many cases, materials successfully produced at lab scale have failed to take the leap to an industrial scale. This is the case of nanomaterials, which after years of profound investigation in laboratories worldwide proving their excellent properties, have not yet found a consolidated market niche due to the so-called *valley of death* (gap between research and industry). For this reason, prototypes for several applications were developed during this thesis in order to take a step forward towards their scaling up for industry.

In the case of starch-based materials, which is a process very similar to the one employed in industry for the production of solid trays was developed to produce some prototypes of a size similar to that of trays found on the market. This process is based on extrusion and thermoforming (*section 6.2.1*). A specifically designed mould for the thermoforming stage was employed which allowed to employ the hydraulic press available in the laboratory to be employed. Foamed starch trays were also produced by microwave foaming using a specifically design mould based on PTFE (*section 6.2.2*) but their inherent brittleness makes this product unsuitable for this application. However, this material and process is suitable for the production of protective-packaging foams of a defined shape, such as the ones employed for household appliances. Moreover, an economic evaluation comparing the price of starch-based formulations with those of synthetic polymers such as PET was performed with the aim of evaluating the economic competitiveness of the materials developed (*section 6.2.3*). The development of these starch-based materials would not be of interest if they were not proved to be biodegradable and compostable under controlled conditions. The use of plasticizers and natural fibres could have influenced the inherent biodegradability of starch. This is why the biodegradation degree of some of the starch-based materials developed in this work was tested by means of a procedure based on several standards, which will be explained in *section 6.2.4.*

On the other hand, the optimization of formulations and parameters in the ICM route allowed rigid foamed panels to be produced with excellent mechanical properties regarding stiffness and strength and of varied shapes and sizes. The PP-based foams used for characterization in chapter 5 were disk-shaped foams with a diameter of 150 mm and cylinders with a diameter of 20 mm (Figure 27). A new mould was developed, which was capable of producing square-shaped foams of larger sizes (220x220 mm^2) in order to analyse the influence of the size in the production of these foams. Good results were obtained indicating that there are good chances of scaling up the ICM process to industrial sizes. The prototypes developed were denominated as *ANICELL* in

reference to their anisotropic structures. There are several versions of these panels depending on the formulation employed and the structures obtained from them: *ANICELL CC* in the case of closed cell foams, *ANICELL OC* in the case of nanoreinforced open cell foams and *ANICELL F* in the case of using flame-retardant additives. The mechanical properties of *ANICELL CC and OC* were compared with those of foamed panels employed in the market such as PVC and PET foams (*section 6.3.2*) The interesting properties of *ANICELL* foams, developed within the NANCORE project, resulted in the filing of a patent, which is included in *section 6.3.3*.

6.2- Bioderived and biodegradable food-packaging trays based on TPS.

There are numerous types of food-packaging trays available on the market. Some examples are shown in Figure 6.1. They differ in their design and dimensions. Some of them are completely flat while others are designed with structural nerves in order to reduce the tray thickness and hence, its cost. In some cases the colour and design is varied with the purpose of making them more attractive for the consumer.

Figure 6.1. Food packaging trays with different designs

But in general there are two main kinds of trays on the market: foamed trays and solid trays. The foamed trays are usually produced from polystyrene (PS), extruded (XPS) and expanded (EPS), while the solid trays are produced from PET and PP. In both cases the production route is very similar because it consists of two common steps: extrusion and thermoforming (Figure 6.2). However, the production of foamed trays requires the employment of more sophisticated extruders (tandem extrusion lines) because a physical blowing agent is injected into the extruder and dissolved into the molten polymer in order to expand the product at the exit of the die.

Figure 6.2. Equipment employed for the production of the packaging trays: a) production of PP and PET solid sheets by extrusion. b) Production of XPS foamed sheets by extrusion foaming. c) Thermoforming moulds for trays

In this work, two production routes for the production of solid and foamed food packaging tray prototypes based on starch formulations were developed. They are described in the following sections.

6.2.1- Solid and flexible starch-based trays.

The steps of the process implemented for the production of solid food packaging trays prototypes based on thermoplastic starch are schematically shown in Figure 6.3. It basically consisted of two main stages: *extrusion* and *thermoforming* but several sub-stages had to be implemented due to the singularities of the equipment employed in the laboratory. The main differences between this process and the one usually employed at industrial scale will be

commented at the end of this section. These sub-stages were denominated by numbers (between parentheses) so as to make reference to them throughout the text.

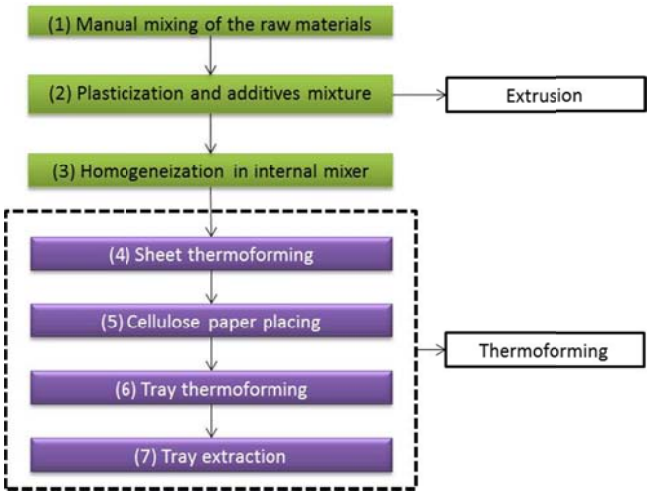

Figure 6.3.Scheme of the production process for solid starch-based trays developed at CellMat Laboratory.

Firstly, the raw materials (starch, plasticizers and processing aids) were manually mixed (1) as seen in Figure 6.4.The raw materials and base formulations were described in sections 3.1.1 and 4.2. In addition, paraffin wax was added in some of the formulations with the aim of lubricating the extrusion process, hence, it acts as a processing aid.

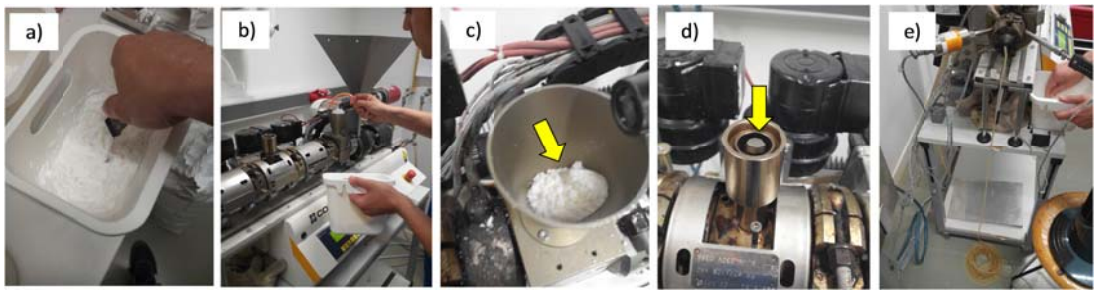

Figure 6.4.a,b) Manual feeding of the raw materials to the extruder. c) Starch powders agglomerated in the hopper. d) Ventilation channel to release steam. e) Molten TPS strand cooled in air.

Secondly, the plasticization process and additives mixture (2) were carried out in a twin-screw extruder (model *ZK 25T, Dr. Collin*). The production parameters were the same ones employed for the production of TPS solid biocomposites (*section3.2.1*). The feeding of the raw materials was performed manually (Figure 6.4b) due to the low diameter of the hopper located at the beginning of the extruder, which caused the agglomeration of the starch batter when it was fed automatically (Figure 6.4c). A ventilation channel was placed in the middle of the extruder barrel (Figure 4d) with the aim of evacuating the steam generated during the process, which could have produced unwanted expansions of the TPS after exiting the extruder. Finally, the plasticized

starch blended with additives came out of the extruder die in the form of a molten strand which was immediately cooled in air (Figure 6.4e) due to the hydrophilic character of TPS.

In the third stage, the formulation produced was homogenized (3) in an internal mixer (*section 3.2.1*)in order to make it more uniform and obtain a compact batter of TPS as the one observed in Figure 6.5.This step was required because the homogeneity of the TPS blend obtained after the extrusion step was not very high due to the feeding problems previously described.

Figure 6.5.Intermediate mixing step. a) Internal mixer employed. b) Chamber with the TPS blend inside and the screws rotating. c) Starch batter formed at the end of the process.

Finally, the thermoforming stage was carried out in a laboratory thermoforming press composed of two independent hydraulic presses: one for heating and the other one for cooling (Figure 6.6a). This laboratory press required the use of a specifically designed aluminium mould as the one shown in Figure 6.6b, which can be manually closed by screws, enabling it to be moved from the heating press to the cooling one without losing the shape of the molten tray.

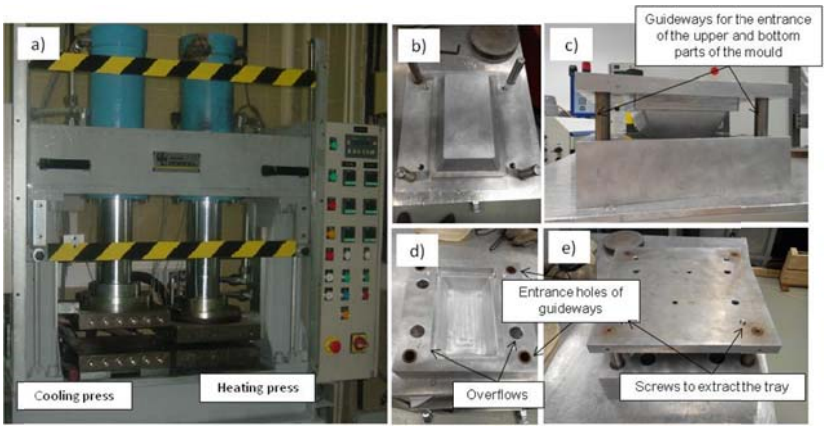

Figure 6.6 a) Laboratory hydraulic press. b) Mould male. c) Mould and female joined by the guide-ways. d) Mould female. e) Upper view of the mould.

The mould was machined with four circular guide-ways in the male part and four circular holes in the female part(Figure 6.6b.c) in order to join both parts with the maximum precision and always produce trays of the same dimensions (high reproducibility). The mould was also designed with overflows in the female part in order to let the excess molten polymer leak out from the cavity (Figure 6.6d). Moreover, a screw system (Figure 6.6e) permitted the separation of the male part from the female part at the end of the process to extract the tray.

The thermoforming stage was in turn split up into four sub-stages as previously shown in Figure 3.Firstly, a certain amount of the TPS batter obtained in the internal mixer was used to produce a sheet of4 mm in thickness as the one shown in Figure 7a. The pressure and the temperature applied were 22,2 bars and 150ºC, respectively, for only one minute. Secondly, two pieces of cellulose paper were placed between the sheet previously produced and the female and male parts of the mould (as shown in Figures 6.7b, c and d). In this way the extraction of the tray after the final thermoforming step was easier because the cellulose paper prevented the starch-based material from sticking to the aluminium mould.

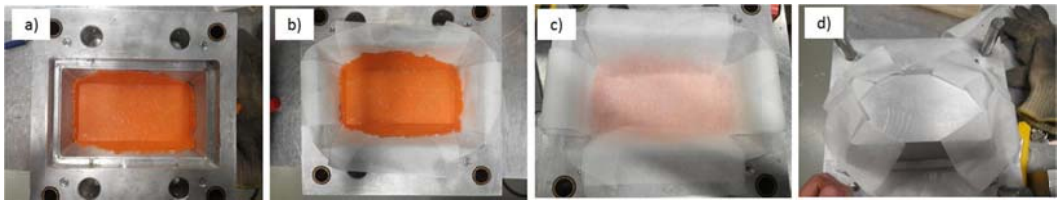

Figure 6.7.a) 4 mm thick sheet produced after the pre-thermoforming step. b) cellulose paper between the female part of the mould and the starch-based sheet. c) cellulose paper placed between the sheet and the male part. d) cellulose paper stuck to the male part.

Thirdly, the mould was closed and placed between the hot-plates of the hydraulic press (Figure 6.8a). A pressure of 22,2 bars and a temperature of 150 ºC were also applied but in this case for 10 minutes with the aim of providing the tray with the final shape (6). After this time, pressure was released, the mould was displaced from the heating plates to the cooling plates and it was cooled under pressure and finally, it was extracted from the mould (7) as shown in Figures 6.8b-d.

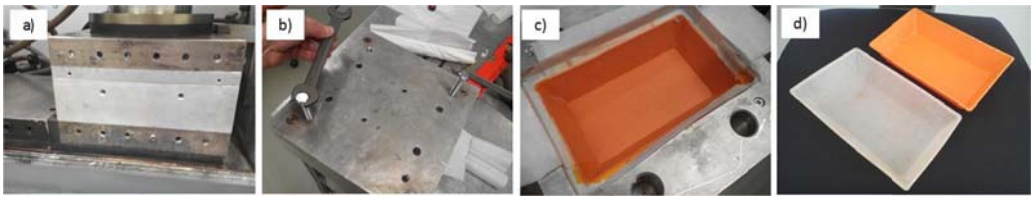

Figure 6.8. a) Mould placed between the hot-plates during thermoforming. b) Extraction of the upper part of the mould by screws. c) Thermoformed tray inside the mould. d) Two kinds of solid flexible trays produced after this process.

Four kinds of solid and flexible food-packaging trays based on TPS and with a final thickness of 2 mm were produced following this production route. All of them are shown in Figure 6.9.

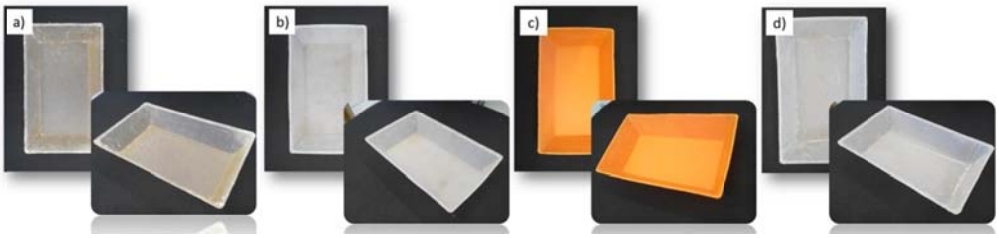

Figure 6.9.a) TPS25. b)TPS23P5. c)TPS23P5C.d)TPS23P5+LDPE film.

The main difference between them was the formulation employed. *TPS25* is based on pure TPS plasticized with 25% of glycerol. *TPS23P5* is thermoplastic starch plasticized with only 23% of glycerol and 5% of paraffin wax and *TPS23P5C* is the same formulation as the previous one but incorporating an orange pigment. The last tray shown in Figure 9 presents the peculiarity of incorporating an LDPE film covering the whole tray in order to isolate it from environmental humidity and from the wetness of the food products. This strategy is usually employed in industry for the production of multi-layers trays in which each single layer plays a different role.

The process described in this section presents some differences with respect to a conventional industrial process, which were unavoidable due to the characteristics of the laboratory equipment employed. One of the differences was found in the extrusion stage. In the process developed in this thesis, the extrusion stage (2) was only employed to plasticize starch and to blend the required additives. A pre-thermoforming step (4) was required later in order to produce a sheet of the required dimensions prior to the final thermoforming stage. This pre-thermoforming stage would not be required in industry because the solid sheets are produced by extrusion, using an extruder equipped with a specific sheet-shaped die and with pumps to displace the molten material up to the shaping unit at high pressures. Moreover, the plasticization process could be carried out in this same extruder. The initial mixing units would produce the plasticization of starch as schematically shown in Figure 6.10. Therefore, processes (2) (3) and (4) could be simplified into one single extrusion step. The other important difference was found in the thermoforming step that had to be performed in several sub-stages due to the singularities of the hydraulic press employed in the laboratory, which is composed of two independent presses: one for heating and the other one for cooling. This fact made the production of a specifically adapted mould (previously described) indispensible, which was able to be displaced from the heating plates to the cooling ones without losing the shape of the tray. In an industrial process, the heating and the cooling of the tray inside the mould are performed in the same press and in only one stage. Moreover, this mould was not coated with TEFLON (a common practice in industrial processes) making it necessary to use a cellulose paper to release the tray at the end of the process properly.

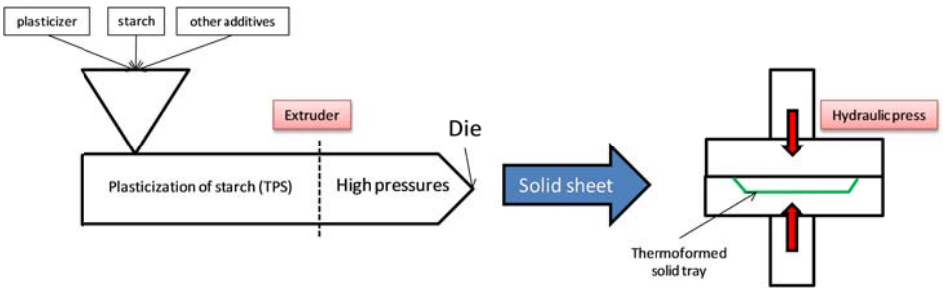

Figure 6.10.Scheme of the industrial production process of the TPS solid trays.

The performance of the solid trays produced (the ones covered with the LDPE film) was evaluated in the ACTIBIOPACK project and the results obtained were compared with those obtained for conventional non-biodegradable trays. The food selected to perform the test was

fresh mushrooms. Several tests were performed (colour, texture, PH etc.) and the results obtained were successful. Even in some cases the performance of the TPS tray was better than that of the commercial non-biodegradable trays. This fact proved that the production and use on the market of a thermoformed tray made of a biodegradable polymer such as starch is possible.

6.2.2- Foamed rigid trays.

A process based on microwave foaming was also developed for the production of foamed starch trays. The design of a PTFE mould was key in order to obtain tray-shaped foams. The processing stages are very similar to those employed for the production of solid trays with two exceptions: firstly, the plasticizer used is water instead of glycerol because it acts as the blowing agent. Secondly, an additional foaming stage is included in which a TPS-based solid precursor is foamed by microwave radiation inside the aforementioned PTFE mould.

The processing parameters employed for the plasticization of starch by water and the homogenization in the internal mixer are those specified in *section 3.2.1* (Figure 3.11). The production parameters in the thermoforming step differ slightly because the size of the sheets obtained (solid precursors) is larger (Figure 6.11c). In this case, a 2 mm in thickness sheet is obtained after thermoforming 170 grams of a TPS batter under 22,2 bars and a temperature of 90 ºC. The initial starch batter and the thermoformed sheet obtained are shown in Figure 6.11.

Figure 6.11. Production of solid precursors. a) TPS batter obtained after homogenization in internal mixer. b) Thermoforming stage in the hot-plates press. c) Thermoformed solid precursor.

Finally, the microwave foaming stage is carried out. The only difference with respect to the process described in *section 3.2.2* is the PTFE mould employed, which was specifically designed for producing trays of the dimensions shown in the scheme of Figure 6.12. The mould consists of a male and female, which are joined by screws as shown in Figure 11. The reasons why PTFE was selected as the mould material were explained in more detail in *section 3.2.2*.

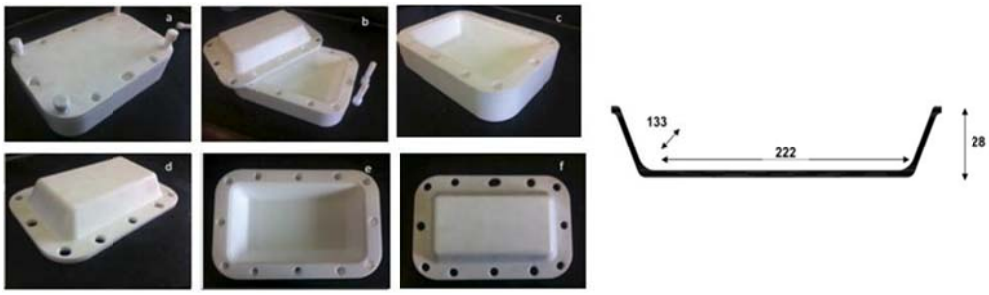

Figure 6.12.PTFE mould employed for the production of the trays from different views. Dimensions of the foamed starch tray produced by microwave radiation.

Figure 6.12 shows the main stages involved in the production of the starch foamed trays by the microwave foaming process developed in the laboratory.

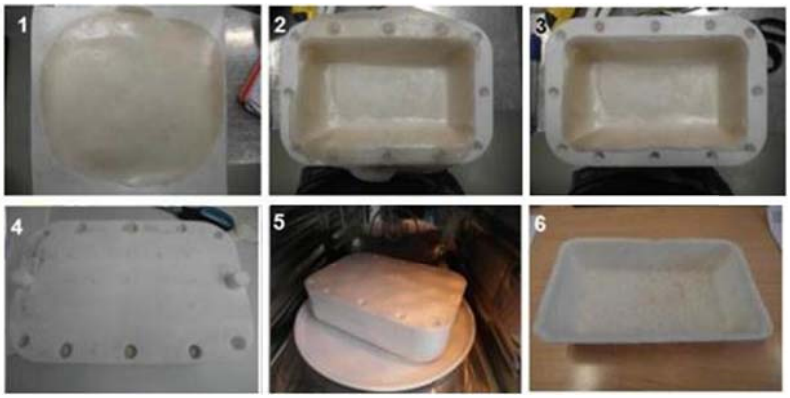

Figure 6.12.Steps of the microwave foaming process for producing starch foamed trays.

The process consists of several sub-stages. Firstly the sheet obtained after thermoforming is placed into the mould cavity (1 and 2) and the excess material is cut off (3) in order to close the mould easily (4). Once the mould is closed by the screws, it is introduced into the microwave oven chamber (5) and microwave radiation is applied for 4 minutes at the maximum power permitted by the oven (900 W). Finally, the mould is extracted from the oven, opened and the tray is extracted (6). Some of the trays obtained are shown in Figure 6.13.

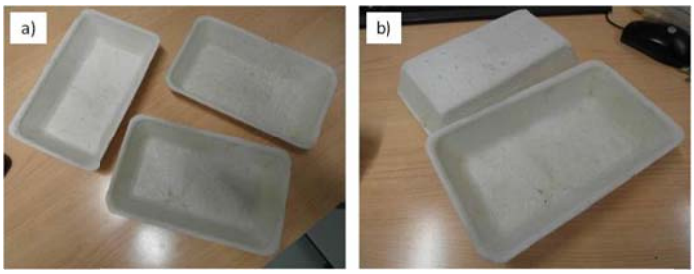

Figure 6.13. Foamed starch trays produced by microwave foaming.

The formulation employed (wheat starch plasticized with 30% of water) and the processing parameters chosen allowed foams with a thickness of 4 mm to be obtained, a weight around 90 grams and a density of 450 kg/m^3.

The main drawback of this process is that the trays obtained are very brittle and therefore, not adequate for packing food products. This application requires flexible products such as the solid TPS trays produced in *section 6.2.1*. On the contrary, this brittle material is more adequate for *protective-packaging* applications in order to replace common synthetic foams employed in this market such as EPS (expanded polystyrene). Moreover, the microwave foaming process is more efficient in terms of energy consumption and cycle-times (*section 3.2.2*) than the ones employed for the production of EPS foams (moulded-bead process).The production of these starch trays proved that the microwave foaming process could be applied for the production of biodegradable *protective-packaging* foams of a defined shape, such as those employed to pack household appliances. Nowadays, the only starch foams applied for protective packaging applications are loose-fill chips obtained by extrusion foaming.

In order to implement this lab-scale process on an industrial scale it is necessary to use more sophisticated microwave ovens, which could allow a continuous production process. The extrusion stage would be very similar to the one described in section 6.2.1 for the production of solid trays on an industrial scale. The only difference is the use of water as the plasticizer. This means that the production parameters should be adapted (lower temperatures) so as to avoid water vaporization inside the extruder. The thermoforming stage would not be required because the industrial extruder would have a sheet-shaped unit. The sheet produced would be finally introduced in an industrial microwave oven with a higher power than the one used in the laboratory and specifically designed to allow PTFE moulds to be introduced in the chamber.

6.2.3- Economic evaluation.

The TPS trays developed should be competitive not only in terms of properties but also in terms of costs. For this reason, an economic evaluation was performed in which the objective was to evaluate if the TPS solid trays developed (section 6.2.1) are economically competitive with respect to conventional trays currently found in the market produced from fossil based polymers such as PET and from biodegradable polymers such as PLA. This evaluation was exclusively based on the raw material cost. The production costs were not considered because the process employed for the production of the TPS trays is very similar to the conventional industrial production route employed for the production of solid food-packaging trays (extrusion and thermoforming). Hence, the energy consumed in both processes would be very similar as well as the equipment employed.

The costs evaluation was performed with solid flexible trays based on TPS plasticized with different contents of glycerol (biodegradable polymer), PET trays (petroleum-based polymer) and PLA trays (biodegradable polymer).The inputs of the evaluation are the elastic modulus of the raw materials, their densities and their price. These data are shown in Table 1. The TPS

mechanical properties and densities were taken from the work developed in *section 4.2*in which materials based on TPS with different amounts of glycerol were produced. The PET and PLA properties were obtained from technical data sheets of conventional commercial polymers.

Formulation	Elastic Modulus (MPa)	Price (€/kg)	Density (kg/m^3)
PET	2500	1.5	1400
PLA	3500	4	1250
TPS (30%Gly)	16	0.95	1372
TPS (25%Gly)	117	0.91	1365
TPS (20%Gly)	1691	0.87	1358

Table 6.1.Inputs of the economic evaluation.

The price of the TPS formulations was calculated considering that the price of native starch is 0,7€/kg and that of glycerol is 1.53€/kg. Hence, decreasing the amount of glycerol is beneficial in two aspects. On the one hand, because the material is more rigid and on the other hand, because the price of the formulation decreases due to the higher cost of glycerol. The material densities are not greatly affected by the variation in the glycerol content.

In spite of the stiffness increment produced when decreasing the amount of glycerol, the stiffness of PET and PLA is still greater. Hence, the tray made of TPS should be produced with a greater thickness in order to support the same bending load. The thickness of this "theoretical" TPS tray can be obtained from equation 6.1,in which the elastic modulus of a squared-cross section beam (Figure 6.14) deformed by a bending load is calculated (simulating the possible deformation mode of trays because of the weight of the packed food).

$$E = \frac{PL^3}{4\,w\,t^3 y} \tag{6.1}$$

where:

- P: load applied in the middle point.
- L: length of the beam.
- w: width.
- t: thickness.
- y: strain.

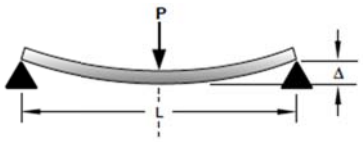

Figure 6.14.Squared cross section beam subjected to a single bending load in the middle.

Assuming that all the terms in equation 6.1 are equal except for the thickness (*t*) and the elastic modulus (*E*), equation 6.1 turns into equation 6.2, which can be used for calculating the thickness of a theoretical TPS tray by simply knowing the elastic modulus and the thickness of a reference tray, which in this case can be made of PET and PLA (in the equation we use PET as a reference).

$$t_{TPS} = \sqrt[3]{\frac{E_{PET}}{E_{TPS}}}\, t_{PET} \tag{6.2}$$

Finally, taking the densities (kg/m^3) and the prices of the raw materials (€/kg)into account, the final cost of the formulations developed (€/m^2) was estimated. They are represented in Figure 6.15 versus the calculated theoretical thicknesses.

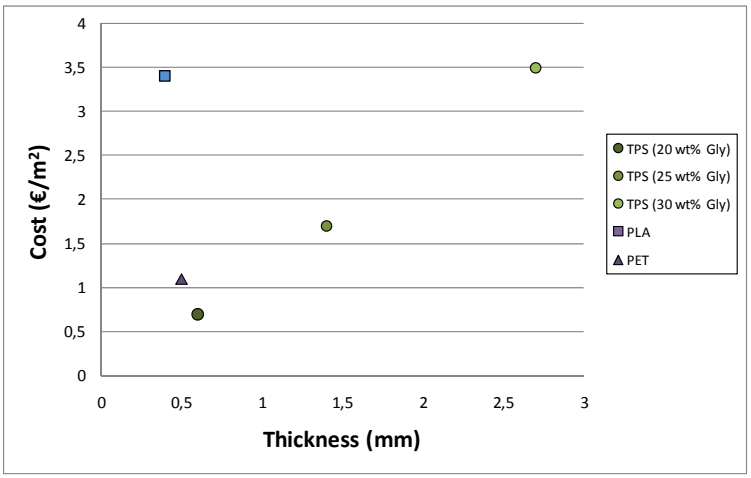

Figure 6.15.Tray thicknesses and costs comparison.

The cost of a theoretical tray made of TPS clearly depends on the amount of glycerol. This is due on the one hand, to the higher price of glycerol with respect to that of native starch and on the other hand, to the increase in thickness required to produce TPS trays with high amounts of glycerol. The thickness of a theoretical TPS tray plasticized with 30% of glycerol is 2.7 mm whereas that of a TPS tray plasticized with only 20% of glycerol is only 0.6 mm and hence, very similar to the current trays found in the supermarkets. In this last case the cost of the material is even lower than that of a PET tray and therefore, this theoretical TPS tray would be economically competitive. The comparison is even more favourable when considering a tray produced from a biodegradable polymer such as PLA whose properties are very similar to those of synthetic polymers but whose price is very high, making the packaging products produced from it non-competitive (the cost per m^2 is 3,4 €, around 5 times higher than that of the TPS material).

In conclusion, the TPS trays developed could compete in the market of food-packaging trays and replace current trays produced from fossil-based polymers such as PET. This fact constitutes one

of the main advantages of thermoplastic starch because the biodegradable polymers currently used in this market are very expensive (such as PLA).

6.2.4- Biodegradability tests.

One of the main environmental concerns of the modern society is the huge amount of plastic waste generated especially that derived from food-packaging products (*chapter 1*). For this reason, the production of more environmentally-friendly packages is nowadays, one of the most important goals of this industrial sector. One interesting strategy to solve this matter is the employment of biodegradable polymers, which decompose biologically under controlled conditions in a few months. The term *biological decomposition* is employed because the material goes through processes different to those undergone by chemical and physical decomposition routes. It is a process, which is basically controlled by microorganisms acting under controlled conditions regarding temperature, humidity and oxygen content. Microorganisms are able to transform organic materials into their most elementary molecules such as carbon dioxide and water throughout the biodegradation process. Equation 3 shows a typical reaction of an aerobic biodegradation process.

$$Organic\ compound + O_2 + microorganisms \rightarrow CO_2 + H_2O + salts + biomass. \quad (6.3)$$

The starch-based materials developed in this thesis should be considered as biodegradable because starch is a natural polymer known for its biodegradability. However, the materials developed present some other components in their formulations (plasticizers, fillers and processing aids) that could decrease the original biodegradability of starch. For this reason, biodegradation tests were carried out within the framework of the *ACTIBIOPACK* project in order to quantify the real biodegradability of the materials developed. These measurements were performed at *CTME* facilities *(Technological Centre of Miranda de Ebro*) and the tests conducted are based on several standards: *UNE-EN 14046*[1], *ASTM D 5988*[2] and *UNE-EN-ISO 17556*[3].

Three kinds of starch-based materials developed during this thesis were characterized: wheat starch plasticized with 30 wt% of glycerol (*solid*), wheat starch-based foam (*foam*) and wheat starch-based foam reinforced with grape waste (*grape foam*). These materials were previously ground and the powders obtained were packed in plastic bags as the ones shown in Figure 6.16. Finally, they were sent to CTME where the tests were carried out. Moreover, a reference material (starch powders), which was completely biodegradable was also measured (*R*).

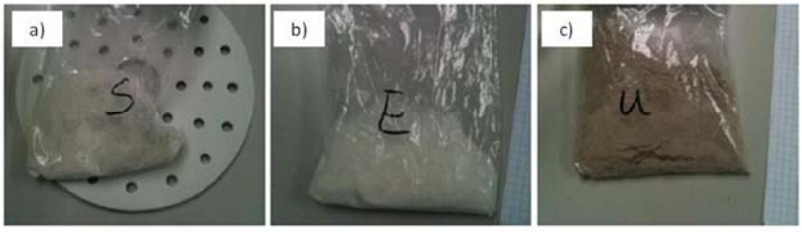

Figure 6.16. Samples measured which correspond to some of the materials developed during this thesis: a) solid TPS plasticized with glycerol (solid), b) starch foam plasticized with water (foam) and c) starch foam plasticized with water and filled with grape particles (grape foam).

First of all, the *total dry solid content* and the *total organic content*(*TOC*) of the samples were determined in order to quantify their potential biodegradability. The results are shown in Table 6.2.

Samples	Total dry solid content (%)	Total organic content (%)
Solid	99	42,6
Foam	99	36,9
Grape foam	100	39,3

Table 6.2. Total dry content and total organic content of the samples.

The TOC was measured by the combustion catalytic oxidation method and by the subsequent measurement of the CO^2 generated in the process by non-dispersive infrared spectroscopy. A TOC analyser Shimadzu model SSM-5000A was used for these experiments. The TOC measurements are important in order to know the exact amount of carbon, which is able to be degraded by microorganisms, that is, the biodegradability potential of the samples.

Secondly, the samples were mixed with an inoculum (Figure 6.17b), which is the microorganism source. The quality of the inoculum is crucial in order to achieve a complete biodegradation of the material organic fraction. For this reason, the inoculum was artificially prepared from mature compost (Figure 6.17a) by mixing carbon-rich materials (woods and mature compost) and nitrogen-rich materials (green plants, urea etc.) in adequate proportions. The microorganisms have to be activated by adding water to the compost and left to stand for a determined period of time. After that, the inocolum is ready and the samples can be mixed with it to proceed with the biodegradation tests.

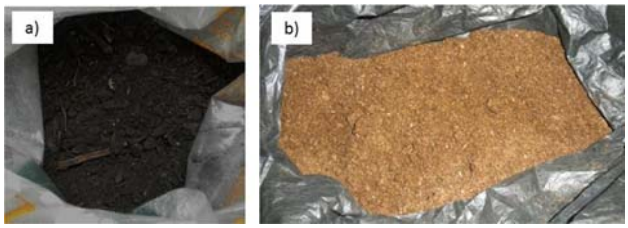

Figure 6.17.a) Mature compost (carbon-rich source). b) Inoculum used for the test.

The sample and the inoculum were mixed inside a glass vessel (Figure 6.18) until a homogenous mixture was achieved. The vessel is hermetically closed and the CO_2 generated during the decomposition reaction is captured by adequate traps (inside glass flasks), which are chemically titrated at specific periods of time in order to know the evolution of the reaction. A glass flask with a blank sample (water in Figure 6.18) is also placed into the vessel. The test requires specific environmental conditions in order to favour the microbial activity (full darkness and controlled conditions of temperature, oxygen and humidity).

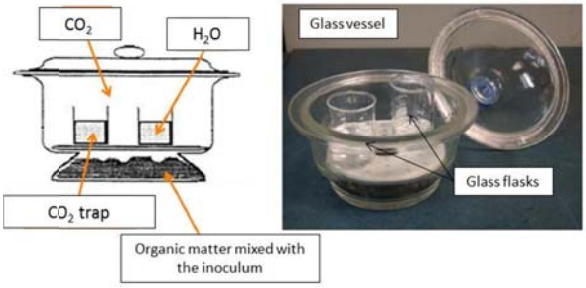

Figure 6.18.Glass vessel in which the biodegradation reaction takes place.

Figure 6.19 shows pictures of the inoculum and samples evolution during the test.

Figure 6.19.Evolution of the samples during the biodegradation test.

The evolution of the biodegradation degree in percentage (D_t) is calculated by equation 6.4.

$$D_t = \frac{\sum m_i - \sum m_B}{Th\ CO_2} \times 100 \qquad (6.4)$$

where:

- D_t: biodegradation degree at time t (%).
- Σmi: carbon dioxide amount in milligrams released in the test vessel for the sample *i* between the beginning of the test and the time *t*.
- Σm_B: carbon dioxide amount in milligrams released in the blank vessel (*B*) for the sample *i* between the beginning of the test and the time *t*.

- $ThCO_2$: Theoretical amount of carbon dioxide (milligrams).

The theoretical amount of carbon dioxide ($ThCO_2$) released by the sample (in grams) is calculated by equation 6.5.

$$ThCO_2 = m \times w_c \times \frac{44}{12} \tag{6.5}$$

where:

- *m: weight of the tested material sample*
- *w_c: TOC expressed in mass fraction.*
- *44 and 12 are the molar mass of CO_2 and the atomic mass of carbon, respectively.*

The results are shown in the plot of Figure 6.20, in which the biodegradation degree (D_t) is represented versus time for all the materials considered. For the sake of reproducibility two samples for each material (*solid*, *foam*, *grape foam*) and two references (*R*) were measured. The test is considered valid if the biodegradation degree is higher than 60% after reaching the stationary state or at the end of the test.

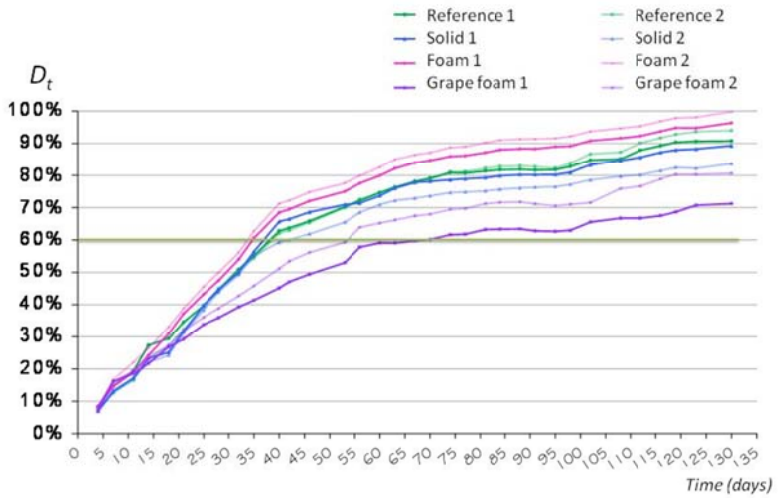

Figure 6.20.Biodegradation degree (Dt) in percentage versus time.

All the materials measured can be considered biodegradable because D_t is higher than 60% at the end of the test (130 days).*Foam* is the material with the highest biodegradability (98,1%), which is even higher than that of the reference (92,4%). The *solid* sample also reached high biodegradability values (85%) in spite of being plasticized with glycerol. The material with the lowest biodegradation rate is the *grape foam* (75%), which consists of a starch-based foam reinforced with grape fibres (value reached). The lignocellulose fraction of this sample could contribute to the slowing down of the decomposition process. Finally, it is important to note that the final biodegradability values of these materials could be higher because the curves did not reach a steady state at the end of the experiments. Therefore, higher biodegradation rates are expected at more elevated times.

6.2.5- Conclusions.

The TPS-based materials developed in this thesis could be applied for the production of solid flexible *food-packaging* trays at industrial scale because the production route developed is very similar to the one employed in industry (*extrusion* and *thermoforming*). In addition, some functional tests (packing of fresh mushrooms) were successful when using TPS trays covered with an LDPE film. Last but not least, the material is economically competitive not only with respect to synthetic polymers such as PET and PP but also with respect to other biodegradable polymers with potential application in the food-packaging market such as PLA.

The production of starch foamed trays by microwave radiation at industrial scale proved to be inviable because of the inherent brittleness of the foams produced that make them non suitable for this application. Nevertheless, this material and process could be suitable for the production of *protective-packaging* foams with defined shapes.

Finally, the main motivation of this thesis within the framework of the ACTIBIOPACK project was the development of sustainable materials based, in this case, on biodegradable and compostable polymers. For this reason the evaluation of their biodegradability was necessary due to the fact that certain additives (plasticizers) and particles (natural fibres) added could diminish or even suppress the inherent biodegradability of starch. The biodegradability was tested by a procedure which follows several standards and the results showed how all the formulations developed can be considered as biodegradable.

6.3- Non cross-linked PP foamed panels as the cores of sandwich panels.

Sandwich panels with foamed cores are employed in a broad bracket of applications and in many industrial sectors. For instance, PVC foamed cores are one of the main structural elements in the hull of yachts because they provide the whole structure with buoyancy. Moreover, their closed cellular structure makes them ideal in this application because water penetration is prevented. Figure 6.21 shows a yacht hull with PVC foams inside. The interiors of trains (roof, side walls and floors) are usually built with light structural elements that incorporate low-density rigid foams (Figure 6.21) because they increase the comfort levels because of higher sound absorptions and thermal insulation. Wind turbine blades are internally composed of sandwich panels with foamed cores in order to support the shear loads to which this element is constantly subjected by wind forces. Last but not least, the automotive sector is nowadays searching for lighter materials with the aim of reducing the weight of the vehicles and in this sense, increasing engine performances and reducing fuel consumption. This is even more important when considering electric vehicles because by using lighter materials such as rigid foams the performance of the current batteries would be increased. This is the aim of one of the European projects in which *CellMat Laboratory* is currently involved: *EVOLUTION*[4] in which the use of PP foams is being considered for the production of the doors panels of electrical cars.

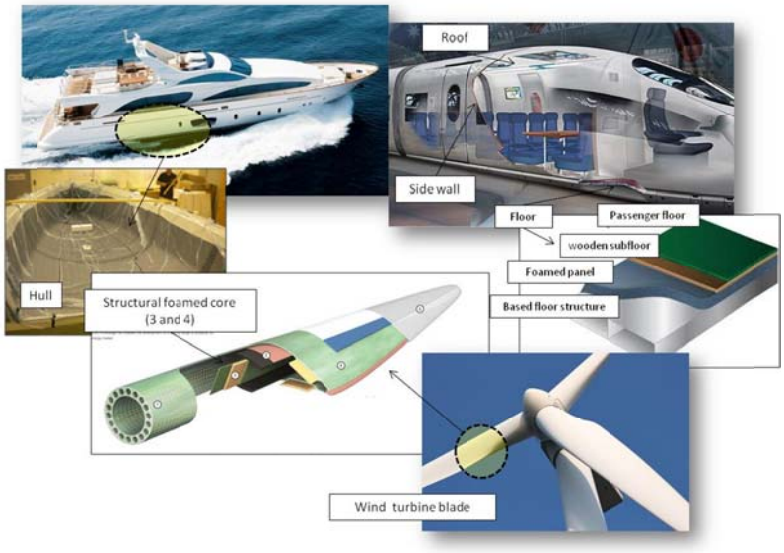

Figure 6.21.Typical applications of rigid foamed panels.

Nevertheless, most of the foams employed in these applications are based on cross-linked polymer foams such as PVC foams which therefore, are non-recyclable. Balsa wood is other material, which is widely employed but its natural origin make their structures and hence, their properties non-homogeneous. There are other solutions based on non cross-linked polymers such as PET foams but their mechanical performance is considerably lower than those of the previously mentioned materials. In addition, these man-made foams (PVC and PET) are produced by very few companies worldwide being the most representative being 3A

COMPOSITES, DIAB and GURIT. This evident lack of competitors makes the final prices of these foams very high. For these reasons, the research conducted in this thesis within the framework of the NANCORE project aimed at developing economically competitive non cross-linked rigid foamed cores with similar or even higher mechanical properties than those of the foams currently employed.

As a first result of our research rigid foamed panels based on PP and with very promising properties were obtained. These properties were shown in the articles of chapter 5.However, the size of the foams produced in this thesis was very small because they were used exclusively for characterization purposes: cylinders of 20 mm in diameter and disks of 150 mm in diameter. On the contrary, at industrial scale the foamed panels produced present considerably larger surfaces and thicknesses in a broad range. Table 6.3 shows the dimensions of some commercial structural foamed panels based on PVC and PET.

Type	Commercial denomination	Producer	Dimensions (mm)		
			Length	Width	Thickness
PET	AIREX T10	3A COMPOSITES	2440	1005	10-45
PET	Divinycell PX	DIAB	2440	1220	-
PVC	AIREX C70	3A COMPOSITES	1500-2850	700-1330	5-80
PVC	Divinycell H	DIAB	1640-2650	800-1250	

Table 6.3.Dimensions of commercial rigid foamed panels

Therefore, when considering the scaling-up of these materials the main problem that they will face up to is increasing their size. This is a very critical aspect in foams because the heating and the cooling process have to be adapted consequently. Moreover, the commercial foams are boards while the foams produced during this thesis were cylinders and disks, as previously commented.

In an attempt to take a step forward in the scalability of these materials a mould with a larger size and square in shape was designed. The design process of this mould was somewhat limited by the size of the available laboratory hydraulic press, whose plates present a surface of 300x300 mm. Finally, a square-shaped mould as the one shown in Figure 6.22 was designed.

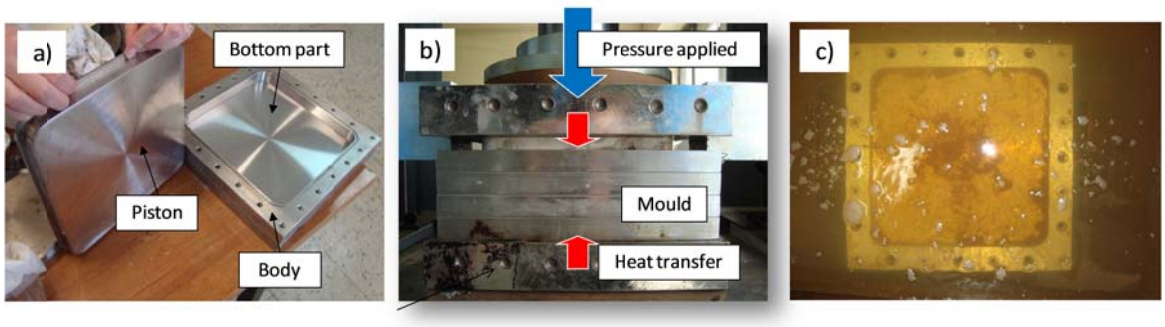

Figure 6.22.Squared-shape mould.

The production process of the foams had to be optimized because of the large size of this new mould. In this sense, the detailed knowledge acquired in chapter 5 with the relation process-structure-properties was fundamental in order to be able to produce these new foamed panels. For instance, the foaming times were higher. The cylinders and disks were produced at foaming times no higher than 15 min while in the case of this new square foamed panels the foaming times required were about 25 min (they varied depending on the formulation employed). Finally, squared shape foams with similar properties to the ones obtained with disks and cylinders were obtained. Some examples are shown in Figure 6.23.

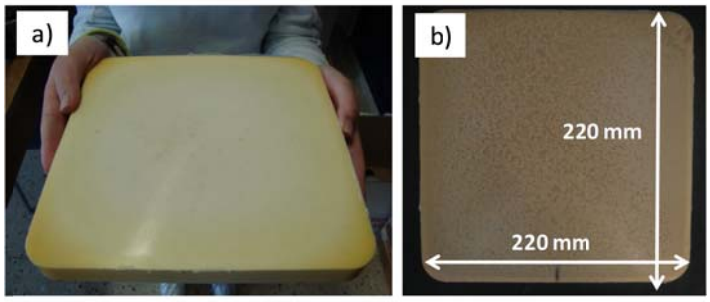

Figure 6.23. Squared-shape foams.

The good properties of the foams obtained (chapter 5) and the possibility of increasing their size without significantly modifying the production process, make attainable the purpose of commercializing the product. For this reason, , a patent was filled (WO 2014/009579 A1: METHOD FOR PRODUCING CELLULAR MATERIALS HAVING A THERMOPLASTIC MATRIX), which is included in an ANEX of this thesis. These foams were denominated as ANICELL and the whole range of properties will be shown in the next section (6.3.1).

6.3.1- An alternative rigid foam for structural applications in the market: ANICELL

Anicell (***ANI****sotropic* ***CELL****ular structures*) is the denomination given to the low density and rigid foamed panels based on polypropylene developed during the NANCORE project. Two versions of ANICELL foams can be found depending on their cellular structures. On the one hand, *ANICELL CC* (***C****losed* ***C****ell*) foams are suitable as structural elements and for buoyancy applications due to their closed cellular structure. On the other hand, *ANICELL OC (**O**pen **C**ell*) foams are adequate as sound absorbers and as a filter element because of the high degree of interconnectivity between cells. Both can be employed as single structural elements or as foamed cores for the production of sandwich panels.

The optimization of formulations (blowing agent content) and production parameters in the ICM foaming route that was carried out in the works performed in *section 5.2* and *section 5.3* constituted a key milestone for the production of low-density foamed panels (90-200kg/m^3) based on branched polypropylenes with closed cellular structures and elongated cells in the expansion direction. This kind of product was denominated as ANICELL CC (closed cell

foams).*ANICELL CC* panels produced in different shapes (discs and rectangular prisms) and their typical cellular structure is shown in Figure 6.24.

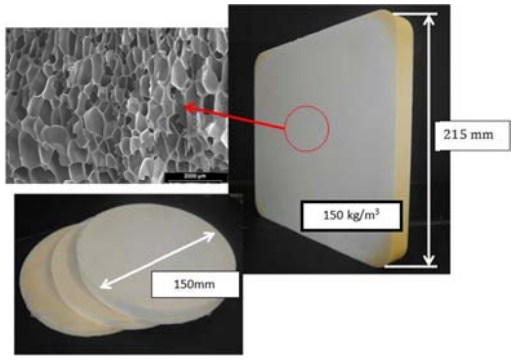

Figure 6.24.ANICELL CC foamed panels and typical cellular structure.

These foams present a very high mechanical performance in terms of stiffness and strength, which is comparable or in some cases higher than those of PVC and PET foams. A comparison between their mechanical properties will be shown in *section 6.3.2*. Table 6.4shows some of the properties of *ANICELL CC* foamed panels for two typical densities: 150 and 180 kg/m^3.

	ANICELL CC 180 Kg/m^3	ANICELL CC 150 Kg/m^3
Compressive modulus (MPa)	180	120
Collapse strength (MPa)	2.8	1.6
Open cell content (%)	<20	<20
Average anisotropy ratio.	2.3	2.6

Table 6.4. Anicell CC properties.

The reinforcement of the polymer matrix with nanoclays produced outstanding results because they induced the formation of bimodal cellular structures with lower than average cell sizes and secondly, because the interconnectivity degree between cells increased considerably with respect to pure foams. This last modification should have resulted in lower mechanical performances but on the contrary, when comparing the properties of the nanoreinforced foams with those of the pure foams at the same open cell content, the nanoreinforced foams were stiffer and stronger, proving the reinforcing effect of nanoclays [5].This new product based on nanoreinforced PP foams was called ***ANICELL OC*** (open-cell) and it is adequate for applications in which high sound absorption levels are required, such as in the interior of trains, or as filtering elements. Figure6.25 shows a typical *ANICELL OC* panel and its characteristic cellular structure composed of a bimodal distribution of cell sizes with a high degree of interconnectivity.

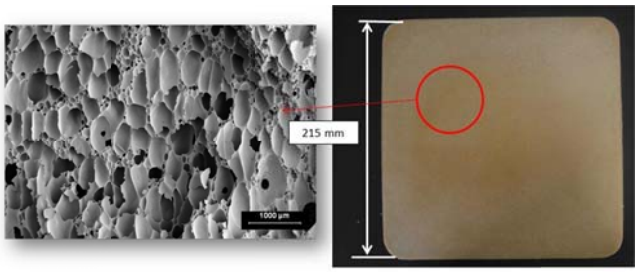

Figure 6.25. ANICELL OC foamed panels and cellular structure.

Table 6.5 shows some of the properties of ANICELL OC foamed panels for two typical densities: 150 and 180 kg/m^3.

	ANICELL OC 180 Kg/m^3	ANICELL OC 150 Kg/m^3
Compressive modulus (Mpa)	120	90
Collapse strength (MPa)	2.6	1.6
Open cell content (%)	95	95
Averge anisotropy	2.3	2.7

Table 6.5. Anicell OC properties.

6.3.2- Comparison with PVC and PET foams

The mechanical properties in compression of *ANICELL* foams, with regards to their compressive modulus, were compared with the mechanical properties of PVC and PET foamed cores employed in the market. The PVC foams were supplied by DIAB and the PET foams by 3A COMPOSITES. The compressive test used for the determination of the compressive modulus was the same as the one used in *chapters 4* and *5,* which is based on the *ASTM standard D1621-00*[6].

The PVC foamed panels (were characterized by means of SEM images and mechanical properties in compression. The cellular structure of one of the foamed panels (55 kg/m^3) is shown in Figure 6.26.

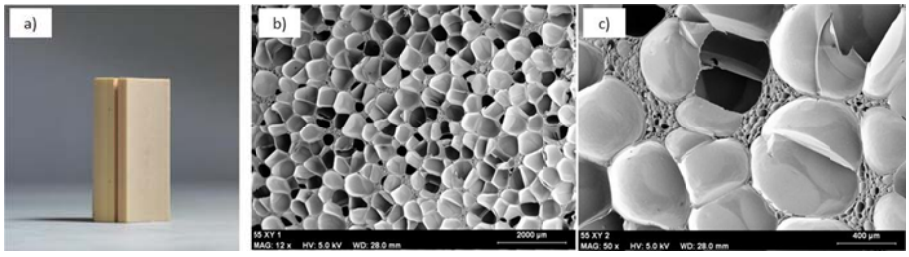

Figure 6.26. PVC foamed panels of 55 kg/m^3.

This foam presents a typical closed cellular structure with a bimodal distribution of cell sizes, as well as the nanoreinforced PP foams (*ANICELL OC*). This closed cellular structure was achieved after crosslinking the polymer matrix, which means that the final product is non-recyclable. More details about their production route can be found in *chapter 1.*

An alternative non-crosslinked foamed panel is based on PET, which is produced by the *strand foaming technology* (*section 2.5.4*). This production process is less costly than that used for the production of PVC foams mainly because it operates in continuous (based on *extrusion foaming*). Figure 6.27shows foamed PET panels sent by *3A COMPOSITES* and their typical cellular structures.

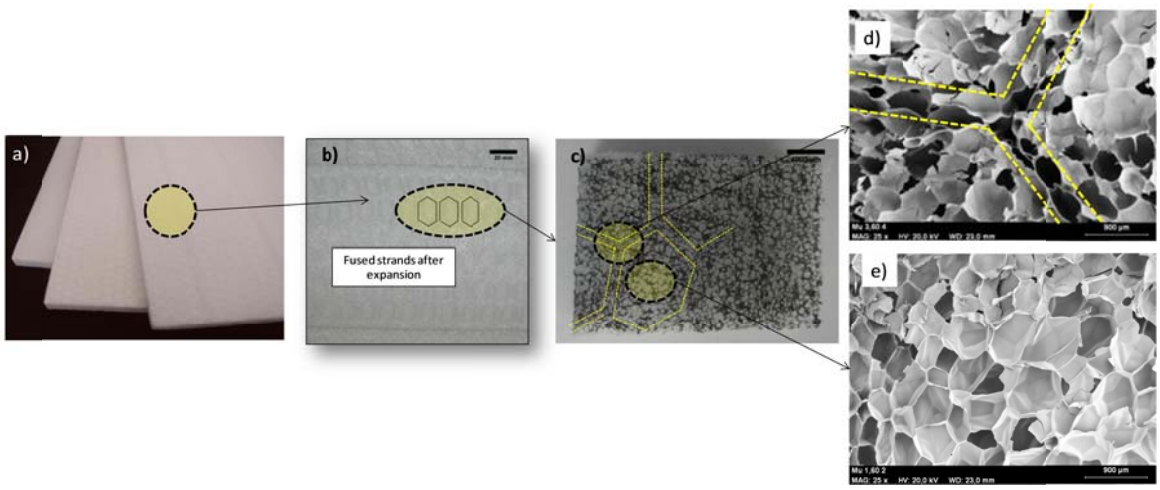

Figure 6.27. a) PET foamed panels of 60 kg/m3. b) Photograph of the panels surface. c) Photograph of the cellular structure of a fused strand. d) SEM micrograph of the borders between fused strands. e) SEM micrograph of the interior of a fused strand.

These pictures and SEM images were taken along the plane perpendicular to the expansion direction which coincides with the extrusion direction. These cellular structures are very interesting because the expansion of the strands and their final adhesion induce deformation of the cells within the borders, as delimited by the yellow lines in Figures 25.c and d.

The mechanical properties of the PVC and PET foamed panels and those of *ANICELL OC* and *ANICELL CC* were compared in Figure 26 by means of a plot in which the compressive modulus is represented versus the density of the foams. In all the cases the thickness of the foams was 10 mm. A theoretical estimation of the PP foam properties is also represented because the density of most of the PVC and PET foamed panels included in this comparison fall below the minimum density (about 150 kg/m^3) of the ANICELL foams included. The cubic cell model of *Gibson* and *Ashby* (*section 2.4*) was employed for this theoretical estimation.

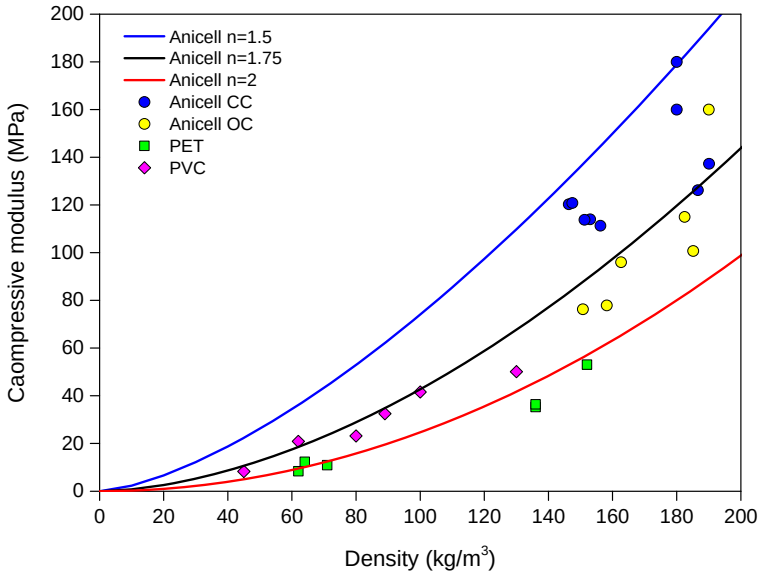

Figure 6.28.Compressive modulus versus density plot.

When comparing the properties of foams with similar densities (in the range between 130 and 160 kg/m^3), the compressive modulus of ANICELL foams, both the closed cell and the open cell versions, are clearly higher than those of PVC and PET foams. The compressive modulus of the PVC foams follow a tendency similar to that predicted for the PP foams but when the exponent n is taken as 1,75 (black line). In the case of the PET foams, the tendency followed is also similar but with an exponent nearer to 2 (red line). Nevertheless, the experimental properties of ANICELL foams are located between the line corresponding to n=1.75 and the line corresponding to n=1.5 (blue line). In addition, the experimental values of *ANICELL CC* are nearer the values predicted with n=1.5. For this reason, it is reasonable to assume that the properties of ANICELL foams produced at lower densities would be higher than those of the PVC and PET foams. PP foams with lower densities than 100 kg/m^3 have been produced by the ICM route although a detailed characterization of their structures and properties has not been carried out so far and for this reason, they were not included in this section.

6.3.3- Conclusions.

The knowledge developed in the relation process-structure-properties of these materials (PP foams) as well as the application of suitable production technology (ICM route) allowed the production of materials with very interesting properties in the field of structural components.

Nevertheless, in spite of the promising results obtained, further research is still necessary to evaluate how *ANICELL* foamed panels behave under other kinds of loads and if they are able to fulfil other requirements. For instance, the production of foamed cores for sandwich panels requires a more detailed evaluation of their shear properties (modulus and strength) because it is the main mode of deformation during their service period (*section 2.5.4*).

Other aspects, which are more closely related to their handling after production, will have to be tackled as well. For instance, the adhesion degree between the foamed core and the skins (usually fibre-based composites) has to be evaluated too. The common adhesion technologies employed in this market are based on resin infusion methods (assisted by vacuum frequently) that employ adhesives based on epoxy resins. A picture of this process is shown in Figure 6.28a, in which a vacuum bag covers both the mould and the core in a yacht hull. The resin is transferred with pressure through multiple inlets and complete wet out is achieved by using grooves, cuts and perforations of the core. Figure 6.28b shows PVC foamed panels drilled on one side to allow resin to transfer throughout the foam and grooved on the other side to facilitate the distribution of resin on the underside of the foam during the vacuum assisted resin infusion process.

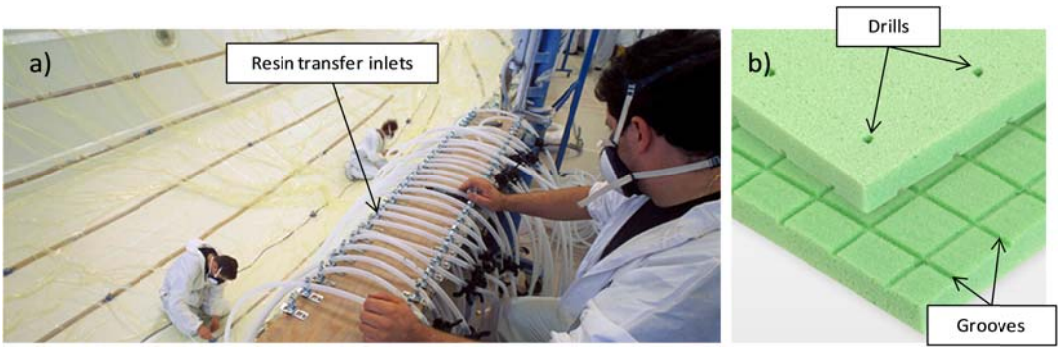

Figure 6.28.a) Vacuum resin infusion method. b) Drilled and grooved PVC foams.

Moreover, the final scaling up of these materials will have to face up to several challenges. First of all, the current commercial boards present larger sizes (Table 6.3). The production of the larger square-shaped mould proved that the production of larger foams is possible. Secondly, the implementation of the ICM technology would present several difficulties mainly derived from the fact that the polymer is not cross-linked during the process. This fact requires the design of sophisticated moulds able to retain the molten polymer inside, especially during the expansion and cooling processes because otherwise, the foam would leak out of the mould. These specifically designed moulds would require large cycle times, especially in the closing and

opening operations, which could increase the production costs considerably. This is especially critical if the product is compared with the commercial PET foams, which are also non cross-linked but produced by a continuous process based on extrusion (explained in section 6.3.2).

Nevertheless, there are not only disadvantages. On the one hand, obtaining a non cross-linked product makes the foam recyclable which is a good point from an environmental point of view. On the other hand, the mechanical properties (at least in compression) of the materials developed (*ANICELL*) are comparable or even higher than those of the foamed panels currently employed in the market. This confirms that these PP foamed panels could represent a real alternative for this application (structural applications) not only due to the fact that they are economically competitive (lower price of the raw material) and sustainable (*non-crosslinked*) but also because they present better mechanical properties.

References.

[1] UNE-EN 14046: envases y embalajes: evaluación de la biodegradabilidad aeróbica última y de la desintegración de los materiales de envase y de embalaje bajo condiciones controladas de formación de compost : método mediante el análisis del dióxido de carbono liberado. Asociación Española de Normalización y Certificación. *AENOR*.

[2] ASTM D5988. Standard test method for determining aerobic biodegradation in soil of plastic materials or residual plastic materials after composting.

[3] UNE-EN-ISO 17556. Plásticos: Determinación de la biodegradabilidad aeróbica última en el suelo mediante la medición de la demanda de oxígeno en un respirómetro o bien mediante la cantidad de dióxido de carbono generada.

[4] http://evolutionproject.eu/about-evolution

[5] Lopez-Gil, A.; Escudero, J.; Laguna-Gutierrez,E.; Saiz-Arroyo,C.; Rodriguez-Perez, M.A. Anicell. Low density and non-crosslinked anisotropic polypropylene foams as a promising option to produce structural panels. EUROTEC 2013.

[6] ASTME D1621-00.Standard test method for compressive properties of rigid cellular plastics.

CHAPTER 7:

CONCLUSIONS AND FUTURE WORK

Contents

7.1- Conclusions.

The research carried out in this thesis reached the targets set at the beginning (chapter 1) by employing more sustainable production routes and by developing solid and foamed materials based on environmentally-friendly polymers such as starch (biodegradable polymer) and a branched polypropylene (non cross-linked polyolefin). The specific conclusions were divided depending on the material employed: starch or polypropylene, in accordance with the general structure of the thesis.

7.1.1- Starch.

Several biobased and biodegradable formulations based on thermoplastic starch (TPS) and with a high potential for being employed for the production of ***solid flexible trays for food-packaging*** and ***rigid shaped protective-packaging foams*** were developed.

In the particular case of the research conducted with solid starch-based materials (section 4.2), the main conclusions obtained were:

- A lab-scale production route consisting of two stages: extrusion and thermoforming were optimized for the production of formulations based on TPS filled with natural fillers.

- Several formulations were produced and studied as a function of the amount of plasticizer (glycerol for solid biocomposites) and the type and amount of natural fillers (barley straw fibres and grape particles).

- The range of glycerol concentrations studied (20-30 wt%) allowed the production of formulations with varied mechanical properties. On the one hand, the plasticization with 20 wt% of glycerol resulted in stiff materials (modulus >1600 MPa; elongation at break < 5%). On the other hand, the plasticization with 30 wt% of glycerol resulted in flexible materials (elongation at break > 120%).

- The natural fillers employed (barley straw fibres and grape waste)were selected because of their very different morphology. Barley straw presents a fibre-shaped morphology with high aspect ratios while grape waste presents a more irregular particle-shaped morphology.

- The reinforcement with natural fillers involved important structural modifications of the materials developed. SEM micrographs of the solid composites obtained showed in general a good dispersion of the fibres along the polymer matrix, suggesting that processing conditions were chosen properly. On the contrary, the adhesion degree varied depending on the fibre employed, which could be due to their different chemical composition. Interphases between grape fillers and the polymer matrix were detected, whereas barley straw fibres presented very good adhesions.

- The mechanical properties measured under tensile tests were positively affected by the addition of barley straw fibres. The stiffness increased more than 3 times and the strength about 2.5 times with respect to the formulation without reinforcement. However, the incorporation of grape particles did not involve any appreciable improvement, which could be due to their lower adhesion degree.

- Several analytical models were employed to describe the mechanical properties of the solid biocomposites produced. The predictions of the ***Halpin& Tsai model*** fit very well with the experimental results obtained in the case of the composite reinforced with barley straw

fibres (fibres with high aspect ratio). Hence, this result could indicate a preferential orientation of the fibres during processing that could not be appreciated experimentally by the SEM micrographs.

In the case of the research performed on foamed starch-based materials (section 4.3), the main conclusions obtained were:

- A lab-scale microwave foaming process was developed and optimized for the production of starch-based foams. This process differs with respect to those previously found in literature because the solid precursor employed is a thermoformed sheet instead of individual pellets. This fact allowed the production of foamed blocks without discontinuities, which in the previous processes were caused by the lack of adhesion between expanded pellets.

- Several formulations were produced and studied, which were based on starch plasticized with water and reinforced with different kinds of natural fillers.

- Water acted not only as the plasticizer but also as the blowing agent. The low boiling point of water involved the employment of softer production conditions (temperatures and pressures in the extruder and in the hydraulic press) than those employed with glycerol (solid formulations) in order to avoid losing it prior to foaming.

- Three natural fillers were employed: barley straw fibres, grape waste and cardoon waste, which were added at the same loading level (5 wt%). These natural fillers were selected because of their different morphology. This was evaluated in detail by image analyses of optical micrographs. The results obtained revealed on the one hand, that the aspect ratio of barley straw fibres was considerably higher than that of grape and cardoon (barley straw fibres with aspect ratios near 10 could be found). On the other hand, grape particles were bigger than cardoon and barley straw (most of the grape particles were larger than 4000 μm^2) although they presented a broad distribution of particle sizes.

- The addition of natural fillers slightly decreased the expansion capacity of the polymer matrix because the densities obtained were higher than that of the pure foam (292 kg/m^3). This reduction of the expansion capacity was more notorious in the case of the foam reinforced with barley straw fibres (347 kg/m^3).

- The cellular structures of the foams obtained were in general non-homogeneous (in terms of cell size and shape) and presented high open cell contents (OC>95%). The distributions of cell sizes were very wide in all cases with sizes between 100 and 1600 μm. The average cell size was normalized with respect to the density of the foam in order to avoid the influence of the expansion ratio (relative cell size).Grape particles did not vary significantly the relative cell size while barley straw fibres and cardoon particles produced considerably reductions. This could be due to a heterogeneous nucleation of cells caused by the high amount of small particles present in barley straw and cardoon waste (higher specific surface, hence, active points capable of acting as nucleating points).

- The mechanical performance of the foams produced was evaluated by means of compression tests. On the one hand, the results obtained within the elastic region (compressive modulus and strength) showed that all the particles reinforced the polymer matrix within the cell walls and struts because the compressive strength values of the reinforced foams were higher than those of the pure foams. However, only grape particles increased the compressive modulus values (when normalized to the density). This could be connected to the cellular structures obtained because this particle did not modify the cell

size appreciably. On the other hand, the total energy absorbed by the pure starch-based foams (W=1.91 MJ/m^3) increased in general with the addition of fibres but this increment was considerably higher in the case of barley straw fibres (W= 4.54 MJ/m^3).

- The stabilization mechanism of the cellular structure in these foams was promoted by a gradual drying of the polymer matrix during the expansion process. The properties of the polymer matrix within the cell walls and struts change during the expansion process. In fact, the process starts with a highly flexible solid precursor and ends up with a brittle foam. The compressive moduli of the foams obtained are even higher than those of the solids, which is in clear disagreement with the predictions of analytical models found in literature able to predict the mechanical properties of foams, such as the cubic cell model of Gibson & Ashby. On the contrary, this model allowed the properties of the solid cell walls and struts to be predicted by introducing the properties (density and modulus) of the foams obtained into the equation.

- The production of continuous foamed blocks from solid precursors based on thermoformed sheets allowed the mechanical properties to be increased with respect to previous works found in literature.

- The previous production routes were optimized for the production of prototypes due to the promising properties obtained. The main conclusions obtained in this part of the research were:

- Prototypes of solid food packaging trays based on the formulations previously developed were successfully produced. The production route employed was very similar to that employed in industry because it consists of two basic stages: extrusion and thermoforming. This fact makes the perspective of using of this material for high volume productions more affordable. Moreover, the prototypes obtained were successfully tested under real conditions, that is, by packing fresh mushrooms (within the framework of the ACTIBIOPACK project).

- Prototypes of foamed food packaging trays were produced by a microwave foaming process. The mechanical properties of these trays were not suitable for packing food products (brittle product), but this foaming method proved to be useful for the production of foams of defined shapes for protective packaging applications, like those usually employed for the protection of household appliances.

- An economic evaluation of the solid TPS formulations developed showed that these bioderived and biodegradable materials are able to compete with the common synthetic polymer employed for food-packaging applications such as PET and PP. This fact constitutes an important achievement in this field because the high price of biopolymers have so far limited their use in the packaging sector.

- The inherent biodegradability and compost ability of starch was not greatly affected by the additives used (plasticizers, natural fillers and processing aids). Biodegradability tests performed following several standards confirmed that the formulations which were developed are biodegradable.

7.1.2- Polypropylene.

Environmentally friendly non-crosslinked rigid foamed panels based on PP were successfully produced by the ICM route in a broad density range (from densities below 200 kg/m^3 to densities up to 600 kg/m^3). These foams present great potential to replace common foams employed for ***structural applications*** based on cross-linked polymers (such as PVC foams) which therefore, are non-recyclable. The conclusions obtained were split up according to the different range of densities obtained and therefore, it follows the same structure of the thesis (chapter 5).

In the case of medium-high density PP foams (relative densities higher than 0.2), which were studied in section 5.2, the main conclusions obtained were:

- The *formulations* (blowing agent content) and *production parameters* in the *ICM foaming route* were optimized for the production of medium-high density PP foam*s* (relative density > 0.2).

- The ICM foaming route allowed an independent control of the density and the cellular structure of the foams to be produced. For instance, foams with very different cellular structures, in terms of cell size, cell density and degree of interconnectivity (open cell content), but with the same expansion ratio were produced by simply modifying the blowing agent content.

- Cellular structures with a high population of cells (cell density) and low average cell sizes(Φ<100 μm) and at the same time, with very narrow cell size distributions were achieved by applying high initial pressures and by adding large amounts of the blowing agent (15 wt%).

- The open cell content proved to be a parameter which was highly dependent on the expansion ratio and on the amount of blowing agent. The higher the expansion ratio, the higher the open cell content. The foams produced with the highest expansion ratio(ER=3) presented open cell contents near 60%, regardless of the amount of blowing agent employed. However, as the expansion ratio decreased, the open cell content did too and at the same time, it became more sensitive to the amount of blowing agent. For instance, when considering foams with ER= 1.6 and when decreasing the amount of blowing agent to 1%, the interconnectivity level between cells drastically decreased and even closed cell foams were obtained.

- The elastic modulus of these foams was measured under different load configurations: compression, tensile and bending and the results were analysed in terms of the exponent n (Gibson & Ashby model). In the case of the tensile loads all the foams followed a tendency of n=2 regardless of the open cell content and the cell size. Therefore, this load configuration was not sensitive to cellular structure variations. However, in the case of the compression and bending loads, those foams with low open cell contents (1 wt% of blowing agent) deviated from the previous general tendency (n=2) resulting in foams with better mechanical performance (1<n<2). Therefore, the role played by the *open cell content* prevailed over that played by the *cell size* when determining the stiffness of PP foams.

- The strength of these foams was also calculated under different configuration loads (compression, tensile and bending). In this case, the foams behaved better under bending loads because the values of n obtained in this configuration were nearer to one. However, the correlation between the cellular structure and the strength values was not as clear as

with the elastic modulus. This parameter seems to be more dependent on the expansion ratio than on the cellular structure.

In the case of the low density PP foams (relative densities lower than 0.2) developed and studied in section 5.3, the main conclusions obtained were:

- A high melt strength branched PP was successfully employed for the production of non-crosslinked and low-density shaped PP foams with fine cellular structures (relative density< 0.2) by the ICM foaming route.

- The foams developed presented cellular structures with elongated cells in the expansion direction due to the unidirectional expansion that the molten polymer experiences in the self-expandable mould. This fact makes the mechanical properties of these foams highly dependent on the direction in which they are tested.

- The reinforcement with nanoclays promoted interesting cellular structure alterations such as the appearance of bimodal distributions of cell sizes in which a large number of small and isotropic cells are gathered surrounding a small number of bigger and anisotropic cells.

- Two reasons explained the previous behaviour: on the one hand, a catalytic effect over the blowing agent decomposition reaction and on the other hand, a two-stage nucleation process.

- The catalytic effect was evaluated by measuring the *onset temperature*(TGA), which decreased from 217,5 to 197,7 C after adding nanoclays. Moreover, the decomposition reaction was accelerated. As a result, larger amounts of gas were produced when using the nanoreinforced formulations, which made these foams more sensitive to pressure variations.

- The employment of low external pressures (< 4 MPa) and the large amount of gas generated when adding nanoclays induced a two-stage nucleating mechanism. The big anisotropic cells were produced during the application of the external pressure (the polymer is not able to dissolve the gas generated) while the small isotropic cells were formed after releasing the external pressure. The cells formed during the first stage had more time and space to grow and for this reason, they became bigger and anisotropic (restriction of the expansion to only one direction).

- Moreover, the presence of nanoclays involved a higher degree of interconnectivity between cells. This was qualitatively observed by SEM micrographs in which small ruptures or holes within the cell walls were detected, giving place to partially open cellular structures. Moreover, gas picnometry measurements revealed that the open cell contents of the nanoreinforced foams were higher (OC>50%) than those of the pure foams (OC<35%). This was due to changes in the rheological behaviour of the molten polymer after adding nanoclays that could induce higher drainage from the walls to the struts. As a consequence the walls are weaker than in the pure foams and they break under the pressure of the gas generated by the blowing agent.

- A new methodology to characterize the morphological anisotropy, different from those traditionally used in literature, was implemented due to the apparent correlation between anisotropy ratio and cell size that was found in this work (bimodal cell size distributions). For this reason, the shape anisotropy of the cells (R) was weighted by their area and a new anisotropy ratio coefficient (R_w) was employed to analyse the mechanical properties.

- The nanoreinforced foams produced with the lower pressures (0.5 and 1.5MPa)and measured in the expansion direction presented higher compressive moduli values (134and 118MPa). Moreover, the compressive moduli of the nanoreinforced foams measured in the transversal direction were higher than their pure counterparts in all the range of pressures studied. This fact confirmed that nanoclays reinforced the polymer matrix within the cell walls and struts, in spite of increasing the degree of interconnectivity.

- Common models employed to describe the mechanical behaviour of anisotropic cellular structures, such as the ***Huber & Gibson*** model (rectangular prismatic cells) and the ***Kelvin model*** (tetrakaidecahedron cells) were used to describe the mechanical behaviour of these PP foams. They provided a good correlation with the experimental results when considering R_w values lower than 1.6. However, in the case of the foams with higher R_W values, which are those with bimodal distribution of cell sizes (nanoreinforced foams produced under low pressures), they did not provide such a good correlation, which could be due to the lack of periodicity of these structures, their non-homogeneous distribution of cell sizes, and their only partially open cellular structures.

Section 6.3 was focused on evaluating the feasibility of scaling up the PP foams developed during this thesis. The main conclusions obtained were:

- Square-shaped prototypes with larger sizes than the ones developed in chapter 5 could be produced by the ICM route, which indicated the great potential of this polymer and this technology to be scaled-up to industry.

- The high mechanical performance of the foams produced and their varied cellular structures make them a very promising, cost-effective and sustainable alternative *(non crosslinked polymer*) to current materials employed in the market of structural lightweight foams, such as PVC and PET foams. A comparison between the mechanical properties of the PP foams developed and those of PET and PVC foams confirmed their great potential.

- These foams were denominated as ANICELL CC (in the case of closed cell foams) and ANICELL OC (in the case of open cell foams) and a patent was elaborated *"Method for producing cellular materials having a thermoplastic matrix*" in order to protect the know-how developed, which is included in an ANNEX of this thesis.

7.2- Future work

In spite of the interesting results obtained in this thesis, some new questions arise, which can only be answered by establishing new research lines in the coming years. Some of these research topics are presented in the following sections:

7.2.1- Development of starch-based materials

Several drawbacks were found with the materials developed so far. On the one hand, the formulations produced in this thesis are only suitable for packaging dry products and the only way of using them for packing wet food products is the adhesion of external hydrophobic layers (such as LDPE films). On the other hand, the application of starch foams produced by microwave foaming for food-packaging applications is limited because of their inherent brittleness. Moreover, the microwave foaming process developed in this thesis, in spite of its promising features, is still far from being an industrially scalable technology for this application. For these reasons, the following challenges will be tackled during the next few years.

- The production of solid and foamed thermoplastic starch based materials suitable for packing wet food products. For this reason, one of the future works that will be carried out will be the development of formulations with lower water affinity. An interesting approach adopted during the ACTIBIOPACK project was based on blending TPS with paraffin wax. The paraffin wax, during processing, migrated to the surface of the thermoformed samples producing a similar protective effect to that produced by external coatings, usually incorporated by co-extrusion (common practice in industrial processes). Moreover, the selection of chemically modified starches with higher water absorption resistance will have to be considered too.

- The development of TPS formulations able to maintain their flexibility after being foamed in processes in which water is the blowing agent. In this sense, the production of thermoplastic starch by using multiple plasticizers could be an interesting approach. One of the plasticizers (water) would be lost during foaming while the other would remain in the final foam because of a higher boiling point, preserving to some extent the flexibility of the product.

- The development of TPS foams by using chemical blowing agents in processes such as extrusion foaming or compression moulding. This research will require the selection of chemical blowing agents with very low decomposition temperatures due to the low thermal resistance of thermoplastic starch (natural polymer) or the use of catalysers to decrease the decomposition temperature of conventional chemical blowing agents.

- The production of TPS foams by foaming processes based on physical blowing agents in an attempt to replicate the production process of XPS foamed trays, which is based on extrusion foaming.

7.2.2- Development of polypropylene foams.

The addition of nanoparticles to polymer foams in general, and to PP foams in particular, and how they affect the different foaming mechanisms (nucleation, expansion and stabilization of the cellular structure)and as a consequence, the cellular structures and final properties obtained is still uncertain. For this reason, the following research lines are proposed:

- The study of the real effect that nanoparticles have on the rheological properties of the polymer matrix in order to understand the cellular structure alterations produced when

foaming nanoreinforced polypropylenes. In this sense, extensional viscosity and shear rheology measurements of pure and nanoreinforced formulations will be very helpful.

- To evaluate in more detail the heterogeneous nucleating effect that nanoparticles have on polymer foams produced under the effect of external pressures, such as in the ICM foaming route. Analyses ex-situ and in-situ of the foaming process based on X-ray radioscopy could be used for this purpose.

- To obtain further understanding of the mechanical response of anisotropic foams reinforced with nanoparticles, analysing the deformation mechanisms and improving the theoretical models.

- To use the ICM route to produce foams based on thermoplastic materials with higher stiffness and strength.

Moreover, a full implementation of these rigid foams in the market of structural foamed panels still requires further research in certain areas.

- The chemical modification of the PP foams surface by grafting reactions (for instance) could be an interesting strategy in order to increase their adhesion capability to solid skins based on epoxy resins composites, which is, in principle, low due to the chemical nature of PP.

- Further development of the formulations and of the self-expandable moulds employed in the ICM process for the production of lower density foams ($\rho \leq 90$ kg/m^3) and with fine cellular structures. For instance, the great thickness of the moulds currently employed avoids high cooling rates and as a result, the cellular structures are more prone to degeneration.

- The adaptation of the concept underlying the ICM route to foaming processes such as injection moulding, which would allow PP foams competing with other rigid foams with lower mechanical performance but produced by more cost-effective processes such as extrusion foaming (PET foams).